Nonconforming boundary elements and finite elements for interface and contact problems with friction – hp-version for mortar, penalty and Nitsche's methods

Von der Fakultät für Mathematik und Physik
der Universität Hannover
zur Erlangung des Grades
Doktor der Naturwissenschaften
Dr. rer. nat.

genehmigte Dissertation

von

Dipl.-Math. Alexey Chernov

geboren am 13.08.1981 in Moskau

2006

Referent:	Prof. Dr. E. P. Stephan, Universität Hannover
Korreferent:	Prof. Dr. P. Hansbo, Chalmers University of Technology, Göteborg
Korreferent:	Prof. Dr. J. Gwinner, Universität der Bundeswehr, München
Tag der Promotion:	27.06.2006

Abstract

The objective of this thesis is the construction, analysis and implementation of high order FE, BE and FE/BE coupling methods for interface and frictional contact problems with nonmatching discretizations, which have a wide industrial application.

A new *hp*-Nitsche's FE/BE coupling method for interface problems is designed and analysed. The method is proven to be consistent and stable, independent of the discretization parameters. A priori error analysis shows that the method is optimal in h and is suboptimal in p on quasiuniform meshes.

The question of unique solvability is addressed for the one-body contact problem with Tresca's friction. Constructing a chain of equivalent formulations the frictional contact problem is approximated with a sequence of frictionless contact problems (Uzawa algorithm). Conditions for the convergence of the algorithm are obtained. An *hp*-penalty BEM for one-body frictionless contact is developed. As the a priori error analysis shows, the penalty parameter ε_n must be chosen proportional to $(h/p)^{1-\epsilon}$, for optimal convergence rate (in the energy norm) of the discrete penalty solution to the solution of the original variational inequality formulation. A residual based a posteriori error estimator for the h-version of penalty FE and BE for one-body contact with Tresca friction is investigated. The error estimator, motivated so far with heuristical arguments and only for FEM, is shown to be reliable and efficient for both FEM and BEM.

The two-body elastoplastic contact problem with Coulomb's law of friction is solved with the FE/BE coupling and pure BE methods. The incremental loading procedure with Newton iterations on each loading step is used. Linearization of the frictional contact and plasticity terms as well as a description of the solution procedure are given in detail. The residual a posteriori error estimate, obtained for one-body frictional contact, is generalized to this two-body frictional contact problem. A novel *hp*-mortar method for two-body contact with Tresca's friction is designed and analysed for a variational inequality formulation. The contact constraints are imposed on the discrete global set of Gauss-Lobatto points. The nonmatched meshes are connected in terms of the *hp*-mortar projection. The a priori error analysis shows the convergence rate $\mathcal{O}((h/p)^{1/4})$ in the energy norm under additional assumptions on the discretization parameters. A Dirichlet-to-Neumann algorithm and an Uzawa algorithm are used to solve the problem. A heuristically motivated error indicator is used to perform an *hp* automatic refinement procedure. The h-version of the constructed method is extended onto two-body elastoplastic frictional contact problems and is compared to the results provided by the penalty method.

The theoretical results are supported by numerical benchmark computations.

Key words. frictional contact, interface problems, finite elements, boundary elements, FE/BE coupling, *hp*-methods, a priori error, a posteriori error, mortar, penalty, Nitsche's method

Zusammenfassung

Das Ziel dieser Dissertation ist die Konstruktion, Analyse und Implementierung von FE, BE und FE/BE Kopplungsverfahren für Interface- und Reibungskontaktprobleme mit unpassenden Diskretisierungen.

Eine neue *hp*-Nitsche FE/BE Kopplungsmethode für Interface-Probleme wird konstruiert und analysiert. Es wird bewiesen, dass das Verfahren konsistent und stabil ist, unabhängig von den Diskretisierungsparametern. Die durchgeführte a priori Fehleranalyse zeigt, dass die Methode optimal in h und suboptimal in p auf den quasiuniformen Gittern ist.

Die Frage der eindeutigen Lösbarkeit wird für das Ein-Körper-Kontaktproblem mit Tresca Reibung untersucht. Die Lösung des Ausgangsproblems mit Reibung wird durch eine Folge von reibungslosen Problemen approximiert (Uzawa Algorithmus). Die Konvergenzbedingungen für den Algorithmus werden hergeleitet. Eine *hp*-Penalty BE Methode für das Ein-Körper-Kontaktproblem wird entwickelt. Wie die a priori Fehleranalyse zeigt, muß der Penalty-Parameter ε_n proportional zu $(h/p)^{1-\epsilon}$, gewählt werden, um die optimale Konvergenzordnung (in der Energienorm) der diskreten Penalty-Lösung gegen die exakte Lösung der variationellen Ungleichung zu erreichen. Als nächstes wird ein residueller a posteriori Fehlerschätzer für die h-Versionen von FEM und BEM untersucht. Für den Fehlerschätzer, der bisher nur mit heuristischen Argumenten motiviert und ausschließlich für FEM benutzt wurde, wird bewiesen, dass er zuverlässig und effizient ist.

Ferner werden die Zwei-Körper-Kontaktprobleme mit Coulomb'scher Reibung für die h-Versionen von FE/BE und reinem BE Verfahren betrachtet. Die inkrementelle Lastaufbringung mit dem Newton-Verfahren in jedem Iterationsschritt wird eingesetzt. Die Linearisierung der Reibungskontaktterme und der Plastizitätsterme sowie die Beschreibung der Lösungsprozedur werden detailliert angegeben. Die residuelle a posteriori Fehlerabschätzung, die im Falle des Ein-Körper-Reibungskontaktproblems gewonnen wurde, wird auf ein Zwei-Körper-Reibungskontaktproblem verallgemeinert. Eine neue *hp*-Mortar Methode für das Zwei-Körper-Kontaktproblem mit Tresca Reibung wird konstruiert und die variationelle Ungleichung analysiert. Die Kontaktbedingungen sind auf der diskreten globalen Menge der Gauß-Lobatto Knoten definiert. Nichtpassende Gitter sind durch die *hp*-Mortarprojektion verbunden. Die a priori Fehleranalyse zeigt die Konvergenzordnung $\mathcal{O}((h/p)^{1/4})$ in der Energienorm unter zusätzlichen Bedingungen für die Diskretisierungsparametern. Dirichlet-zu-Neumann Verfahren und Uzawa Verfahren werden als Lösungsprozedur benutzt. Ein Fehlerindikator wird heuristisch begründet und in einer automatischen *hp* Gitterverfeinerungsprozedur eingesetzt. Die h-Version des obigen Verfahrens wird auf Zwei-Körper elastoplastische Kontaktprobleme mit Reibung generalisiert und mit den Ergebnissen des Penalty-Verfahrens verglichen.

Die theoretische Ergebnisse werden durch die Benchmark-Rechnungen unterstützt.

Schlagworte: Reibungskontakt, Interface-Probleme, finite Elemente, Randelemente, FE/BE Kopplung, *hp*-Methoden, a priori, a posteriori, Mortar, Penalty, Nitsche Verfahren

Acknowledgements

It is a great pleasure for me to thank my advisor, Prof. Dr. Ernst P. Stephan, for inspiring me to work in this area. I am very grateful to him for his intensive guidance of my work, for helpful discussions and important remarks. Also I would like to thank PD Dr. Matthias Maischak for his support and help in my theoretical investigations as well as in the programming. His software package `maiprogs` became a basis for implementation of numerical experiments, presented in the thesis.

I am very grateful to my co-advisor and my co-referee Prof. Dr. Peter Hansbo (Chalmers University of Technology, Gothenburg, Sweden) for his hospitality and numerous discussions during my visit in Gothenburg. I would like to thank my co-referee Prof. Dr. Joachim Gwinner (Universität der Bundeswehr, München, Germany) for his support and readiness to examine this thesis in a very short period of time. I would also like to thank Prof. Dr. Patrick Hild (Laboratoire de Mathématiques, Université de Franche-Comté, Besançon, France) for his comments and sending me several important papers.

Furthermore, I would like to give my thanks to the members of our working group in the Institute of Applied Mathematics, University of Hanover, for the friendly and stimulating atmosphere. My special thanks go to Dipl.-Math. Sergey Geyn for his cooperation, particularly for performing several numerical examples from Section 4.2.7. Also I am very grateful to all members of the DFG Graduiertenkolleg 615 for their collaboration and interest in my work.

Finally, I would like to thank wholeheartedly my family and give a very special thanks to my wife Natalia for her strong support and patience during my work on this thesis.

This thesis was supported by the *DFG Graduiertenkolleg 615 "Interaction of Modeling, Computation Methods and Software Concepts for Scientific-Technological Problems"*.

Hanover, May 2006 Alexey Chernov

Contents

List of Figures

List of Tables

Introduction

The last decades are the time of booming development in many branches of industry and computer technologies. A new generation of powerful computers allow to go beyond the academic examples and solve complicated high dimensional problems of industrial interest. On the other hand, there is an undisputed tendency to move as most as possible of the product design process from the experimental studies on prototypes to the numerical simulation. In spite of fast growing computer capacities, the commercial software (ABAQUS, ANSYS, etc.) often does not provide acceptable computing time or the required precision. Therefore the development of new fast convergent, accurate and efficient methods for the numerical simulation is of high importance for many branches of industry and engineering.

The physical problem is transformed into a system of partial differential equations, which can be solved with different discretization methods. The Finite Element Method (FEM) is one of the mostly used methods in modern computational mechanics. It is a well-established universal approach, which can be applied to problems with geometrical and material nonlinearities, as well as to anisotropic problems, see e.g. Braess [13], Wriggers [72], Simo and Hughes [60]. A different technique, the Boundary Element Method (BEM), has also turned out to be an accurate and effective approach for a wide range of problems (Stephan [62], Sauter and Schwab [55]), however, applying BEM is relatively seldom. In this thesis the boundary element method and FE/BE coupling method are developed for interface and frictional contact problems. In BEM, only the boundaries of the bodies are discretized. This automatically reduces the number of unknowns, but, in contrast to FEM, due to nonlocal boundary integral operators, the matrices of the problem are fully populated. There exist several methods, reducing the computational costs of standard BEM, see e.g. Maischak et al. [48], Tran and Stephan [66]. Another advantage of BEM is the significant reduction of expenses for mesh generation, since the dimension of the problem is reduced by one.

Problems of industrial interest are usually very complicated. They often have a complex geometry and varying material parameters or different material laws in different subdomains. It may be in many cases very convenient to decompose the domain of the original problem into several simpler subproblems, which are easier to handle. For example, if a large elastoplastic body is considered and the zone of the plastic deformation is small, it can be more efficient to extract a small subdomain containing this plastic zone and use the elastoplastic material law inside it. Then the complement domain can be treated as pure elastic. Another example of a strong industrial interest with natural decomposition of the original domain is the problem of sound radiation of a rolling tire, cf. Nackenhorst and von Estorff [50]. Here a multifield problem must be considered: strongly nonlinear mechanical deformation inside the tire must be coupled with the wave equation in the infinite exterior domain, simulating sound radiation in the air.

It happens very often that one discretization method is especially good for some particular material behaviour or geometry and is of no advantage in other cases. In the framework of interface problems coupling of different discretization methods, chosen to be optimal in different parts of the problem domain Ω, can be realized. For example, in the sound radiation problem of rolling tire it is natural to apply the boundary element method in the infinitely large exterior domain (air simulation), while the finite element method suites better for simulation of high nonlinear behaviour inside the tire. In this thesis a FE/BE coupling based on Nitsche's method is developed and analysed for bounded domains. With similar arguments it can be extended to the case of an unbounded BE domain.

Using independent discretizations in the different subdomains is often very convenient. It simplifies the task of global mesh generation and opens some important options such as possibility of independent automatic mesh refinement in the subdomains. Moreover, recent studies show that the high order methods, as p- and hp-FEM are quasioptimal even in case of nonmatching discretizations, cf. Ben Belgacem et al. [7]. The aim of this thesis is to construct and analyse high order methods allowing independent discretizations for interface and frictional contact problems.

As soon as a decomposition of the original domain is done, the corresponding transmission conditions, yielding continuity of displacement and traction, must be imposed on the interfaces between subdomains. There are several methods for the interface problems, known from the literature, which allow to treat nonmatching discretizations on the interface. An auxiliary variable for enforcing the interface conditions is used in the mortar method, cf. Bernardi et al. [12]. A different approach is given by interior penalty methods, see e.g. Lazarov et al. [43], where the interface conditions are enforced by introducing additional penalty terms, depending on a small penalty parameter. The drawback of this approach is that the formulation is not consistent any more, i.e. the penalty parameter must tend to zero together with the discretization parameters to guarantee convergence of the numerical solution to the exact one, which increases the condition number of the corresponding algebraic system and herewith the computational time. However, these troubles can be partially reduced with the augmented Lagrangian techniques, developed e.g. by Le Tallec and Sassi [44]. In the framework of Nitsche's methods, e.g. Becker et al. [5], Hansbo et al. [31], the additional terms enforcing consistency of the formulation are introduced. In this thesis a high order hp-Nitsche's method is constructed, analysed and applied for enforcing the interface conditions for a FE/BE coupling discretization. As the a priori error analysis shows, the method is optimal with respect to the mesh size h and is suboptimal with respect to the polynomial degree p on quasiuniform meshes.

A more general and involved class of problems, which often appear in industrial applications, are frictional contact problems. Actually, frictional contact happens in every device or during forming of any product. Such branches as automobile industry or metal forging have a number of applications, where frictional contact appears. Very often the bodies coming into contact can not be treated as rigid. Then multibody frictional contact problems must be considered. Therefore construction and developing of methods for accurate and efficient numerical simulation of frictional contact problems became a very important and fast developing part of modern applied mathematics and mechanics.

In the framework of frictional contact problems, Signorini conditions are enforced on the normal components of displacement and of boundary traction. This represents noninterpenetration of the contacting bodies. The tangential components of displacement and of boundary traction are connected with a friction law (e.g. Coulomb's friction law). Moreover, the zone of contact is not known in advance and must be obtained during the solution procedure. These nonlinearities of different types make the frictional contact problem much more complicated, then pure interface problems.

Also for frictional contact problems nonmatching discretizations are strongly desirable. Furthermore, in many cases, as for large deformation or sliding boundaries, it is the only way to avoid a time consuming remeshing procedure.

The h-version of the FEM is commonly used together with the penalty method for simulation of multibody frictional contact problems, where penalizing of penetration and regularizing of Coulomb's frictional law are performed by introducing penalty parameters, see e.g. Wriggers [72], Laursen [41]. Here we use a pure BE and a FE/BE coupling approaches with the penalty method for two-body frictional contact problem. Similarly to the interior penalty approach for interface problems, the lack of consistency of the formulation and the increase of the condition number of the algebraic system with decreasing penalty parameters are the major problems of the approach. To reduce these drawbacks the augmented Lagrangian technique was extended onto contact problems with friction, cf. Laursen and Simo [42]. The alternative mortar approach was also extended onto the h-version of FEM for frictionless and frictional contact problems in Ben Belgacem et al. [8], Hild [34], see also the paper of Hild and Laborde [35] for extension onto quadratic FEM.

The special emphasis in this thesis lies in the construction, analysis and implementation of high order FE, BE and FE/BE coupling methods for solving interface and contact problems with and without friction with nonmatched discretizations. In many cases the hp-techniques are shown to be particularly powerful, where the solution of the discrete problem converges exponentially fast towards the exact solution of the continuous problem, see the works of Szabó, Babuška [65] for FEM and of Babuška, Guo and Stephan [2] for BEM. Employing $hp-$methods to contact problems is very seldom done. The first attempt to construct an hp boundary element method for the Signorini problem, modelling unilateral contact of an elastic body and a rigid obstacle goes back to Maischak and Stephan [45], [46]. In this thesis an hp-BEM with penalty contact discretization is analysed, see also in Chernov et al. [19]. In case of multibody frictional contact independent discretizations should be used, but, as shown in this thesis, the mathematical analysis as well as the numerical implementation are automatically more complicated. In this thesis a novel approach employing hp-techniques with FE, BE or FE/BE coupling methods to contact problems with and without friction is constructed. For brevity we present here the analysis for the boundary element method only, whilst the finite element method can be treated analogously. Our method allows to handle nonmatching discretizations by using mortar technique and can be easily implemented.

A very important question in modern computational mechanics is the mesh optimization. In other words, a mesh, where the error is uniformly distributed over the elements, is preferable, since it provides the prescribed tolerance with minimal amount of computing time and memory resources. The approach is based on corresponding error estimators, which give the information about the local error between exact and discrete solution of the problem based only on the computed (and therefore known) discrete solution, cf. Verfürth [67], Bangerth and Rannacher [3], Carstensen and Stephan [17], Eck and Wendland [27]. Residual-based local error estimators for frictional contact with linear boundary elements and finite elements are obtained in this thesis. We prove that they are reliable and efficient, and therefore, fully describe the local behaviour of the error. Furthermore, based on indicators for the mortar method for interface problems, an hp-automatic mesh refinement procedure is introduced. A series of numerical experiments for FEM, BEM and FEM/BEM coupling confirms our theoretical results and shows the wide applicability and flexibility of the constructed methods.

The thesis is organized as follows. In **Chapter 1** main concepts and definitions, needed in the forthcoming analysis, are recalled. In **Chapter 2** a new hp-FE/BE coupling approach for interface problems with nonmatched meshes, based on Nitsche's method, is introduced. The a priori error analysis is carried out in case of quasiuniform meshes, which are compatible across the interface. It yields an optimal convergence rate with respect to the mesh size h and a suboptimal convergence rate with respect to the polynomial degree p. Then numerical examples are presented, confirming the theoretical analysis.

The frictional contact problem between an elastic body and a rigid obstacle is addressed in **Chapter 3**. First, the boundary integral formulation is given for the frictional contact problem with Tresca's law of friction. It is shown that the resulting variational inequality has a unique solution. Then, a mixed formulation, containing an auxiliary variable, which corresponds to the tangential traction, is derived, and equivalence between the mixed formulation and the original variational inequality is shown. The solution of the mixed formulation is approximated with a sequence of solutions of suitably defined frictionless problems with updated right-hand side. It is proven that this sequence converges in the energy norm to the exact solution of the original frictional contact problem. This solution procedure can be treated as an Uzawa algorithm. We prove that the algorithm converges for sufficiently small damping parameter. The results of this section are also employed in the Chapter 4, Section 4.3 in construction of the solution algorithm for *hp*-mortar BEM for two-body frictional contact problems.

Then the *hp*-penalty approach for the frictionless contact problem is formulated and investigated. An a priori error analysis, including treatment of the consistency and approximation error, is carried out. The convergence rate of order $\mathcal{O}((h/p)^{1-\epsilon})$ in the energy norm is obtained, if the exact solution of the original variational inequality formulation $\boldsymbol{u}$ lies in $\tilde{\boldsymbol{H}}^{3/2}(\Sigma)$ and the penalty parameter $\varepsilon_n \gtrsim (h/p)^{1-\epsilon}$. Here $\epsilon > 0$ is some fixed small parameter.

Further, the question of automatic mesh refinement is investigated in the framework of the *h*-version of penalty FEM and BEM for a one-body frictional contact problem. The error measure, based on the energy norm of the solution, combined with normal and tangential contact terms is introduced for FEM and BEM. Then, the local residual-based error estimators are derived for both FEM and BEM and their reliability and efficiency are shown. It is worth to say that the similar error indicators were motivated so far only with heuristical arguments and only for FEM, see e.g. Wriggers [72]. An automatic mesh refinement procedure, based on these indicators is introduced. Finally the suggested method is illustrated on several numerical examples.

Chapter 4 is devoted to two-body contact problems with friction. First, piecewise linear boundary elements and a corresponding FE/BE coupling on nonmatching meshes with penalty method is considered in the framework of elastoplastic frictional contact problems. The incremental loading method combined with Newton's method and return mapping algorithm is applied to solve the problem. An implicit Euler scheme for both plasticity and frictional contact is applied in case of FE/BE coupling. In the pure BEM case, an explicit Euler scheme for plasticity and an implicit scheme for frictional contact are used. Linearization of normal, tangential contact terms and of plasticity terms are presented in detail. The a posteriori error estimate for one-body frictional contact, derived in Chapter 3, is extended to the two-body case. The above mentioned methods are demonstrated by a number of numerical examples.

The direct application of the *hp*-penalty method to two-body frictional contact problems on nonmatched meshes seems to be problematic, due to the required pointwise contact. Therefore, the *hp*-mortar method is constructed, which does not have this requirement. Here the contact conditions are defined in the weak sense. The contact constraints are imposed on the discrete global set of affinely transformed Gauss-Lobatto points on the individual elements. The data transfer is realized in terms of the mortar projection. The problem is reformulated as a variational inequality of the second kind with the Steklov-Poincaré operator over a convex cone of admissible solutions. We obtain an upper error bound in the energy norm. Due to the nonconformity of our approach, the error is decomposed into the approximation error and the consistency error. Finally, we show that the discrete solution converges to the exact solution as $\mathcal{O}((h/p)^{1/4})$ in the energy norm. under additional assumptions on the discretization parameters. We solve the discrete problem with a Dirichlet-to-Neumann algorithm. The original two-body formulation is rewritten as a one-body contact problem and a one-body Neumann problem (see also Chernov et al. [18]). Then the global problem is solved by fixed point iterations. An alternative approach is the Uzawa algorithm, which consists of solving two independent one-body problems with a subsequent update for the contact traction. The error indicator obtained for the pure FE approach for interface problems by Wohlmuth [70] is applied here to frictional contact problems (also with boundary elements) and is employed in an automatic mesh refinement procedure together with the three-step *hp*-refinement algorithm from Maischak and Stephan [47]. Finally, the *h*-version of the suggested approach is generalized onto elastoplastic two-body frictional contact problems. Then numerical examples are given, which underline the proposed approach.

The analysis, presented in this thesis is mostly restricted to the two-dimensional case. However, many results can be directly applied in the three-dimensional case, when product meshes are used.

1 Foundations

In this section we recall some important and often used concepts and properties from functional analysis and the theory of boundary elements. First the framework of Sobolev spaces is considered. Then we turn to the boundary integral operators and their properties. The discretization of the boundary integral operators is also described.

1.1 Sobolev spaces

Here we briefly introduce the main concepts and definitions connected with the Sobolev spaces, see e.g. [1], [61].

Let $\Omega \subset \mathbb{R}^d$ some bounded, simply connected domain, $d \in \{1, 2, 3\}$. Let $\Gamma = \partial\Omega$ be its boundary. We define with $C^k(\Omega)$, $k \in \mathbb{N}_0$, the set of all k-times continuously differentiable functions $u : \Omega \to \mathbb{R}$ with the norm

$$||u||_{C^k(\Omega)} := \sum_{|\alpha| \leq k} \sup_{x \in \Omega} |D^\alpha u(x)|,$$

where $\alpha = (\alpha_1, ..., \alpha_d)$ is a multiindex, $|\alpha| := \alpha_1 + \cdots + \alpha_d$ and the partial derivative of order α is given by

$$D^\alpha u(x) := \left(\frac{\partial}{\partial x_1}\right)^{\alpha_1} ... \left(\frac{\partial}{\partial x_d}\right)^{\alpha_d} u(x_1, ..., x_d)$$

The support of a function u is given by $\text{supp}\,(u) := \overline{\{x \in \Omega : u(x) \neq 0\}}$. We define the set of all k-times continuously differentiable functions $u : \Omega \to \mathbb{R}$ with the compact support by

$$C_0^k(\Omega) := \{u \in C^k(\Omega) : \text{supp}\,(u) \subset \Omega\}.$$

Corresponding spaces of infinitely differentiable functions we denote with $C^\infty(\Omega)$ and $C_0^\infty(\Omega)$. For $k \in \mathbb{N}_0, \kappa \in (0, 1]$ we introduce the space of Hölder-continuous functions $C^{k,\kappa}(\Omega)$ on Ω with the norm

$$||u||_{C^{k,\kappa}(\Omega)} := ||u||_{C^k(\Omega)} + \sum_{|\alpha|=k} \sup_{\substack{x, y \in \Omega, \\ x \neq y}} \frac{|D^\alpha u(x) - D^\alpha u(y)|}{|x - y|^\kappa}.$$

The function $u : \Omega \to \mathbb{R}$ is called Lipschitz-continuous, if $u \in C^{0,1}(\Omega)$. The boundary $\Gamma = \partial\Omega$ is called Lipschitz, if it can be piecewise represented with a Lipschitz-continuous parameterization. In that case the domain Ω is also called a Lipschitz domain.

Further, we define by $L_2(\Omega)$ the space of all Lebesgue-measurable functions defined in Ω, which are square-integrable. The corresponding norm is given by

$$||u||_{L_2(\Omega)} := \left(\int_\Omega |u(x)|^2 \, dx \right)^{1/2}.$$

We define for $k \in \mathbb{N}_0$ a norm

$$||u||_{H^k(\Omega)} := \left(\sum_{|\alpha| \le k} ||D^\alpha u||^2_{L_2(\Omega)} \right)^{1/2}$$

and the Sobolev spaces with a nonnegative integer parameter $k \in \mathbb{N}_0$ as the closure of the space $\{u \in C^\infty(\Omega) : ||u||_{H^k(\Omega)} < \infty\}$ with respect to $|| \cdot ||_{H^k(\Omega)}$, i.e.

$$H^k(\Omega) := \overline{C^\infty(\Omega)}^{||\cdot||_{H^k(\Omega)}}.$$

This definition can be generalized to the case of Sobolev spaces with real positive parameter $s := k + r$, $k \in \mathbb{N}_0$, $r \in (0, 1)$. The corresponding Sobolev-Slobodeckii norm is given by

$$||u||_{H^s(\Omega)} := \left(||u||^2_{H^k(\Omega)} + |u|^2_{H^r(\Omega)} \right)^{1/2},$$

with the half-norm

$$|u|_{H^r(\Omega)} := \left(\sum_{|\alpha| = k} \int_\Omega \int_\Omega \frac{|D^\alpha u(x) - D^\alpha u(y)|^2}{|x - y|^{d+2r}} dx dy \right)^{1/2}.$$

We define the L_2 scalar product on Ω by

$$(u, v)_\Omega := \int_\Omega u(x) v(x) \, dx.$$

In the BE analysis the Sobolev spaces on the boundary of the domain $\Gamma = \partial\Omega$ are of special meaning. The L_2-space on Γ is defined similarly to the space $L_2(\Omega)$ and equipped with the norm

$$||u||_{L_2(\Gamma)} := \left(\int_\Gamma |u(x)|^2 \, ds_x \right)^{1/2}.$$

Here it is assumed, that there exists a piecewise parameterization of the boundary

$$\chi : \xi \mapsto x, \quad \xi = (\xi_1, \dots, \xi_{d-1}) \in \mathfrak{V}, \quad x \in \Gamma.$$

The definition of higher order Sobolev spaces on Γ requires the partial derivatives with respect to the parameters ξ

$$\partial^\alpha u(x) := \left(\frac{\partial}{\partial \xi_1}\right)^{\alpha_1} \dots \left(\frac{\partial}{\partial \xi_{d-1}}\right)^{\alpha_{d-1}} u(x(\xi_1, \dots, \xi_{d-1})), \qquad x \in \Gamma.$$

It should be noted, that existence of the derivative $\partial^\alpha u(x)$ with $|\alpha| \leq l$ depends on the smoothness of Γ. In particular, $\Gamma \in C^{l-1,1}(\mathfrak{V})$ provides existence of $\partial^\alpha u(x)$ for $|\alpha| \leq l$. Now we can define the Sobolev spaces on the boundary of order $k \in \mathbb{N}_0$, $k \leq l$ as the closure of the space $\{u \in C^\infty(\Gamma) : ||u||_{H^k(\Gamma)} < \infty\}$ with respect to the norm

$$||u||_{H^k(\Gamma)} := \left(\sum_{|\alpha| \leq k} ||\partial^\alpha u||^2_{L_2(\Gamma)}\right)^{1/2}.$$

The generalization onto the case of the Sobolev spaces of real positive order $s = k + r$, where $k \in \mathbb{N}_0$, $r \in (0,1)$ is realized by the corresponding Sobolev-Slobodeckii norm

$$||u||_{H^s(\Gamma)} := \left(||u||^2_{H^k(\Gamma)} + |u|^2_{H^r(\Gamma)}\right)^{1/2}$$

with the half-norm

$$|u|_{H^r(\Gamma)} := \left(\sum_{|\alpha|=k} \int_\Gamma \int_\Gamma \frac{|\partial^\alpha u(x) - \partial^\alpha u(y)|^2}{|x-y|^{d-1+2r}}\, ds_x ds_y\right)^{1/2}.$$

Employing the dual product

$$\langle u, v \rangle_\Gamma := \int_\Gamma u(x) v(x)\, ds_x$$

we introduce the Sobolev spaces $H^{-s}(\Gamma)$ of negative order for $s \in (0, l]$ as the dual spaces to $H^s(\Gamma)$

$$H^{-s}(\Gamma) = (H^s(\Gamma))', \qquad s < 0,$$

with the norm

$$||u||_{H^{-s}(\Gamma)} := \sup_{0 \neq v \in H^s(\Gamma)} \frac{\langle u, v \rangle_\Gamma}{||u||_{H^s(\Gamma)}}.$$

In the forthcoming analysis we will also use the Sobolev spaces, defined on the part of the boundary. Let $\Gamma_0 \subset \Gamma$ be an open subset of the boundary Γ. We define Sobolev spaces of positive order $s \in \mathbb{R}_{\geq 0}$, $s \in (0, l]$ by

$$H^s(\Gamma_0) := \{u : \exists v \in H^s(\Gamma) : u = v|_{\Gamma_0}\},$$
$$\tilde{H}^s(\Gamma_0) := \{u : \exists v \in H^s(\Gamma) : u = v|_{\Gamma_0},\ \text{supp}\,(v) \subset \overline{\Gamma}_0\}$$

with the standard norms

$$||u||_{H^s(\Gamma_0)} := \inf_{\substack{v \in H^s(\Gamma) \\ v|_{\Gamma_0} = u}} ||v||_{H^s(\Gamma)},$$
$$||u||_{\tilde{H}^s(\Gamma_0)} := ||u_0||_{H^s(\Gamma)},$$

where u_0 is the extension of u onto Γ by zero. The Sobolev spaces of negative order on Γ_0 are defined by duality again

$$H^{-s}(\Gamma_0) := (\tilde{H}^s(\Gamma_0))', \qquad \tilde{H}^{-s}(\Gamma_0) := (H^s(\Gamma_0))', \qquad s \in (0, l]. \tag{1.1}$$

Remark 1.1.1. *The notation $\tilde{H}^s(\Gamma_0)$ is commonly used in the boundary element literature. In the finite element literature the notation $H^s_{00}(\Gamma_0)$ is used. Then the different notation for the dual spaces is used (see e.g. [6]).*

$$H^{-s}(\Gamma_0) := (H^s(\Gamma_0))', \qquad H^{-s}_{00}(\Gamma_0) := (H^s_{00}(\Gamma_0))', \qquad s > 0.$$

We will use notations (1.1).

Remark 1.1.2. *The boundary Γ of a polygonal domain Ω belongs to the class $C^{0,1}$. Nethertheless, following Costabel and Stephan [22], Sobolev spaces $H^s(\Gamma)$ with $s > 1$ can be also defined due to Grisvard, [22, Lemma 2.7]*

For the spaces of vector-valued functions we use the bold symbols, e.g.

$$\boldsymbol{H}^s(\Gamma) := [H^s(\Gamma)]^d$$

stands for the space of d-dimensional vectors, which components lie in space $H^s(\Gamma)$.

1.2 Boundary integral operators for elliptic problems

In this section we will introduce the boundary integral operators, arising in the boundary formulation of the elliptic boundary value problems. We consider the Poisson's equation and the equations of linear elasticity. The fundamental solutions of Laplace and Lamé operators give rise to the corresponding representation formulae, which allows to transform the domain formulation to the boundary.

The scalar Poisson's equation in a domain $\Omega \subset \mathbb{R}^d$ with piecewise Lipschitz boundary $\Gamma = \partial\Omega$ is given by

$$-\Delta u(\boldsymbol{x}) = f(\boldsymbol{x}), \qquad \boldsymbol{x} \in \Omega,$$

where Δ is the Laplace operator, $u : \Omega \to \mathbb{R}$ is unknown and the volume force $f : \Omega \to \mathbb{R}$ is prescribed. The equations of linear elasticity are

$$-\Delta^* \boldsymbol{u}(\boldsymbol{x}) = \boldsymbol{f}(\boldsymbol{x}), \qquad \boldsymbol{x} \in \Omega.$$

Here $\boldsymbol{u} : \Omega \to \mathbb{R}^d$ is unknown and the volume force $\boldsymbol{f} : \Omega \to \mathbb{R}^d$ is known in advance. Further down, we will omit the space variable x, where it does not lead to misunderstanding. The Lamé operator Δ^* is given by

$$\Delta^* \boldsymbol{u} := (\overline{\lambda} + \overline{\mu}) \operatorname{grad} \operatorname{div} \boldsymbol{u} + \overline{\mu} \Delta \boldsymbol{u},$$

where $\overline{\lambda}$ and $\overline{\mu}$ are the Lamé elasticity coefficients, if $d = 3$, or modified Lamé elasticity coefficients in case $d = 2$ (see e.g. [61]). It can also be expressed in terms of the stress tensor σ as

$$\Delta^* \boldsymbol{u} = \operatorname{div} \sigma(\boldsymbol{u}),$$

where the Hook's law represents the stress-strain relationship

$$\sigma(\boldsymbol{u}) := \overline{\lambda} \operatorname{tr} \varepsilon(\boldsymbol{u}) + 2\overline{\mu}\varepsilon(\boldsymbol{u})$$

and the linearized strain tensor ε is the symmetrized gradient of $\boldsymbol{u}$, i.e.

$$\varepsilon(\boldsymbol{u}) := \frac{1}{2}(\nabla \boldsymbol{u} + (\nabla \boldsymbol{u})^T).$$

Let $\boldsymbol{G}(\boldsymbol{x}, \boldsymbol{y})$ be the fundamental solution of the operator L, $L = \Delta$ or Δ^*, i.e.

$$\int_\Omega L_y \boldsymbol{G}(\boldsymbol{x}, \boldsymbol{y}) \cdot \boldsymbol{u}(\boldsymbol{y})\, d\boldsymbol{y} = \boldsymbol{u}(\boldsymbol{x}), \qquad \boldsymbol{x} \in \Omega.$$

The fundamental solution for the Laplace equation is given by

$$\boldsymbol{G}(\boldsymbol{x}, \boldsymbol{y}) = \begin{cases} -\dfrac{1}{2\pi} \log |\boldsymbol{x} - \boldsymbol{y}|, & \text{for } d = 2, \\ \dfrac{1}{4\pi} \dfrac{1}{|\boldsymbol{x} - \boldsymbol{y}|}, & \text{for } d = 3 \end{cases}$$

and the fundamental solution for the Lamé equation is given by

$$\boldsymbol{G}(\boldsymbol{x}, \boldsymbol{y}) = \begin{cases} \dfrac{\overline{\lambda} + 3\overline{\mu}}{4\pi\overline{\mu}(\overline{\lambda} + 2\overline{\mu})} \left\{ \log \dfrac{1}{|\boldsymbol{x} - \boldsymbol{y}|} \boldsymbol{I} + \dfrac{\overline{\lambda} + \overline{\mu}}{\overline{\lambda} + 3\overline{\mu}} \dfrac{(\boldsymbol{x} - \boldsymbol{y}) \otimes (\boldsymbol{x} - \boldsymbol{y})}{|\boldsymbol{x} - \boldsymbol{y}|^2} \right\}, & \text{for } d = 2, \\ \dfrac{\overline{\lambda} + 3\overline{\mu}}{8\pi\overline{\mu}(\overline{\lambda} + 2\overline{\mu})} \left\{ \dfrac{1}{|\boldsymbol{x} - \boldsymbol{y}|} \boldsymbol{I} + \dfrac{\overline{\lambda} + \overline{\mu}}{\overline{\lambda} + 3\overline{\mu}} \dfrac{(\boldsymbol{x} - \boldsymbol{y}) \otimes (\boldsymbol{x} - \boldsymbol{y})}{|\boldsymbol{x} - \boldsymbol{y}|^3} \right\}, & \text{for } d = 3. \end{cases}$$

(cf. [61]) We use here the bold symbols also in the scalar case of the Laplace operator, treating the scalars as vectors of the dimension one. Then the second Green's formula provides the *representation formula*: for arbitrary $\boldsymbol{x} \in \Omega \setminus \partial\Omega$

$$\begin{aligned} \boldsymbol{u}(\boldsymbol{x}) = \int_\Gamma \boldsymbol{G}(\boldsymbol{x}, \boldsymbol{y}) \cdot \mathcal{T}_{n_y} \boldsymbol{u}(\boldsymbol{y})\, ds_y - \int_\Gamma \mathcal{T}_{n_y} \boldsymbol{G}(\boldsymbol{x}, \boldsymbol{y}) \cdot \boldsymbol{u}(\boldsymbol{y})\, ds_y \\ + \int_\Omega \boldsymbol{G}(\boldsymbol{x}, \boldsymbol{y}) \cdot \boldsymbol{f}(\boldsymbol{y})\, ds_y. \end{aligned} \tag{1.2}$$

Here $\mathcal{T}_{n_y}$ stands for the traction operator with respect to the $\boldsymbol{y}$-variable and it is given by $\mathcal{T}_{n_y} \boldsymbol{u}(\boldsymbol{y}) := \nabla \boldsymbol{u}(\boldsymbol{y}) \cdot \boldsymbol{n}(\boldsymbol{y})|_\Gamma$ in the Laplace case and by $\mathcal{T}_{n_y} \boldsymbol{u}(\boldsymbol{y}) := \sigma(\boldsymbol{u}(\boldsymbol{y})) \cdot \boldsymbol{n}(\boldsymbol{y})|_\Gamma$ in the Lamé case. The operator $\mathcal{T}_n$ is also called the inner conormal derivative and is denoted by γ_1^{int}. The inner trace operator $(\cdot)|_\Gamma$ is denoted also by γ_0^{int}, see [61]. The representation formula (1.2) is also called the *Somigliana's identity* in case of Lamé equations.

Remark 1.2.1. *It follows from (1.2), that for the solution of Poisson's equation or of the problem of linear elastostatic, it is sufficient to find the complete boundary data, i.e. the unknown $\boldsymbol{u}$ and its boundary traction $\mathcal{T}_n\boldsymbol{u}$. Then the values inside the domain can be obtained with (1.2).*

Then taking a limit $\Omega \setminus \partial\Omega \ni \boldsymbol{x} \to \Gamma$ we obtain the well-known system of boundary integral equations for $\boldsymbol{\phi} := \mathcal{T}_n\boldsymbol{u}$

$$\begin{pmatrix} \boldsymbol{u} \\ \boldsymbol{\phi} \end{pmatrix} = \begin{pmatrix} 1/2 - K & V \\ W & 1/2 + K' \end{pmatrix} \begin{pmatrix} \boldsymbol{u} \\ \boldsymbol{\phi} \end{pmatrix} + \begin{pmatrix} N_0\boldsymbol{f} \\ N_1\boldsymbol{f} \end{pmatrix}, \tag{1.3}$$

where the single layer potential V, the double layer potential K, the adjoint double layer potential K' and hypersingular integral operator are given for $\boldsymbol{x} \in \Gamma$ by

$$\begin{aligned} V\boldsymbol{\phi}(\boldsymbol{x}) &:= \int_\Gamma \boldsymbol{G}(\boldsymbol{x},\boldsymbol{y}) \cdot \boldsymbol{\phi}(\boldsymbol{y})\, ds_y, \\ K\boldsymbol{u}(\boldsymbol{x}) &:= \int_\Gamma (\mathcal{T}_{n_y}\boldsymbol{G}(\boldsymbol{x},\boldsymbol{y})^T) \cdot \boldsymbol{u}(\boldsymbol{y})\, ds_y, \\ K'\boldsymbol{\phi}(\boldsymbol{x}) &:= \mathcal{T}_{n_x}\int_\Gamma \boldsymbol{G}(\boldsymbol{x},\boldsymbol{y}) \cdot \boldsymbol{\phi}(\boldsymbol{y})\, ds_y, \\ W\boldsymbol{u}(\boldsymbol{x}) &:= -\mathcal{T}_{n_x}\int_\Gamma (\mathcal{T}_{n_y}\boldsymbol{G}(\boldsymbol{x},\boldsymbol{y})^T) \cdot \boldsymbol{u}(\boldsymbol{y})\, ds_y \end{aligned} \tag{1.4}$$

and the Newton potentials N_0, N_1 are given for $\boldsymbol{x} \in \Gamma$ by

$$\begin{aligned} N_0\boldsymbol{f}(\boldsymbol{x}) &:= \int_\Gamma \boldsymbol{G}(\boldsymbol{x},\boldsymbol{y}) \cdot \boldsymbol{f}(\boldsymbol{y})\, ds_y, \\ N_1\boldsymbol{f}(\boldsymbol{x}) &:= \mathcal{T}_{n_x}\int_\Gamma \boldsymbol{G}(\boldsymbol{x},\boldsymbol{y}) \cdot \boldsymbol{f}(\boldsymbol{y})\, ds_y. \end{aligned}$$

The following well-known properties will we widely used in the forthcoming analysis.

Lemma 1.2.1. *[21] Let $\Gamma := \partial\Omega$ be the boundary of a Lipschitz domain Ω. Then the integral operators*

$$\begin{aligned} V &: \boldsymbol{H}^{-1/2+s}(\Gamma) \to \boldsymbol{H}^{1/2+s}(\Gamma), \\ K &: \boldsymbol{H}^{1/2+s}(\Gamma) \to \boldsymbol{H}^{1/2+s}(\Gamma), \\ K' &: \boldsymbol{H}^{-1/2+s}(\Gamma) \to \boldsymbol{H}^{-1/2+s}(\Gamma), \\ W &: \boldsymbol{H}^{1/2+s}(\Gamma) \to \boldsymbol{H}^{-1/2+s}(\Gamma), \end{aligned}$$

are bounded for all $s \in [-1/2, 1/2]$, i.e. there exists constants $C_V, C_K, C_{K'}, C_W > 0$ such that

$$\begin{aligned} ||V\boldsymbol{\phi}||_{\boldsymbol{H}^{1/2+s}(\Gamma)} &\le C_V ||\boldsymbol{\phi}||_{\boldsymbol{H}^{-1/2+s}(\Gamma)}, \qquad & ||K'\boldsymbol{\phi}||_{\boldsymbol{H}^{-1/2+s}(\Gamma)} &\le C_{K'} ||\boldsymbol{\phi}||_{\boldsymbol{H}^{-1/2+s}(\Gamma)}, \\ ||K\boldsymbol{u}||_{\boldsymbol{H}^{1/2+s}(\Gamma)} &\le C_K ||\boldsymbol{u}||_{\boldsymbol{H}^{1/2+s}(\Gamma)}, \qquad & ||W\boldsymbol{u}||_{\boldsymbol{H}^{-1/2+s}(\Gamma)} &\le C_W ||\boldsymbol{u}||_{\boldsymbol{H}^{1/2+s}(\Gamma)}. \end{aligned}$$

Lemma 1.2.2. *(see e.g. [61]) Let* $\Gamma := \partial\Omega \subset \mathbb{R}^d$ *be the boundary of a Lipschitz domain* Ω*. Let* $cap(\Omega) < 1$ *in case* $d = 2$*. Then the single layer potential* V *is* $\boldsymbol{H}^{-1/2}(\Gamma)$*-elliptic, i.e. there exists a constant* $c_V > 0$*, such that*

$$\langle V\boldsymbol{\phi}, \boldsymbol{\phi}\rangle_\Gamma \geq c_V ||\boldsymbol{\phi}||^2_{\boldsymbol{H}^{-1/2}(\Gamma)}, \qquad \forall \boldsymbol{\phi} \in \boldsymbol{H}^{-1/2}(\Gamma).$$

Since the single layer potential $V : \boldsymbol{H}^{-1/2}(\Gamma) \to \boldsymbol{H}^{1/2}(\Gamma)$ is bounded and elliptic, the Lax-Milgram lemma yields that its inverse operator $V^{-1} : \boldsymbol{H}^{1/2}(\Gamma) \to \boldsymbol{H}^{-1/2}(\Gamma)$ exists and is bounded, i.e.

$$||V^{-1}\boldsymbol{u}||_{\boldsymbol{H}^{-1/2}(\Gamma)} \leq c_V^{-1} ||\boldsymbol{u}||_{\boldsymbol{H}^{1/2}(\Gamma)}, \qquad \forall \boldsymbol{u} \in \boldsymbol{H}^{-1/2}(\Gamma),$$

where c_V is the ellipticity constant of V.

Lemma 1.2.3. *(see e.g. [61]) Let* $\Gamma := \partial\Omega \subset \mathbb{R}^d$ *be the boundary of a Lipschitz domain* Ω *and* $\Gamma_0 \subset \Gamma$*. Then the hypersingular operator* W *is* $\tilde{\boldsymbol{H}}^{1/2}(\Gamma_0)$*-elliptic, i.e. there exists a constant* $c_W > 0$*, such that*

$$\langle W\boldsymbol{u}, \boldsymbol{u}\rangle_\Gamma \geq c_W ||\boldsymbol{u}||^2_{\tilde{\boldsymbol{H}}^{1/2}(\Gamma_0)}, \qquad \forall \boldsymbol{u} \in \tilde{\boldsymbol{H}}^{1/2}(\Gamma_0).$$

1.3 Symmetric boundary element formulation for mixed boundary value problems

It follows from (1.3), that the traction variable $\boldsymbol{\phi} := \mathcal{T}\boldsymbol{u}$ can be represented in terms of $\boldsymbol{u}$ and the volume force $\boldsymbol{f}$. Since $V : \boldsymbol{H}^{-1/2}(\Gamma) \to \boldsymbol{H}^{1/2}(\Gamma)$ is invertible (in case $cap(\Gamma) < 1$, the case of general Γ can be treated with the scaling arguments) we obtain

$$\boldsymbol{\phi} = V^{-1}(K + 1/2)\boldsymbol{u} - V^{-1}N_0\boldsymbol{f},$$
$$\boldsymbol{\phi} = W\boldsymbol{u} + (K' + 1/2)\boldsymbol{\phi} + N_1\boldsymbol{f}$$

and therefore

$$\boldsymbol{\phi} = S\boldsymbol{u} - N\boldsymbol{f}, \tag{1.5}$$

with the symmetric Steklov-Poincaré operator S and the Newton potential are given by

$$S := W + (K' + 1/2)V^{-1}(K + 1/2) \tag{1.6}$$

$$N := (K' + 1/2)V^{-1}N_0 - N_1. \tag{1.7}$$

The alternative representation is

$$\boldsymbol{\phi} = T\boldsymbol{u} - V^{-1}N_0\boldsymbol{f},$$

where the nonsymmetric Steklov-Poincaré operator T is given by

$$T := V^{-1}(K + 1/2). \tag{1.8}$$

Lemmas 1.2.1 - 1.2.3 for boundary integral operators yield the following lemma.

Lemma 1.3.1. *Let* $\Gamma := \partial\Omega \subset \mathbb{R}^d$ *be the boundary of a Lipschitz domain* Ω *and* $\Gamma_0 \subset \Gamma$. *Then the Steklov-Poincaré operator* $S : \boldsymbol{H}^{1/2}(\Gamma) \to \boldsymbol{H}^{-1/2}(\Gamma)$ *is continuous and* $\tilde{\boldsymbol{H}}^{1/2}(\Gamma_0)$*-elliptic, i.e. there exists* $c_S, C_S > 0$ *such that*

$$||S\boldsymbol{u}||_{\boldsymbol{H}^{-1/2}(\Gamma)} \leq C_S ||\boldsymbol{u}||_{\boldsymbol{H}^{1/2}(\Gamma)}, \qquad \forall \boldsymbol{u} \in \boldsymbol{H}^{1/2}(\Gamma), \tag{1.9}$$

$$\left\langle S\boldsymbol{u}, \boldsymbol{u} \right\rangle_\Gamma \geq c_S ||\boldsymbol{u}||^2_{\tilde{\boldsymbol{H}}^{1/2}(\Gamma_0)}, \qquad \forall \boldsymbol{u} \in \tilde{\boldsymbol{H}}^{1/2}(\Gamma_0). \tag{1.10}$$

Note that due to (1.5), if $\boldsymbol{f} \equiv 0$, then S maps $\boldsymbol{u}$ to its traction. Therefore the Steklov-Poincaré operator is sometimes called the Dirichlet-to-Neumann mapping. Furthermore, in case $\boldsymbol{f} \equiv 0$ there holds

$$S = T.$$

Recalling the definition of the internal trace operator γ_0^{int} and of the internal conormal derivative γ_1^{int} the operators S and T can be rewritten for $\boldsymbol{f} \equiv 0$ as

$$S = T = \gamma_1^{int}(\gamma_0^{int})^{-1},$$

when γ_0^{int} is invertible.

Assume that we have a mixed boundary value problem in Ω, i.e. its boundary $\Gamma = \partial\Omega$ is divided into two disjoint parts $\Gamma = \Gamma_D \cup \Gamma_N$ and on the part Γ_D we have some prescribed displacements $\hat{\boldsymbol{u}}$ and the part Γ_N is subjected to some given tractions $\hat{\boldsymbol{t}}$. The weak formulation, corresponding to (1.5) is obtained by testing it with some test-function $\boldsymbol{v} \in \tilde{\boldsymbol{H}}^{1/2}(\Gamma_N)$ which provides the problem of finding $\boldsymbol{u} \in \{\boldsymbol{w} \in \boldsymbol{H}^{1/2}(\Gamma) : \boldsymbol{w} = \hat{\boldsymbol{u}} \text{ on } \Gamma_D\}$, such that

$$\left\langle S\boldsymbol{u}, \boldsymbol{v} \right\rangle_{\Gamma_N} = \left\langle \hat{\boldsymbol{t}}, \boldsymbol{v} \right\rangle_{\Gamma_N} + \left\langle N\boldsymbol{f}, \boldsymbol{v} \right\rangle_{\Gamma_N}, \qquad \forall \boldsymbol{v} \in \tilde{\boldsymbol{H}}^{1/2}(\Gamma_N). \tag{1.11}$$

1.4 Discretization of the Steklov-Poincaré operator

While discretizing the formulation (1.11) we meet a problem of computing of V^{-1}, which, in general, is not explicitly known. To overcone this difficulty, the approximation $\hat{S}$ of the Steklov-Poincaré operator is constructed. We introduce a mesh $\mathcal{T}_h$ on Γ, i.e.

$$\overline{\Gamma} = \bigcup_{I \in \mathcal{T}_h} \overline{I}.$$

Based on $\mathcal{T}_h$ we define the piecewise polynomial space of discrete tractions

$$\boldsymbol{\mathcal{W}}_{hp} := \{\boldsymbol{\Phi} \in \boldsymbol{L}_2(\Gamma) : \forall I \in \mathcal{T}_h, \boldsymbol{\Phi}|_I \in [\mathcal{P}_{p_I - 1}(I)]^{d-1}\} \subset \boldsymbol{H}^{-1/2}(\Gamma),$$

where $\mathcal{P}_{p_I}(I)$ stands for the space of all polynomials on I with degree not exceeding $p_I - 1$. We introduce an auxiliary problem of finding $\boldsymbol{\Psi} \in \boldsymbol{\mathcal{W}}_{hp}$, such that

$$\left\langle V\boldsymbol{\Psi}, \boldsymbol{\Phi} \right\rangle_\Gamma = \left\langle (K + 1/2)\boldsymbol{u}, \boldsymbol{\Phi} \right\rangle_\Gamma \qquad \forall \boldsymbol{\Phi} \in \boldsymbol{\mathcal{W}}_{hp}$$

for some $\boldsymbol{u}$. Then the approximation $\hat{S}$ of the Steklov-Poincaré operator is given by

$$\hat{S}\boldsymbol{u} := W\boldsymbol{u} + (K' + 1/2)\,\boldsymbol{\Psi}.$$

Lemma 1.4.1. *Let $\Gamma := \partial\Omega \subset \mathbb{R}^d$ be the boundary of a Lipschitz domain Ω and $\Gamma_0 \subset \Gamma$. Then the approximation of the Steklov-Poincaré operator $\hat{S} : \boldsymbol{H}^{1/2}(\Gamma) \to \boldsymbol{H}^{-1/2}(\Gamma)$ is continuous and $\tilde{\boldsymbol{H}}^{1/2}(\Gamma_0)$-elliptic, i.e. there exists $c_{\hat{S}}, C_{\hat{S}} > 0$ such that*

$$||\hat{S}\boldsymbol{u}||_{\boldsymbol{H}^{-1/2}(\Gamma)} \le C_{\hat{S}}||\boldsymbol{u}||_{\boldsymbol{H}^{1/2}(\Gamma)}, \qquad \forall \boldsymbol{u} \in \boldsymbol{H}^{1/2}(\Gamma), \tag{1.12}$$

$$\left\langle \hat{S}\boldsymbol{u}, \boldsymbol{u} \right\rangle_\Gamma \ge c_{\hat{S}}||\boldsymbol{u}||^2_{\tilde{\boldsymbol{H}}^{1/2}(\Gamma_0)}, \qquad \forall \boldsymbol{u} \in \tilde{\boldsymbol{H}}^{1/2}(\Gamma_0). \tag{1.13}$$

We define the operator $\hat{E} := S - \hat{S}$, reflecting the consistency error in the approximation of the Steklov-Poincaré operator.

Lemma 1.4.2. *[46, Lemma 15] The operator $\hat{E}$ is bounded, i.e. there exists $C_{\hat{E}} > 0$ such that*

$$||\hat{E}\boldsymbol{u}||_{\boldsymbol{H}^{-1/2}(\Gamma)} \le C_{\hat{E}}||\boldsymbol{u}||_{\boldsymbol{H}^{1/2}(\Gamma)}.$$

Furthermore there exists a constant $C_0 > 0$, such that

$$||\hat{E}\boldsymbol{u}||_{\boldsymbol{H}^{-1/2}(\Gamma)} \le C_0 \inf_{\boldsymbol{\Phi} \in \boldsymbol{\mathcal{W}}_{hp}} ||V^{-1}(K + 1/2)\boldsymbol{u} - \boldsymbol{\Phi}||_{\boldsymbol{H}^{-1/2}(\Gamma)}.$$

Hence, the consistency error in the approximation of S is optimally bounded and therefore makes no affect to the convergence rate of the corresponding method.

In order to discretize the other boundary integral operators we introduce the continuous piecewise polynomial space for the discretization of $\boldsymbol{u}$.

$$\boldsymbol{\mathcal{V}}_{hp} := \{\boldsymbol{U} \in \boldsymbol{C}(\Gamma) : \forall I \in \mathcal{T}_h,\, \boldsymbol{\Phi}|_I \in [\mathcal{P}_{p_I}(I)]^{d-1}\} \subset \boldsymbol{H}^{1/2}(\Gamma).$$

In general, $\boldsymbol{\mathcal{V}}_{hp}$ can be defined over some other mesh, different from $\mathcal{T}_h$, but for the sake of simplicity we use $\mathcal{T}_h$ here as well. Let $\{\overline{\boldsymbol{U}}_k\}_{k=1}^{N_D}$ and $\{\overline{\boldsymbol{\Phi}}_l\}_{l=1}^{N_N}$ be the (polynomial) bases in $\boldsymbol{\mathcal{V}}_{hp}$ and $\boldsymbol{\mathcal{W}}_{hp}$ respectively. Then the discrete analogues of the boundary integral operators are given by

$$V_{hp} := \left\{\left\langle V\boldsymbol{\Phi}_k, \boldsymbol{\Phi}_l\right\rangle_\Gamma\right\}_{k,l=1}^{N_N,N_N}, \qquad K_{hp} := \left\{\left\langle K\boldsymbol{U}_k, \boldsymbol{\Phi}_l\right\rangle_\Gamma\right\}_{k,l=1}^{N_D,N_N},$$

$$K'_{hp} := \left\{\left\langle K'\boldsymbol{\Phi}_k, \boldsymbol{U}_l\right\rangle_\Gamma\right\}_{k,l=1}^{N_N,N_D}, \qquad W_{hp} := \left\{\left\langle W\boldsymbol{U}_k, \boldsymbol{U}_l\right\rangle_\Gamma\right\}_{k,l=1}^{N_D,N_D}.$$

Computation of the discrete Newton potentials requires some finite element discretization in the domain. Let $\{\overline{\boldsymbol{\Xi}}_k\}_{k=1}^{N_\Omega}$ be the polynomial basis of that discrete space $\boldsymbol{X}_{hp}$. Then the discrete Newton potentials are

$$N_{0hp} := \left\{\left\langle N_0\boldsymbol{\Xi}_k, \boldsymbol{\Phi}_l\right\rangle_\Gamma\right\}_{k,l=1}^{N_\Omega,N_N}, \qquad N_{1hp} := \left\{\left\langle N_1\boldsymbol{\Xi}_k, \boldsymbol{U}_l\right\rangle_\Gamma\right\}_{k,l=1}^{N_\Omega,N_D}.$$

We introduce the canonical embeddings

$$\begin{aligned} i_{hp} &:= \boldsymbol{\mathcal{W}}_{hp} \hookrightarrow \boldsymbol{H}^{-1/2}(\Gamma), \\ j_{hp} &:= \boldsymbol{\mathcal{V}}_{hp} \hookrightarrow \boldsymbol{H}^{1/2}(\Gamma), \\ k_{hp} &:= \boldsymbol{X}_{hp} \hookrightarrow \boldsymbol{H}^{1}(\Omega) \end{aligned} \tag{1.14}$$

and their duals $i^*_{hp}, j^*_{hp}, k^*_{hp}$. Then the discrete boundary integral operators and the Newton potentials can be represented by

$$\begin{aligned} V_{hp} &= i^*_{hp} V i_{hp}, & K_{hp} &= i^*_{hp} K j_{hp}, \\ K'_{hp} &= j^*_{hp} K' i_{hp}, & W_{hp} &= j^*_{hp} W j_{hp}, \\ N_{0hp} &= i^*_{hp} N_0 k_{hp}, & N_{1hp} &= j^*_{hp} N_1 k_{hp}. \end{aligned}$$

According to this notations we obtain for $\hat{S}$ and $\hat{E}$ the representation

$$\begin{aligned} \hat{S} &= W + (K' + 1/2) i_{hp} V^{-1}_{hp} i^*_{hp} (K + 1/2), \\ \hat{E} &= (K' + 1/2)(V - i_{hp} V^{-1}_{hp} i^*_{hp})(K + 1/2). \end{aligned}$$

2 Nonconforming methods for interface problems

In this chapter we consider a nonconforming elliptic boundary value problem (Poisson equation) with mixed boundary data in some Lipschitz domain $\Omega \subset \mathbb{R}^2$. The domain Ω is decomposed into two parts Ω^1 and Ω^2. The boundary element discretization is employed on the boundary of Ω^2 and the finite element discretization is used in the complement domain Ω^1. An independent discretization of both subdomains is considered, and hence, nonmatched meshes on the artificial interface of the decomposition are allowed. We construct and analyse an *hp*-FE/BE coupling on nonmatched meshes, based on Nitsche's method. Both, the mesh size and the polynomial degree are changed to improve accuracy. Nitsche's method leads to a positive definite formulation. Therefore, unlike the mortar method, it does not require the *Babuška-Brezzi* condition for stability. We derive a priori estimates for our method and demonstrate it in several numerical examples. The given analysis can be easily extended to the pure FE or the pure BE decomposition as well as to the case of more then two subdomains. The problem with a bounded domain Ω is considered in detail, but the case of an unbounded BE subdomain and a bounded FE subdomain follows with similar arguments.

2.1 The model problem

Let us consider a bounded domain $\Omega \subset \mathbb{R}^2$ decomposed into two disjoint parts, $\overline{\Omega} = \overline{\Omega^1} \cup \overline{\Omega^2}$. Define also $\Gamma := \partial\Omega$, $\Gamma^i := \partial\Omega^i$, $i = 1, 2$, $\Gamma_I := \Gamma^1 \cap \Gamma^2$.

As a model problem we take the Poisson problem in Ω with mixed boundary conditions: Find $u : \Omega \to \mathbb{R}$ such that

$$\begin{aligned} -\Delta u &= f && \text{in } \Omega, \\ u &= 0 && \text{on } \Gamma_D, \\ \partial_n u &= \hat{t} && \text{on } \Gamma_N, \end{aligned} \tag{2.1}$$

with a disjoint decomposition $\overline{\Gamma} = \overline{\Gamma}_D \cup \overline{\Gamma}_N$, prescribed volume forces f and boundary tractions $\hat{t}$. For simplicity of presentation, we assume that there are no body forces acting in the subdomain Ω^2, i.e. $f|_{\Omega^2} \equiv 0$. If the solution u is sufficiently smooth along Γ_I, problem (2.1) in Ω is equivalent to the following interface problem in Ω^1, Ω^2, [5]:

Find $u : \Omega^1 \cup \Omega^2 \to \mathbb{R}$

$$
\begin{aligned}
-\Delta u &= f && \text{in } \Omega^1, \\
-\Delta u &= 0 && \text{in } \Omega^2, \\
u &= 0 && \text{on } \Gamma_D, \\
\partial_n u &= \hat{t} && \text{on } \Gamma_N, \\
[u] &= 0 && \text{on } \Gamma_I, \\
[\partial_n u] &= 0 && \text{on } \Gamma_I,
\end{aligned}
\tag{2.2}
$$

where the jump $[u] := u_1|_{\Gamma_I} - u_2|_{\Gamma_I}$ is defined with restrictions $u_i := u|_{\Omega^i}$, $\partial_n u := \nabla u \cdot \boldsymbol{n}^1$ on Γ_I and therefore $[\partial_n u] = \nabla u_1|_{\Gamma_I} \cdot \boldsymbol{n}^1 - \nabla u_2|_{\Gamma_I} \cdot \boldsymbol{n}^1$. Here $\boldsymbol{n}^1$ denotes the unit outer normal vector to Ω^1. We define for brevity $\Gamma^i_A := \Gamma_A \cap \Gamma^i$ and $\Sigma^i := \Gamma^i_N \cap \Gamma_I$ with $i = 1, 2$ and $A = D, N$.

We shall use a finite element discretization in Ω^1 and a boundary element discretization on Γ^2. Let $\mathcal{T}^1_{h,\Omega}$ be a shape-regular decomposition of the finite element part Ω^1 into triangular or quadrilateral elements, and let $\mathcal{T}^2_{h,\Gamma}$ be a decomposition of Γ^2 into straight line segments

$$
\overline{\Omega^1} = \bigcup_{K \in \mathcal{T}^1_{h,\Omega}} \overline{K}, \qquad \overline{\Gamma^2} = \bigcup_{I \in \mathcal{T}^2_{h,\Gamma}} \overline{I}.
$$

Assume that the meshes $\mathcal{T}^1_{h,\Omega}$, $\mathcal{T}^2_{h,\Gamma}$ are quasiuniform. Let h_K and h_I stand for the diameter of K and I respectively, and define

$$
h_1 := \max_{K \in \mathcal{T}^1_{h,\Omega}} h_K, \qquad h_2 := \max_{I \in \mathcal{T}^2_{h,\Gamma}} h_I.
$$

Further we introduce the continuous spaces

$$
\begin{aligned}
\mathcal{V}^1_\Omega &:= H^1_{D_0}(\Omega^1) \equiv \left\{ u \in H^1(\Omega^1) : \; u|_{\Gamma^1_D} = 0 \right\}, \\
\mathcal{V}^2_\Gamma &:= \tilde{H}^{1/2}(\Sigma^2) \equiv \left\{ u \in H^{1/2}(\Sigma^2) : \; \text{supp } u \subset \Sigma^2 \right\}, \\
\mathcal{V} &= \mathcal{V}^1_\Omega \times \mathcal{V}^2_\Gamma,
\end{aligned}
$$

and their discrete analogues based on $\mathcal{T}^1_{h,\Omega}$, $\mathcal{T}^2_{h,\Gamma}$

$$
\begin{aligned}
\mathcal{V}^1_{hp,\Omega} &:= \left\{ U \in \mathcal{V}^1_\Omega : \; U|_K \in \mathcal{P}_{p_K}(K) \; \forall K \in \mathcal{T}^1_{h,\Omega} \right\}, \\
\mathcal{V}^2_{hp,\Gamma} &:= \left\{ U \in \mathcal{V}^2_\Gamma : \; U|_I \in \mathcal{P}_{p_I}(I) \; \forall I \in \mathcal{T}^2_{h,\Gamma} \right\}, \\
\mathcal{V}_{hp} &= \mathcal{V}^1_{hp,\Omega} \times \mathcal{V}^2_{hp,\Gamma}.
\end{aligned}
$$

Here $\mathcal{P}_p$ stands for the space of polynomials, with degree not exceeding p. We assume that the polynomial degree distributions in $\mathcal{V}^1_{hp,\Omega}, \mathcal{V}^2_{hp,\Gamma}$ are quasiuniform and set

$$
p_1 := \min_{K \in \mathcal{T}^1_{h,\Omega}} p_K, \qquad p_2 := \min_{i \in \mathcal{T}^2_{h,\Gamma}} p_I.
$$

We define with $\mathcal{T}^1_{h,I}$ and $\mathcal{T}^2_{h,I}$ the trace meshes on Γ_I induced by the partitions $\mathcal{T}^1_{h,\Omega}$ and $\mathcal{T}^2_{h,\Gamma}$ respectively. Note, that the functions in the discrete space $\mathcal{V}_{hp}$ are in general discontinuous over Γ_I. Moreover, continuity in the strong sense can not be imposed, in case of nonmatched meshes, i.e. $\mathcal{T}^1_{h,I} \neq \mathcal{T}^2_{h,I}$. *hp*-Nitsche's method, imposing continuity of the solution u in the weak sense, is constructed and analysed below.

The h-version of Nitsche's finite element method was recently introduced and studied e.g. by Becker, Hansbo and Stenberg [5], Hansbo, Hansbo and Larson [31]. It can be treated as a mesh-dependent penalty method with additional terms, which, in contrast to the original internal penalty methods (described e.g. by Lazarov, Tomov and Vassilevski [43]), provide consistency of the coupling. Stability of Nitsche's method is provided by the penalty-like parameter λ^{Nit}, which should be chosen sufficiently large. Due to consistency of the method there is no need to take higher values of λ^{Nit} if the stability is already achieved. In the context of the penalty method, the penalty parameter should be increased together with decreasing mesh size and/or increasing polynomial degree to capture the consistency error. For example, in the framework of a frictionless contact between an elastic body and a rigid obstacle, the relation between the penalty parameter and the discretization parameters is obtained in Section 3.2.

An alternative method is the mortar method (see e.g. Seshaiyer and Suri [59] for *hp*-FEM). In the context of the mortar method, the weak continuity of u is enforced with the help of a Lagrange multiplier λ. This yields a saddle point formulation. It is well known from the literature (see e.g. Ben Belgacem [6], Wohlmuth [71]), not every discretization of u and λ leads to a stable method. The *Babuška-Brezzi condition* is the crucial inequality which guarantees the stable discretization for the mortar method. Nitsche's method leads to the positive definite system of algebraic equations, and therefore, it is always stable for large enough penalty-like parameters λ^{Nit}.

We use a symmetric boundary element formulation with the Steklov-Poincaré operator S (see e.g. Carstensen and Stephan [17]) in the BE subdomain. As the operator S cannot be discretized directly, its approximation $\hat{S}$ is used, which yields a consistency error. This consistency error can be bounded by the approximation error of the discrete traction space, Lemma 1.4.2, which is optimal and does not damage the convergence rate of the methods.

2.2 hp-Nitsche's method

The discrete weak formulation with Nitsche's coupling across Γ_I corresponding to the problem (2.2) can be written as follows: Find $U = (U^1, U^2) \in \mathcal{V}_{hp}$ such that

$$a_h(U, \Phi) = l(\Phi) \qquad \forall \Phi \in \mathcal{V}_{hp}, \tag{2.3}$$

where

$$l(\Phi) := (f, \Phi_1)_{\Omega^1} + \left\langle \hat{t}, \Phi \right\rangle_{\Gamma_N},$$

$$
\begin{aligned}
a_h(U,\varPhi) := (\nabla U, \nabla \varPhi)_{\Omega^1} + \left\langle \hat{S}U, \varPhi \right\rangle_{\Sigma^2} \\
- \langle \{\partial_n U\}, [\varPhi] \rangle_{\Gamma_I} - \langle [U], \{\partial_n \varPhi\} \rangle_{\Gamma_I} + \left\langle \lambda^{Nit} h_1^{-1} p_1^{\alpha} [U], [\varPhi] \right\rangle_{\Gamma_I}
\end{aligned} \tag{2.4}
$$

for some $\alpha \in \mathbb{R}$, where $\hat{S}$ is the discrete Steklov-Poincaré operator. For the normal flux on the coupling interface we choose, as in [31], the one sided approximation from the FE subdomain $\{\partial_n \varPhi\} := \partial_n \varPhi_1$. The piecewise constant functions $h_1(x)$ and $p_1(x)$ represent the local meshsize and the local polynomial degree from the *FE side* on Γ_I

$$
h_1(x) := h_K, \qquad p_1(x) := p_K, \qquad x \in K \in \mathcal{T}^1_{h,\Omega}, \quad K \subset \overline{\Gamma}_I.
$$

Due to the consistency error, yielding by the approximation of the Steklov-Poincaré operator $\hat{S}$ the Galerkin orthogonality property does not hold for our method. Instead, the following theorem holds.

Theorem 2.2.1. *(Consistency error) The discrete problem (2.3) is consistent up to an error in the approximation of the Steklov-Poincaré operator, i.e. for $u \in \mathcal{V}$ solving (2.2) and $\hat{E} := S - \hat{S}$ there holds*

$$
a_h(u,\varPhi) - l(\varPhi) = -\left\langle \hat{E}u_2, \varPhi_2 \right\rangle_{\Sigma^2},
$$

and therefore for $U \in \mathcal{V}_{hp}$ solving (2.3) there holds

$$
a_h(u - U,\varPhi) = -\left\langle \hat{E}u_2, \varPhi_2 \right\rangle_{\Sigma^2}.
$$

Proof. For $u \in \mathcal{V}$ solving (2.2) there holds

$$
[u] = 0, \qquad \{\partial_n u\} := \nabla u_1 \cdot \boldsymbol{n}^1 = -\nabla u_2 \cdot \boldsymbol{n}^2 \qquad \text{on } \Gamma_I.
$$

Therefore

$$
\begin{aligned}
a_h(u,\varPhi) &= (\nabla u_1, \nabla \varPhi_1)_{\Omega^1} + \left\langle \hat{S}u_2, \varPhi_2 \right\rangle_{\Sigma^2} \\
&\quad - \langle \{\partial_n u\}, [\varPhi] \rangle_{\Gamma_I} - \langle [u], \{\partial_n \varPhi\} \rangle_{\Gamma_I} + \left\langle \lambda^{Nit} h_1^{-1} p_1^{\alpha} [u], [\varPhi] \right\rangle_{\Gamma_I} \\
&= (\nabla u_1, \nabla \varPhi_1)_{\Omega^1} + \left\langle \hat{S}u_2, \varPhi_2 \right\rangle_{\Sigma^2} - \left\langle \nabla u_1 \cdot \boldsymbol{n}^1, \varPhi_1 \right\rangle_{\Gamma_I} - \left\langle \nabla u_2 \cdot \boldsymbol{n}^2, \varPhi_2 \right\rangle_{\Gamma_I}
\end{aligned}
$$

The Steklov-Poincaré operator S is a Dirichlet-to-Neumann mapping, therefore the Green's formula provides

$$
(\nabla u_2, \nabla \phi_2)_{\Omega^2} = \langle S u_2, \phi_2 \rangle_{\Sigma^2} \qquad \forall \phi_2 \in \mathcal{V}^2_\Gamma.
$$

Hence, with partial integration we get

$$
\begin{aligned}
a_h(u,\varPhi) - l(\varPhi) &= (\nabla u_1, \nabla \varPhi_1)_{\Omega^1} - \left\langle \nabla u_1 \cdot \boldsymbol{n}^1, \varPhi_1 \right\rangle_{\Gamma_I} - \left\langle \hat{t}, \varPhi_1 \right\rangle_{\Gamma^1_N} - (f, \varPhi_1)_{\Omega^1} \\
&\quad + (\nabla u_2, \nabla \varPhi_2)_{\Omega^2} - \left\langle \nabla u_2 \cdot \boldsymbol{n}^2, \varPhi_2 \right\rangle_{\Gamma_I} - \left\langle \hat{t}, \varPhi_2 \right\rangle_{\Gamma^2_N} \\
&\quad - \left\langle (S - \hat{S}) u_2, \varPhi_2 \right\rangle_{\Sigma^2} \\
&= (-\Delta u_1 - f, \varPhi_1)_{\Omega^1} + (-\Delta u_2, \varPhi_2)_{\Omega^2} - \left\langle (S - \hat{S}) u_2, \varPhi_2 \right\rangle_{\Sigma^2},
\end{aligned}
$$

which together with (2.3) gives the assertion of the theorem. □

The nodes of $\mathcal{T}^1_{h,I}$ and $\mathcal{T}^2_{h,I}$ together produce a finer partition $\mathcal{T}^{12}_{h,I}$ of Γ_I, i.e.

$$\overline{\Gamma}_I = \bigcup_{J \in \mathcal{T}^{12}_{h,I}} \overline{J}$$

and

$$\forall J \in \mathcal{T}^{12}_{h,I} \qquad \exists K_J \in \mathcal{T}^1_{h,\Omega}: \; J \subset \overline{K_J}, \qquad \exists I_J \in \mathcal{T}^2_{h,\Gamma}: \; J \subset \overline{I_J}.$$

In the forthcoming analysis we will need the mesh dependent norms (see e.g. [31])

$$\begin{aligned} ||\phi||^2_{1/2,h,\Gamma_I} &:= ||h^{-1/2} p^{\gamma/2} \phi||^2_{L_2(\Gamma_I)} = \sum_{J \in \mathcal{T}^{12}_{h,I}} h^{-1}_{K_J} p^{\gamma}_{K_J} ||\phi||^2_{L_2(J)}, \\ ||\phi||^2_{-1/2,h,\Gamma_I} &:= ||h^{1/2} p^{-\gamma/2} \phi||^2_{L_2(\Gamma_I)} = \sum_{J \in \mathcal{T}^{12}_{h,I}} h_{K_J} p^{-\gamma}_{K_J} ||\phi||^2_{L_2(J)}, \end{aligned} \tag{2.5}$$

and

$$|||\phi|||^2_h := ||\nabla \phi||^2_{L_2(\Omega^1)} + \left\langle \hat{S}\phi, \phi \right\rangle_{\Sigma^2} + ||\{\partial_n \phi\}||^2_{-1/2,h,\Gamma_I} + ||[\phi]||^2_{1/2,h,\Gamma_I}.$$

It is easy to see that with the Cauchy-Schwarz inequality there holds

$$\langle \phi, \psi \rangle_{\Gamma_I} \leq \sum_{J \in \mathcal{T}^{12}_{h,I}} h^{-1/2}_{K_J} p^{\gamma/2}_{K_J} ||\phi||_{L_2(\Gamma_I)} h^{1/2}_{K_J} p^{-\gamma/2}_{K_J} ||\psi||_{L_2(\Gamma_I)} \leq ||\phi||_{1/2,h,\Gamma_I} ||\psi||_{-1/2,h,\Gamma_I}.$$

2.2.1 Continuity and coercivity of $a_h(\cdot,\cdot)$

Continuity and coercivity of the bilinear form $a_h(\cdot,\cdot)$ are needed to be shown to ensure convergence of our method.

Lemma 2.2.1. *(Continuity of a_h) The bilinear form $a_h(\cdot,\cdot)$ is continuous in the space $\mathcal{V}$ with the $|||\cdot|||_h$-norm, i.e. there exists a constant $C > 0$, independent of the discretization parameters, such that*

$$a_h(\phi, \psi) \leq C p_1^{\max\{\alpha-\gamma,0\}} |||\phi|||_h |||\psi|||_h, \qquad \forall \phi, \psi \in \mathcal{V}.$$

Proof. The assertion follows directly from the definitions and the Cauchy-Schwarz inequality. For arbitrary $\phi, \psi \in \mathcal{V}$ there holds

$$(\nabla\phi, \nabla\psi)_{\Omega^1} \leq ||\nabla\phi||_{L_2(\Omega^1)} ||\nabla\psi||_{L_2(\Omega^1)} \leq |||\phi|||_h |||\psi|||_h,$$

$$\begin{aligned} \left\langle \hat{S}\phi, \psi \right\rangle_{\Sigma^2} &= \left\langle \hat{S}^{1/2}\phi, \hat{S}^{1/2}\psi \right\rangle_{\Sigma^2} \leq \left\langle \hat{S}^{1/2}\phi, \hat{S}^{1/2}\phi \right\rangle^{1/2}_{\Sigma^2} \left\langle \hat{S}^{1/2}\psi, \hat{S}^{1/2}\psi \right\rangle^{1/2}_{\Sigma^2} \\ &= \left\langle \hat{S}\phi, \phi \right\rangle^{1/2}_{\Sigma^2} \left\langle \hat{S}\psi, \psi \right\rangle^{1/2}_{\Sigma^2} \leq |||\phi|||_h |||\psi|||_h, \end{aligned}$$

$$\langle\{\partial_n\phi\},[\psi]\rangle_{\Gamma_I} \le ||\{\partial_n\phi\}||_{-1/2,h,\Gamma_I}||[\psi]||_{1/2,h,\Gamma_I} \le |||\phi|||_h|||\psi|||_h,$$

$$\langle\lambda^{Nit}h_1^{-1}p_1^{\alpha}[\phi],[\psi]\rangle_{\Gamma_I} \le \lambda^{Nit}p_1^{\alpha-\gamma}||\phi||_{1/2,h,\Gamma_I}||\psi||_{1/2,h,\Gamma_I} \le \lambda^{Nit}p_1^{\alpha-\gamma}|||\phi|||_h|||\psi|||_h.$$

The choice $C := \max\{\lambda^{Nit},1\}$ completes the proof. □

We need the following Lemma to prove coercivity of $a_h(\cdot,\cdot)$.

Lemma 2.2.2. *(Inverse inequality) For all $\Phi \in \mathcal{V}^1_{hp,\Omega}$ there exists a constant $C_{inv} > 0$, independent of the discretization parameters, such that*

$$||\Phi||_{1/2,h,\Gamma_I} \le C_{inv}\frac{p_1^{1+\gamma/2}}{h_1}||\Phi||_{L_2(\Omega^1)}, \tag{2.6}$$

$$||\nabla\Phi\cdot\boldsymbol{n}^1||_{-1/2,h,\Gamma_I} \le C_{inv}p_1^{1-\gamma/2}||\nabla\Phi||_{L_2(\Omega^1)}. \tag{2.7}$$

Proof. We recall the result of Warburton and Hesthaven [68] that for some d-dimensional simplex D and some polynomial $\Psi \in [\mathcal{P}_{p_D}(D)]^d$ there holds

$$||\Psi||_{L_2(\partial D)} \le \left(\frac{(p_D+1)(p_D+d)}{d}\frac{\text{Volume }(\partial D)}{\text{Volume }(D)}\right)^{1/2}||\Psi||_{L_2(D)} \le C\frac{p_D}{h_D^{1/2}}||\Psi||_{L_2(D)}$$

for some $C > 0$, independent of h_D and p_D. We denote by $K_J \in \mathcal{T}^1_{h,\Omega}$ a volume element, including the part of the interface $J \in \mathcal{T}^{12}_{h,I}$. Thus,

$$\begin{aligned}||\Psi||_{1/2,h,\Gamma_I} = \left(\sum_{J\in\mathcal{T}^{12}_{h,I}}\frac{p_{K_J}^{\gamma}}{h_{K_J}}||\Psi||^2_{L_2(J)}\right)^{1/2} &\le \left(\sum_{J\in\mathcal{T}^{12}_{h,I}}C\frac{p_{K_J}^{2+\gamma}}{h_{K_J}^2}||\Psi||^2_{L_2(K_J)}\right)^{1/2}\\ &\le C\frac{p_1^{1+\gamma/2}}{h_1}||\Psi||_{L_2(\Omega^1)},\end{aligned}$$

which is inequality (2.6). Similarly we obtain

$$\begin{aligned}||\Psi||_{-1/2,h,\Gamma_I} = \left(\sum_{J\in\mathcal{T}^{12}_{h,I}}\frac{h_{K_J}}{p_{K_J}^{\gamma}}||\Psi||^2_{L_2(J)}\right)^{1/2} &\le \left(\sum_{J\in\mathcal{T}^{12}_{h,I}}Cp_{K_J}^{2-\gamma}||\Psi||^2_{L_2(K_J)}\right)^{1/2}\\ &\le Cp_1^{1-\gamma/2}||\Psi||_{L_2(\Omega^1)}.\end{aligned}$$

The inequality (2.7) follows by setting $\Psi := |\nabla\Phi|$ and noting that $\nabla\Phi\cdot\boldsymbol{n}^1 \le |\nabla\Phi|$. □

Lemma 2.2.3. *(Coercivity of a_h) The bilinear form $a_h(\cdot,\cdot)$ is coercive in the discrete space $\mathcal{V}_{hp}$ with the $|||\cdot|||_h$-norm, i.e. there exists a constant $C > 0$, independent of the discretization parameters, such that*

$$a_h(\Phi,\Phi) \ge Cp_1^{-\max\{2-\gamma,0\}}|||\Phi|||_h^2, \qquad \forall\Phi\in\mathcal{V}_{hp},$$

if the penalty-like parameter λ^{Nit} fulfils $\lambda^{Nit} \ge 1/2p_1^{\gamma-\alpha} + C_{inv}p_1^{2-\alpha}$, where the constant C_{inv} comes from the inverse inequality (2.7).

Proof. With the definition (2.4) of the bilinear form $a_h(\cdot,\cdot)$ we obtain

$$a_h(\Phi,\Phi) \geq ||\nabla\Phi||^2_{L_2(\Omega^1)} + \left\langle \hat{S}\Phi, \Phi \right\rangle_{\Sigma^2} - 2\left\langle \{\partial_n \Phi\}, [\Phi] \right\rangle_{\Gamma_I} + \lambda^{Nit} p_1^{\alpha-\gamma} ||[\Phi]||^2_{1/2,h,\Gamma_I}.$$

Lemma 2.2.2 provides for arbitrary $\epsilon > 0$

$$\begin{aligned} 2\left\langle \{\partial_n \Phi\}, [\Phi] \right\rangle_{\Gamma_I} &\leq 2||\{\partial_n \Phi\}||_{-1/2,h,\Gamma_I} ||[\Phi]||_{1/2,h,\Gamma_I} \\ &\leq \epsilon^{-1} ||\{\partial_n \Phi\}||^2_{-1/2,h,\Gamma_I} + \epsilon ||[\Phi]||^2_{1/2,h,\Gamma_I} \\ &\leq C_{inv} p_1^{2-\gamma} \epsilon^{-1} ||\nabla\Phi||^2_{L_2(\Omega^1)} + \epsilon ||[\Phi]||^2_{1/2,h,\Gamma_I}. \end{aligned}$$

That gives

$$a_h(\Phi,\Phi) \geq (1 - C_{inv} p_1^{2-\gamma}\epsilon^{-1}) ||\nabla\Phi||^2_{L_2(\Omega^1)} + \left\langle \hat{S}\Phi, \Phi \right\rangle_{\Sigma^2} + (\lambda^{Nit} p_1^{\alpha-\gamma} - \epsilon) ||[\Phi]||^2_{1/2,h,\Gamma_I}.$$

We choose $\epsilon := 2\,C_{inv}\,p_1^{2-\gamma}$ and $\lambda^{Nit} \geq (1/2+\epsilon)/p_1^{\alpha-\gamma} = 1/2 p_1^{\gamma-\alpha} + C_{inv} p_1^{2-\alpha}$. Therefore

$$a_h(\Phi,\Phi) \geq \frac{1}{2}\left(||\nabla\Phi||^2_{L_2(\Omega^1)} + \left\langle \hat{S}\Phi, \Phi \right\rangle_{\Sigma^2} + ||[\Phi]||^2_{1/2,h,\Gamma_I} \right).$$

Employing inequality (2.7) from Lemma 2.2.2 we obtain

$$||\{\partial_n \Phi\}||_{-1/2,h,\Gamma_I} \leq C_{inv} p_1^{1-\gamma/2} ||\nabla\Phi||_{L_2(\Omega^1)},$$

and hence

$$|||\Phi|||^2_h \leq (1 + C_{inv} p_1^{2-\gamma}) \left(||\nabla\Phi||^2_{L_2(\Omega^1)} + \left\langle \hat{S}\Phi, \Phi \right\rangle_{\Sigma^2} + ||[\Phi]||^2_{1/2,h,\Gamma_I} \right).$$

This yields

$$a_h(\Phi,\Phi) \geq (2(1 + C_{inv} p_1^{2-\gamma}))^{-1} |||\Phi|||^2_h,$$

which is the assertion of the lemma. □

The right hand side $l(\cdot)$ in the discrete formulation (2.3) is obviously continuous. The bilinear form $a_h(\cdot,\cdot)$, thanks to Lemmas 2.2.1 and 2.2.3 is continuous and coercive. Thus the Lax-Milgram lemma guarantees that the discrete problem (2.3) has a unique solution.

2.2.2 Interpolation in the $|||\cdot|||_h$-norm

The approximation properties of the *hp*-Lagrange interpolation operator in the Gauss-Lobatto nodes are needed for further analysis. Let $\mathcal{I}^1_{hp,\Omega}, \mathcal{I}^2_{hp,\Gamma}$ be the *hp*-Lagrangian interpolation operator in the Gauss-Lobatto nodes of the elements of $\mathcal{T}^1_{hp,\Omega}$, $\mathcal{T}^2_{hp,\Gamma}$, respectively. Define an interpolation operator on $\Omega^1 \cup \Gamma^2$ such that

$$\mathcal{I}_{hp}\phi|_{\Omega^1} := \mathcal{I}^1_{hp,\Omega}\phi|_{\Omega^1}, \qquad \mathcal{I}_{hp}\phi|_{\Gamma^2} := \mathcal{I}^2_{hp,\Gamma}\phi|_{\Gamma^2}.$$

Lemma 2.2.4. *Let J be a straight line segment, $h := |J|$ and let $\mathcal{I}_{hp}^J$ be the hp-Lagrange interpolation operator on the Gauss-Lobatto nodes of J. For any real numbers $\nu \in [0,1]$, $\mu > \nu/2$, there exists a positive constant C depending on μ, such that the following approximation property holds for any function $\phi \in H^{\mu+1/2}(J)$*

$$||\phi - \mathcal{I}_{hp}^J\phi||_{H^\nu(J)} \le C\left(\frac{h}{p}\right)^{\mu+1/2-\nu} ||\phi||_{H^{\mu+1/2}(J)}.$$

Further, let K is a triangle or a plane quadrilateral, $h := diam(K)$ and let $\mathcal{I}_{hp}^K$ be the hp-Lagrange interpolation operator on the Gauss-Lobatto nodes of K. For any real numbers $\nu \in [0,1]$, $\mu > \nu/2$, there exists a positive constant C depending on μ, such that the following approximation property holds for any function $\phi \in H^{\mu+1}(K)$

$$||\phi - \mathcal{I}_{hp}^K\phi||_{H^\nu(K)} \le C\left(\frac{h}{p}\right)^{\mu+1-\nu} ||\phi||_{H^{\mu+1}(K)},$$

$$||\phi - \mathcal{I}_{hp}^K\phi||_{H^\nu(\partial K)} \le C\left(\frac{h}{p}\right)^{\mu+1/2-\nu} ||\phi||_{H^{\mu+1}(K)}.$$

Proof. For quadrilaterals the statement of the theorem follows from [10, Theorem 4.7] and [10, Theorem 5.9] by scaling. We adopt the techniques of regularity preserving extension from a triangle to a quadrilateral (see e.g. [56, Remark 4.74]) to obtain the corresponding result for triangles. □

Lemma 2.2.5. *Let $\mathcal{I}_{hp}$ be the Lagrange interpolation operator in the Gauss-Lobatto nodes of $\mathcal{T}_{h,\Omega}^1$ and $\mathcal{T}_{h,\Gamma}^2$. Assume that the discrete spaces $\mathcal{V}_{hp,\Omega}^1$ and $\mathcal{V}_{hp,\Gamma}^2$ have quasiuniform and compatible meshes and polynomial degree distributions, with characteristical discretization parameters denoted by h and p, respectively. Then for arbitrary $\phi_1 \in H_{D_0}^1(\Omega^1) \cap H^{r+1}(\Omega^1)$ and for arbitrary $\phi_2 \in \tilde{H}^{r+1/2}(\Sigma^2), r \ge 1$, and $\phi := (\phi_1, \phi_2)$ there exists a constant $C > 0$ independent of h and p, such that*

$$|||\phi - \mathcal{I}_{hp}\phi|||_h \le Cp^{|1/2-\gamma/2|}\left(\frac{h}{p}\right)^r \left(||\phi_1||_{H^{r+1}(\Omega^1)} + ||\phi_2||_{\tilde{H}^{r+1/2}(\Sigma^2)}\right), \quad r \ge 1. \tag{2.8}$$

Proof. We estimate the four terms composing the mesh dependent energy norm $|||\cdot|||_h$

According to Lemma 2.2.4 for the volume term there holds

$$\begin{aligned}||\nabla(\phi_1 - \mathcal{I}_{hp}\phi_1)||^2_{L_2(\Omega^1)} &= \sum_{K\in\mathcal{T}_{h,\Omega}^1} ||\nabla(\phi_1 - \mathcal{I}_{hp}^K\phi_1)||^2_{L_2(K)} \le \sum_{K\in\mathcal{T}_{h,\Omega}^1} ||\phi_1 - \mathcal{I}_{hp}^K\phi_1||^2_{H^1(K)} \\ &\le C\sum_{K\in\mathcal{T}_{h,\Omega}^1}\left(\frac{h_K}{p_K}\right)^{2r} ||\phi_1||^2_{H^{r+1}(K)} \le C\left(\frac{h}{p}\right)^{2r} ||\phi_1||^2_{H^{r+1}(\Omega^1)}.\end{aligned}$$

The discrete Steklov-Poincaré operator $\hat{S}$ is bounded, therefore, due to Lemma 2.2.4, there holds

$$\left\langle \hat{S}(\phi_2 - \mathcal{I}_{hp}\phi_2), \phi_2 - \mathcal{I}_{hp}\phi_2 \right\rangle_{\Sigma^2} \le C_{\hat{S}} ||\phi_2 - \mathcal{I}_{hp}\phi_2||^2_{\tilde{H}^{1/2}(\Sigma^2)} \le C \left(\frac{h}{p}\right)^{2r} ||\phi_2||^2_{\tilde{H}^{r+1/2}(\Sigma^2)}.$$

The triangle inequality provides for the jump term

$$\frac{1}{2}|||[\phi - \mathcal{I}_{hp}\phi]|||^2_{1/2,h,\Gamma_I} \le ||\phi_1 - \mathcal{I}_{hp}\phi_1||^2_{1/2,h,\Gamma_I} + ||\phi_2 - \mathcal{I}_{hp}\phi_2||^2_{1/2,h,\Gamma_I}$$
$$\le \sum_{K\in\mathcal{T}^1_{h,\Omega}} \sum_{\substack{J \in \mathcal{T}^{12}_{h,I} \\ J \subset \overline{K}}} \frac{p_K^\gamma}{h_K} ||\phi_1 - \mathcal{I}^K_{hp}\phi_1||^2_{L_2(J)} + \frac{p_K^\gamma}{h_K} ||\phi_2 - \mathcal{I}^I_{hp}\phi_2||^2_{L_2(J)},$$

where $J \subset \overline{I} \in \mathcal{T}^2_{h,\Gamma}$. Lemma 2.2.4 gives on each interval J

$$\frac{p_K^\gamma}{h_K} ||\phi_1 - \mathcal{I}^K_{hp}\phi_1||^2_{L_2(J)} \le C \left(\frac{h_K}{p_K}\right)^{2r} p_K^{\gamma-1} ||\phi_1||^2_{H^{r+1}(K)},$$
$$\frac{p_K^\gamma}{h_K} ||\phi_2 - \mathcal{I}^I_{hp}\phi_2||^2_{L_2(J)} \le C \left(\frac{h_I}{p_I}\right)^{2r} \frac{h_I}{h_K} \frac{p_K^\gamma}{p_I} ||\phi_2||^2_{H^{r+1/2}(I)}.$$

The meshsize and the polynomial degrees are compatible across the interface Γ_I, thus the second inequality becomes

$$\frac{p_K^\gamma}{h_K} ||\phi_2 - \mathcal{I}_{hp}\phi_2||^2_{L_2(J)} \le C \left(\frac{h_I}{p_I}\right)^{2r} p_K^{\gamma-1} ||\phi_2||^2_{H^{r+1/2}(I)}.$$

That yields

$$|||[\phi - \mathcal{I}_{hp}\phi]|||^2_{1/2,h,\Gamma_I} \le C p^{\gamma-1} \left(\frac{h}{p}\right)^{2r} \left(||\phi_1||^2_{H^{r+1}(\Omega^1)} + ||\phi_2||^2_{\tilde{H}^{r+1/2}(\Sigma^2)} \right).$$

Finally, Lemma 2.2.4 gives for the flux term

$$||\{\partial_n(\phi - \mathcal{I}_{hp}\phi)\}||^2_{-1/2,\partial\Omega} \le C \sum_{K\in\mathcal{T}^1_{h,\Omega}} \sum_{\substack{J \in \mathcal{T}^{12}_{h,I} \\ J \subset \overline{K}}} \frac{h_K}{p_K^\gamma} ||\nabla(\phi_1 - \mathcal{I}_{hp}\phi_1)||^2_{L_2(J)}$$
$$\le C \sum_{K\in\mathcal{T}^1_{h,\Omega}} \sum_{\substack{J \in \mathcal{T}^{12}_{h,I} \\ J \subset \overline{K}}} \left(\frac{h_K}{p_K}\right)^{2r} p_K^{1-\gamma} ||\phi_1||^2_{H^{r+1}(K)}$$
$$\le \left(\frac{h}{p}\right)^{2r} p^{1-\gamma} ||\phi_1||^2_{H^{r+1}(\Omega^1)}.$$

Combining above estimates we obtain (2.8), which completes the lemma. □

2.2.3 A priori error analysis

Now we are in the position to prove the following a priori error estimate.

Theorem 2.2.2. *(A priori error estimate) Let* $u = (u_1, u_2)$ *with* $u_1 \in H^1_{D_0}(\Omega^1) \cap H^{r+1}(\Omega^1)$, $u_2 \in \tilde{H}^{r+1/2}(\Sigma^2)$, $r \geq 1$, *be the solution of (2.2) and let* $U \in \mathcal{V}_{hp} := \mathcal{V}^1_{hp,\Omega} \times \mathcal{V}^2_{hp,\Gamma}$ *be the solution of the discrete problem (2.3). Assume that the discrete spaces* $\mathcal{V}^1_{hp,\Omega}$ *and* $\mathcal{V}^2_{hp,\Gamma}$ *have quasiuniform and compatible meshes and polynomial degree, with characteristical discretization parameters denoted by* h *and* p*, respectively. Then the following a priori error estimate holds*

$$|||u - U|||_h \leq C \left(\frac{h}{p}\right)^r p^{\max\{2-\gamma,0\}+\max\{\alpha-\gamma,0\}+|1/2-\gamma/2|} \left(||u_1||_{H^{r+1}(\Omega^1)} + ||u_2||_{\tilde{H}^{r+1/2}(\Sigma^2)}\right),$$

where the parameter α *stands for the exponent of* p *in the definition of the bilinear form (2.4) and the parameter* γ *is the exponent of* p *in the definition of the discrete norms (2.5).*

Proof. For some $\Phi \in \mathcal{V}_{hp}$ there holds

$$|||u - U|||_h \leq |||u - \Phi|||_h + |||U - \Phi|||_h.$$

Coercivity and continuity of $a_h(\cdot,\cdot)$ shown in Lemma 2.2.3 and Lemma 2.2.1 respectively combined with Theorem 2.2.1 provide for the second term

$$\begin{aligned} |||U - \Phi|||_h^2 &\leq Cp^{\max\{2-\gamma,0\}}\, a_h(U - \Phi, U - \Phi) \\ &= Cp^{\max\{2-\gamma,0\}} \left(a_h(u - \Phi, U - \Phi) + \left\langle \hat{E}u_2, U_2 - \Phi_2 \right\rangle_{\Sigma^2}\right) \\ &\leq Cp^{\max\{2-\gamma,0\}} \left(p^{\max\{\alpha-\gamma,0\}}|||u - \Phi|||_h + ||\hat{E}u_2||_{H^{-1/2}(\Gamma^2)}\right) |||U - \Phi|||_h \end{aligned}$$

and therefore with Lemma 1.4.2 we obtain

$$\begin{aligned} |||u - U|||_h &\leq Cp^{\max\{2-\gamma,0\}} \left(p^{\max\{\alpha-\gamma,0\}}|||u - \Phi|||_h + ||\hat{E}u_2||_{H^{-1/2}(\Gamma^2)}\right) \\ &\leq C \left(\frac{h}{p}\right)^r p^{\max\{2-\gamma,0\}+\max\{\alpha-\gamma,0\}+|1/2-\gamma/2|} \left(||u_1||_{H^{r+1}(\Omega^1)} + ||u_2||_{\tilde{H}^{r+1/2}(\Sigma^2)}\right). \end{aligned}$$

□

As shown in Lemma 2.2.3, to ensure coercivity of the bilinear form the penalty-like parameter λ^{Nit} must be chosen such that

$$\lambda^{Nit} \geq 1/2p^{\gamma-\alpha} + C_{inv}p^{2-\alpha}.$$

It can be chosen independent of the polynomial degree, if

$$\alpha \geq \max\{\gamma, 2\}. \tag{2.9}$$

On the other hand, the parameter α in the definition of the bilinear form (2.4) should not be too large, since, due to Theorem 2.2.2, large values of α will damage the convergence rate. To find the optimal values of α and γ we note that

$$\inf\{\max\{2-\gamma,0\}+\max\{\alpha-\gamma,0\}+|1/2-\gamma/2|\}=1/2$$

and the infimum is achieved if and only if $\gamma=2,\ \alpha\leq\gamma$, which together with (2.9) yields that $\alpha=2$ and $\gamma=2$ are optimal parameters, and therefore the following theorem holds.

Theorem 2.2.3. *(A priori error estimate) Let $u=(u_1,u_2)$ with $u_1\in H^1_{D_0}(\Omega^1)\cap H^{r+1}(\Omega^1), u_2\in\tilde{H}^{r+1/2}(\Gamma^2)$ be the solution of (2.2) and let $U\in\mathcal{V}_{hp}:=\mathcal{V}^1_{hp,\Omega}\times\mathcal{V}^2_{hp,\Gamma}$ be the solution of the discrete problem (2.3). Assume that the discrete spaces $\mathcal{V}^1_{hp,\Omega}$ and $\mathcal{V}^2_{hp,\Gamma}$ have quasiuniform and compatible meshes and polynomial degree, with characteristical discretization parameters denoted by h and p, respectively. Then for $\alpha=2$ in the definition of the bilinear form (2.4) and for $\gamma=2$ in the definition of the discrete norms (2.5) the following a priori error estimate holds*

$$|||u-U|||_h\leq C\left(\frac{h}{p}\right)^r p^{1/2}\left(||u_1||_{H^{r+1}(\Omega^1)}+||u_2||_{\tilde{H}^{r+1/2}(\Sigma^2)}\right).$$

2.2.4 Algebraic formulation

The algebraic system corresponding to the weak formulation (2.3) will be described in this section. We denote by u_I and D_I the coefficient vectors associated with the interface from the FE side and from the BE side, respectively. The rest of the coefficients from the FE side we denote by u_N and from the BE side we denote by D_N. Then the algebraic problem has the following structure

$$(\mathfrak{A}+\mathfrak{B}+\mathfrak{C})\begin{pmatrix}u_N\\u_I\\D_I\\D_N\end{pmatrix}=\begin{pmatrix}l_u\\0\\0\\l_D\end{pmatrix}.$$

The matrix $\mathfrak{A}$ is the stiffness matrix of the finite element and the boundary element part produced with the term $(\nabla U,\nabla V)_{\Omega^1}+\langle S_hU,V\rangle_{\partial\Omega^2}$ without the coupling terms

$$\mathfrak{A}:=\begin{pmatrix}A_{NN}&A_{IN}^T&0&0\\A_{IN}&A_{II}&0&0\\0&0&S_{II}&S_{IN}^T\\0&0&S_{IN}&S_{NN}\end{pmatrix}:=\begin{pmatrix}\mathcal{A}&0\\0&\mathcal{S}\end{pmatrix}.$$

The mixed terms $-\langle\{\nabla_nU\},[V]\rangle_{\Gamma_I}-\langle[U],\{\nabla_nV\}\rangle_{\Gamma_I}$ yield the matrix $\mathfrak{B}$, given by

$$\mathfrak{B}:=\begin{pmatrix}0&0&(B_{NI}^{uD})^T&0\\0&0&(B_{II}^{uD})^T&0\\B_{NI}^{uD}&B_{II}^{uD}&B_{II}^{DD}+(B_{II}^{DD})^T&0\\0&0&0&0\end{pmatrix}.$$

Finally, the penalty-like term $\left\langle \lambda h_1^{-1} p_1^{\alpha}[U],[V]\right\rangle_{\Gamma_I}$ yields the matrix $\mathfrak{C}$

$$\mathfrak{C} := \begin{pmatrix} 0 & 0 & 0 & 0 \\ 0 & C^{uu} & (C^{uD})^T & 0 \\ 0 & C^{uD} & C^{DD} & 0 \\ 0 & 0 & 0 & 0 \end{pmatrix}.$$

The matrices $\mathfrak{B}$, $\mathfrak{C}$ are sparse as well as the finite element part $\mathcal{A}$ of the matrix $\mathfrak{A}$. The boundary element part $\mathcal{S}$ of the matrix $\mathfrak{A}$ is a dense matrix.

2.2.5 Numerical experiments

We present a series of numerical examples for the hp-FE/BE coupling with Nitsche's method on uniform meshes, nonmatched across the coupling interface. First, we consider an example with a smooth solution and investigate convergence of the h-version for different polynomial degrees. We also show that the p-version converges with an exponential rate. Then, an example with a singular solution will be presented. We compare the convergence of h- and p-versions. Finally, we study dependence of the convergence rates on the penalty-like parameter λ^{Nit}. We show that there exists a threshold value, such that for smaller λ^{Nit} no convergence, or a reduced convergence rate takes place, and for larger λ^{Nit}, no improvement of the convergence rate is observed. This threshold value can be interpreted as a coercivity threshold of the bilinear form $a_h(\cdot,\cdot)$ in the weak problem (2.3), which coincides with our theoretical results.

Example 1: smooth solution

In the first example we consider a square domain $\Omega := [-1,1]\times[-1,1]$. We introduce the boundary element domain Ω^2 and its complement Ω^1, where finite elements will be employed (Figure 2.1)

$$\begin{aligned} \Omega^2 &:= [-1,0]\times[-\tfrac{1}{2},\tfrac{1}{2}], \\ \Omega^1 &:= \Omega\setminus\Omega^2. \end{aligned} \tag{2.10}$$

The interface boundary is given by

$$\Gamma_I := \partial\Omega^1 \cap \partial\Omega^2. \tag{2.11}$$

Let $G(\boldsymbol{\xi},\boldsymbol{\eta})$ stand for the fundamental solution of the two-dimensional Laplace operator

$$G(\boldsymbol{\xi},\boldsymbol{\eta}) := -\frac{1}{2\pi}\log|\boldsymbol{\xi}-\boldsymbol{\eta}|.$$

In particular for $\boldsymbol{\eta}\notin\overline{\Omega}$ there holds

$$\Delta_{\boldsymbol{\xi}} G(\boldsymbol{\xi},\boldsymbol{\eta}) = 0, \qquad \forall\boldsymbol{\xi}\in\Omega\subset\mathbb{R}^2.$$

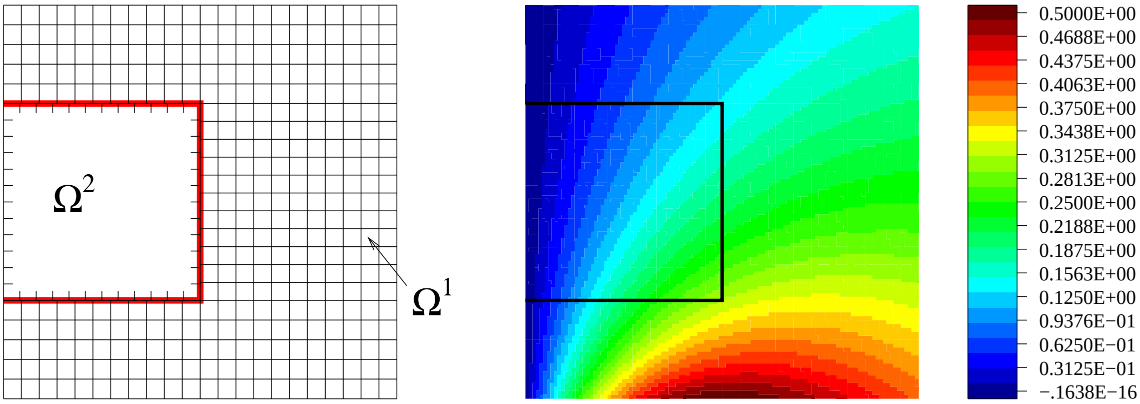

Figure 2.1: Geometry and the numerical solution: smooth case
$$u(x,y) = \frac{x+1}{(x+1)^2+(y+2)^2}$$

We fix $\boldsymbol{\eta} = (-1,-2)$ and let $\boldsymbol{\xi} = (x,y)$ be variable. We define

$$u(x,y) := -2\pi \frac{\partial}{\partial x} G((-1,-2),(x,y)) = \frac{x+1}{(x+1)^2+(y+2)^2}. \tag{2.12}$$

The function $u(x,y)$ is an exact solution of problem (2.1) with

$$\Gamma_D := \{-1\} \times [-1,1], \qquad \Gamma_N = \partial\Omega \setminus \Gamma_D, \qquad f = 0, \qquad \hat{t} = \left.\frac{\partial u}{\partial n}\right|_{\Gamma_N}.$$

Moreover, the function $u(x,y)$ is an exact solution of the interface problem (2.2) with the decomposition (2.10) and with the interface boundary (2.11).

In order to study the convergence of the method we choose $\lambda^{Nit} := 10.0$ and perform a series of experiments for the uniform h- and p-version. The error reduction for the h-version for $p_1 = p_2 = 1,2,3$ in the BE and FE parts is presented in Table 2.1 and in Table 2.2, respectively.

The numerical experiments for the p-version are obtained for the fixed meshes with the meshsize relation $h_1/h_2 = 6/5$ on the interface boundary with 24 boundary elements and 75 finite elements with increasing $p_1 \equiv p_2$. Since the exact solution $u(x,y)$ is an infinitely differentiable function, the exponential convergence of the p-version is observed. The results, obtained for the h-version with $p = 2$, are compared with the p-version and given in Figure 2.2.

h^{-1}	p	L_2-norm	convergence rate	H_0^1-norm	convergence rate
3	1	0.0045807		0.0263224	
6	1	0.0009919	2.2073015	0.0124597	1.0790217
12	1	0.0001865	2.4110190	0.0061552	1.0173917
24	1	.3870E-04	2.2687702	0.0030679	1.0045543
48	1	.9604E-05	2.0106263	0.0015314	1.0024003
3	2	0.0001306		0.0022084	
6	2	.1248E-04	3.3874651	0.0004878	2.1786398
12	2	.1520E-05	3.0374747	0.0001188	2.0377549
24	2	.1887E-06	3.0099050	.2944E-04	2.0126853
48	2	.2354E-07	3.0029082	.7331E-05	2.0056958
3	3	.8771E-05		0.0001550	
6	3	.2772E-06	4.9837422	.1629E-04	3.2502097
12	3	.1771E-07	3.9682911	.1991E-05	3.0324215
24	3	.1126E-08	3.9752855	.2469E-06	3.0114945
48	3	.9843E-10	3.5159649	.3077E-07	3.0043305

Table 2.1: Convergence rates for h-version: BE part

h^{-1}	p	L_2-norm	convergence rate	H_0^1-norm	convergence rate
2	1	0.0090366		0.1020531	
5	1	0.0017310	1.8035583	0.0462404	0.8639609
11	1	0.0003120	2.1731693	0.0196812	1.0833687
23	1	.6483E-04	2.1302020	0.0088135	1.0891816
47	1	.1567E-04	1.9870058	0.0043547	0.9865327
2	2	0.0009280		0.0153579	
5	2	0.0001072	2.3555138	0.0031937	1.7139209
11	2	.8249E-05	3.2526861	0.0005648	2.1972827
23	2	.7335E-06	3.2809424	0.0001119	2.1947782
47	2	.8861E-07	2.9574937	.2732E-04	1.9729656
2	3	0.0003011		0.0069455	
5	3	.5454E-05	4.3775333	0.0002450	3.6501417
11	3	.1662E-06	4.4275225	.1710E-04	3.3764410
23	3	.7526E-08	4.1958143	.1780E-05	3.0673378
47	3	.4995E-09	3.7955622	.1774E-06	3.2266853

Table 2.2: Convergence rates for h-version: FE part

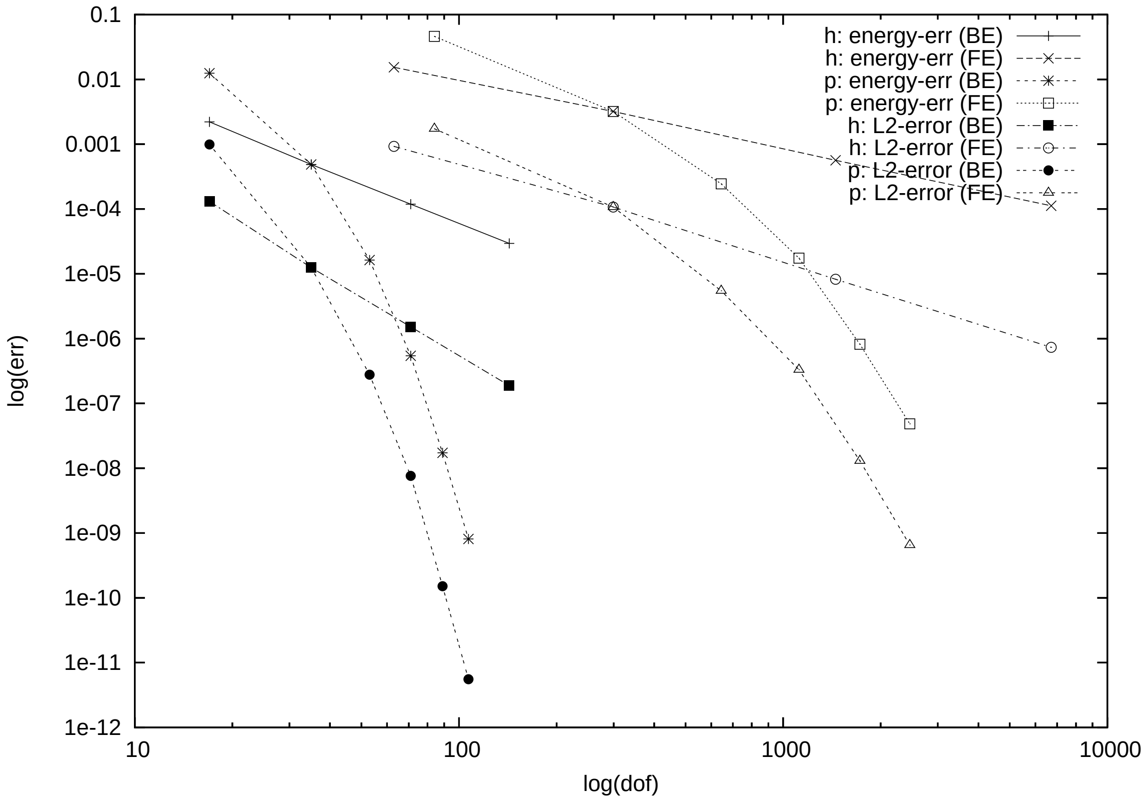

Figure 2.2: h-version with $p_1 = p_2 = 2$ vs. p-version with $h_1 = 1/5$ $h_2 = 1/6$

Example 2: singular solution

For our second example we choose Ω to be an L-shaped domain

$$\Omega := \{[-1,1] \times [-1,1]\} \setminus \{[0,1] \times [-1,0]\} \tag{2.13}$$

and the decomposition

$$\begin{aligned} \Omega^2 &:= \{[-\tfrac{1}{2}, \tfrac{1}{2}] \times [-\tfrac{1}{2}, \tfrac{1}{2}]\} \setminus \{[0, \tfrac{1}{2}] \times [-\tfrac{1}{2}, 0]\}, \\ \Omega^1 &:= \Omega \setminus \Omega^2. \end{aligned} \tag{2.14}$$

as shown in Figure 2.3. We define also

$$\begin{aligned} &\Gamma_D := \{\{0\} \times [-1,0]\} \cup \{[0,1] \times \{0\}\}, \\ &\Gamma_N := \partial\Omega \setminus \Gamma_D, \qquad \Gamma_I := \partial\Omega^1 \cap \partial\Omega^2. \end{aligned} \tag{2.15}$$

For this kind of domain, $r^{2/3}$ is a typical singularity, located in the origin. Here (r, θ) stand for the spherical coordinates on the plane. We choose

$$u(r, \theta) := r^{2/3} \sin(2\theta/3).$$

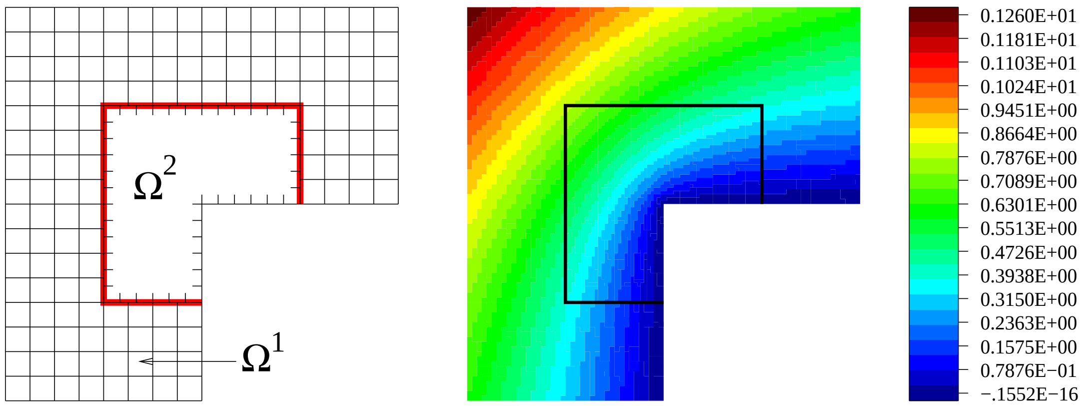

Figure 2.3: Geometry and the numerical solution: singular case $u(r, \theta) = r^{2/3} \sin(2\theta/3)$

It is easy to check that $u(r, \theta)$ is an exact solution of (2.1) and (2.2) with (2.13)-(2.15). There holds

$$u \in H^1(\Omega), \quad u \notin H^2(\Omega),$$

therefore even the h-version does not provide linear convergence in the energy norm and quadratic convergence in the L_2-norm, respectively. Corresponding results are given in Table 2.3 and Table 2.4. It is possible to show that $u \in H^{5/3}(\Omega)$, therefore the convergence rate $2/3$ for the h-version in the H_0^1-norm, is optimal. The theoretical convergence rate agrees with the numerical convergence rate ≈ 0.66, as shown in Table 2.3.

Furthermore, Table 2.3 and Figure 2.4 show that in the BE domain Ω^2, which includes the singularity, the p-version gives a better convergence rate in the energy norm than the h-version (0.8 vs. 0.66), but a worse convergence rate in the L_2-norm (1.19 vs. 1.4). In the FE domain Ω^1 the p-version provides a significantly better convergence rate than the h-version (see Table 2.4, Figure 2.4), although the singularity affects the FE domain across the coupling interface.

It is known from the work of Stephan and Suri [64], that the convergence rate for the p-version of the BEM in the energy norm is twice that the corresponding convergence rate of the h-version. Therefore, we expect the convergence rate $4/3$ in the energy norm in our example. Due to Theorem 2.2.3, the p-version of our FE/BE Nitsche's coupling is suboptimal, caused by the factor $p^{1/2}$. Thus, for our example the convergence rate $4/3 - 1/2 = 5/6 \approx 0.83$ is expected. This result is in agreement with the numerical experiments. As shown in Table 2.3, the numerical rate of convergence is ≈ 0.8, which is very near to the theoretical estimate 0.83.

h^{-1}	p	L_2-norm	convergence rate	H_0^1-norm	convergence rate
8	1	0.0025194		0.0885605	
12	1	0.0013665	1.5088057	0.0681681	0.6454544
20	1	0.0006334	1.5052218	0.0489318	0.6490458
36	1	0.0002642	1.4876073	0.0333037	0.6545895
68	1	0.0001044	1.4598948	0.0219059	0.6586791
132	1	.4043E-04	1.4302214	0.0141255	0.6615079
260	1	.1561E-04	1.4038779	0.0090096	0.6633788
6	1	0.0039545		0.1061839	
6	2	0.0012297	1.6851889	0.0525158	1.0157416
6	3	0.0006871	1.4355013	0.0364846	0.8982865
6	4	0.0004864	1.2007996	0.0285718	0.8497924
6	5	0.0003743	1.1740143	0.0238089	0.8172352
6	6	0.0003023	1.1717633	0.0205406	0.8098661
6	7	0.0002515	1.1934875	0.0181426	0.8053202

Table 2.3: Convergence rates for BE part: h-version (above) and p-version (below)

h^{-1}	p	L_2-norm	convergence rate	H_0^1-norm	convergence rate
4	1	0.0011601		0.0316011	
8	1	0.0005921	0.9703364	0.0158300	0.9973135
16	1	0.0003858	0.6179877	0.0079073	1.0014042
32	1	0.0001986	0.9579875	0.0039502	1.0012595
64	1	.9029E-04	1.1372275	0.0019737	1.0010230
128	1	.3852E-04	1.2289585	0.0009864	1.0006580
256	1	.1590E-04	1.2765809	0.0004930	1.0005852
4	1	0.0013727		0.0316477	
4	2	0.0006130	1.1630574	0.0020695	3.9347465
4	3	0.0002444	2.2679108	0.0006354	2.9122298
4	4	0.0001239	2.3613965	0.0001039	6.2945383
4	5	.7227E-04	2.4157798	.5954E-04	2.4951675
4	6	.4618E-04	2.4564418	.3801E-04	2.4615799
4	7	.3149E-04	2.4837826	.2606E-04	2.4485634

Table 2.4: Convergence rates for FE part: h-version (above) and p-version (below)

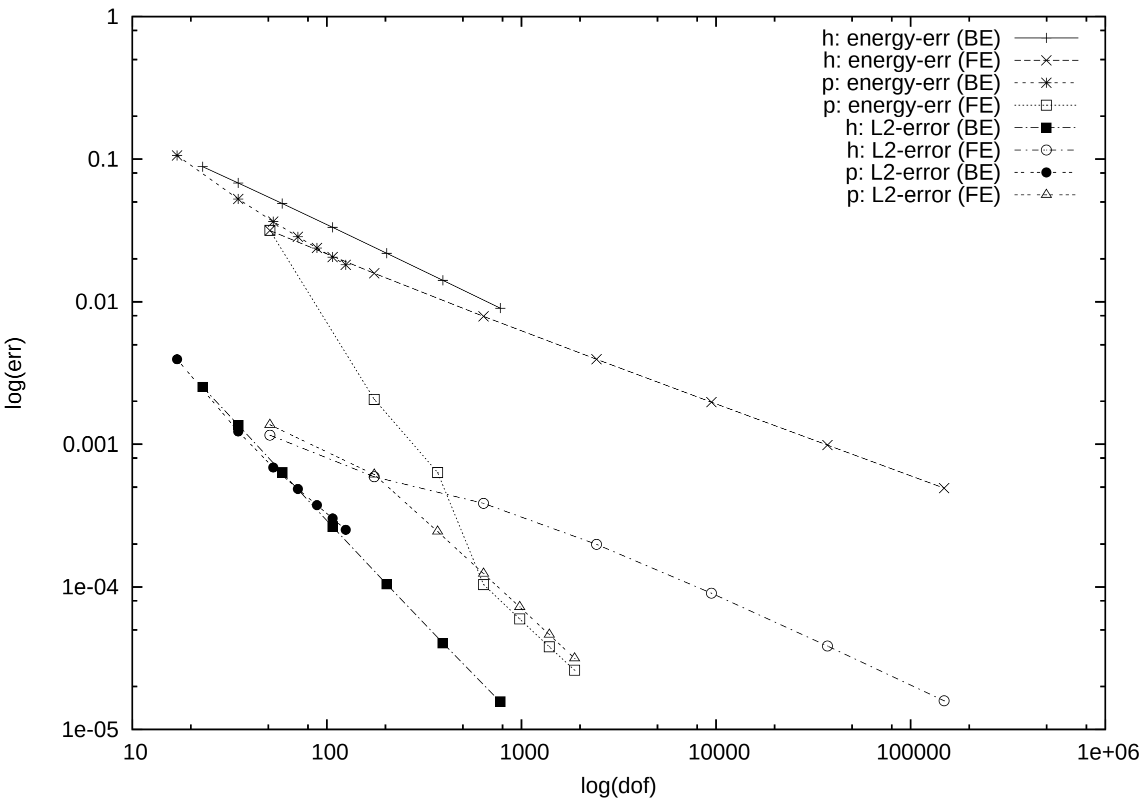

Figure 2.4: h-version with $p_1 = p_2 = 1$ vs. p-version with $h_1 = 1/6$ $h_2 = 1/8$

Example 3: choice of λ^{Nit}

In this section we study convergence of the method for different values of the penalty-like parameter λ^{Nit}. We perform a series of tests for a smooth exact solution and the geometry, described in Example 1. The convergence rates for the h-version for $p_1 = p_2 = 1, 2, 3$ are shown in Figures 2.5–2.8.

For $\lambda^{Nit} = 1.0$ we observe no convergence in the piecewise linear case. Furthermore, for $\lambda^{Nit} = 5.0$ we observe a reduced convergence rate for the piecewise cubic case. On the other hand, the convergence rates for $\lambda^{Nit} = 10.0$ and $\lambda^{Nit} = 20.0$ are almost the same, i.e. the bilinear form becomes coercive. Since our coupling method is consistent (unlike the penalty method), we do not observe any improvement of the convergence rate with increase of λ^{Nit}, if coercivity of the bilinear form is already achieved.

A similar behaviour we have for the singular example, described in Example 2. As it is shown in Figures 2.9–2.12, the convergence curves do not change starting from $\lambda^{Nit} = 5.0$.

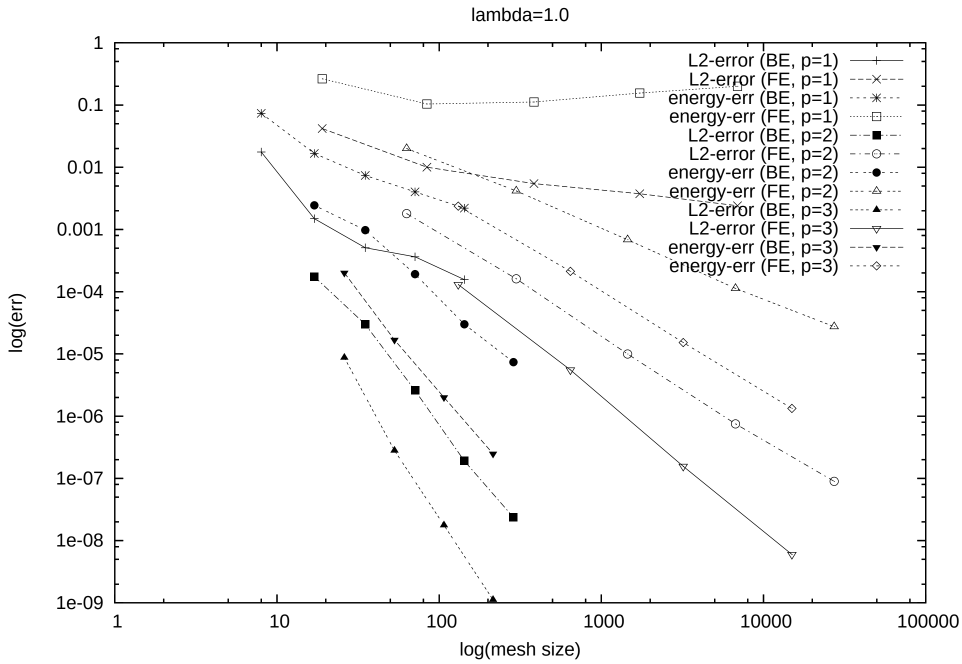

Figure 2.5: h-version with $\lambda^{Nit} = 1$: smooth solution

$$u(x,y) = \frac{x+1}{(x+1)^2 + (y+2)^2}$$

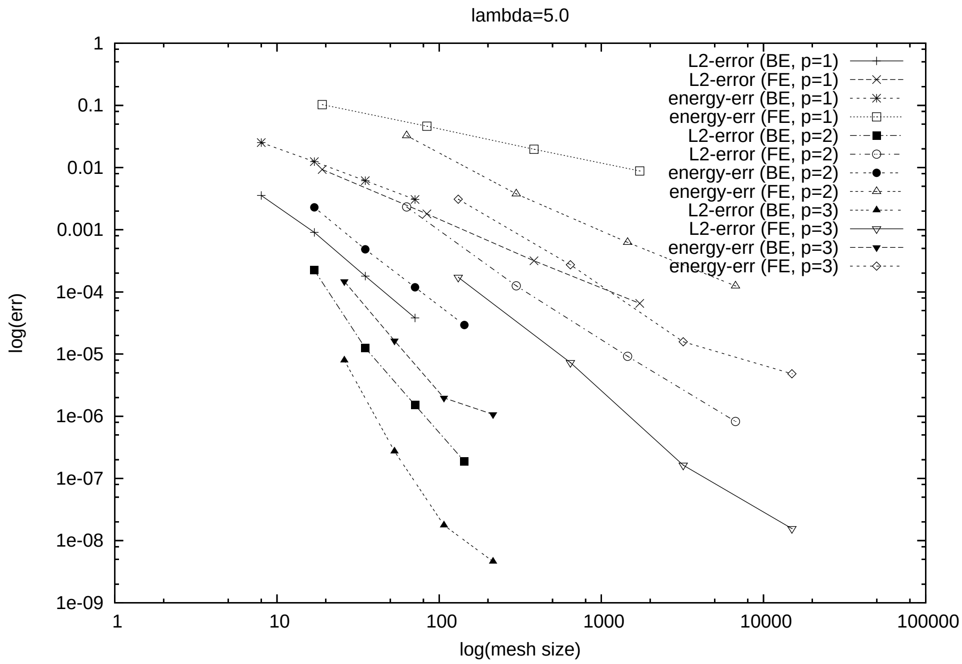

Figure 2.6: h-version with $\lambda^{Nit} = 5$: smooth solution

$$u(x,y) = \frac{x+1}{(x+1)^2 + (y+2)^2}$$

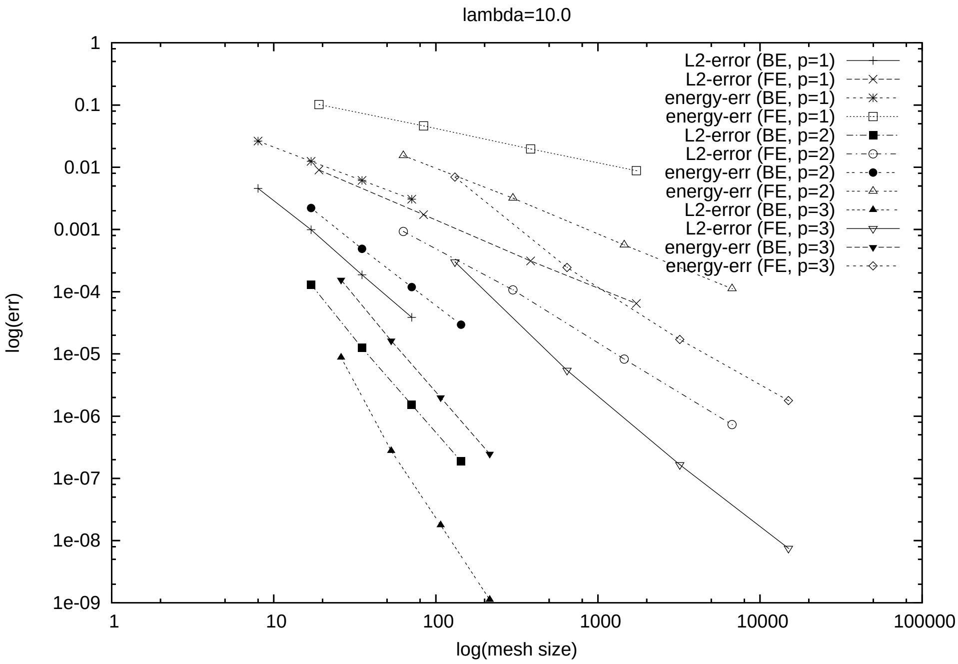

Figure 2.7: h-version with $\lambda^{Nit} = 10$: smooth solution
$$u(x,y) = \frac{x+1}{(x+1)^2 + (y+2)^2}$$

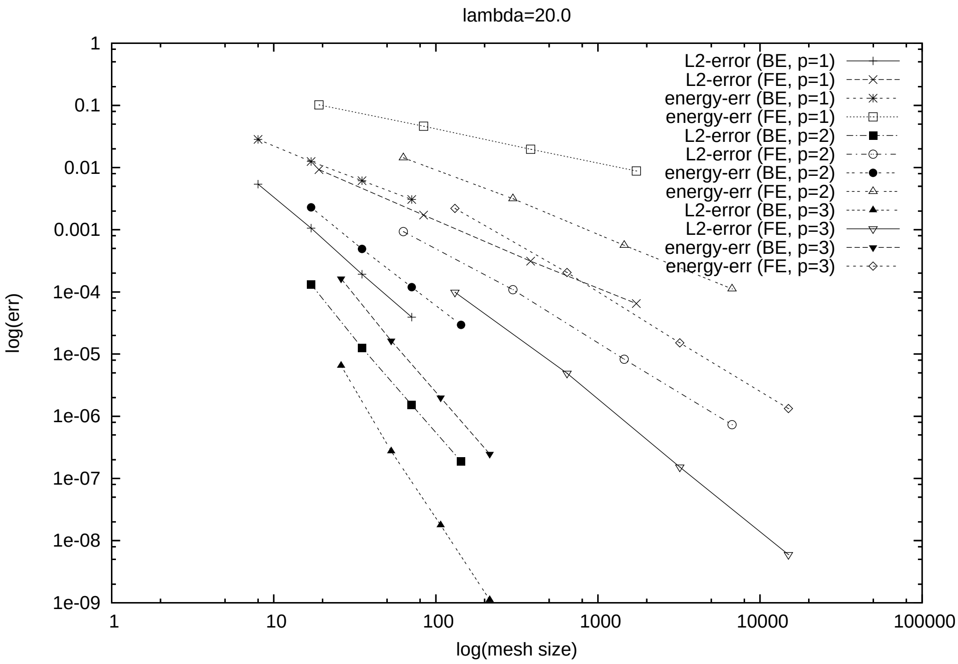

Figure 2.8: h-version with $\lambda^{Nit} = 20$: smooth solution
$$u(x,y) = \frac{x+1}{(x+1)^2 + (y+2)^2}$$

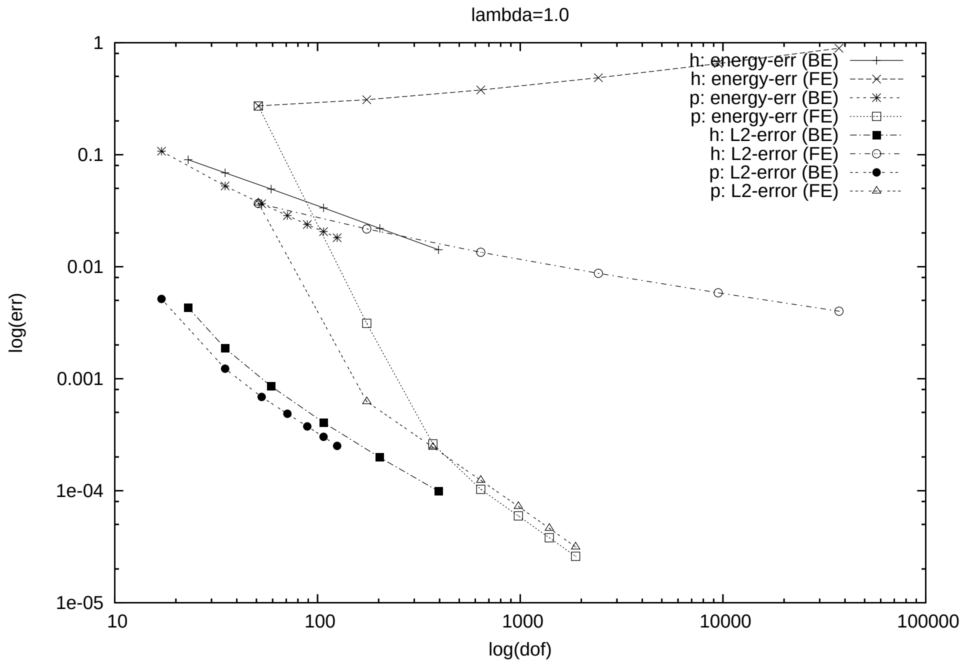

Figure 2.9: h- and p-version for $\lambda^{Nit} = 1$: singular solution $u(r,\theta) = r^{2/3}\sin(2\theta/3)$

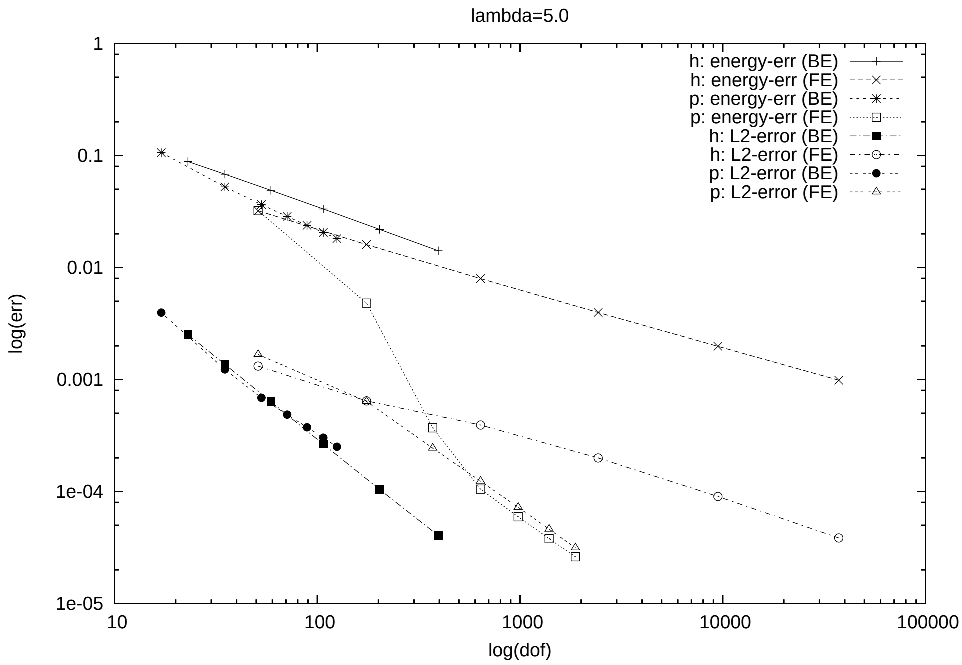

Figure 2.10: h- and p-version for $\lambda^{Nit} = 5$: singular solution $u(r,\theta) = r^{2/3}\sin(2\theta/3)$

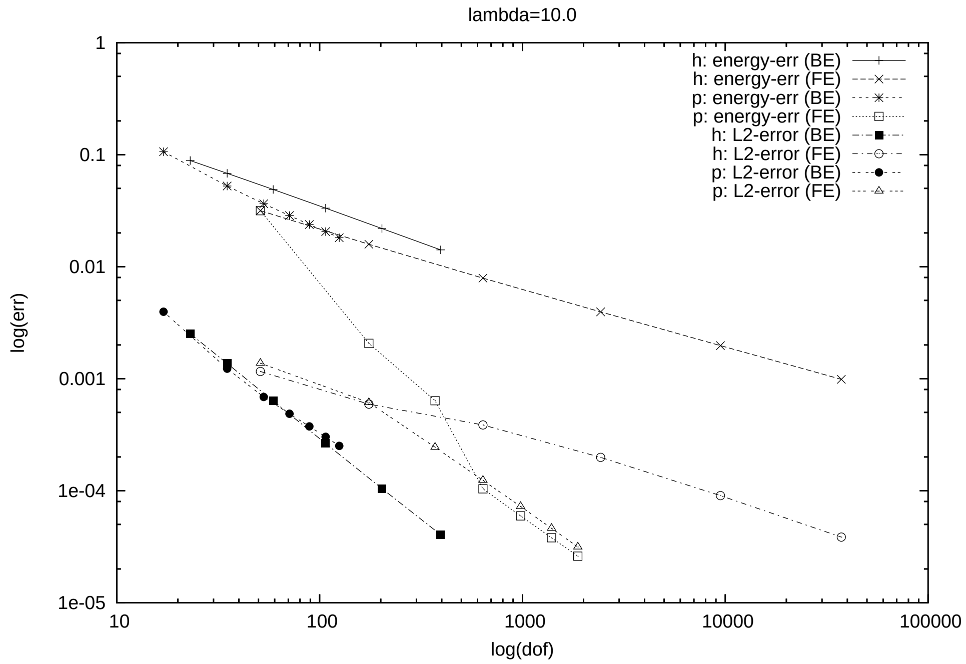

Figure 2.11: h- and p-version for $\lambda^{Nit} = 10$: singular solution $u(r, \theta) = r^{2/3} \sin(2\theta/3)$

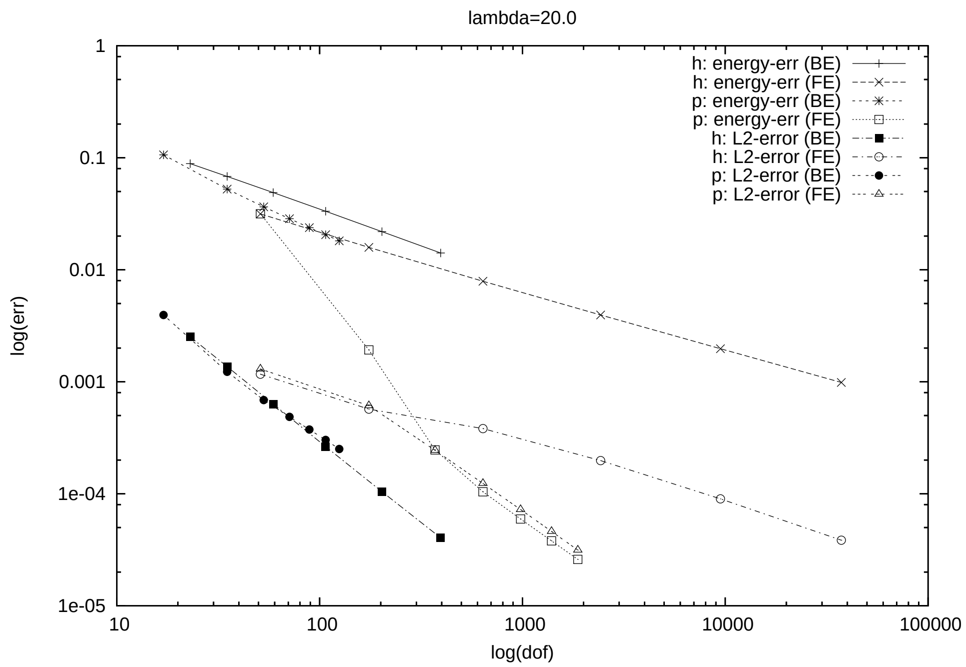

Figure 2.12: h- and p-version for $\lambda^{Nit} = 20$: singular solution $u(r, \theta) = r^{2/3} \sin(2\theta/3)$

3 Contact between a body and a rigid obstacle

Contact problems between an elastic body and a rigid obstacle are addressed in this chapter. We investigate questions related to variational formulation (such as well-posedness of the problem), as well as topics connected with discretization, convergence of numerical methods and automatic mesh refinement procedures.

In Section 3.1 we derive a boundary integral formulation for contact problems with Tresca's law of friction. Constructing a chain of equivalent formulations we approximate the frictional contact problem with a sequence of the frictionless problems. This procedure can be treated as an Uzawa-type algorithm. We prove that the sequence of approximate solutions converges to the exact solution of the problem with friction in the energy norm, when the damping parameter is sufficiently small.

The rest of the chapter is devoted to the investigation of the numerical solution procedures with the penalty method. In Section 3.2 we formulate an *hp*-penalty Boundary Element Method for frictionless problems and investigate its convergence. The solution of the variational inequality $\boldsymbol{u}$ is approximated with the continuous piecewise polynomial solution of the discrete penalty formulation $\boldsymbol{U}^{\varepsilon}$. The a priori error analysis shows, that under additional regularity assumptions on $\boldsymbol{u}$ and on corresponding traction $\mathcal{T}\boldsymbol{u}$ that the error $\boldsymbol{u} - \boldsymbol{U}^{\varepsilon}$ converges as $\mathcal{O}((h/p)^{1-\epsilon})$ in the energy norm. This convergence rate is achieved if the penalty parameter ε_n is proportional to $(h/p)^{1-\epsilon}$ for arbitrary small fixed $\epsilon > 0$.

In Section 3.3 we derive residual-based a posteriori error estimates and employ them in the automatic mesh refinement procedures. We obtain the a posteriori error estimates for the h-version of penalty BEM and FEM for one-body contact with Tresca's friction. Furthermore, we prove that the error estimates are reliable and efficient. Finally, we introduce an automatic mesh refinement procedure, based on these estimates, and illustrate the suggested method on several numerical examples.

The classical formulation of a contact problem between an elastic body and a rigid obstacle with *Tresca's law* of friction, considered in this chapter, is given as follows. Let a linear elastic body occupy a bounded polygonal two-dimensional domain Ω with (Lipschitz) boundary Γ with the exterior normal vector $\boldsymbol{n}$. We assume that Γ is decomposed into three disjoint parts $\overline{\Gamma} = \overline{\Gamma}_D \cup \overline{\Gamma}_N \cup \overline{\Gamma}_C$. We denote for brevity $\overline{\Sigma} := \overline{\Gamma}_N \cup \overline{\Gamma}_C$. For the sake of simplicity we assume that the volume force vanishes. The case of a nonvanishing volume force can be treated with the similar arguments employing Newton potentials, as in the works of Eck, Steinbach and Wendland [26],[27]. We fix the body along Γ_D and prescribe some surface tractions $\hat{\boldsymbol{t}}$ along Γ_N. Γ_C is the zone of possible frictional contact of the body with a rigid smooth obstacle. Let $g : \Gamma_C \to \mathbb{R}^+ \cup \{0\}$ be a continuous mapping associating every point $x \in \Gamma_C$ with its distance to the rigid obstacle measured in the direction of $\boldsymbol{n}(x)$ (cf. [73], see also [38], [26]).

Then the displacement field $\boldsymbol{u}$ satisfies the following boundary value problem

$$\begin{aligned} -\mathrm{div}\ \sigma(\boldsymbol{u}) &= 0 && \text{in } \Omega,\\ \boldsymbol{u} &= 0 && \text{on } \Gamma_D,\\ \sigma(\boldsymbol{u}) \cdot \boldsymbol{n} &= \hat{\boldsymbol{t}} && \text{on } \Gamma_N,\\ \left.\begin{array}{c} \sigma_n \leq 0, \quad u_n \leq g, \quad \sigma_n(u_n - g) = 0,\\ |\sigma_t| \leq \mathcal{F}, \quad \sigma_t u_t + \mathcal{F}|u_t| = 0, \end{array}\right\} && && \text{on } \Gamma_C. \end{aligned} \tag{3.1}$$

Here σ stands for the stress tensor. It is connected with the displacement field $\boldsymbol{u}$ by Hook's law of elasticity, i.e. under small strain assumption there holds

$$\sigma(\boldsymbol{u}) = \mathbb{C} : \varepsilon(\boldsymbol{u}) = \overline{\lambda}\mathrm{tr}\varepsilon(\boldsymbol{u})\boldsymbol{I} + 2\overline{\mu}\varepsilon(\boldsymbol{u}), \qquad \varepsilon(\boldsymbol{u}) = \frac{1}{2}(\nabla\boldsymbol{u} + \nabla\boldsymbol{u}^T),$$

where $\overline{\lambda}$, $\overline{\mu}$ are the Lamé constants and $\boldsymbol{I}$ is the unit tensor of the second order. The normal and tangential stress on the contact boundary is given by

$$\sigma_n = \boldsymbol{n} \cdot \sigma(\boldsymbol{u}) \cdot \boldsymbol{n}, \qquad \sigma_t \boldsymbol{t} = \sigma(\boldsymbol{u}) \cdot \boldsymbol{n} - \sigma_n \boldsymbol{n}.$$

The so-called given friction function $\mathcal{F} \geq 0$ defines pointwise the sticking threshold of the bodies. As it can be seen from (3.1), if the absolute value of the tangential stress does not exceed the value of the given friction function $|\sigma_t| < \mathcal{F}$, then $u_t = 0$. Moreover, $u_t \neq 0$ is only possible if $|\sigma_t| = \mathcal{F}$. It is worth to mention that in the Tresca's model of friction the tangential stress is not necessarily zero when the body does not touch the obstacle. This nonphysical phenomenon disappears for the more general and realistic *Coulomb's law* of friction. This model consists of setting $\mathcal{F} := \mu_f \sigma_n$, where μ_f is the friction coefficient. Now, opening of the gap yields $\sigma_n = 0$, which provides $\mathcal{F} = 0$ and $\sigma_t = 0$.

3.1 Boundary weak formulations for contact problems with Tresca's law of friction

In this section we derive and analyse a boundary integral variational inequality formulation for contact problems with Tresca's law of friction. We introduce a constraint minimization problem and prove its equivalence to the original boundary integral variational inequality formulation. We show that the both problems are well-posed, i.e. that they have unique identical solutions. Further, we obtain a mixed formulation, which includes an auxiliary variable corresponding to the tangential traction. We prove equivalence between the mixed formulation and the original variational inequality. Then we formulate an Uzawa-type algorithm for solution of the mixed problem. It allows to obtain a solution of the contact problem with friction as a sequence of frictionless problems with changing right hand side. Finally, convergence of the Uzawa algorithm is investigated and conditions, which guarantee the convergence, are obtained. The results of this section will be also employed in Section 4.3, where we construct a solution algorithm for *hp*-mortar BEM applied for two-body frictional contact problems.

3.1.1 Boundary integral variational inequality

In order to derive the weak formulation of (3.1) we assume that $\mathcal{F} \in L_2(\Gamma_C)$ and $\hat{\boldsymbol{t}} \in \boldsymbol{H}^{-1/2}(\Gamma_N)$. For simplicity of presentation we assume that the gap function g is zero, i.e. *the body is in contact* with the obstacle along the whole $\overline{\Gamma}_C$, but the gap can open during the deformation process. After testing the first equation with $\boldsymbol{v} \in \boldsymbol{\mathcal{V}}_F := \{\boldsymbol{v} \in \boldsymbol{H}^1(\Omega) : \boldsymbol{v}|_{\Gamma_D} = 0\}$ we obtain

$$0 = \int_\Omega \operatorname{div} \sigma(\boldsymbol{u}) \cdot \boldsymbol{v}\, dx = \int_\Omega \operatorname{div}(\sigma(\boldsymbol{u}) \cdot \boldsymbol{v})\, dx - \int_\Omega \sigma(\boldsymbol{u}) : \nabla \boldsymbol{v}\, dx. \tag{3.2}$$

Application of Gauss theorem gives for the traction operator $\boldsymbol{\mathcal{T}}(\boldsymbol{u}) := \sigma(\boldsymbol{u}) \cdot \boldsymbol{n}$

$$\int_\Omega \operatorname{div}(\sigma(\boldsymbol{u}) \cdot \boldsymbol{v})\, dx = \int_\Gamma \boldsymbol{\mathcal{T}}(\boldsymbol{u}) \cdot \boldsymbol{v}\, ds,$$

and, due to symmetry of σ the last summand in (3.2) becomes

$$\int_\Omega \sigma(\boldsymbol{u}) : \nabla \boldsymbol{v}\, dx = \int_\Omega \sigma(\boldsymbol{u}) : \varepsilon(\boldsymbol{v})\, dx = \int_\Omega \varepsilon(\boldsymbol{u}) : \mathbb{C} : \varepsilon(\boldsymbol{v})\, dx.$$

We define a bilinear form $\beta(\cdot,\cdot)$ on $\boldsymbol{H}^1(\Omega)$ by

$$\beta(\boldsymbol{u}, \boldsymbol{v}) := \int_\Omega \varepsilon(\boldsymbol{u}) : \mathbb{C} : \varepsilon(\boldsymbol{v}) dx = \int_\Omega 2\mu\varepsilon(\boldsymbol{u}) : \varepsilon(\boldsymbol{v}) + \lambda \operatorname{tr}\varepsilon(\boldsymbol{u}) \operatorname{tr}\varepsilon(\boldsymbol{v})\, dx.$$

Hence, (3.2) can be rewritten as

$$\beta(\boldsymbol{u}, \boldsymbol{v}) = \int_\Gamma \boldsymbol{\mathcal{T}}(\boldsymbol{u}) \cdot \boldsymbol{v}\, ds. \tag{3.3}$$

Further we introduce $\boldsymbol{\mathcal{K}}_F := \{\boldsymbol{v} \in \boldsymbol{\mathcal{V}}_F : v_n|_{\Gamma_C} \leq 0\}$. Note, that for the solution $\boldsymbol{u}$ of problem (3.1) there holds $\boldsymbol{u} \in \boldsymbol{\mathcal{K}}_F$. Next, we set $\boldsymbol{v} = \boldsymbol{w} - \boldsymbol{u} \in \boldsymbol{\mathcal{V}}_F$ for arbitrary $\boldsymbol{w} \in \boldsymbol{\mathcal{K}}_F$. Introducing the functional

$$L(\boldsymbol{v}) = \int_{\Gamma_N} \hat{\boldsymbol{t}} \cdot \boldsymbol{v}\, ds \tag{3.4}$$

we observe that (3.3) yields for arbitrary $\boldsymbol{w} \in \boldsymbol{\mathcal{K}}_F$

$$\beta(\boldsymbol{u}, \boldsymbol{w} - \boldsymbol{u}) = L(\boldsymbol{w} - \boldsymbol{u}) + \int_{\Gamma_C} \sigma_n(w_n - u_n) ds + \int_{\Gamma_C} \sigma_t(w_t - u_t)\, ds. \tag{3.5}$$

The contact boundary conditions in (3.1) provide

$$\sigma_n(w_n - u_n) = \sigma_n w_n \geq 0$$

and

$$-\sigma_t(w_t - u_t) \leq |\sigma_t||w_t| - \mathcal{F}|u_t| \leq \mathcal{F}(|w_t| - |u_t|).$$

Further, we define the frictional functional

$$j(\boldsymbol{v}) = \int_{\Gamma_C} \mathcal{F}|v_t| ds. \tag{3.6}$$

Note, that $j(\cdot)$ is non-differentiable, due to the absolute value function under the integral sign. Now the problem (3.5) can be reformulated as the following domain formulation: Find $\boldsymbol{u} \in \boldsymbol{\mathcal{K}}_F$ such that

$$\beta(\boldsymbol{u}, \boldsymbol{w} - \boldsymbol{u}) + j(\boldsymbol{w}) - j(\boldsymbol{u}) \geq L(\boldsymbol{w} - \boldsymbol{u}) \qquad \text{for } \forall \boldsymbol{w} \in \boldsymbol{\mathcal{K}}_F. \tag{3.7}$$

In order to derive a symmetric boundary integral formulation we employ the Steklov-Poincaré operator S. It is a Dirichlet-to-Neumann mapping, i.e. (cf. (1.5))

$$\boldsymbol{\mathcal{T}}(\boldsymbol{u}) = S\boldsymbol{u} := W\boldsymbol{u} + (K' + 1/2)V^{-1}(K + 1/2)\boldsymbol{u},$$

which is a continuous mapping $S : \tilde{\boldsymbol{H}}^{1/2}(\Sigma) \to \boldsymbol{H}^{-1/2}(\Gamma)$. Looking back to (3.3) we note that

$$\beta(\boldsymbol{u}, \boldsymbol{v}) = \int_{\Sigma} \boldsymbol{\mathcal{T}}(\boldsymbol{u}) \cdot \boldsymbol{v}\, ds = \int_{\Sigma} S\boldsymbol{u} \cdot \boldsymbol{v}\, ds =: \langle S\boldsymbol{u}, \boldsymbol{v}\rangle_{\Sigma}. \tag{3.8}$$

Here and further down, when a function defined in a domain is integrated over some part of its boundary, the boundary trace operator is ommited for brevity. Introducing the boundary functional sets

$$\boldsymbol{\mathcal{V}} := \tilde{\boldsymbol{H}}^{1/2}(\Sigma), \qquad \boldsymbol{\mathcal{K}} := \{\boldsymbol{v} \in \boldsymbol{\mathcal{V}} : v_n \leq 0 \text{ on } \Gamma_C\},$$

we rewrite the domain formulation (3.7) in terms of boundary integral operators: Find $\boldsymbol{u} \in \boldsymbol{\mathcal{K}}$ such that

$$\langle S\boldsymbol{u}, \boldsymbol{w} - \boldsymbol{u}\rangle_{\Sigma} + j(\boldsymbol{w}) - j(\boldsymbol{u}) \geq L(\boldsymbol{w} - \boldsymbol{u}) \qquad \forall \boldsymbol{w} \in \boldsymbol{\mathcal{K}}. \tag{3.9}$$

Now we are in a position to find a connection between formulations (3.1) and (3.9).

Theorem 3.1.1. *The solution of the classical formulation (3.1) is a solution of problem (3.9). Let $\boldsymbol{u}$ be a solution of (3.9). If the prescribed data $\hat{\boldsymbol{t}}, \mathcal{F}$ are sufficiently regular, such that the function $\boldsymbol{u}(\boldsymbol{x})$, $\boldsymbol{x} \in \Omega$, obtained with the representation formula (1.2) lies in $\boldsymbol{C}^2(\Omega)$, then $\boldsymbol{u}$ solves the classical problem (3.1).*

Proof. It remains only to show the second part of the statement. Equivalence between (3.9) and (3.7) follows from (3.8). Let the boundary data $\hat{\boldsymbol{t}}, \mathcal{F}$ be smooth enough such that the solution of (3.7) has continuous second partial derivatives (the existence and uniqueness of solution (3.7) will be shown later). Then for any $\boldsymbol{w} \in \boldsymbol{\mathcal{K}}_F$ we set $\boldsymbol{v} = \boldsymbol{w} - \boldsymbol{u} \in \boldsymbol{\mathcal{V}}_F$ and insert in (3.7). Then

$$\begin{aligned}
0 &\leq \beta(\boldsymbol{u}, \boldsymbol{v}) + j(\boldsymbol{v} + \boldsymbol{u}) - j(\boldsymbol{u}) - L(\boldsymbol{v}) \\
&= -\int_\Omega \operatorname{div} \sigma(\boldsymbol{u}) \cdot \boldsymbol{v} dx + \int_{\Gamma_N} (\sigma(\boldsymbol{u}) \cdot \boldsymbol{n} - \hat{\boldsymbol{t}}) \cdot \boldsymbol{v} ds + \\
&\quad \int_{\Gamma_C} \sigma_n v_n ds + \int_{\Gamma_C} \mathcal{F}(|v_t + u_t| - |u_t|) + \sigma_t v_t ds.
\end{aligned}$$

Choosing $\boldsymbol{v} := \pm\boldsymbol{\phi}$ with $\boldsymbol{\phi} \in \{\boldsymbol{\psi} \in \boldsymbol{\mathcal{V}}_F : \ \operatorname{supp} \boldsymbol{\psi} \subset\subset \Omega\}$ we derive $\operatorname{div} \sigma(\boldsymbol{u}) = 0$, which is the equilibrium equation in (3.1). Next, we take $\boldsymbol{v} = \pm\boldsymbol{\phi}$ with $\boldsymbol{\phi} \in \{\boldsymbol{\psi} \in \boldsymbol{\mathcal{V}}_F : \boldsymbol{\psi} = 0 \text{ on } \Gamma_C\}$. That yields $\sigma(\boldsymbol{u}) \cdot \boldsymbol{n} = \hat{\boldsymbol{t}}$ on Γ_N. It remains to obtain the frictional contact conditions in the strong form from

$$0 \leq \int_{\Gamma_C} \sigma_n v_n ds + \int_{\Gamma_C} \mathcal{F}(|v_t + u_t| - |u_t|) + \sigma_t v_t ds. \tag{3.10}$$

Let us take $\boldsymbol{v} \in \{\boldsymbol{\psi} \in \boldsymbol{\mathcal{V}}_F : \psi_n = 0 \text{ on } \Gamma_C\}$ such that $v_t|_{\Gamma_C} = \pm u_t$. Then $|\sigma_t| \leq \mathcal{F}$ and the equation $\sigma_t u_t + \mathcal{F}|u_t| = 0$ holds on Γ_C. These are frictional conditions on Γ_C. Finally, we consider $\boldsymbol{w} \in \{\boldsymbol{\psi} \in \boldsymbol{\mathcal{K}}_F : w_t = u_t \text{ on } \Gamma_C\}$, $w_n|_{\Gamma_C} = 0$ and $2u_n$. Note that in both cases $\boldsymbol{w} \in \boldsymbol{\mathcal{K}}_F$. Hence, $v_n = \pm u_n$, which yields $\sigma_n u_n = 0$. It remains to show that $\sigma_n \leq 0$. Assume the opposite, i.e. $\exists \Gamma' \subset \Gamma : \sigma_n > 0$. Then we choose $\boldsymbol{w} \in \boldsymbol{\mathcal{K}}$, with $w_n|_{\Gamma'} = u_n - \chi_{\Gamma'} < 0, w_n|_{\Gamma_C \setminus \Gamma'} = u_n$ and $w_t|_{\Gamma_C} = u_t$, where $\chi_{\Gamma'}$ is some strictly positive function on $\Gamma' \setminus \partial\Gamma'$ and $\chi_{\Gamma'} = 0$ in $\partial\Gamma'$. Therefore

$$\int_{\Gamma_C} \sigma_n (w_n - u_n) ds < 0,$$

which is a contradiction to (3.10). □

3.1.2 Existence and uniqueness of the weak solution

In this paragraph we prove that the variational problem (3.9) is well-posed, i.e. that it has a unique solution.

Theorem 3.1.2. *The solution of the variational problem (3.9) is unique.*

Proof. Assume the contrary, i.e. that there exist $\boldsymbol{u}_1$, $\boldsymbol{u}_2 \in \boldsymbol{\mathcal{K}}$, two not identical solutions of (3.9). Then there holds holds

$$\begin{aligned} \langle S\boldsymbol{u}_1, \boldsymbol{u}_2 - \boldsymbol{u}_1\rangle_\Sigma + j(\boldsymbol{u}_2) - j(\boldsymbol{u}_1) &\geq L(\boldsymbol{u}_2 - \boldsymbol{u}_1), \\ \langle S\boldsymbol{u}_2, \boldsymbol{u}_1 - \boldsymbol{u}_2\rangle_\Sigma + j(\boldsymbol{u}_1) - j(\boldsymbol{u}_2) &\geq L(\boldsymbol{u}_1 - \boldsymbol{u}_2). \end{aligned}$$

Summing up we obtain

$$-\langle S(\boldsymbol{u}_1 - \boldsymbol{u}_2), \boldsymbol{u}_1 - \boldsymbol{u}_2\rangle_\Gamma \geq 0,$$

which yields $\boldsymbol{u}_1 \equiv \boldsymbol{u}_2$, since the Steklov-Poincaré operator S is positive definite on $\tilde{\boldsymbol{H}}^{1/2}(\Sigma)$. □

In order to prove existence of the solution of problem (3.9) we show that (3.9) is equivalent to the following minimization problem: Find $\boldsymbol{u} \in \boldsymbol{\mathcal{K}}$:

$$J(\boldsymbol{w}) \geq J(\boldsymbol{u}), \qquad \forall \boldsymbol{w} \in \boldsymbol{\mathcal{K}}, \tag{3.11}$$

where

$$J(\boldsymbol{w}) := \frac{1}{2}\langle S\boldsymbol{w}, \boldsymbol{w}\rangle_\Sigma + j(\boldsymbol{w}) - L(\boldsymbol{w}). \tag{3.12}$$

We show that the problem (3.11) has a solution, which automatically guarantees solvability of the boundary integral variational inequality (3.9).

Theorem 3.1.3. *The minimization problem (3.11) and the variational problem (3.9) are equivalent.*

Proof. Let $\boldsymbol{u} \in \boldsymbol{\mathcal{K}}$ solve (3.9). Since the bilinear form $\langle S\cdot, \cdot\rangle_\Sigma$ is symmetric, for arbitrary $\boldsymbol{w} \in \boldsymbol{\mathcal{K}}$ there holds

$$J(\boldsymbol{w}) - \frac{1}{2}\langle S(\boldsymbol{w} - \boldsymbol{u}), \boldsymbol{w} - \boldsymbol{u}\rangle_\Sigma \geq J(\boldsymbol{u}).$$

Noting that $\langle S\cdot, \cdot\rangle_\Sigma$ is positive definite we obtain the formulation (3.11).

Now, let $\boldsymbol{u}$ solve the minimization problem (3.11). Note that the set of admissible solutions $\boldsymbol{\mathcal{K}}$ is convex, i.e.

$$\forall \boldsymbol{v}, \boldsymbol{w} \in \boldsymbol{\mathcal{K}}, \quad \forall \lambda \in (0,1) \quad \text{there holds} \quad \boldsymbol{w} + \lambda(\boldsymbol{v} - \boldsymbol{w}) \in \boldsymbol{\mathcal{K}}.$$

And therefore $J(\boldsymbol{u}+\lambda(\boldsymbol{v}-\boldsymbol{u})) \geq J(\boldsymbol{u})$ for arbitrary $\boldsymbol{v} \in \boldsymbol{\mathcal{K}}$ and $\lambda \in (0,1)$. This together with symmetry of $\langle S\cdot,\cdot\rangle_\Sigma$ provides

$$\lambda\langle S\boldsymbol{u}, \boldsymbol{v}-\boldsymbol{u}\rangle_\Sigma + j(\boldsymbol{u}+\lambda(\boldsymbol{v}-\boldsymbol{u})) - j(\boldsymbol{u}) - \lambda L(\boldsymbol{v}-\boldsymbol{u}) + \frac{\lambda^2}{2}\langle S(\boldsymbol{v}-\boldsymbol{u}), \boldsymbol{v}-\boldsymbol{u}\rangle_\Sigma \geq 0. \quad (3.13)$$

The frictional functional $j(\cdot)$ is convex, i.e. $j(\boldsymbol{u}+\lambda(\boldsymbol{v}-\boldsymbol{u})) \leq j(\boldsymbol{u}) + \lambda(j(\boldsymbol{v}) - j(\boldsymbol{u}))$, hence, dividing (3.13) by $\lambda > 0$ we obtain

$$\langle S\boldsymbol{u}, \boldsymbol{v}-\boldsymbol{u}\rangle_\Sigma + j(\boldsymbol{v}) - j(\boldsymbol{u}) - L(\boldsymbol{v}-\boldsymbol{u}) + \frac{\lambda}{2}\langle S(\boldsymbol{v}-\boldsymbol{u}), \boldsymbol{v}-\boldsymbol{u}\rangle_\Sigma \geq 0. \quad (3.14)$$

Finally, we let $\lambda \to 0+$ and obtain the formulation (3.9). □

Two following auxiliary lemmas are needed in the existence analysis for (3.11).

Lemma 3.1.1. *The functional $J(\cdot)$, defined in (3.12), is coercive, i.e. $J(\boldsymbol{v}) \to \infty$, when $\boldsymbol{v} \in \boldsymbol{\mathcal{K}}$ and $\|\boldsymbol{v}\|_{\tilde{\boldsymbol{H}}^{1/2}(\Sigma)} \to \infty$.*

Proof. The Steklov-Poincaré operator S is positive definite on $\tilde{\boldsymbol{H}}^{1/2}(\Sigma)$ and the functional L is continuous on $\tilde{\boldsymbol{H}}^{1/2}(\Sigma)$, i.e. there exist constants $c_S, C_L > 0$, such that

$$\langle S\boldsymbol{v}, \boldsymbol{v}\rangle_\Sigma \geq c_S\|\boldsymbol{v}\|^2_{\tilde{\boldsymbol{H}}^{1/2}(\Sigma)}, \qquad L(\boldsymbol{v}) \leq C_L\|\boldsymbol{v}\|_{\tilde{\boldsymbol{H}}^{1/2}(\Sigma)}.$$

Thus

$$J(\boldsymbol{v}) \geq \frac{1}{2}\langle S\boldsymbol{v}, \boldsymbol{v}\rangle_\Sigma - L(\boldsymbol{v}) \geq c_S\|\boldsymbol{v}\|^2_{\tilde{\boldsymbol{H}}^{1/2}(\Sigma)} - C_L\|\boldsymbol{v}\|_{\tilde{\boldsymbol{H}}^{1/2}(\Sigma)}.$$

The quadratic term dominates for $\|\boldsymbol{v}\|_{\tilde{\boldsymbol{H}}^{1/2}(\Sigma)} \to \infty$, which provides coercivity of $J(\cdot)$. □

Definition 3.1.1. *(Gâteaux derivative) [38, Chapter 3] A functional $F : \boldsymbol{\mathcal{K}} \to \mathbb{R}$ is Gâteaux differentiable at a point $\boldsymbol{u} \in \boldsymbol{\mathcal{K}} \subset \boldsymbol{\mathcal{V}}$ if there exists a linear functional $DF(\boldsymbol{u}) \in \boldsymbol{\mathcal{V}}'$ such that*

$$\lim_{\varepsilon\to 0}\frac{\partial}{\partial\varepsilon}F(\boldsymbol{u}+\varepsilon\boldsymbol{v}) = \langle DF(\boldsymbol{u}), \boldsymbol{v}\rangle, \qquad \forall \boldsymbol{v} \in \boldsymbol{\mathcal{K}}.$$

Definition 3.1.2. *(Subdifferentiability) [38, Chapter 3] Let F be a functional on $\boldsymbol{\mathcal{K}}$. The set $\partial F(\boldsymbol{u}) \subset \boldsymbol{\mathcal{V}}'$ of all linear functionals q_u such that*

$$F(\boldsymbol{v}) - F(\boldsymbol{u}) \geq q_u(\boldsymbol{v}-\boldsymbol{u}), \qquad \boldsymbol{v} \in \boldsymbol{\mathcal{V}}, \qquad |F(\boldsymbol{u})| < \infty$$

is called the subdifferential of F at $\boldsymbol{u}$, and any $q_u \in \partial F(\boldsymbol{u})$ is a subgradient of F at $\boldsymbol{u}$.

Lemma 3.1.2. *The functional $J(\boldsymbol{u})$, defined in (3.12), is weakly lower semicontinuous, i.e. for any sequence $\{\boldsymbol{u}_k\} \subset \boldsymbol{\mathcal{K}}$, such that $\boldsymbol{u}_k$ converges weakly to $\boldsymbol{u} \in \boldsymbol{\mathcal{K}}$ ($\boldsymbol{u}_k \rightharpoonup \boldsymbol{u}$), there holds*

$$\liminf_{k\to\infty} J(\boldsymbol{u}_k) \geq J(\boldsymbol{u}).$$

Proof. We define $H(\boldsymbol{v}) := \frac{1}{2}\langle S\boldsymbol{v},\boldsymbol{v}\rangle_\Sigma - L(\boldsymbol{v})$ and hence $J(\boldsymbol{v}) = H(\boldsymbol{v}) + j(\boldsymbol{v})$. It is easy to see that the functional $H(\cdot)$ is Gâteaux differentiable with derivative

$$\langle DH(\boldsymbol{u}),\boldsymbol{v}\rangle_\Sigma = \langle S\boldsymbol{u},\boldsymbol{v}\rangle_\Sigma - L(\boldsymbol{v}) \qquad \forall \boldsymbol{v} \in \boldsymbol{\mathcal{K}}.$$

Note that for any $\boldsymbol{v} \in \boldsymbol{\mathcal{K}}$

$$|v_t| - |u_t| = v_t\text{sign}(v_t) - u_t\text{sign}(u_t) \geq \text{sign}(u_t)(v_t - u_t).$$

This provides that the frictional functional $j(\cdot)$ is subdifferentiable at $\boldsymbol{u}$. Indeed, there holds $\mathcal{F} \geq 0$ and therefore

$$j(\boldsymbol{v}) - j(\boldsymbol{u}) = \int_{\Gamma_C} \mathcal{F}(|v_t| - |u_t|)\,ds \geq \int_{\Gamma_C} \mathcal{F}\text{sign}(u_t)(v_t - u_t)\,ds =: q_u(\boldsymbol{v} - \boldsymbol{u}).$$

Further, for the convex functional $J(\cdot)$ there holds

$$J(\boldsymbol{u} + \varepsilon(\boldsymbol{u}_k - \boldsymbol{u})) - J(\boldsymbol{u}) \leq \varepsilon(J(\boldsymbol{u}_k) - J(\boldsymbol{u})) \qquad \varepsilon \in (0,1).$$

or

$$\frac{1}{\varepsilon}(H(\boldsymbol{u} + \varepsilon(\boldsymbol{u}_k - \boldsymbol{u})) - H(\boldsymbol{u})) + \frac{1}{\varepsilon}(j(\boldsymbol{u} + \varepsilon(\boldsymbol{u}_k - \boldsymbol{u})) - j(\boldsymbol{u})) \leq J(\boldsymbol{u}_k) - J(\boldsymbol{u}).$$

Then taking the limit $\varepsilon \to \infty$ we obtain

$$J(\boldsymbol{u}_k) - J(\boldsymbol{u}) \geq \langle DH(\boldsymbol{u}), \boldsymbol{u}_k - \boldsymbol{u}\rangle_\Sigma + q_u(\boldsymbol{u}_k - \boldsymbol{u}).$$

It was supposed that $\{\boldsymbol{u}_k\}$ converges weakly to $\boldsymbol{u}$, therefore

$$\liminf_{k\to\infty} J(\boldsymbol{u}_k) - J(\boldsymbol{u}) \geq \liminf_{k\to\infty}(\langle DH(\boldsymbol{u}), \boldsymbol{u}_k - \boldsymbol{u}\rangle_\Sigma + q_u(\boldsymbol{u}_k - \boldsymbol{u})) = 0,$$

which finishes the proof. □

Now we are at the position to prove existence of the solution of the minimization problem (3.11).

Theorem 3.1.4. *Problem (3.11) has a solution.*

Proof. Due to Lemma 3.1.1 there exists a constant $M > 0$ such that for any $\boldsymbol{v}$ with $\|\boldsymbol{v}\|_{\tilde{\boldsymbol{H}}^{1/2}(\Sigma)} \geq M$ there holds $J(\boldsymbol{v}) \geq 1$. Let us consider a closed functional set

$$\boldsymbol{\mathcal{A}} := \{\boldsymbol{v} \in \boldsymbol{\mathcal{K}} : \|\boldsymbol{v}\|_{\tilde{\boldsymbol{H}}^{1/2}(\Sigma)} \leq M\} \subset \boldsymbol{\mathcal{K}}.$$

This provides

$$\inf_{\boldsymbol{v}\in\boldsymbol{\mathcal{K}}} J(\boldsymbol{v}) = \inf_{\boldsymbol{v}\in\boldsymbol{\mathcal{A}}} J(\boldsymbol{v}).$$

The Steklov-Poincaré operator S, the frictional functional j and the load functional L are continuous, i.e. there exists constants $C_S, C_1, C_2 > 0$ such that

$$|J(\boldsymbol{v})| \leq |\langle S\boldsymbol{v}, \boldsymbol{v}\rangle| + |j(\boldsymbol{v})| + |L(\boldsymbol{v})| \leq C_S ||\boldsymbol{v}||^2_{\tilde{\boldsymbol{H}}^{1/2}(\Sigma)} + (C_1 + C_2)||\boldsymbol{v}||_{\tilde{\boldsymbol{H}}^{1/2}(\Sigma)}$$

and therefore with $\bar{M} := C_S M^2 + (C_1 + C_2)M$

$$-\bar{M} < \inf_{\boldsymbol{v}\in\boldsymbol{\mathcal{A}}} J(\boldsymbol{v}) = \inf_{\boldsymbol{v}\in\boldsymbol{\mathcal{K}}} J(\boldsymbol{v}) < \bar{M}.$$

Then there exists $a \in [-\bar{M}, \bar{M}]$ and a sequence $\{\boldsymbol{u}_n\} \subset \boldsymbol{\mathcal{A}}$ such that

$$a = \inf_{\boldsymbol{v}\in\boldsymbol{\mathcal{A}}} J(\boldsymbol{v}) = \lim_{n\to\infty} J(\boldsymbol{u}_n).$$

Since $\boldsymbol{\mathcal{A}}$ is a closed subspace of the Hilbert space $\tilde{\boldsymbol{H}}^{1/2}(\Sigma)$ there exists a subsequence $\{\boldsymbol{u}_{n_k}\} \subset \{\boldsymbol{u}_n\}$ which converges weakly to some function $\bar{\boldsymbol{u}} \in \boldsymbol{\mathcal{A}}$. From Lemma 3.1.2 we have

$$a = \liminf_{k\to\infty} J(\boldsymbol{u}_{n_k}) \geq J(\bar{\boldsymbol{u}}), \tag{3.15}$$

which implies that $a = J(\bar{\boldsymbol{u}})$ and therefore $\bar{\boldsymbol{u}}$ solves the minimization problem (3.11). □

3.1.3 Saddle point formulation - Uzawa algorithm

In this paragraph we introduce a dual formulation equivalent to the variational formulation (3.9), and hence to the minimization problem (3.11). The derived formulation does not include the non-differentiable frictional functional $j(\cdot)$ and is more suitable for implementation. The obtained problem can be solved with the Uzawa algorithm. Here we follow ideas of [29, Chapter 4], see also [47].

Let us define the space of Lagrangian multipliers $\Lambda = \{\sigma \in L_2(\Gamma_C) : |\sigma| \leqslant 1 \text{ a.e. on } \Gamma_C\}$ and the bilinear functional

$$q(\sigma, \boldsymbol{w}) = \int_{\Gamma_C} \mathcal{F}\sigma w_t \, ds.$$

Let us consider the following mixed formulation: Find $\boldsymbol{u} \in \boldsymbol{\mathcal{K}}, \sigma_u \in \Lambda$:

$$\begin{aligned} &\langle S\boldsymbol{u}, \boldsymbol{w} - \boldsymbol{u}\rangle_\Sigma + q(\sigma_u, \boldsymbol{w}) - q(\sigma_u, \boldsymbol{u}) \geq L(\boldsymbol{w} - \boldsymbol{u}), \qquad \forall \boldsymbol{w} \in \boldsymbol{\mathcal{K}}, \\ &\sigma_u u_t = |u_t| \text{ a.e. on } \Gamma_C \end{aligned} \tag{3.16}$$

and the saddle point problem: Find $\boldsymbol{u} \in \boldsymbol{\mathcal{K}}, \sigma_u \in \Lambda$:

$$F(\boldsymbol{u}, \sigma) \leq F(\boldsymbol{u}, \sigma_u) \leq F(\boldsymbol{w}, \sigma_u), \qquad \forall \boldsymbol{w} \in \boldsymbol{\mathcal{K}}, \quad \forall \sigma \in \Lambda, \tag{3.17}$$

with

$$F(\boldsymbol{w}, \sigma) = \frac{1}{2}\langle S\boldsymbol{w}, \boldsymbol{w}\rangle_\Sigma + q(\sigma, \boldsymbol{w}) - L(\boldsymbol{w}).$$

Theorem 3.1.5. *Problems (3.16) and (3.17) are equivalent*

Proof. Let $(\boldsymbol{u}, \sigma_u)$ solve (3.17), then for $\boldsymbol{w} \in \boldsymbol{\mathcal{K}}$ and $\varepsilon \in (0,1)$ there holds

$$
\begin{aligned}
0 &\leq \frac{1}{\varepsilon}(F(\boldsymbol{u} + \varepsilon(\boldsymbol{w} - \boldsymbol{u}), \sigma_u) - F(\boldsymbol{u}, \sigma_u)) \\
&= \langle S\boldsymbol{u}, \boldsymbol{w} - \boldsymbol{u} \rangle_\Sigma - L(\boldsymbol{w} - \boldsymbol{u}) + \int_{\Gamma_C} \mathcal{F}\sigma_u(w_t - u_t)ds + \frac{\varepsilon}{2}\langle S(\boldsymbol{w} - \boldsymbol{u}), \boldsymbol{w} - \boldsymbol{u} \rangle_\Sigma.
\end{aligned}
$$

Taking the limit $\varepsilon \to 0+$ we obtain the first inequality in (3.16). Further, for every $\sigma \in \Lambda$ there holds

$$
0 \leq F(\boldsymbol{u}, \sigma_u) - F(\boldsymbol{u}, \sigma) = \int_{\Gamma_C} \mathcal{F}(\sigma_u - \sigma)u_t ds,
$$

Choosing $\sigma := \operatorname{sign}(u_t)$ we obtain

$$
\int_{\Gamma_C} \mathcal{F}(\sigma_u u_t - |u_t|)ds \geq 0.
$$

But $\sigma_u u_t \leq |u_t|$ due to definition of Λ. This implies that $\sigma_u \equiv \operatorname{sign}(u_t)$ a.e. on Γ_C and $(\boldsymbol{u}, \sigma_u) \in \boldsymbol{\mathcal{K}} \times \Lambda$ solve (3.16).

Now let us assume that $(\boldsymbol{u}, \sigma_u) \in \boldsymbol{\mathcal{K}} \times \Lambda$ solve (3.16). Basic calculations show that for any $\boldsymbol{w} \in \boldsymbol{\mathcal{K}}$ there holds

$$
F(\boldsymbol{w}, \sigma_u) - \frac{1}{2}\langle S(\boldsymbol{w} - \boldsymbol{u}), \boldsymbol{w} - \boldsymbol{u} \rangle_\Sigma \geq F(\boldsymbol{u}, \sigma_u)
$$

and the right inequality in (3.17) follows.

Taking into account that for arbitrary $\sigma \in \Lambda$ there holds $(\sigma - \sigma_u)u_t = \sigma u_t - |u_t| \leq 0$, we obtain

$$
\int_{\Gamma_C} \mathcal{F}(\sigma - \sigma_u)u_t ds \leq 0.
$$

Hence,

$$
F(\boldsymbol{u}, \sigma) = F(\boldsymbol{u}, \sigma_u) + \int_{\Gamma_C} \mathcal{F}(\sigma - \sigma_u)u_t ds \leq F(\boldsymbol{u}, \sigma_u),
$$

and herewith the left inequality in (3.17) follows. □

In order to prove equivalence between the minimization problem (3.11) and the mixed problem (3.16) we introduce a sequence of their regularized versions. First, we employ the regularization $\Psi_k(x)$ of the absolute value function and its derivative $\varphi_k(x) := \Psi_k'(x)$

$$
\Psi_k(x) = \begin{cases} |x| - \frac{1}{2k}, & |x| \geq \frac{1}{k}, \\ \frac{kx^2}{2}, & |x| \leq \frac{1}{k}, \end{cases} \qquad \varphi_k(x) = \begin{cases} 1, & x \geq \frac{1}{k}, \\ kx, & |x| \leq \frac{1}{k}. \end{cases} \tag{3.18}
$$

For an integer k let us introduce a parameter dependent family of regularized minimization problem as follows: Find $\boldsymbol{u}_k \in \boldsymbol{\mathcal{K}}$:

$$F_k(\boldsymbol{w}) \geq F_k(\boldsymbol{u}_k), \qquad \forall \boldsymbol{w} \in \boldsymbol{\mathcal{K}} \tag{3.19}$$

with the family of functionals

$$F_k(\boldsymbol{w}) = \frac{1}{2}\langle S\boldsymbol{w}, \boldsymbol{w}\rangle + j_k(\boldsymbol{w}) - L(\boldsymbol{w}), \qquad j_k(\boldsymbol{w}) := \int_{\Gamma_C} \mathcal{F}\Psi_k(w_t)ds,$$

and a parameter dependent family of regularized variational inequalities: Find $u_k \in \boldsymbol{\mathcal{K}}$:

$$\langle S\boldsymbol{u}_k, \boldsymbol{w} - \boldsymbol{u}_k\rangle + \int_{\Gamma_C} \mathcal{F}\varphi_k((u_k)_t)(w_t - (u_k)_t)ds \geq L(\boldsymbol{w} - \boldsymbol{u}_k), \qquad \forall w \in \boldsymbol{\mathcal{K}}. \tag{3.20}$$

Theorem 3.1.6. *Problems (3.19) and (3.20) are equivalent for some positive $k \in \mathbb{N}$. Moreover, they have unique solutions.*

Proof. First, we show equivalence between (3.19) and (3.20). Let us assume that $\boldsymbol{u}_k \in \boldsymbol{\mathcal{K}}$ solves (3.19), i.e. for some $\varepsilon \in (0,1)$ there holds

$$F_k(\boldsymbol{u}_k + \varepsilon(\boldsymbol{w} - \boldsymbol{u}_k)) \geq F_k(\boldsymbol{u}_k), \qquad \forall \boldsymbol{w} \in \boldsymbol{\mathcal{K}}.$$

This leads to the following inequality (cf. Theorem 3.1.5)

$$\begin{aligned} 0 &\leq \frac{1}{\varepsilon}(F_k(\boldsymbol{u}_k + \varepsilon(\boldsymbol{w} - \boldsymbol{u}_k)) - F_k(\boldsymbol{u}_k)) \\ &= \langle S\boldsymbol{u}_k, \boldsymbol{w} - \boldsymbol{u}_k\rangle_\Sigma + \int_{\Gamma_C} \mathcal{F}\frac{\Psi_k((u_k)_t + \varepsilon(w_t - (u_k)_t)) - \Psi((u_k)_t)}{\varepsilon}\,ds - L(\boldsymbol{w} - \boldsymbol{u}_k) \\ &\quad + \frac{\varepsilon}{2}\langle S(\boldsymbol{w} - \boldsymbol{u}_k), \boldsymbol{w} - \boldsymbol{u}_k\rangle_\Sigma . \end{aligned}$$

Taking the limit $\varepsilon \to 0+$ leads to the formulation (3.20). Note, that the function Ψ_k is differentiable with $\Psi_k' = \varphi_k$, therefore

$$\frac{\Psi_k((u_k)_t + \varepsilon(w_t - (u_k)_t)) - \Psi((u_k)_t)}{\varepsilon} \to \varphi_k((u_k)_t)(w_t - (u_k)_t), \qquad \varepsilon \to 0+ .$$

Now, let $\boldsymbol{u}_k$ be a solution of (3.20). After some calculation we obtain for arbitrary $\boldsymbol{w} \in \boldsymbol{\mathcal{K}}$

$$\begin{aligned} F_k(\boldsymbol{w}) &- \frac{1}{2}\langle S(\boldsymbol{w} - \boldsymbol{u}_k), \boldsymbol{w} - \boldsymbol{u}_k\rangle_\Sigma \\ &- \int_{\Gamma_C} \mathcal{F}(\Psi(w_t) - \Psi((u_k)_t) - \Psi'((u_k)_t)(w_t - (u_k)_t)) \geq F_k(\boldsymbol{u}_k). \end{aligned}$$

The function Ψ_k is convex and is piecewise quadratic, then

$$\Psi(w_t) - \Psi((u_k)_t) - \Psi'((u_k)_t)(w_t - (u_k)_t) \geq 0.$$

The formulation (3.19) follows since $\langle S\cdot, \cdot\rangle_\Sigma$ is positive definite. The functional F_k is strictly convex, Gâteaux differentiable and coercive on $\boldsymbol{\mathcal{K}}$. Applying arguments similar to that in Section 3.1.2 we obtain that problem (3.19), and herewith problem (3.20), have unique solutions. □

Lemma 3.1.3. *Let* $\{\boldsymbol{u}_k\}_{k\in\mathbb{N}}$ *be the family of solutions of the regularized problem (3.19) and* $\boldsymbol{u}$ *solve the variational inequality (3.9). Assume that the given friction function* $\mathcal{F} \in L_1(\Gamma_C)$*. Then*

$$\lim_{k\to\infty} \boldsymbol{u}_k = \boldsymbol{u}.$$

Proof. The variational inequality provides for $\forall \boldsymbol{w} \in \boldsymbol{\mathcal{K}}$

$$\langle S\boldsymbol{u}, \boldsymbol{w} - \boldsymbol{u}\rangle_\Sigma + j(\boldsymbol{w}) - j(\boldsymbol{u}) \geq L(\boldsymbol{w} - \boldsymbol{u}). \tag{3.21}$$

The minimization problem can be rewritten as follows (cf. Theorem 3.1.3)

$$\langle S\boldsymbol{u}_k, \boldsymbol{w} - \boldsymbol{u}_k\rangle_\Sigma + j_k(\boldsymbol{w}) - j_k(\boldsymbol{u}_k) \geq L(\boldsymbol{w} - \boldsymbol{u}_k), \qquad \forall \boldsymbol{w} \in \boldsymbol{\mathcal{K}}. \tag{3.22}$$

Substituting $\boldsymbol{w} = \boldsymbol{u}_k$ and $\boldsymbol{w} = \boldsymbol{u}$ in (3.21), (3.22) respectively and adding them we obtain

$$\langle S(\boldsymbol{u}_k - \boldsymbol{u}), \boldsymbol{u}_k - \boldsymbol{u}\rangle_\Sigma \leq j_k(\boldsymbol{u}) - j(\boldsymbol{u}) + j(\boldsymbol{u}_k) - j_k(\boldsymbol{u}_k). \tag{3.23}$$

From definition of Ψ_k it follows that $0 \leq |\xi| - \Psi_k(\xi) \leq (2k)^{-1}$, therefore

$$0 \leq j_k(\boldsymbol{w}) - j(\boldsymbol{w}) \leq \frac{1}{2k}||\mathcal{F}||_{L_1(\Gamma_C)}, \qquad \forall \boldsymbol{w} \in \boldsymbol{\mathcal{K}}.$$

This together with (3.23) gives

$$\langle S(\boldsymbol{u}_k - \boldsymbol{u}), \boldsymbol{u}_k - \boldsymbol{u}\rangle_\Sigma \leq \frac{1}{k}||\mathcal{F}||_{L_1(\Gamma_C)} \to 0, \qquad k \to \infty. \tag{3.24}$$

The bilinear form $\langle S\cdot, \cdot\rangle_\Sigma$ is positive definite, hence $\boldsymbol{u}_k \to \boldsymbol{u}$ when $k \to \infty$. □

Theorem 3.1.7. *Problems (3.9) and (3.16) are equivalent.*

Proof. Let $(\boldsymbol{u}, \sigma_u) \in \boldsymbol{\mathcal{K}} \times \Lambda$ solve (3.16). Noting that

$$\int_{\Gamma_C} \sigma_u \mathcal{F} w_t ds \leq \int_{\Gamma_C} \mathcal{F}|w_t|ds, \qquad \int_{\Gamma_C} \sigma_u \mathcal{F} u_t ds = \int_{\Gamma_C} \mathcal{F}|u_t|ds$$

we obtain the variational inequality (3.9) directly from the first line in (3.16).

Let us assume now that $\boldsymbol{u} \in \boldsymbol{\mathcal{K}}$ is a solution of (3.9). Due to Theorem 3.1.6 and Lemma 3.1.3, $\boldsymbol{u}$ can be represented as a limit $\lim_{k\to\infty} \boldsymbol{u}_k = \boldsymbol{u}$, where $\{\boldsymbol{u}_k\}$ is a sequence of solutions of the problem (3.20), i.e.

$$\langle S\boldsymbol{u}_k, \boldsymbol{w} - \boldsymbol{u}_k\rangle_\Sigma + \int_{\Gamma_C} \mathcal{F}\varphi_k((u_k)_t)(w_t - (u_k)_t)ds \geq L(\boldsymbol{w} - \boldsymbol{u}_k), \qquad \forall \boldsymbol{w} \in \boldsymbol{\mathcal{K}}, \tag{3.25}$$

where φ_k defined by (3.18), hence $\varphi_k((u_k)_t) \in \Lambda, \forall k$. The convex set Λ is weakly compact in $L_2(\Gamma_C)$, cf. [29, Chapter 4, Theorem 2.2], therefore there exists a subsequence $\{\varphi_{n_k}\}$, converging weakly to some $\sigma \in \Lambda$. Taking the limit $k \to \infty$ in (3.25) we obtain

$$\langle S\boldsymbol{u}, \boldsymbol{w} - \boldsymbol{u}\rangle_\Sigma + \int_{\Gamma_C} \sigma\mathcal{F}(w_t - u_t)ds \geq L(\boldsymbol{w} - \boldsymbol{u}), \tag{3.26}$$

which is the first line in (3.16). Now, set $\boldsymbol{w} = 0, 2\boldsymbol{u} \in \boldsymbol{\mathcal{K}}$ in (3.9) and in (3.26), which yields

$$\langle S\boldsymbol{u}, \boldsymbol{u}\rangle_\Sigma + \int_{\Gamma_C} \mathcal{F}|u_t| ds = L(\boldsymbol{u}). \tag{3.27}$$

$$\langle S\boldsymbol{u}, \boldsymbol{u}\rangle_\Sigma + \int_{\Gamma_C} \mathcal{F}\sigma u_t ds = L(\boldsymbol{u}), \tag{3.28}$$

respectively. Subtracting (3.28) and (3.27) provides

$$\int_{\Gamma_C} \mathcal{F}(|u_t| - \sigma u_t) ds = 0. \tag{3.29}$$

Since $\sigma \in \Lambda$, there holds $|\sigma| \leq 1$ a.e. on Γ_C, and therefore $|u_t| - \sigma u_t \geq 0$ a.e. on Γ_C. This together with (3.29) leads to

$$|u_t| = \sigma u_t \text{ a.e. on } \Gamma_C, \tag{3.30}$$

which is the second line in (3.16). □

The formulation (3.16) gives a natural algorithm for solving the contact problem with Tresca's friction law.

Algorithm 3.1. *(Uzawa algorithm)*

---

1. *Choose* $\sigma^0 \in \Lambda$.
2. *For* $n = 0, 1, 2, \dots$ *determine* $\boldsymbol{u}^n \in \boldsymbol{\mathcal{K}}$, *such that*

$$F(\boldsymbol{u}^n, \sigma^n) \leq F(\boldsymbol{w}, \sigma^n) \quad \forall \boldsymbol{w} \in \boldsymbol{\mathcal{K}},$$

   i.e. find $\boldsymbol{u}^n \in \boldsymbol{\mathcal{K}}$ *such that*

$$\langle S\boldsymbol{u}^n, \boldsymbol{w} - \boldsymbol{u}^n\rangle \geq L(\boldsymbol{w} - \boldsymbol{u}^n) - \int_{\Gamma_C} \mathcal{F}\sigma^n(\boldsymbol{w} - \boldsymbol{u}^n)\, ds \quad \forall \boldsymbol{w} \in \boldsymbol{\mathcal{K}}. \tag{3.31}$$

3. *Set*

$$\sigma^{n+1} = P_\Lambda(\sigma^n + \rho\mathcal{F}u_t^n),$$

   where $\rho > 0$ *is a sufficiently small parameter that will be specified later on, and* P_Λ *denotes the projection operator from* $L_2(\Gamma_C)$ *to* Λ

$$P_\Lambda(\mu)(\boldsymbol{x}) = \sup\{-1, \inf\{1, \mu(\boldsymbol{x})\}\}, \qquad \boldsymbol{x} \in \Gamma_C, \quad \forall \mu \in L_2(\Gamma_C).$$

4. *Set* $n := n + 1$. *Repeat with 2. until the convergence criterion is satisfied.*

Theorem 3.1.8. *Let $\mathcal{F} \in L_\infty(\Gamma_C)$ and $0 < \rho < 2c_S \|\mathcal{F}\|^{-2}_{L_\infty(\Gamma_C)}$, where c_S is the ellipticity constant of the Steklov-Poincaré operator S. Then the Uzawa algorithm converges for arbitrary starting function $\sigma^0 \in \Lambda$, i.e. $\boldsymbol{u}^n \to \boldsymbol{u}$ strongly in $\tilde{\boldsymbol{H}}^{1/2}(\Sigma)$.*

Proof. Let $(\boldsymbol{u}, \sigma_u) \in \boldsymbol{\mathcal{K}} \times \Lambda$ be the solution of problem (3.16). Then $\sigma_u u_t = |u_t|$ a.e. on Γ_C and hence $\sigma_u^2 = 1$ a.e. on Γ_C. That gives

$$P_\Lambda(\sigma_u + \rho \mathcal{F} u_t) = P_\Lambda(\sigma_u(1 + \rho\mathcal{F}|u_t|)) = P_\Lambda(\sigma_u) = \sigma_u, \tag{3.32}$$

since $\rho\mathcal{F}|u_t| > 0$. The projection operator P_Λ is a contraction, therefore

$$\begin{aligned} \|\sigma^{n+1} - \sigma_u\|^2_{L_2(\Gamma_C)} &\leq \|\sigma^n - \sigma_u + \rho\mathcal{F}(u_t^n - u_t)\|^2_{L_2(\Gamma_C)} \\ &\leq \|\sigma^n - \sigma_u\|^2_{L_2(\Gamma_C)} + 2\rho \int_{\Gamma_C} \mathcal{F}(\sigma^n - \sigma_u)(u_t^n - u_t)\, ds \\ &\quad + \rho^2 \|\mathcal{F}\|^2_{L_\infty(\Gamma_C)} \|u_t^n - u_t\|^2_{L_2(\Gamma_C)}. \end{aligned}$$

The first line in (3.16) combined with (3.31) provides with $\boldsymbol{e}^n := \boldsymbol{u} - \boldsymbol{u}^n$

$$-\int_{\Gamma_C} \mathcal{F}(\sigma_u - \sigma^n)(u_t - u_t^n)\, ds \geq \langle S\boldsymbol{e}^n, \boldsymbol{e}^n \rangle_\Sigma . \tag{3.33}$$

Since the Steklov-Poincaré operator S is elliptic on $\tilde{\boldsymbol{H}}^{1/2}(\Sigma)$ (cf. (1.10)), there exists a constant $c_S > 0$ such that

$$-\|u_t^n - u_t\|^2_{\boldsymbol{L}_2(\Gamma_C)} \geq -\|u_t^n - u_t\|^2_{\boldsymbol{H}^{1/2}(\Sigma)} \geq -c_S^{-1} \langle S\boldsymbol{e}^n, \boldsymbol{e}^n \rangle_\Sigma .$$

Hence

$$\|\sigma^n - \sigma\|^2_{L_2(\Gamma_C)} - \|\sigma^{n+1} - \sigma\|^2_{L_2(\Gamma_C)} \geq \rho(2 - \rho c_S^{-1} \|\mathcal{F}\|^2_{L_\infty(\Gamma_C)}) \langle S\boldsymbol{e}^n, \boldsymbol{e}^n \rangle_\Sigma . \tag{3.34}$$

If $0 < \rho < 2c_S \|\mathcal{F}\|^{-2}_{L_\infty(\Gamma_C)}$ we have $(2 - \rho c_S^{-1} \|\mathcal{F}\|^2_{L_\infty(\Gamma_C)}) > 0$, which gives

$$\|\sigma^n - \sigma\|^2_{L_2(\Gamma_C)} > \|\sigma^{n+1} - \sigma\|^2_{L_2(\Gamma_C)}$$

for $\boldsymbol{e}^n \neq 0$. The sequence $\|\sigma^n - \sigma\|^2_{L_2(\Gamma_C)}$ converges, because it is monotone decreasing and has a lower bound, i.e.

$$\lim_{n\to\infty} (\|\sigma^n - \sigma\|^2_{L_2(\Gamma_C)} - \|\sigma^{n+1} - \sigma\|^2_{L_2(\Gamma_C)}) = 0$$

and therefore $\lim_{n\to\infty} \langle S\boldsymbol{e}^n, \boldsymbol{e}^n \rangle_\Sigma = 0$. Using again ellipticity of S on $\tilde{\boldsymbol{H}}^{1/2}(\Sigma)$ we obtain that $\boldsymbol{u}^n \to \boldsymbol{u}$ strongly in $\tilde{\boldsymbol{H}}^{1/2}(\Sigma)$. □

The constructed Uzawa algorithm (Algorithm 3.1) will be also employed in Section 4.3, where we construct a solution algorithm for *hp*-mortar BEM for two-body frictional contact problems.

3.2 Penalty hp-BEM for one-body contact problem

In this section we obtain a priori error estimates for the hp-version of penalty boundary element method, used for solving one-body contact problems in elasticity. The error analysis is divided into two parts. At first we consider the error caused by the approximation of the variational inequality (or Lagrange multiplier) formulation with the penalty formulation. Under additional regularity assumptions we derive a linear convergence rate with respect to the penalty parameter. Then we consider the discretization error between the solution of the penalty formulation and its Galerkin approximation. We show two types of the best approximation property, which are similar to Cea's lemma, but here the estimate depends on the penalty parameter. Finally, an a priori estimate for the error between the exact solution of the variational inequality and the boundary element Galerkin solution of the penalty problem is obtained. For the displacement $\boldsymbol{u} \in \tilde{\boldsymbol{H}}^{3/2}(\Gamma_C \cup \Gamma_N)$ solving the variational inequality formulation, and for the corresponding boundary traction $T\boldsymbol{u} \in \boldsymbol{H}^{1/2}(\Gamma)$ we obtain a quasioptimal convergence rate $\mathcal{O}((h/p)^{1-\epsilon})$ for the penalty parameter $\varepsilon \gtrsim (h/p)^{1-\epsilon}$. Here $\epsilon > 0$ is some fixed small parameter. We finish the section with a numerical example for the h-version of BEM, which provides the linear convergence rate, since ϵ may be chosen arbitrary close to zero.

3.2.1 Variational inequality, Lagrange multiplier, and penalty formulation

First, recall the classical formulation of the one-body contact problem described in the introduction to Chapter 3, where in addition no friction occurs between the elastic body and the rigid obstacle ($\sigma_t \equiv 0$, or equivalently $\mathcal{F} \equiv 0$). Let the domain Ω, boundary parts $\Gamma_D, \Gamma_N, \Gamma_C, \Sigma$ and the gap function g be defined as in the introduction to Chapter 3. Then the classical formulation of the one-body frictionless contact problem is given as follows (cf. (3.1))

$$\begin{aligned} \operatorname{div} \sigma(\boldsymbol{u}) &= 0 && \text{in } \Omega, \\ \boldsymbol{u} &= 0 && \text{on } \Gamma_D, \\ \sigma(\boldsymbol{u}) \cdot \boldsymbol{n} &= \hat{\boldsymbol{t}} && \text{on } \Gamma_N, \\ \sigma_n \le 0, \quad u_n - g \le 0, \quad \sigma_n(u_n - g) &= 0, \quad \sigma_t = 0, && \text{on } \Gamma_C. \end{aligned} \tag{3.35}$$

Further, we introduce the functional spaces and sets required for the forthcoming analysis

$$\boldsymbol{\mathcal{V}} := \tilde{\boldsymbol{H}}^{1/2}(\Sigma), \tag{3.36}$$

$$\boldsymbol{\mathcal{W}} := \boldsymbol{H}^{-1/2}(\Sigma), \tag{3.37}$$

$$\boldsymbol{\mathcal{K}} := \{\boldsymbol{v} \in \boldsymbol{\mathcal{V}} : (v_n - g) \le 0 \text{ on } \Gamma_C\}, \tag{3.38}$$

$$\Lambda := \left\{ \lambda \in \tilde{H}^{-1/2}(\Gamma_C) : \ \forall v \in H^{1/2}(\Gamma_C), \ v \le 0, \ \int_{\Gamma_C} \lambda v \, ds \ge 0 \right\}. \tag{3.39}$$

We introduce the single layer potential V, the double layer potential K, the adjoint double layer potential K' and the the hypersingular integral operator W as in (1.4) and recall the definition Steklov-Poincaré operator S (1.6)

$$S = W + (K' + 1/2)V^{-1}(K + 1/2). \tag{3.40}$$

As before, we denote the duality pairing over some (closed or unclosed) curve γ by $\langle \cdot, \cdot \rangle_\gamma$. Let the linear functional $L(\boldsymbol{v})$ be defined by $L(\boldsymbol{v}) := \langle \hat{\boldsymbol{t}}, \boldsymbol{v} \rangle_{\Gamma_N}$. As it was shown in Section 3.1, the classical problem (3.35) can be reformulated in a weak form as a variational inequality, cf. (3.9): Find $\boldsymbol{u} \in \boldsymbol{\mathcal{K}}$:

$$\langle S\boldsymbol{u}, \boldsymbol{v} - \boldsymbol{u} \rangle_\Sigma \geq L(\boldsymbol{v} - \boldsymbol{u}) \qquad \forall \boldsymbol{v} \in \boldsymbol{\mathcal{K}}, \tag{3.41}$$

or equivalently as a minimization problem, cf. (3.11): Find $\boldsymbol{u} \in \boldsymbol{\mathcal{K}}$:

$$J(\boldsymbol{v}) \geq J(\boldsymbol{u}), \qquad \forall \boldsymbol{v} \in \boldsymbol{\mathcal{K}}. \tag{3.42}$$

with $J(\boldsymbol{v}) := \frac{1}{2}\langle S\boldsymbol{v}, \boldsymbol{v} \rangle_\Sigma - L(\boldsymbol{v})$. In both formulations (3.41) and (3.42) the set of admissible solutions $\boldsymbol{\mathcal{K}} \subset \boldsymbol{\mathcal{V}}$ includes the inequality constraint, which is often undesirable. Sometimes it may be more convenient to remove the constraint from the displacement by introducing an auxiliary variable $\lambda \in \Lambda$. Now the solution is sought in the whole space $\boldsymbol{u} \in \boldsymbol{\mathcal{V}}$. The problem can be reformulated in a saddle point form: Find $\boldsymbol{u} \in \boldsymbol{\mathcal{V}}, \lambda \in \Lambda$:

$$\mathcal{L}(\boldsymbol{u}, \mu) \leq \mathcal{L}(\boldsymbol{u}, \lambda) \leq \mathcal{L}(\boldsymbol{v}, \lambda) \qquad \forall \boldsymbol{v} \in \boldsymbol{\mathcal{V}}, \lambda \in \Lambda, \tag{3.43}$$

with $\mathcal{L}(\boldsymbol{v}, \mu) := \frac{1}{2}\langle S\boldsymbol{v}, \boldsymbol{v} \rangle_\Sigma - L(\boldsymbol{v}) - \langle \mu, v_n - g \rangle_{\Gamma_C}$, which is equivalent to the following dual variational formulation with Lagrange multiplier: Find $\boldsymbol{u} \in \boldsymbol{\mathcal{V}}, \lambda \in \Lambda$:

$$\begin{array}{rcll} \langle S\boldsymbol{u}, \boldsymbol{v} \rangle_\Sigma - \langle \lambda, v_n \rangle_{\Gamma_C} & = & L(\boldsymbol{v}) & \qquad \forall \boldsymbol{v} \in \boldsymbol{\mathcal{V}}, \\ \langle \mu - \lambda, u_n - g \rangle_{\Gamma_C} & \geq & 0 & \qquad \forall \mu \in \Lambda. \end{array} \tag{3.44}$$

The existence and uniqueness of the solution of the variational inequality, and therefore of the solution of (3.43) and (3.44) is guaranteed by results of Section 3.1. Note that the inequality constraint is completely removed from the set of admissible displacements and the *equality* is obtained for the variation of the displacement (first line in (3.44)). On the other hand, the inequality constraints are associated now with the auxiliary variable λ, which has a meaning of the normal contact traction, acting from the side of the rigid obstacle and resisting the penetration of the body through the obstacle. The inequality constraints remain in the set of admissible contact tractions Λ and in the second line of the dual variational formulation (3.44).

To remove the inequality constraints completely from the functional sets and from the variational formulation, which makes the implementation much easier, the penalty formulation is used, see e.g. [26], [72]. Here some penetration of the body through the obstacle is allowed and the resisting contact force is defined to be proportional to the value of penetration. The proportionality coefficient ε is called penalty parameter. The penalty formulation is given as follows: Find $\boldsymbol{u}^\varepsilon \in \boldsymbol{\mathcal{V}}$:

$$\langle S\boldsymbol{u}^\varepsilon, \boldsymbol{v}\rangle - \langle p_n^\varepsilon, v_n\rangle_{\Gamma_C} = L(\boldsymbol{v}) \qquad \forall \boldsymbol{v} \in \boldsymbol{\mathcal{V}}, \tag{3.45}$$

$$p_n^\varepsilon := -\frac{1}{\varepsilon}(u_n^\varepsilon - g)^+. \tag{3.46}$$

Here the penalty parameter $\varepsilon > 0$ must be chosen in advance. The positive and the negative part of some function $f \in H^{1/2}(\Gamma_C)$ are defined with

$$\left.\begin{array}{l} f^+ := (|f| + f)/2 \geq 0 \\ f^- := (|f| - f)/2 \geq 0 \end{array}\right\} \Rightarrow f = f^+ - f^-. \tag{3.47}$$

The main aim of this section is to find a relation between the penalty parameter ε and the characteristical meshsize h and polynomial degree p in the quasiuniform *hp*-discretization of the problem with boundary elements, such that the optimal convergence rate is achieved.

For simplicity of presentation we assume that both Γ_D and Γ_C are connected open curves. Furthermore, we consider only the case $\overline{\Gamma}_D \cap \overline{\Gamma}_C = \emptyset$.

Remark 3.2.1. *In fact, the case $\overline{\Gamma}_D \cap \overline{\Gamma}_C = \emptyset$, or equivalently the case when Γ_N has two disjoint connected components, is the most general case. Indeed, for $\Gamma_N = \emptyset$ we obtain $\Gamma_C \equiv \Sigma$ and the set of admissible normal contact tractions Λ is not a subset of $\tilde{H}^{-1/2}(\Gamma_C)$, but a subset of $H^{-1/2}(\Gamma_C)$. Therefore, do not need the inf-sup condition in the form of (3.52). On the other hand, if we replace the space $\tilde{H}^{-1/2}(\Gamma_C)$ with $H^{-1/2}(\Gamma_C)$ in the right-hand side of (3.52), we obtain a condition, which holds trivially, since $(H^{-1/2}(\Gamma_C))' = \tilde{H}^{1/2}(\Gamma_C) = \tilde{H}^{1/2}(\Sigma)$. Moreover, the case of connected Γ_N can be treated by combining the arguments for vanishing Γ_N with the arguments presented in this section below.*

Further down, if no missunderstanding can occur, we omit the domain of integration γ when writing the dual product $\langle \cdot, \cdot \rangle_\gamma$.

3.2.2 Inf-sup condition

In this paragraph we prove an *inf-sup* condition, which is intensively used in the forthcoming a priori error estimation. The main result is given by the following abstract theorem.

Theorem 3.2.1. *Let Γ be a closed Lipschitz curve with two open connected disjoint subsets $\gamma_0 \subset \Gamma, \gamma_1 \subset \Gamma, \overline{\gamma}_0 \cap \overline{\gamma}_1 = \emptyset$. Let also $\gamma_0^* := \Gamma \setminus \overline{\gamma}_0$, $\gamma_{01}^* := \Gamma \setminus (\overline{\gamma}_0 \cup \overline{\gamma}_1)$. Then there holds the following inf-sup condition:*

$$\exists \alpha > 0 : \qquad \sup_{v \in \tilde{H}^{1/2}(\gamma_0^*)\setminus\{0\}} \frac{\langle \mu, v\rangle_{\gamma_1}}{||v||_{\tilde{H}^{1/2}(\gamma_0^*)}} \geq \alpha ||\mu||_{\tilde{H}^{-1/2}(\gamma_1)} \qquad \forall \mu \in \tilde{H}^{-1/2}(\gamma_1). \tag{3.48}$$

Moreover, the constant $\alpha > 0$ depends only on $\min_{i=1,2} |(\gamma_{01}^*)^i|$, where $(\gamma_{01}^*)^i, i = 1, 2$ are connected components of γ_{01}^*.

To prove the above theorem we need two following auxiliary lemmas.

Lemma 3.2.1. *Let us adopt notations of Theorem 3.2.1 and let*

$$X_{\gamma_0,\gamma_1} := \left\{\chi \geq 0 : \ \ ||\chi||_{L_\infty(\Gamma)} = 1, \ \chi' \in L_\infty(\Gamma), \ \chi|_{\gamma_0} \equiv 0 \ \ \text{and} \ \ \chi|_{\gamma_1} \equiv 1\right\}.$$

Then for arbitrary $v \in H^{1/2}(\Gamma)$ and for arbitrary $\chi \in X_{\gamma_0,\gamma_1}$, there holds

$$\chi v \in H^{1/2}(\Gamma), \qquad \chi v|_{\gamma_0^*} \in \tilde{H}^{1/2}(\gamma_0^*),$$

and

$$||\chi v||_{\tilde{H}^{1/2}(\gamma_0^*)} := ||\chi v||_{H^{1/2}(\Gamma)} \leq C_{\chi'} ||v||_{H^{1/2}(\gamma_0^*)} \leq C_{\chi'} ||v||_{H^{1/2}(\Gamma)}. \tag{3.49}$$

where $C_{\chi'} = 2^{1/4}\left(1 + ||\chi'||^2_{L_\infty(\gamma_{01}^*)}\right)^{1/4}$.

Proof. Obviously there holds $||\chi v||_{L_2(\Gamma)} \leq ||v||_{L_2(\gamma_0^*)}$. Further, for $v \in H^1(\Gamma)$ we obtain

$$\begin{aligned}
||\chi v||_{H^1(\Gamma)} &= \left(\int_\Gamma (\chi' v + \chi v')^2 \, ds + ||\chi v||^2_{L_2(\Gamma)}\right)^{1/2} \\
&\leq \left(2\int_\Gamma (\chi' v)^2 + (\chi v')^2 \, ds + ||\chi v||^2_{L_2(\Gamma)}\right)^{1/2} \\
&\leq \sqrt{2}\left(||\chi'||^2_{L_\infty(\gamma_{01}^*)} ||v||^2_{L_2(\gamma_{01}^*)} + ||v'||^2_{L_2(\gamma_0^*)} + ||v||^2_{L_2(\gamma_0^*)}\right)^{1/2} \\
&\leq \sqrt{2}\left(1 + ||\chi'||^2_{L_\infty(\gamma_{01}^*)}\right)^{1/2} ||v||_{H^1(\gamma_0^*)}.
\end{aligned}$$

Then the first inequality in the assertion of the lemma follows by the real interpolation between L_2 and H^1. The second inequality follows trivially by definition of the Sobolev spaces on open curves. □

Lemma 3.2.2. *Under notations of Theorem 3.2.1 the following statement holds. For all $\phi \in H^{1/2}(\gamma_1)$ there exists an extension $f_\phi \in \tilde{H}^{1/2}(\gamma_0^*)$ of ϕ onto γ_0^*, such that $f_\phi|_{\gamma_1} = \phi$ and*

$$\exists \alpha > 0 : \qquad ||\phi||_{H^{1/2}(\gamma_1)} \geq \alpha ||f_\phi||_{\tilde{H}^{1/2}(\gamma_0^*)}, \tag{3.50}$$

where the constant $\alpha > 0$ depends only on $\min_{i=1,2} |(\gamma_{01}^*)^i|$, where $(\gamma_{01}^*)^i$ are connected components of γ_{01}^*.

Proof. Using the definition of the $H^{1/2}$-norm on open curve, and Lemma 3.2.1 we obtain for arbitrary fixed $\chi \in X_{\gamma_0,\gamma_1}$

$$\begin{aligned}||\phi||_{H^{1/2}(\gamma_1)} :=& \inf_{v\in H^{1/2}(\Gamma)} \{||v||_{H^{1/2}(\Gamma)} : v|_{\gamma_1} = \phi\} \\ \geq& C_{\chi'}^{-1} \inf_{v\in H^{1/2}(\Gamma)} \left\{||\chi v||_{\tilde{H}^{1/2}(\gamma_0^*)} : \chi v|_{\gamma_1} = \phi\right\} \\ \geq& C_{\chi'}^{-1} \inf_{f\in \tilde{H}^{1/2}(\gamma_0^*)} \left\{||f||_{\tilde{H}^{1/2}(\gamma_0^*)} : f|_{\gamma_1} = \phi\right\}.\end{aligned}$$

The last inequality holds due to inclusion

$$\left\{\chi v|_{\gamma_0^*} : v \in H^{1/2}(\Gamma)\right\} \subset \tilde{H}^{1/2}(\gamma_0^*) \qquad \forall \chi \in X_{\gamma_0,\gamma_1}.$$

Further, there exists $f_\phi \in \left\{w \in \tilde{H}^{1/2}(\gamma_0^*) : w|_{\gamma_1} = \phi\right\}$ such that

$$||f_\phi||_{\tilde{H}^{1/2}(\gamma_0^*)} \leq 2 \inf_{f\in \tilde{H}^{1/2}(\gamma_0^*)} \left\{||f||_{\tilde{H}^{1/2}(\gamma_0^*)} : f|_{\gamma_1} = \phi\right\}.$$

and therefore

$$||\phi||_{H^{1/2}(\gamma_1)} \geq (2C_{\chi'})^{-1}||f_\phi||_{\tilde{H}^{1/2}(\gamma_0^*)},$$

The largest constant α in the above estimate is given by

$$\alpha := \left(2 \inf_{\chi\in X_{\gamma_0,\gamma_1}} C_{\chi'}\right)^{-1} = 2^{-5/4}\left(1 + \inf_{\chi\in X_{\gamma_0,\gamma_1}} ||\chi'||^2_{L_\infty(\gamma_{01}^*)}\right)^{-1/4}.$$

The infimum is obviously achieved for continuous, piecewise linear χ. Therefore

$$\alpha = 2^{-5/4}\left(1 + \min_{i=1,2} \left(\arctan|(\gamma_{01}^*)^i|^{-1}\right)^2\right)^{-1/4}. \tag{3.51}$$

□

Proof. (of Theorem 3.2.1)

The statement of Theorem 3.2.1 follows by definition of Sobolev norm via duality pairing

$$\begin{aligned}||\mu||_{\tilde{H}^{-1/2}(\gamma_1)} =& \sup_{\phi\in H^{1/2}(\gamma_1)\setminus\{0\}} \frac{\langle\mu,\phi\rangle_{\gamma_1}}{||\phi||_{H^{1/2}(\gamma_1)}} \\ \leq& \alpha^{-1} \sup_{\phi\in H^{1/2}(\gamma_1)\setminus\{0\}} \frac{\langle\mu,f_\phi\rangle_{\gamma_1}}{||f_\phi||_{\tilde{H}^{1/2}(\gamma_0^*)}} \\ \leq& \alpha^{-1} \sup_{v\in \tilde{H}^{1/2}(\gamma_0^*)\setminus\{0\}} \frac{\langle\mu,v\rangle_{\gamma_1}}{||v||_{\tilde{H}^{1/2}(\gamma_0^*)}}\end{aligned}$$

where the constant α is defined in (3.51). The last inequality holds, since $f_\phi \in \tilde{H}^{1/2}(\gamma_0^*)$ for arbitrary $\phi \in H^{1/2}(\gamma_1)$ by construction. □

Corollary 3.2.1. *Theorem 3.2.1 trivially yields for* $\gamma_0 = \Gamma_D, \gamma_1 = \Gamma_C, \gamma_{01}^* = \Gamma_N$ *and* $\gamma_0^* = \Sigma$ *the following result*

$$\exists \alpha > 0 : \qquad \sup_{\boldsymbol{v} \in \tilde{\boldsymbol{H}}^{1/2}(\Sigma)\setminus\{0\}} \frac{\langle \mu, v_n \rangle_{\Gamma_C}}{||\boldsymbol{v}||_{\tilde{\boldsymbol{H}}^{1/2}(\Sigma)}} \geq \alpha ||\mu||_{\tilde{H}^{-1/2}(\Gamma_C)} \qquad \forall \mu \in \tilde{H}^{-1/2}(\Gamma_C), \tag{3.52}$$

where the constant $\alpha > 0$ *depends only on* $\min_{i=1,2} |\Gamma_N^i|$, *where* $\Gamma_N^i, i = 1, 2$ *are connected components of* Γ_N.

3.2.3 Consistency error in the penalty approximation

First, we prove some auxiliary results required in the proof of Theorem 3.2.2.

Lemma 3.2.3. *Let* $\boldsymbol{u} \in \boldsymbol{\mathcal{V}}$, $\lambda \in \Lambda$ *solve the Lagrange multiplier formulation (3.44), let* $\boldsymbol{u}^\varepsilon \in \boldsymbol{\mathcal{V}}$ *solve the penalty formulation (3.45) and let* p_n^ε *be defined with (3.46). Then there holds*

$$\langle \lambda - p_n^\varepsilon, u_n - g \rangle \leq 0.$$

Proof. Inserting $\mu = 0 \in \Lambda$, $\mu = 2\lambda \in \Lambda$ in the second equation in (3.44) gives

$$\left.\begin{array}{c} \langle -\lambda, u_n - g \rangle \geq 0 \\ \langle \lambda, u_n - g \rangle \geq 0 \end{array}\right\} \Rightarrow \langle \lambda, u_n - g \rangle = 0.$$

Equivalence of the Lagrange multiplier formulation (3.44) and the variational inequality (3.41) yields $\boldsymbol{u} \in \boldsymbol{\mathcal{K}}$ and therefore $(u_n - g)^+ \equiv 0$. Thus

$$\begin{aligned} \langle \lambda - p_n^\varepsilon, u_n - g \rangle &= \langle -p_n^\varepsilon, u_n - g \rangle \\ &= \langle \frac{1}{\varepsilon}(u_n^\varepsilon - g)^+, (u_n - g)^+ \rangle - \langle \frac{1}{\varepsilon}(u_n^\varepsilon - g)^+, (u_n - g)^- \rangle \\ &= -\langle \frac{1}{\varepsilon}(u_n^\varepsilon - g)^+, (u_n - g)^- \rangle \leq 0, \end{aligned}$$

since $(u_n^\varepsilon - g)^+ \geq 0$ and $(u_n - g)^- \geq 0$ on Γ_C provided by (3.47). □

Lemma 3.2.4. *Let* $\boldsymbol{u} \in \boldsymbol{\mathcal{V}}$, $\lambda \in \Lambda$ *solve the Lagrange multiplier formulation (3.44), let* $\boldsymbol{u}^\varepsilon \in \boldsymbol{\mathcal{V}}$ *solve the penalty formulation (3.45) and let* p_n^ε *be defined with (3.46). Then there holds*

$$\langle p_n^\varepsilon - \lambda, (u_n^\varepsilon - g)^- \rangle \geq 0.$$

Proof. For every function $f \in H^{1/2}(\Gamma_C)$ there holds $\langle f^+, f^- \rangle = 0$, because $\mathrm{supp} f^+ \cap \mathrm{supp} f^-$ has the Lebesgue measure zero. This yields $\langle p_n^\varepsilon, (u_n^\varepsilon - g)^- \rangle = 0$, and therefore

$$\langle p_n^\varepsilon - \mu, (u_n^\varepsilon - g)^- \rangle = \langle \mu, -(u_n^\varepsilon - g)^- \rangle \geq 0 \qquad \forall \mu \in \Lambda.$$

The last inequality follows from the definition of Λ (3.39). □

Lemma 3.2.5. *Let $\boldsymbol{u} \in \boldsymbol{\mathcal{V}}$, $\lambda \in \Lambda$ solve the Lagrange multiplier formulation (3.44), let $\boldsymbol{u}^\varepsilon \in \boldsymbol{\mathcal{V}}$ solve the penalty formulation (3.45) and let p_n^ε be defined with (3.46). Then there holds*

$$||\lambda - p_n^\varepsilon||_{\tilde{H}^{-1/2}(\Gamma_C)} \leq \frac{C_S}{\alpha}||\boldsymbol{u} - \boldsymbol{u}^\varepsilon||_{\tilde{\boldsymbol{H}}^{1/2}(\Sigma)},$$

where C_S is the continuity constant of the Steklov-Poincaré operator S and the constant $\alpha > 0$ comes from the inf-sup condition (3.52).

Proof. Inf-sup condition (3.52) combined with penalty formulation (3.44) and Lagrange multiplier formulation (3.45) gives

$$\begin{aligned}
\alpha||\lambda - p_n^\varepsilon||_{\tilde{H}^{-1/2}(\Gamma_C)} &\leq \sup_{\boldsymbol{v}\in\boldsymbol{\mathcal{V}}} \frac{\langle \lambda - p_n^\varepsilon, v_n\rangle_{\Gamma_C}}{||\boldsymbol{v}||_{\tilde{\boldsymbol{H}}^{1/2}(\Sigma)}} \\
&= \sup_{\boldsymbol{v}\in\boldsymbol{\mathcal{V}}} \frac{\langle S\boldsymbol{u}, \boldsymbol{v}\rangle_\Sigma - L(\boldsymbol{v}) - \langle S\boldsymbol{u}^\varepsilon, \boldsymbol{v}\rangle_\Sigma + L(\boldsymbol{v})}{||\boldsymbol{v}||_{\tilde{\boldsymbol{H}}^{1/2}(\Sigma)}} \\
&= \sup_{\boldsymbol{v}\in\boldsymbol{\mathcal{V}}} \frac{\langle S(\boldsymbol{u} - \boldsymbol{u}^\varepsilon), \boldsymbol{v}\rangle_\Sigma}{||\boldsymbol{v}||_{\tilde{\boldsymbol{H}}^{1/2}(\Sigma)}} \leq C_S||\boldsymbol{u} - \boldsymbol{u}^\varepsilon||_{\tilde{\boldsymbol{H}}^{1/2}(\Sigma)}.
\end{aligned}$$

□

Now we are in the position to derive an upper bound for the error, caused by penalization.

Theorem 3.2.2. *Let $\boldsymbol{u} \in \boldsymbol{\mathcal{V}}$, $\lambda \in \Lambda$ solve the Lagrange multiplier formulation (3.44), let $\boldsymbol{u}^\varepsilon \in \boldsymbol{\mathcal{V}}$ solve the penalty formulation (3.45) and let p_n^ε be defined with (3.46). We assume that $\lambda \in H^{1/2}(\Gamma_C)$. Then there holds*

$$||\boldsymbol{u} - \boldsymbol{u}^\varepsilon||_{\tilde{\boldsymbol{H}}^{1/2}(\Sigma)} \leq \frac{C_S}{c_S\alpha}||\varepsilon\lambda||_{H^{1/2}(\Gamma_C)}, \tag{3.53}$$

$$||\lambda - p_n^\varepsilon||_{\tilde{H}^{-1/2}(\Gamma_C)} \leq \frac{C_S^2}{c_S\alpha^2}||\varepsilon\lambda||_{H^{1/2}(\Gamma_C)}, \tag{3.54}$$

where C_S and c_S are continuity and ellipticity constants of S respectively, and the constant $\alpha > 0$ comes from the inf-sup condition (3.52).

Proof. According to (3.44), (3.45) we obtain

$$\langle S\boldsymbol{u}, \boldsymbol{v}\rangle - \langle \lambda, v_n\rangle = L(\boldsymbol{v}) \qquad \forall \boldsymbol{v} \in \boldsymbol{\mathcal{V}},$$

$$\langle S\boldsymbol{u}^\varepsilon, \boldsymbol{v}\rangle - \langle p_n^\varepsilon, v_n\rangle = L(\boldsymbol{v}) \qquad \forall \boldsymbol{v} \in \boldsymbol{\mathcal{V}},$$

Subtracting these variational equations and choosing $\boldsymbol{v} := \boldsymbol{u} - \boldsymbol{u}^\varepsilon \in \boldsymbol{\mathcal{V}}$ we obtain

$$\begin{aligned}
\langle S(\boldsymbol{u} - \boldsymbol{u}^\varepsilon), \boldsymbol{u} - \boldsymbol{u}^\varepsilon\rangle &= \langle \lambda - p_n^\varepsilon, u_n - u_n^\varepsilon\rangle \\
&= \langle \lambda - p_n^\varepsilon, u_n - g\rangle + \langle p_n^\varepsilon - \lambda, u_n^\varepsilon - g\rangle
\end{aligned}$$

Lemma 3.2.3 provides $\langle \lambda - p_n^\varepsilon, u_n - g \rangle \leq 0$, Lemma 3.2.4 gives $\langle p_n^\varepsilon - \lambda, (u_n^\varepsilon - g)^- \rangle \geq 0$. Thus

$$\begin{aligned}\langle S(\boldsymbol{u} - \boldsymbol{u}^\varepsilon), \boldsymbol{u} - \boldsymbol{u}^\varepsilon \rangle &\leq \langle p_n^\varepsilon - \lambda, u_n^\varepsilon - g \rangle \\ &= \langle p_n^\varepsilon - \lambda, (u_n^\varepsilon - g)^+ \rangle - \langle p_n^\varepsilon - \lambda, (u_n^\varepsilon - g)^- \rangle \\ &\leq \langle p_n^\varepsilon - \lambda, (u_n^\varepsilon - g)^+ \rangle.\end{aligned}$$

Recalling the definition (3.46) we rewrite $\langle p_n^\varepsilon - \lambda, (u_n^\varepsilon - g)^+ \rangle = \langle p_n^\varepsilon - \lambda, -\varepsilon p_n^\varepsilon \rangle$. Further, since $\langle p_n^\varepsilon - \lambda, \varepsilon(p_n^\varepsilon - \lambda) \rangle \geq 0$ there holds

$$\begin{aligned}\langle S(\boldsymbol{u} - \boldsymbol{u}^\varepsilon), \boldsymbol{u} - \boldsymbol{u}^\varepsilon \rangle &\leq \langle p_n^\varepsilon - \lambda, -\varepsilon p_n^\varepsilon \rangle \\ &\leq \langle p_n^\varepsilon - \lambda, -\varepsilon p_n^\varepsilon \rangle + \langle p_n^\varepsilon - \lambda, \varepsilon(p_n^\varepsilon - \lambda) \rangle \\ &= \langle \lambda - p_n^\varepsilon, \varepsilon \lambda \rangle \\ &\leq ||\lambda - p_n^\varepsilon||_{\tilde{H}^{-1/2}(\Gamma_C)} ||\varepsilon \lambda||_{H^{1/2}(\Gamma_C)} \\ &\leq \frac{C_S}{\alpha} ||\boldsymbol{u} - \boldsymbol{u}^\varepsilon||_{\tilde{\boldsymbol{H}}^{1/2}(\Sigma)} ||\varepsilon \lambda||_{H^{1/2}(\Gamma_C)},\end{aligned}$$

where we applied Lemma 3.2.5 in the last inequality. Ellipticity of the Steklov-Poincaré operator (1.10) provides

$$c_S ||\boldsymbol{u} - \boldsymbol{u}^\varepsilon||^2_{\tilde{\boldsymbol{H}}^{1/2}(\Sigma)} \leq \langle S(\boldsymbol{u} - \boldsymbol{u}^\varepsilon), \boldsymbol{u} - \boldsymbol{u}^\varepsilon \rangle$$

and therefore

$$||\boldsymbol{u} - \boldsymbol{u}^\varepsilon||_{\tilde{\boldsymbol{H}}^{1/2}(\Sigma)} \leq \frac{C_S}{c_S \alpha} ||\varepsilon \lambda||_{H^{1/2}(\Gamma_C)}.$$

We apply Lemma 3.2.5 again and get

$$||\lambda - p_n^\varepsilon||_{\tilde{H}^{-1/2}(\Gamma_C)} \leq \frac{C_S}{\alpha} ||\boldsymbol{u} - \boldsymbol{u}^\varepsilon||_{\tilde{\boldsymbol{H}}^{1/2}(\Sigma)} \leq \frac{C_S^2}{c_S \alpha^2} ||\varepsilon \lambda||_{H^{1/2}(\Gamma_C)}.$$

□

3.2.4 A priori error analysis

Discretization

In order to discretize the problem, we decompose the boundary Γ into disjoint straight line segments $I \in \mathcal{T}_h$, with diameters not exceeding h. We allow only conforming meshes $\mathcal{T}_h$, i.e. the points $\bar{\Gamma}_D \cap \bar{\Gamma}_N$, $\bar{\Gamma}_D \cap \bar{\Gamma}_C$, $\bar{\Gamma}_N \cap \bar{\Gamma}_C$, are nodes of $\mathcal{T}_h$. Let $\mathcal{P}_{p_I}(I)$ be the space of polynomials on a segment I, with degree less or equal p_I. We define the boundary element spaces on Γ as follows

$$\begin{aligned}\overline{\boldsymbol{\mathcal{V}}}_{hp} &:= \left\{ \boldsymbol{U} \in \boldsymbol{\mathcal{V}} : \ \forall I \in \mathcal{T}_h, \ \boldsymbol{U} \in [\mathcal{P}_{p_I}(I)]^2 \right\}, \\ \overline{\boldsymbol{\mathcal{W}}}_{hp} &:= \left\{ \boldsymbol{U} \in \boldsymbol{\mathcal{W}} : \ \forall I \in \mathcal{T}_h, \ \boldsymbol{U} \in [\mathcal{P}_{p_I - 1}(I)]^2 \right\},\end{aligned}$$

where $\boldsymbol{\mathcal{V}}$ and $\boldsymbol{\mathcal{W}}$ are given by (3.36) and (3.37) respectively. We assume that the meshes $\mathcal{T}_h$ and the polynomial degree distributions in $\overline{\boldsymbol{\mathcal{V}}}_{hp}$ are quasiuniform and let h and p be the characteristic mesh size and polynomial degree respectively.

In order to define discrete boundary integral operators, we introduce canonical embeddings $j_{hp} : \overline{\boldsymbol{\mathcal{V}}}_{hp} \hookrightarrow \boldsymbol{H}^{1/2}(\Gamma)$, $i_{hp} : \overline{\boldsymbol{\mathcal{W}}}_{hp} \hookrightarrow \boldsymbol{H}^{-1/2}(\Gamma)$, and their duals j^*_{hp}, i^*_{hp} with respect to the dual pairing $\langle \cdot, \cdot \rangle$, cf. (1.14). Now, we define discrete boundary integral operators as follows

$$\begin{aligned} V_{hp} &:= i^*_{hp} V i_{hp}, \quad & K_{hp} &:= i^*_{hp} K j_{hp}, \\ K'_{hp} &:= j^*_{hp} K' i_{hp}, \quad & W_{hp} &:= j^*_{hp} W j_{hp}, \end{aligned} \tag{3.55}$$

$$\begin{aligned} \hat{S} &:= W + (K' + 1/2) i_{hp} V_{hp}^{-1} i^*_{hp} (K + 1/2), \\ \hat{E} &:= S - \hat{S} = (K' + 1/2)(V^{-1} - i_{hp} V_{hp}^{-1} i^*_{hp})(K + 1/2). \end{aligned} \tag{3.56}$$

We introduce discrete spaces $\boldsymbol{\mathcal{V}}_{hp}$ and $\boldsymbol{\mathcal{W}}_{hp}$ associated with $\overline{\boldsymbol{\mathcal{V}}}_{hp}$ and $\overline{\boldsymbol{\mathcal{W}}}_{hp}$ respectively, and given by

$$\boldsymbol{\mathcal{V}}_{hp} = \left\{ j_{hp} \boldsymbol{u}_{hp} : \boldsymbol{u}_{hp} \in \overline{\boldsymbol{\mathcal{V}}}_{hp} \right\}, \qquad \boldsymbol{\mathcal{W}}_{hp} = \left\{ i_{hp} \boldsymbol{\phi}_{hp} : \boldsymbol{\phi}_{hp} \in \overline{\boldsymbol{\mathcal{W}}}_{hp} \right\}.$$

For clarity of presentation we will distinguish between spaces $\overline{\boldsymbol{\mathcal{V}}}_{hp}$, $\overline{\boldsymbol{\mathcal{W}}}_{hp}$ and $\boldsymbol{\mathcal{V}}_{hp}$, $\boldsymbol{\mathcal{W}}_{hp}$, respectively. This will be convenient e.g. in the proof of Lemma 3.2.7. Now, we introduce the discrete penalty formulation as follows: For given $\varepsilon > 0$ find $\boldsymbol{U}^\varepsilon \in \boldsymbol{\mathcal{V}}_{hp}$:

$$\left\langle \hat{S} \boldsymbol{U}^\varepsilon, \boldsymbol{v} \right\rangle - \left\langle P_n^\varepsilon, v_n \right\rangle = L(\boldsymbol{v}) \qquad \forall \boldsymbol{v} \in \boldsymbol{\mathcal{V}}_{hp}, \tag{3.57}$$

where

$$P_n^\varepsilon := -\frac{1}{\varepsilon} (U_n^\varepsilon - g)^+. \tag{3.58}$$

Furthermore, for $\boldsymbol{u}^\varepsilon \in \boldsymbol{\mathcal{V}}$ and $\boldsymbol{U}^\varepsilon \in \boldsymbol{\mathcal{V}}_{hp}$ we define the traction-like functions

$$\begin{aligned} \boldsymbol{\psi} &:= V^{-1}(K + 1/2) \boldsymbol{u}^\varepsilon, \\ \boldsymbol{\Psi}^* &:= V^{-1}(K + 1/2) \boldsymbol{U}^\varepsilon, \\ \boldsymbol{\Psi} &:= i_{hp} V_{hp}^{-1} i^*_{hp} (K + 1/2) \boldsymbol{U}^\varepsilon. \end{aligned} \tag{3.59}$$

Lemma 3.2.6. *(cf. [15, Proposition 5.1]) Let $\boldsymbol{u}^\varepsilon \in \boldsymbol{\mathcal{V}}$, $\boldsymbol{U}^\varepsilon \in \boldsymbol{\mathcal{V}}_{hp}$ and traction-like functions defined by (3.59). Then the following identity holds*

$$||\boldsymbol{u}^\varepsilon - \boldsymbol{U}^\varepsilon||_W^2 + ||\boldsymbol{\psi} - \boldsymbol{\Psi}||_V^2 = \left\langle S \boldsymbol{u}^\varepsilon - \hat{S} \boldsymbol{U}^\varepsilon, \boldsymbol{u}^\varepsilon - \boldsymbol{U}^\varepsilon \right\rangle + \left\langle V(\boldsymbol{\Psi}^* - \boldsymbol{\Psi}), \boldsymbol{\psi} - \boldsymbol{\Psi} \right\rangle,$$

where

$$\begin{aligned} ||\boldsymbol{u}^\varepsilon - \boldsymbol{U}^\varepsilon||_W &:= \left\langle W(\boldsymbol{u}^\varepsilon - \boldsymbol{U}^\varepsilon), \boldsymbol{u}^\varepsilon - \boldsymbol{U}^\varepsilon \right\rangle^{1/2}, \\ ||\boldsymbol{\psi} - \boldsymbol{\Psi}||_V &:= \left\langle V(\boldsymbol{\psi} - \boldsymbol{\Psi}), \boldsymbol{\psi} - \boldsymbol{\Psi} \right\rangle^{1/2}. \end{aligned}$$

Proof. The definition of the Steklov-Poincaré operator (3.40) yields

$$\begin{aligned}
\left\langle S(\boldsymbol{u}^\varepsilon - \boldsymbol{U}^\varepsilon), \boldsymbol{u}^\varepsilon - \boldsymbol{U}^\varepsilon \right\rangle &= \left\langle (W + (K' + 1/2)V^{-1}(K + 1/2))(\boldsymbol{u}^\varepsilon - \boldsymbol{U}^\varepsilon), \boldsymbol{u}^\varepsilon - \boldsymbol{U}^\varepsilon \right\rangle \\
&= \left\langle W(\boldsymbol{u}^\varepsilon - \boldsymbol{U}^\varepsilon), \boldsymbol{u}^\varepsilon - \boldsymbol{U}^\varepsilon \right\rangle \\
&\quad + \left\langle (K + 1/2))(\boldsymbol{u}^\varepsilon - \boldsymbol{U}^\varepsilon), V^{-1}(K + 1/2)(\boldsymbol{u}^\varepsilon - \boldsymbol{U}^\varepsilon) \right\rangle \\
&= ||\boldsymbol{u}^\varepsilon - \boldsymbol{U}^\varepsilon||_W^2 + \left\langle V(\boldsymbol{\psi} - \boldsymbol{\Psi}^*), \boldsymbol{\psi} - \boldsymbol{\Psi}^* \right\rangle,
\end{aligned}$$

Further, (3.56) gives

$$\begin{aligned}
\left\langle (S - \hat{S})\boldsymbol{U}^\varepsilon, \boldsymbol{u}^\varepsilon - \boldsymbol{U}^\varepsilon \right\rangle &= \left\langle (K' + 1/2)(V - i_{hp}V_{hp}^{-1}i_{hp}^*)(K + 1/2)\boldsymbol{U}^\varepsilon, \boldsymbol{u}^\varepsilon - \boldsymbol{U}^\varepsilon \right\rangle \\
&= \left\langle (V - i_{hp}V_{hp}^{-1}i_{hp}^*)(K + 1/2)\boldsymbol{U}^\varepsilon, (K + 1/2)(\boldsymbol{u}^\varepsilon - \boldsymbol{U}^\varepsilon) \right\rangle \\
&= \left\langle \boldsymbol{\Psi}^* - \boldsymbol{\Psi}, V(\boldsymbol{\psi} - \boldsymbol{\Psi}^*) \right\rangle \\
&= \left\langle V(\boldsymbol{\Psi}^* - \boldsymbol{\Psi}), \boldsymbol{\psi} - \boldsymbol{\Psi}^* \right\rangle.
\end{aligned}$$

Combining the upper identities we get

$$\begin{aligned}
\left\langle S\boldsymbol{u}^\varepsilon - \hat{S}\boldsymbol{U}^\varepsilon, \boldsymbol{u}^\varepsilon - \boldsymbol{U}^\varepsilon \right\rangle &= \left\langle S(\boldsymbol{u}^\varepsilon - \boldsymbol{U}^\varepsilon), \boldsymbol{u}^\varepsilon - \boldsymbol{U}^\varepsilon \right\rangle + \left\langle (S - \hat{S})\boldsymbol{U}^\varepsilon, \boldsymbol{u}^\varepsilon - \boldsymbol{U}^\varepsilon \right\rangle \\
&= ||\boldsymbol{u}^\varepsilon - \boldsymbol{U}^\varepsilon||_W^2 + \left\langle V(\boldsymbol{\psi} - \boldsymbol{\Psi}^*), \boldsymbol{\psi} - \boldsymbol{\Psi}^* \right\rangle \\
&\qquad + \left\langle V(\boldsymbol{\Psi}^* - \boldsymbol{\Psi}), \boldsymbol{\psi} - \boldsymbol{\Psi}^* \right\rangle \\
&= ||\boldsymbol{u}^\varepsilon - \boldsymbol{U}^\varepsilon||_W^2 + \left\langle V(\boldsymbol{\psi} - \boldsymbol{\Psi}), \boldsymbol{\psi} - \boldsymbol{\Psi}^* \right\rangle \\
&= ||\boldsymbol{u}^\varepsilon - \boldsymbol{U}^\varepsilon||_W^2 + \left\langle V(\boldsymbol{\psi} - \boldsymbol{\Psi}), \boldsymbol{\psi} - \boldsymbol{\Psi} \right\rangle \\
&\qquad + \left\langle V(\boldsymbol{\psi} - \boldsymbol{\Psi}), \boldsymbol{\Psi} - \boldsymbol{\Psi}^* \right\rangle \\
&= ||\boldsymbol{u}^\varepsilon - \boldsymbol{U}^\varepsilon||_W^2 + ||\boldsymbol{\psi} - \boldsymbol{\Psi}||_V^2 - \left\langle V(\boldsymbol{\Psi}^* - \boldsymbol{\Psi}), \boldsymbol{\psi} - \boldsymbol{\Psi} \right\rangle,
\end{aligned}$$

or equivalently

$$||\boldsymbol{u}^\varepsilon - \boldsymbol{U}^\varepsilon||_W^2 + ||\boldsymbol{\psi} - \boldsymbol{\Psi}||_V^2 = \left\langle S\boldsymbol{u}^\varepsilon - \hat{S}\boldsymbol{U}^\varepsilon, \boldsymbol{u}^\varepsilon - \boldsymbol{U}^\varepsilon \right\rangle + \left\langle V(\boldsymbol{\Psi}^* - \boldsymbol{\Psi}), \boldsymbol{\psi} - \boldsymbol{\Psi} \right\rangle.$$

□

Lemma 3.2.7. *For $\boldsymbol{\Psi}^*$, $\boldsymbol{\Psi}$ defined in (3.59) there holds*

$$\left\langle V(\boldsymbol{\Psi}^* - \boldsymbol{\Psi}), \boldsymbol{\Phi} \right\rangle = 0, \qquad \forall \boldsymbol{\Phi} \in \boldsymbol{\mathcal{W}}_{hp}.$$

Proof. Using definitions (3.59), (3.55) for $\boldsymbol{\Phi} = i_{hp}\boldsymbol{\eta}_{hp}$, $\boldsymbol{\eta}_{hp} \in \overline{\boldsymbol{\mathcal{W}}}_{hp}$ we obtain

$$\begin{aligned}
\left\langle V\boldsymbol{\Psi}^*, \boldsymbol{\Phi} \right\rangle &= \left\langle (K + 1/2)\boldsymbol{U}^\varepsilon, \boldsymbol{\Phi} \right\rangle = \left\langle i_{hp}^*(K + 1/2)\boldsymbol{U}^\varepsilon, \boldsymbol{\eta}_{hp} \right\rangle \\
&= \left\langle V_{hp}V_{hp}^{-1}i_{hp}^*(K + 1/2)\boldsymbol{U}^\varepsilon, \boldsymbol{\eta}_{hp} \right\rangle \\
&= \left\langle i_{hp}^*Vi_{hp}V_{hp}^{-1}i_{hp}^*(K + 1/2)\boldsymbol{U}^\varepsilon, \boldsymbol{\eta}_{hp} \right\rangle \\
&= \left\langle i_{hp}^*V\boldsymbol{\Psi}, \boldsymbol{\eta}_{hp} \right\rangle = \left\langle V\boldsymbol{\Psi}, \boldsymbol{\Phi} \right\rangle.
\end{aligned}$$

□

Similarly to [16] we prove the following lemma.

Lemma 3.2.8. *(cf. [16, Lemma 4.1]) For p_n^ε and P_n^ε given by (3.46), (3.58) respectively the following inequality holds*

$$||\varepsilon^{1/2}(p_n^\varepsilon - P_n^\varepsilon)||^2_{L_2(\Gamma_C)} \leq -\langle p_n^\varepsilon - P_n^\varepsilon, u_n^\varepsilon - U_n^\varepsilon \rangle.$$

Proof. To prove the lemma we use the simple observation, that

$$((u_n^\varepsilon - g)^+ - (U_n^\varepsilon - g)^+)(u_n^\varepsilon - U_n^\varepsilon) = (a^+ - b^+)(a - b), \tag{3.60}$$

where $a := u_n^\varepsilon - g, b := U_n^\varepsilon - g$. Recalling (3.47) we obtain

$$\begin{aligned}(a^+ - b^+)(a - b) &= |a^+ - b^+|^2 - (a^+ - b^+)(a^- - b^-)\\ &= |a^+ - b^+|^2 + (a^+ b^- + a^- b^+)\\ &\geq |a^+ - b^+|^2 = |(u_n^\varepsilon - g)^+ - (U_n^\varepsilon - g)^+|^2,\end{aligned}$$

since $a^+a^- = 0 = b^+b^-$ and $a^+, a^-, b^+, b^- \geq 0$. That yields

$$\begin{aligned}-\langle p_n^\varepsilon - P_n^\varepsilon, u_n^\varepsilon - U_n^\varepsilon \rangle &= \int_{\Gamma_C} \frac{1}{\varepsilon}((u_n^\varepsilon - g)^+ - (U_n^\varepsilon - g)^+))(u_n^\varepsilon - U_n^\varepsilon)\, ds\\ &\geq \int_{\Gamma_C} \frac{1}{\varepsilon}|(u_n^\varepsilon - g)^+ - (U_n^\varepsilon - g)^+)|^2\, ds\\ &= \int_{\Gamma_C} \varepsilon|p_n^\varepsilon - P_n^\varepsilon|^2\, ds = ||\varepsilon^{1/2}(p_n^\varepsilon - P_n^\varepsilon)||^2_{L_2(\Gamma_C)}.\end{aligned}$$

□

A priori estimate of the penalty discretization error

Theorem 3.2.3. *Let $\boldsymbol{u}^\varepsilon$ solve the continuous penalty problem (3.45), let $\boldsymbol{U}^\varepsilon$ solve the discrete penalty problem (3.57). Let $\boldsymbol{\psi}$, $\boldsymbol{\Psi}$ be defined by (3.59). Then there exists $C > 0$ independent of h, p, ε such that $\forall \boldsymbol{w} \in \boldsymbol{\mathcal{V}}_{hp}$, $\forall \boldsymbol{\Phi} \in \boldsymbol{\mathcal{W}}_{hp}$ there holds*

$$\begin{aligned}&||\boldsymbol{u}^\varepsilon - \boldsymbol{U}^\varepsilon||_{\tilde{\boldsymbol{H}}^{1/2}(\Sigma)} + ||\boldsymbol{\psi} - \boldsymbol{\Psi}||_{\boldsymbol{H}^{-1/2}(\Gamma)} + ||\varepsilon^{1/2}(p_n^\varepsilon - P_n^\varepsilon)||_{L_2(\Gamma_C)}\\ &\quad \leq C(||\boldsymbol{u}^\varepsilon - \boldsymbol{w}||_{\tilde{\boldsymbol{H}}^{1/2}(\Sigma)} + ||\boldsymbol{\psi} - \boldsymbol{\Phi}||_{\boldsymbol{H}^{-1/2}(\Gamma)} + ||\varepsilon^{-1/2}(w_n - u_n^\varepsilon)||_{L_2(\Gamma_C)}).\end{aligned}$$

Proof. We choose $\boldsymbol{v} \in \boldsymbol{\mathcal{V}}_{hp} \subset \boldsymbol{\mathcal{V}}$ in the variational penalty formulation (3.45) and subtract (3.45) from the discrete penalty formulation (3.57). The obtained result is similar to the Galerkin orthogonality property and is given by

$$\langle S\boldsymbol{u}^\varepsilon - \hat{S}\boldsymbol{U}^\varepsilon, \boldsymbol{v} \rangle - \langle p_n^\varepsilon - P_n^\varepsilon, v_n \rangle = 0, \qquad \forall \boldsymbol{v} \in \boldsymbol{\mathcal{V}}_{hp}. \tag{3.61}$$

We choose $\boldsymbol{v} := \boldsymbol{U}^\varepsilon - \boldsymbol{w} \in \boldsymbol{\mathcal{V}}_{hp}$. Then

$$\langle S\boldsymbol{u}^\varepsilon - \hat{S}\boldsymbol{U}^\varepsilon, \boldsymbol{U}^\varepsilon - \boldsymbol{w} \rangle - \langle p_n^\varepsilon - P_n^\varepsilon, U_n^\varepsilon - w_n \rangle = 0, \qquad \forall \boldsymbol{w} \in \boldsymbol{\mathcal{V}}_{hp}.$$

Therefore

$$\begin{aligned}\big\langle S\boldsymbol{u}^\varepsilon - \hat{S}\boldsymbol{U}^\varepsilon, \boldsymbol{u}^\varepsilon - \boldsymbol{U}^\varepsilon\big\rangle - \big\langle p_n^\varepsilon - P_n^\varepsilon, u_n^\varepsilon - U_n^\varepsilon\big\rangle \\ = \big\langle S\boldsymbol{u}^\varepsilon - \hat{S}\boldsymbol{U}^\varepsilon, \boldsymbol{u}^\varepsilon - \boldsymbol{U}^\varepsilon\big\rangle - \big\langle p_n^\varepsilon - P_n^\varepsilon, u_n^\varepsilon - U_n^\varepsilon\big\rangle \\ + \big\langle S\boldsymbol{u}^\varepsilon - \hat{S}\boldsymbol{U}^\varepsilon, \boldsymbol{U}^\varepsilon - \boldsymbol{w}\big\rangle - \big\langle p_n^\varepsilon - P_n^\varepsilon, U_n^\varepsilon - w_n\big\rangle \\ = \big\langle S\boldsymbol{u}^\varepsilon - \hat{S}\boldsymbol{U}^\varepsilon, \boldsymbol{u}^\varepsilon - \boldsymbol{w}\big\rangle - \big\langle p_n^\varepsilon - P_n^\varepsilon, u_n^\varepsilon - w_n\big\rangle.\end{aligned}$$

Thus, according to Lemma 3.2.6 we obtain

$$\begin{aligned}&||\boldsymbol{u}^\varepsilon - \boldsymbol{U}^\varepsilon||_W^2 + ||\boldsymbol{\psi} - \boldsymbol{\Psi}||_V^2 - \big\langle p_n^\varepsilon - P_n^\varepsilon, u_n^\varepsilon - U_n^\varepsilon\big\rangle \qquad (3.62)\\ &= \big\langle S\boldsymbol{u}^\varepsilon - \hat{S}\boldsymbol{U}^\varepsilon, \boldsymbol{u}^\varepsilon - \boldsymbol{U}^\varepsilon\big\rangle - \big\langle p_n^\varepsilon - P_n^\varepsilon, u_n^\varepsilon - U_n^\varepsilon\big\rangle + \big\langle V(\boldsymbol{\Psi}^* - \boldsymbol{\Psi}), \boldsymbol{\psi} - \boldsymbol{\Psi}\big\rangle \\ &= \big\langle S\boldsymbol{u}^\varepsilon - \hat{S}\boldsymbol{U}^\varepsilon, \boldsymbol{u}^\varepsilon - \boldsymbol{w}\big\rangle - \big\langle p_n^\varepsilon - P_n^\varepsilon, u_n^\varepsilon - w_n\big\rangle + \big\langle V(\boldsymbol{\Psi}^* - \boldsymbol{\Psi}), \boldsymbol{\psi} - \boldsymbol{\Psi}\big\rangle \\ &=: A + B + C.\end{aligned}$$

For the term A there holds

$$A \le ||S\boldsymbol{u}^\varepsilon - \hat{S}\boldsymbol{U}^\varepsilon||_{\boldsymbol{H}^{-1/2}(\Gamma)} ||\boldsymbol{u}^\varepsilon - \boldsymbol{w}||_{\tilde{\boldsymbol{H}}^{1/2}(\Sigma)}.$$

With the following identity

$$S\boldsymbol{u}^\varepsilon - \hat{S}\boldsymbol{U}^\varepsilon = S(\boldsymbol{u}^\varepsilon - \boldsymbol{U}^\varepsilon) + \hat{E}\boldsymbol{U}^\varepsilon = S(\boldsymbol{u}^\varepsilon - \boldsymbol{U}^\varepsilon) + \hat{E}(\boldsymbol{U}^\varepsilon - \boldsymbol{u}^\varepsilon) + \hat{E}\boldsymbol{u}^\varepsilon$$

we estimate

$$\begin{aligned}A &\le \Big((C_S + C_{\hat{E}})||\boldsymbol{u}^\varepsilon - \boldsymbol{U}^\varepsilon||_{\tilde{\boldsymbol{H}}^{1/2}(\Sigma)} + ||\hat{E}\boldsymbol{u}^\varepsilon||_{\boldsymbol{H}^{-1/2}(\Sigma)}\Big) ||\boldsymbol{u}^\varepsilon - \boldsymbol{w}||_{\tilde{\boldsymbol{H}}^{1/2}(\Sigma)} \qquad (3.63)\\ &\le (C_S + C_{\hat{E}})||\boldsymbol{u}^\varepsilon - \boldsymbol{U}^\varepsilon||_{\tilde{\boldsymbol{H}}^{1/2}(\Sigma)} ||\boldsymbol{u}^\varepsilon - \boldsymbol{w}||_{\tilde{\boldsymbol{H}}^{1/2}(\Sigma)} \qquad (3.64)\\ &\quad + C_0||\boldsymbol{\psi} - \boldsymbol{\Phi}||_{\boldsymbol{H}^{-1/2}(\Gamma)} ||\boldsymbol{u}^\varepsilon - \boldsymbol{w}||_{\tilde{\boldsymbol{H}}^{1/2}(\Sigma)} \qquad \forall \boldsymbol{\Phi} \in \boldsymbol{\mathcal{W}}_{hp}, \qquad (3.65)\end{aligned}$$

where Lemma 1.4.2 yields the last inequality. For the term B we have

$$B = \big\langle p_n^\varepsilon - P_n^\varepsilon, w_n - u_n^\varepsilon\big\rangle \le ||\varepsilon^{1/2}(p_n^\varepsilon - P_n^\varepsilon)||_{L_2(\Gamma_C)} ||\varepsilon^{-1/2}(w_n - u_n^\varepsilon)||_{L_2(\Gamma_C)}. \qquad (3.66)$$

Finally for the term C we employ the orthogonality property from Lemma 3.2.7 and get

$$\begin{aligned}C &= \big\langle V(\boldsymbol{\Psi}^* - \boldsymbol{\Psi}), \boldsymbol{\psi} - \boldsymbol{\Phi}\big\rangle \\ &= \big\langle V(\boldsymbol{\Psi}^* - \boldsymbol{\psi}), \boldsymbol{\psi} - \boldsymbol{\Phi}\big\rangle + \big\langle V(\boldsymbol{\psi} - \boldsymbol{\Psi}), \boldsymbol{\psi} - \boldsymbol{\Phi}\big\rangle \\ &\le \big\langle (K + 1/2)(\boldsymbol{U}^\varepsilon - \boldsymbol{u}^\varepsilon), \boldsymbol{\psi} - \boldsymbol{\Phi}\big\rangle + C_V||\boldsymbol{\psi} - \boldsymbol{\Psi}||_{\boldsymbol{H}^{-1/2}(\Gamma)} ||\boldsymbol{\psi} - \boldsymbol{\Phi}||_{\boldsymbol{H}^{-1/2}(\Gamma)} \\ &\le (C_K + 1/2)||\boldsymbol{U}^\varepsilon - \boldsymbol{u}^\varepsilon||_{\tilde{\boldsymbol{H}}^{1/2}(\Sigma)} ||\boldsymbol{\psi} - \boldsymbol{\Phi}||_{\boldsymbol{H}^{-1/2}(\Gamma)} \\ &\quad + C_V||\boldsymbol{\psi} - \boldsymbol{\Psi}||_{\boldsymbol{H}^{-1/2}(\Gamma)} ||\boldsymbol{\psi} - \boldsymbol{\Phi}||_{\boldsymbol{H}^{-1/2}(\Gamma)} \qquad \forall \boldsymbol{\Phi} \in \boldsymbol{\mathcal{W}}_{hp}.\end{aligned}$$

As shown in Lemma 3.2.8, the contact term in the left hand side of (3.62) satisfies

$$||\varepsilon^{1/2}(p_n^\varepsilon - P_n^\varepsilon)||_{L_2(\Gamma_C)}^2 \le -\big\langle p_n^\varepsilon - P_n^\varepsilon, u_n^\varepsilon - U_n^\varepsilon\big\rangle.$$

Gathering the above results we obtain from (3.62) the following estimate

$$
\begin{aligned}
||\boldsymbol{u}^\varepsilon - \boldsymbol{U}^\varepsilon||_W^2 + ||\boldsymbol{\psi} - \boldsymbol{\Psi}||_V^2 + ||\varepsilon^{1/2}(p_n^\varepsilon - P_n^\varepsilon)||_{L_2(\Gamma_C)}^2 \\
\leq (C_S + C_{\hat{E}})||\boldsymbol{u}^\varepsilon - \boldsymbol{U}^\varepsilon||_{\tilde{\boldsymbol{H}}^{1/2}(\Sigma)}||\boldsymbol{u}^\varepsilon - \boldsymbol{w}||_{\tilde{\boldsymbol{H}}^{1/2}(\Sigma)} \\
+ C_0||\boldsymbol{\psi} - \boldsymbol{\Phi}||_{\boldsymbol{H}^{-1/2}(\Gamma)}||\boldsymbol{u}^\varepsilon - \boldsymbol{w}||_{\tilde{\boldsymbol{H}}^{1/2}(\Sigma)} \\
+ ||\varepsilon^{1/2}(p_n^\varepsilon - P_n^\varepsilon)||_{L_2(\Gamma_C)}||\varepsilon^{-1/2}(w_n - u_n^\varepsilon)||_{L_2(\Gamma_C)} \\
+ (C_K + 1/2)||\boldsymbol{U}^\varepsilon - \boldsymbol{u}^\varepsilon||_{\tilde{\boldsymbol{H}}^{1/2}(\Sigma)}||\boldsymbol{\psi} - \boldsymbol{\Phi}||_{\boldsymbol{H}^{-1/2}(\Gamma)} \\
+ C_V||\boldsymbol{\psi} - \boldsymbol{\Psi}||_{\boldsymbol{H}^{-1/2}(\Gamma)}||\boldsymbol{\psi} - \boldsymbol{\Phi}||_{\boldsymbol{H}^{-1/2}(\Gamma)}.
\end{aligned}
$$

The standard arguments give

$$
\begin{aligned}
c_1||\boldsymbol{u}^\varepsilon - \boldsymbol{U}^\varepsilon||_{\tilde{\boldsymbol{H}}^{1/2}(\Sigma)}^2 + c_2||\boldsymbol{\psi} - \boldsymbol{\Psi}||_{\boldsymbol{H}^{-1/2}(\Gamma)}^2 + ||\varepsilon^{1/2}(p_n^\varepsilon - P_n^\varepsilon)||_{L_2(\Gamma_C)}^2 \\
\leq c_3||\boldsymbol{u}^\varepsilon - \boldsymbol{w}||_{\tilde{\boldsymbol{H}}^{1/2}(\Sigma)}^2 + c_4||\boldsymbol{\psi} - \boldsymbol{\Phi}||_{\boldsymbol{H}^{-1/2}(\Gamma)}^2 + ||\varepsilon^{-1/2}(w_n - u_n^\varepsilon)||_{L_2(\Gamma_C)}^2
\end{aligned}
\tag{3.67}
$$

where the constants

$$
\begin{aligned}
c_1 &= 2c_W - \theta_1 - \theta_2 \\
c_2 &= 2c_V - \theta_3 \\
c_3 &= (C_S + C_{\hat{E}})^2/\theta_1 + C_0 \\
c_4 &= C_0 + (C_K + 1/2)^2/\theta_2 + C_V^2\theta_3
\end{aligned}
$$

are independent of h, p, ε and c_V, c_W are the ellipticity constants of V, W. The constants c_1, c_2 are positive if $\theta_1, \theta_2, \theta_3 > 0$ are small enough. □

Assume that $\boldsymbol{u}^\varepsilon \in \tilde{\boldsymbol{H}}^{3/2}(\Sigma)$ and $\boldsymbol{\psi} \in \boldsymbol{H}^{1/2}(\Gamma)$. According to [10], [64], there exists a constant $C > 0$, such that there hold the following approximation properties

$$\inf_{\boldsymbol{w}\in\boldsymbol{\mathcal{V}}_{hp}} ||\boldsymbol{u}^\varepsilon - \boldsymbol{w}||_{\tilde{\boldsymbol{H}}^{1/2}(\Sigma)} \leq C\frac{h}{p}||\boldsymbol{u}^\varepsilon||_{\tilde{\boldsymbol{H}}^{3/2}(\Sigma)}, \tag{3.68}$$

$$\inf_{\boldsymbol{\Phi}\in\boldsymbol{\mathcal{W}}_{hp}} ||\boldsymbol{\psi} - \boldsymbol{\Phi}||_{\boldsymbol{H}^{-1/2}(\Gamma)} \leq C\frac{h}{p}||\boldsymbol{\psi}||_{\boldsymbol{H}^{1/2}(\Gamma)}, \tag{3.69}$$

$$\inf_{\boldsymbol{w}\in\boldsymbol{\mathcal{V}}_{hp}} ||\varepsilon^{-1/2}(w_n - u_n^\varepsilon)||_{L_2(\Gamma_C)} \leq C\left(\frac{h}{p}\right)^{3/2} ||\varepsilon^{-1/2}u_n^\varepsilon||_{H^{3/2}(\Gamma_C)}. \tag{3.70}$$

Here we define the Sobolev space $H^{3/2}$ on the part of the boundary of the polygonal domain Ω according to [22].

We recall the equivalent nonsymmetric definition of the Steklov-Poincaré operator (1.8)

$$T = V^{-1}(K + 1/2). \tag{3.71}$$

From (3.59) we have $\psi = Tu^{\varepsilon_n}$.

The approximation properties (3.68)–(3.70) combined with Theorem 3.2.3 yield the following a priori error estimate for the solution of the penalty formulation (3.45).

Theorem 3.2.4. *Let* $\boldsymbol{u}^\varepsilon \in \tilde{\boldsymbol{H}}^{3/2}(\Sigma)$ *be a solution of (3.45) and* $T\boldsymbol{u}^\varepsilon \in \boldsymbol{H}^{1/2}(\Gamma)$. *Let* $\boldsymbol{U}^\varepsilon \in \boldsymbol{\mathcal{V}}_{hp}$ *be a solution of (3.57). Then there exists a constant* $C > 0$ *independent of* h, p, ε, *such that*

$$\begin{aligned}&||\boldsymbol{u}^\varepsilon - \boldsymbol{U}^\varepsilon||^2_{\tilde{\boldsymbol{H}}^{1/2}(\Sigma)} + ||T\boldsymbol{u}^\varepsilon - \boldsymbol{\Psi}||^2_{\boldsymbol{H}^{-1/2}(\Gamma)} + ||\varepsilon^{1/2}(p^\varepsilon - P^\varepsilon)||^2_{L_2(\Gamma_C)} \\ &\leq C\left(\frac{h}{p}||\boldsymbol{u}^\varepsilon||_{\tilde{\boldsymbol{H}}^{3/2}(\Sigma)} + \frac{h}{p}||T\boldsymbol{u}^\varepsilon||_{\boldsymbol{H}^{1/2}(\Gamma)} + \left(\frac{h}{p}\right)^{3/2}||\varepsilon^{-1/2}u_n^\varepsilon||_{H^{3/2}(\Gamma_C)}\right).\end{aligned}$$

A priori error estimate of the total error

In order to obtain an a priori error estimate for the total error between the solutions of problems (3.45) and (3.57) in terms of the solution of the variational inequality (3.45), we need to combine the results of Theorem 3.2.2 and Theorem 3.2.3. Unfortunately, lack of stability estimates of type (3.53) for the penalized problem in the L_2-norm yields to the reduced convergence rate. We prove the modified version of Theorem 3.2.3, where the L_2-term on the right hand side of the estimate is absorbed by the $H^{1/2}$-term. This becomes possible under additional conditions on penalty parameter's growth leading to the quasioptimal rate of convergence for the total error.

The following lemma is important for the proof of Theorem 3.2.5.

Lemma 3.2.9. *There exists an operator* $G_{hp} : \tilde{\boldsymbol{H}}^{1/2}(\Sigma) \to \boldsymbol{\mathcal{V}}_{hp}$, *which is stable in the* $\tilde{\boldsymbol{H}}^{1/2}$*-norm and has the quasioptimal approximation properties in the* $\boldsymbol{L}_2$*-norm, i.e. there exists a constant* C, *independent of* h *and* p *such that for all* $\boldsymbol{u} \in \tilde{\boldsymbol{H}}^{1/2}(\Sigma)$ *there holds*

$$||G_{hp}\boldsymbol{u}||_{\tilde{\boldsymbol{H}}^{1/2}(\Sigma)} \leq C||\boldsymbol{u}||_{\tilde{\boldsymbol{H}}^{1/2}(\Sigma)}, \tag{3.72}$$

$$||\boldsymbol{u} - G_{hp}\boldsymbol{u}||_{\boldsymbol{L}_2(\Sigma)} \leq C\left(\frac{h}{p}\right)^{(1-\epsilon)/2}||\boldsymbol{u}||_{\tilde{\boldsymbol{H}}^{1/2}(\Sigma)} \tag{3.73}$$

with arbitrary small $\epsilon \in (0; 1/2)$.

Proof. Let W be the hypersingular integral operator associated with the Lamé operator. We consider a weak formulation for the one-dimensional hypersingular integral equation, which consists of finding $\boldsymbol{u} \in \tilde{\boldsymbol{H}}^{1/2}(\Sigma)$ such that for given $\boldsymbol{f} \in \boldsymbol{H}^{-1/2}(\Sigma)$ there holds

$$\langle W\boldsymbol{u}, \boldsymbol{v}\rangle = \langle \boldsymbol{f}, \boldsymbol{v}\rangle, \qquad \forall \boldsymbol{v} \in \tilde{\boldsymbol{H}}^{1/2}(\Sigma). \tag{3.74}$$

The Galerkin formulation corresponding to (3.74) is given as follows:
Find $\boldsymbol{U} \in \boldsymbol{\mathcal{V}}_{hp}$:

$$\langle W\boldsymbol{U}, \boldsymbol{v}\rangle = \langle \boldsymbol{f}, \boldsymbol{v}\rangle, \qquad \forall \boldsymbol{v} \in \boldsymbol{\mathcal{V}}_{hp}. \tag{3.75}$$

It is well known that both problems have unique solutions for arbitrary $\boldsymbol{f} \in \boldsymbol{H}^{-1/2}(\Sigma)$ (see e.g. [69]). Now, we define the operator G_{hp} as the Galerkin projection, related to (3.74), (3.75), i.e.

$$G_{hp}\boldsymbol{u} := \boldsymbol{U}. \tag{3.76}$$

Stability of the Galerkin projection G_{hp} follows directly from continuity (Lemma 1.2.1) and ellipticity (Lemma 1.2.3) of the hypersingular integral operator on the space $\tilde{H}^{1/2}(\Sigma)$ (see also [61],[69])

$$||G_{hp}\boldsymbol{u}||_{\tilde{H}^{1/2}(\Sigma)} \leq \frac{1}{c_W}\frac{\langle W\boldsymbol{U},\boldsymbol{U}\rangle}{||\boldsymbol{U}||_{\tilde{\boldsymbol{H}}^{1/2}(\Sigma)}} = \frac{1}{c_W}\frac{\langle W\boldsymbol{u},\boldsymbol{U}\rangle}{||\boldsymbol{U}||_{\tilde{\boldsymbol{H}}^{1/2}(\Sigma)}} \leq \frac{C_W}{c_W}||\boldsymbol{u}||_{\tilde{\boldsymbol{H}}^{1/2}(\Sigma)}.$$

Here c_W and C_W stand for ellipticity and continuity constants of W. In order to prove the approximation property, we apply the Aubin-Nitsche type duality arguments [64], [23]. There holds

$$||\boldsymbol{u}-\boldsymbol{U}||_{\boldsymbol{L}_2(\Sigma)} = \sup_{\boldsymbol{\psi}\in\boldsymbol{L}_2(\Sigma)\setminus\{0\}} \frac{\langle \boldsymbol{u}-\boldsymbol{U},\boldsymbol{\psi}\rangle}{||\boldsymbol{\psi}||_{\boldsymbol{L}_2(\Sigma)}}. \tag{3.77}$$

Further, we introduce an auxiliary problem: For $\boldsymbol{\psi} \in \boldsymbol{L}_2(\Sigma)$ find $\boldsymbol{\phi} \in \tilde{\boldsymbol{H}}^{1/2}(\Sigma)$, such that

$$W\boldsymbol{\phi} = \boldsymbol{\psi}.$$

Using Galerkin orthogonality and continuity of W we obtain for arbitrary $\boldsymbol{\Phi} \in \mathcal{V}_{hp}$

$$\begin{aligned}\langle \boldsymbol{u}-\boldsymbol{U},\psi\rangle &= \langle \boldsymbol{u}-\boldsymbol{U},W\boldsymbol{\phi}\rangle = \langle W(\boldsymbol{u}-\boldsymbol{U}),\boldsymbol{\phi}\rangle\\ &= \langle W(\boldsymbol{u}-\boldsymbol{U}),\boldsymbol{\phi}-\boldsymbol{\Phi}\rangle\\ &\leq C_W||\boldsymbol{u}-\boldsymbol{U}||_{\tilde{\boldsymbol{H}}^{1/2}(\Sigma)}||\boldsymbol{\phi}-\boldsymbol{\Phi}||_{\tilde{\boldsymbol{H}}^{1/2}(\Sigma)}\end{aligned} \tag{3.78}$$

Stability of G_{hp} (3.72) provides

$$||\boldsymbol{u}-\boldsymbol{U}||_{\tilde{\boldsymbol{H}}^{1/2}(\Sigma)} \leq ||\boldsymbol{u}||_{\tilde{\boldsymbol{H}}^{1/2}(\Sigma)} + ||\boldsymbol{U}||_{\tilde{\boldsymbol{H}}^{1/2}(\Sigma)} \leq 2||\boldsymbol{u}||_{\tilde{\boldsymbol{H}}^{1/2}(\Sigma)}. \tag{3.79}$$

According to Wendland and Stephan [69] the hypersingular integral operator is a bijective mapping

$$W: \tilde{\boldsymbol{H}}^{1/2+s}(\Sigma) \to \boldsymbol{H}^{-1/2+s}(\Sigma)$$

for $|s| < 1/2$. This provides for $\boldsymbol{\psi} \in \boldsymbol{L}_2(\Sigma)$ that $\boldsymbol{\phi} = W^{-1}\boldsymbol{\psi} \in \boldsymbol{H}^{1-\epsilon}(\Sigma)$ for arbitrary small $\epsilon > 0$. Following [10] we obtain for some fixed $\epsilon \in (0;1/4)$

$$\inf_{\boldsymbol{\Phi}\in\boldsymbol{\mathcal{V}}_{hp}} ||\boldsymbol{\phi}-\boldsymbol{\Phi}||_{\tilde{\boldsymbol{H}}^{1/2}(\Sigma)} \leq \left(\frac{h}{p}\right)^{1/2-\epsilon} ||\boldsymbol{\phi}||_{\tilde{H}^{1-\epsilon}(\Sigma)} \leq \left(\frac{h}{p}\right)^{1/2-\epsilon} ||\boldsymbol{\phi}||_{\tilde{H}^{1-\epsilon}(\Sigma)}. \tag{3.80}$$

Furthermore, since W is continuous for $|s| \leq 1/2$, the inverse mapping theorem provides that the inverse operator W^{-1} is continuous for $|s| < 1/2$. It means that

$$||\boldsymbol{\phi}||_{\tilde{\boldsymbol{H}}^{1-\epsilon}(\Sigma)} = ||W^{-1}\boldsymbol{\psi}||_{\tilde{\boldsymbol{H}}^{1-\epsilon}(\Sigma)} \leq C||\boldsymbol{\psi}||_{\tilde{\boldsymbol{H}}^{-\epsilon}(\Sigma)} \leq C||\boldsymbol{\psi}||_{\boldsymbol{L}_2(\Sigma)},$$

which together with (3.77)–(3.80) gives (3.73). □

The following theorem is a modification of Theorem 3.2.3 avoiding the L_2-term on the left-hand side of the estimate.

Theorem 3.2.5. *Let $\boldsymbol{u}^\varepsilon$ solve the variational penalty problem (3.45), let $\boldsymbol{U}^\varepsilon$ solve the discrete penalty problem (3.57). Let $\boldsymbol{\psi}$, $\boldsymbol{\Psi}$ be defined by (3.59). Assume that $\exists \tilde{C} \geq 0 : \varepsilon \geq \tilde{C}(h/p)^{1-\epsilon}$ for some fixed $\epsilon \in (0; 1/2)$. Then there exists a constant $C > 0$ independent of h, p, ε such that $\forall \boldsymbol{w} \in \boldsymbol{\mathcal{V}}_{hp}$, $\forall \boldsymbol{\Phi} \in \boldsymbol{\mathcal{W}}_{hp}$ there holds*

$$\begin{aligned} ||\boldsymbol{u}^\varepsilon - \boldsymbol{U}^\varepsilon||_{\tilde{\boldsymbol{H}}^{1/2}(\Sigma)} + ||\boldsymbol{\psi} - \boldsymbol{\Psi}||_{\boldsymbol{H}^{-1/2}(\Gamma)} + ||\varepsilon^{1/2}(p_n^\varepsilon - P_n^\varepsilon)||_{L_2(\Gamma_C)} \\ \leq C(||\boldsymbol{u}^\varepsilon - \boldsymbol{w}||_{\tilde{\boldsymbol{H}}^{1/2}(\Sigma)} + ||\boldsymbol{\psi} - \boldsymbol{\Phi}||_{\boldsymbol{H}^{-1/2}(\Gamma)}). \end{aligned}$$

Proof. Using similar arguments as in Theorem 3.2.2 we estimate the term B now by

$$B = \langle p_n^\varepsilon - P_n^\varepsilon, w_n - u_n^\varepsilon \rangle \leq ||p_n^\varepsilon - P_n^\varepsilon||_{\tilde{H}^{-1/2}(\Gamma_C)} ||w_n - u_n^\varepsilon||_{H^{1/2}(\Gamma_C)}.$$

Further following the proof we obtain instead of (3.67)

$$\begin{aligned} & c_1||\boldsymbol{u}^\varepsilon - \boldsymbol{U}^\varepsilon||^2_{\tilde{\boldsymbol{H}}^{1/2}(\Sigma)} + c_2||\boldsymbol{\psi} - \boldsymbol{\Psi}||^2_{\boldsymbol{H}^{-1/2}(\Gamma)} \\ & +2||\varepsilon^{1/2}(p_n^\varepsilon - P_n^\varepsilon)||^2_{L_2(\Gamma_C)} - \theta_4||p_n^\varepsilon - P_n^\varepsilon||^2_{\tilde{H}^{-1/2}(\Gamma_C)} \\ & \qquad \leq c_3||\boldsymbol{u}^\varepsilon - \boldsymbol{w}||^2_{\tilde{\boldsymbol{H}}^{1/2}(\Sigma)} + c_4||\boldsymbol{\psi} - \boldsymbol{\Phi}||^2_{\boldsymbol{H}^{-1/2}(\Gamma)} + 1/\theta_4||w_n - u_n^\varepsilon||^2_{H^{1/2}(\Gamma_C)} \\ & \qquad \leq (c_3 + 1/\theta_4)||\boldsymbol{u}^\varepsilon - \boldsymbol{w}||^2_{\tilde{\boldsymbol{H}}^{1/2}(\Sigma)} + c_4||\boldsymbol{\psi} - \boldsymbol{\Phi}||^2_{\boldsymbol{H}^{-1/2}(\Gamma)} \end{aligned}$$

for some suitable $\theta_4 > 0$. We only need to show that the negative term on the left hand side can be controlled by the positive terms.

Let G_{hp} be the projection operator defined in Lemma 3.2.9. Then, using inf-sup condition (3.52) we get

$$\begin{aligned} \alpha||p_n^\varepsilon - P_n^\varepsilon||_{\tilde{H}^{-1/2}(\Gamma_C)} &\leq \sup_{\boldsymbol{v} \in \tilde{\boldsymbol{H}}^{1/2}(\Sigma)} \frac{\langle p_n^\varepsilon - P_n^\varepsilon, v_n \rangle}{||\boldsymbol{v}||_{\tilde{\boldsymbol{H}}^{1/2}(\Sigma)}} \\ &= \sup_{\boldsymbol{v} \in \tilde{\boldsymbol{H}}^{1/2}(\Sigma)} \left(\frac{\langle p_n^\varepsilon - P_n^\varepsilon, G_{hp} v_n \rangle}{||\boldsymbol{v}||_{\tilde{\boldsymbol{H}}^{1/2}(\Sigma)}} + \frac{\langle p_n^\varepsilon - P_n^\varepsilon, v_n - G_{hp} v_n \rangle}{||\boldsymbol{v}||_{\tilde{\boldsymbol{H}}^{1/2}(\Sigma)}} \right) \end{aligned}$$

The Galerkin orthogonality property (3.61) yields for the first term (cf. (3.63))

$$\begin{aligned} \frac{\langle p_n^\varepsilon - P_n^\varepsilon, G_{hp} v_n \rangle}{||\boldsymbol{v}||_{\tilde{\boldsymbol{H}}^{1/2}(\Sigma)}} &= \frac{\langle S\boldsymbol{u}^\varepsilon - \hat{S}\boldsymbol{U}^\varepsilon, G_{hp}\boldsymbol{v} \rangle}{||\boldsymbol{v}||_{\tilde{\boldsymbol{H}}^{1/2}(\Sigma)}} \\ &\leq ||S\boldsymbol{u}^\varepsilon - \hat{S}\boldsymbol{U}^\varepsilon||_{\boldsymbol{H}^{-1/2}(\Sigma)} \frac{||G_{hp}\boldsymbol{v}||_{\tilde{\boldsymbol{H}}^{1/2}(\Sigma)}}{||\boldsymbol{v}||_{\tilde{\boldsymbol{H}}^{1/2}(\Sigma)}} \\ &\leq C||S\boldsymbol{u}^\varepsilon - \hat{S}\boldsymbol{U}^\varepsilon||_{\boldsymbol{H}^{-1/2}(\Sigma)} \\ &\leq C(C_S + C_{\hat{E}})||\boldsymbol{u}^\varepsilon - \boldsymbol{U}^\varepsilon||_{\tilde{\boldsymbol{H}}^{1/2}(\Sigma)} + CC_0||\boldsymbol{\psi} - \boldsymbol{\Phi}||_{\boldsymbol{H}^{-1/2}(\Gamma)} \quad \forall \boldsymbol{\Phi} \in \boldsymbol{\mathcal{W}}_{hp}, \end{aligned}$$

since G_{hp} is stable with respect to the $\tilde{H}^{1/2}-$norm due to (3.72). The approximation property (3.73) yields for the second term

$$\frac{\langle p_n^\varepsilon - P_n^\varepsilon, v_n - G_{hp} v_n \rangle}{||\boldsymbol{v}||_{\tilde{\boldsymbol{H}}^{1/2}(\Sigma)}} \leq ||p_n^\varepsilon - P_n^\varepsilon||_{L_2(\Gamma_C)} \frac{||\boldsymbol{v} - G_{hp}\boldsymbol{v}||_{\boldsymbol{L}_2(\Gamma_C)}}{||\boldsymbol{v}||_{\tilde{\boldsymbol{H}}^{1/2}(\Sigma)}} \leq C \left(\frac{h}{p}\right)^{(1-\epsilon)/2} ||p_n^\varepsilon - P_n^\varepsilon||_{L_2(\Gamma_C)}.$$

It is only left to show that one can choose a constant $\theta_4 > 0$ such that

$$||\varepsilon^{1/2}(p_n^\varepsilon - P_n^\varepsilon)||^2_{L_2(\Gamma_C)} - \theta_4 \left(\frac{h}{p}\right)^{1-\epsilon} ||p_n^\varepsilon - P_n^\varepsilon||^2_{L_2(\Gamma_C)} \geq \frac{1}{2} ||\varepsilon^{1/2}(p_n^\varepsilon - P_n^\varepsilon)||^2_{L_2(\Gamma_C)}.$$

According to the assumption on ε there exists a constant $\tilde{C} > 0$ such that $\varepsilon \geq \tilde{C}(h/p)^{1-\epsilon}$, therefore the assertion follows with $\theta_4 = \tilde{C}/2$. □

Now we are able to show the optimal rate of convergence of the total error.

Theorem 3.2.6. *Let $\boldsymbol{u} \in \boldsymbol{\mathcal{V}} \cap \tilde{\boldsymbol{H}}^{3/2}(\Sigma), \lambda \in \Lambda \cap H^{1/2}(\Gamma_C)$ be a solution of (3.44) and let $T\boldsymbol{u} \in H^{1/2}(\Gamma)$, where T is defined by (3.71). Let $\boldsymbol{U}^\varepsilon \in \boldsymbol{\mathcal{V}}_{hp}$ solve (3.57). Assume that $\exists \tilde{C} \geq 0 : \varepsilon \geq \tilde{C}(h/p)^{1-\epsilon}$ for some fixed $\epsilon \in (0; 1/2)$. Then there exists a constant $C > 0$ independent of h, p, ε such that*

$$||\boldsymbol{u} - \boldsymbol{U}^\varepsilon||_{\tilde{\boldsymbol{H}}^{1/2}(\Sigma)} \leq C \left(\frac{h}{p} ||\boldsymbol{u}||_{\tilde{\boldsymbol{H}}^{3/2}(\Sigma)} + \left(\varepsilon + \frac{h}{p}\right) ||T\boldsymbol{u}||_{\boldsymbol{H}^{1/2}(\Gamma)}\right). \tag{3.81}$$

Proof. Theorem 3.2.5, the triangle inequality and (3.71) yield

$$\begin{aligned} ||\boldsymbol{u}^\varepsilon - \boldsymbol{U}^\varepsilon||_{\tilde{\boldsymbol{H}}^{1/2}(\Sigma)} &\leq C(||\boldsymbol{u}^\varepsilon - \boldsymbol{w}||_{\tilde{\boldsymbol{H}}^{1/2}(\Sigma)} + ||\boldsymbol{\psi} - \boldsymbol{\Phi}||_{\boldsymbol{H}^{-1/2}(\Gamma)}) \\ &\leq C(||\boldsymbol{u} - \boldsymbol{u}^\varepsilon||_{\tilde{\boldsymbol{H}}^{1/2}(\Sigma)} + ||\boldsymbol{u} - \boldsymbol{w}||_{\tilde{\boldsymbol{H}}^{1/2}(\Sigma)} \\ &\quad + ||\boldsymbol{\psi} - V^{-1}(K + 1/2)\boldsymbol{u}||_{\boldsymbol{H}^{-1/2}(\Gamma)} + ||T\boldsymbol{u} - \boldsymbol{\Phi}||_{\boldsymbol{H}^{-1/2}(\Gamma)}). \end{aligned}$$

The approximation properties of $\boldsymbol{\mathcal{V}}_{hp}, \boldsymbol{\mathcal{W}}_{hp}$ (3.68)–(3.70) provide

$$\inf_{\boldsymbol{w} \in \boldsymbol{\mathcal{V}}_{hp}} ||\boldsymbol{u} - \boldsymbol{w}||_{\tilde{\boldsymbol{H}}^{1/2}(\Sigma)} \leq C \frac{h}{p} ||\boldsymbol{u}||_{\tilde{\boldsymbol{H}}^{3/2}(\Sigma)},$$

$$\inf_{\boldsymbol{\Phi} \in \boldsymbol{\mathcal{W}}_{hp}} ||T\boldsymbol{u} - \boldsymbol{\Phi}||_{\boldsymbol{H}^{-1/2}(\Gamma)} \leq C \frac{h}{p} ||T\boldsymbol{u}||_{\boldsymbol{H}^{1/2}(\Gamma)}.$$

Therefore continuity of $V^{-1}(K+1/2) : \boldsymbol{H}^{1/2}(\Gamma) \to \boldsymbol{H}^{-1/2}(\Gamma)$ and Theorem 3.2.2 provide

$$\begin{aligned} ||\boldsymbol{u} - \boldsymbol{U}^\varepsilon||_{\tilde{\boldsymbol{H}}^{1/2}(\Sigma)} &\leq ||\boldsymbol{u} - \boldsymbol{u}^\varepsilon||_{\tilde{\boldsymbol{H}}^{1/2}(\Sigma)} + ||\boldsymbol{u}^\varepsilon - \boldsymbol{U}^\varepsilon||_{\tilde{\boldsymbol{H}}^{1/2}(\Sigma)} \\ &\leq C \left(||\boldsymbol{u} - \boldsymbol{u}^\varepsilon||_{\tilde{\boldsymbol{H}}^{1/2}(\Sigma)} + \frac{h}{p} ||\boldsymbol{u}||_{\tilde{\boldsymbol{H}}^{3/2}(\Gamma)} + \frac{h}{p} ||T\boldsymbol{u}||_{\boldsymbol{H}^{1/2}(\Gamma)} \right) \\ &\leq C \left(||\varepsilon\lambda||_{H^{1/2}(\Gamma_C)} + \frac{h}{p} ||\boldsymbol{u}||_{\tilde{\boldsymbol{H}}^{3/2}(\Gamma)} + \frac{h}{p} ||T\boldsymbol{u}||_{\boldsymbol{H}^{1/2}(\Gamma)} \right). \end{aligned}$$

The weak formulation (3.44) provides that $\lambda = T\boldsymbol{u} \cdot \boldsymbol{n}|_{\Gamma_C}$, which gives (3.81). □

3.2.5 Numerical example

We consider a model problem of an elastic body Ω contacting with a rigid straight line obstacle. The domain $\Omega = [-1,1]\times[-1,1]$ is fixed along $\Gamma_D := [-1,1]\times\{1\}$ (i.e. $\boldsymbol{u} = 0$ on Γ_D). The contact boundary $\Gamma_C := [-1,1]\times\{-1\}$ comes in contact with the rigid obstacle $[-2,2]\times\{-1+d\}$ thanks to the shift $d = 2\cdot 10^{-4}$. The boundary traction vanishes on the Neumann boundary, given by $\Gamma_N = \partial\Omega \setminus (\Gamma_D \cup \Gamma_C)$. The Young's modulus and the Poisson's ratio are $E = 266926.0, \nu = 0.29$ respectively.

We use h-version of the BEM with piecewise linear basis functions on a uniform mesh. We connect the mesh size h and the penalty parameter ε with a proportionality constant C_ε, i.e. $\varepsilon := C_\varepsilon h$, which balances the penalization error and the discretization error in the estimate (3.81). We study convergence of the method for different values of C_ε.

C_ε	DOF	ε	err($\boldsymbol{U}^\varepsilon$)
10^{-4}	22	$0.25000\cdot10^{-4}$	0.12173862
10^{-4}	46	$0.12500\cdot10^{-4}$	0.10046317
10^{-4}	94	$0.62500\cdot10^{-5}$	0.07444925
10^{-4}	190	$0.31250\cdot10^{-5}$	0.04905021
10^{-4}	382	$0.15625\cdot10^{-5}$	0.02915712
10^{-4}	766	$0.78125\cdot10^{-6}$	0.01609924
10^{-5}	22	$0.25000\cdot10^{-5}$	0.04185280
10^{-5}	46	$0.12500\cdot10^{-5}$	0.02421500
10^{-5}	94	$0.62500\cdot10^{-6}$	0.01314311
10^{-5}	190	$0.31250\cdot10^{-6}$	0.00686598
10^{-5}	382	$0.15625\cdot10^{-6}$	0.00351204
10^{-5}	766	$0.78125\cdot10^{-7}$	0.00177676
10^{-6}	22	$0.25000\cdot10^{-6}$	0.00540834
10^{-6}	46	$0.12500\cdot10^{-6}$	0.00277935
10^{-6}	94	$0.62500\cdot10^{-7}$	0.00141103
10^{-6}	190	$0.31250\cdot10^{-7}$	0.00071157
10^{-6}	382	$0.15625\cdot10^{-7}$	0.00035767
10^{-6}	766	$0.78125\cdot10^{-8}$	0.00017959
10^{-7}	22	$0.25000\cdot10^{-7}$	0.00042198
10^{-7}	46	$0.12500\cdot10^{-7}$	0.00024092
10^{-7}	94	$0.62500\cdot10^{-8}$	0.00012970
10^{-7}	190	$0.31250\cdot10^{-8}$	$0.67760\cdot10^{-4}$
10^{-7}	382	$0.15625\cdot10^{-8}$	$0.34964\cdot10^{-4}$
10^{-7}	766	$0.78125\cdot10^{-9}$	$0.18041\cdot10^{-4}$

Table 3.1: Error behaviour for various penalty parameters $\varepsilon = C_\varepsilon h$

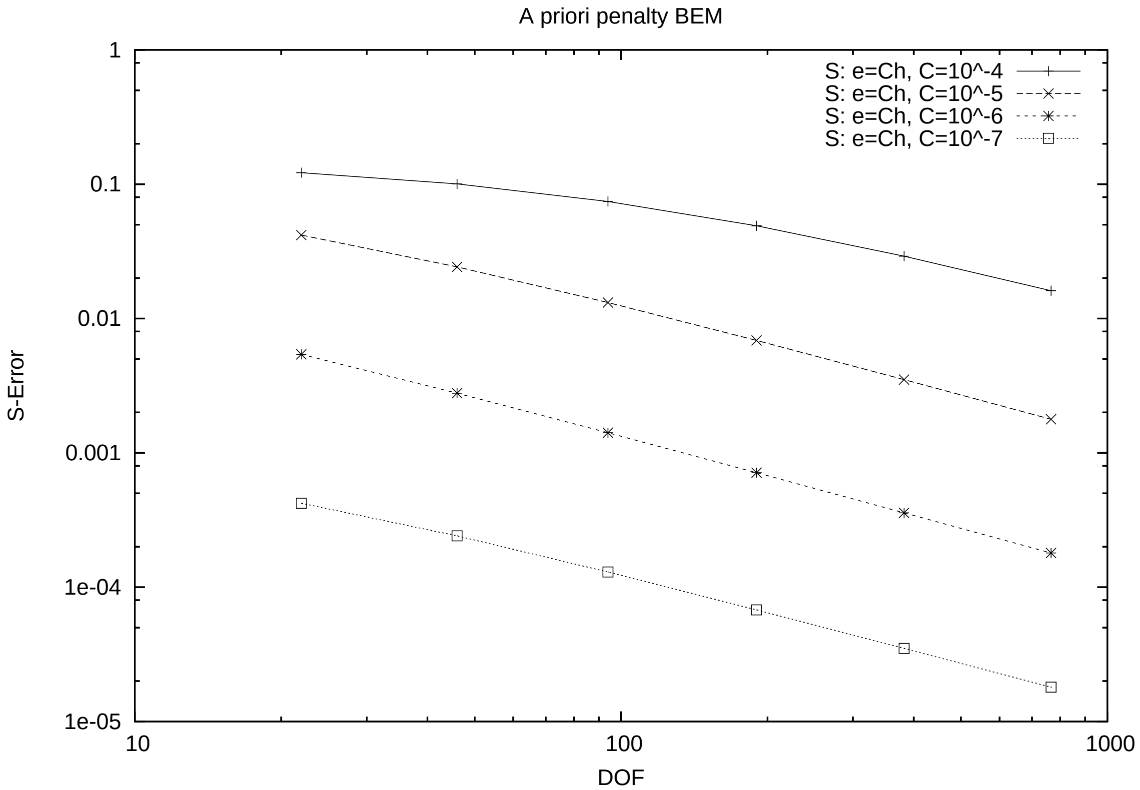

Figure 3.1: Error behaviour for varied penalty parameter $\varepsilon = C_\varepsilon h$

The results of numerical experiments are presented in Table 3.1 and in Figure 3.1. The error is given by $\mathrm{err}(\boldsymbol{U}^\varepsilon) = \left\langle \hat{S}\boldsymbol{U}^\varepsilon, \boldsymbol{U}^\varepsilon \right\rangle^{1/2} - ||\boldsymbol{u}_{lim}||_S$, where the value $||\boldsymbol{u}_{lim}||_S = 0.154398$ is obtained by the Aitken extrapolation. We see that with decreasing of the proportionality constant C_ε the linear rate of convergence is achieved for smaller number of unknowns. For $C_\varepsilon \leq 10^{-5}$ the linear rate of convergence is achieved even for low number of unknowns. Numerical experiments for fixed penalty parameter show that the error does not decrease if the mesh size is reduced.

3.3 Residual FE and BE a posteriori error estimates for contact with friction

The question of automatic mesh refinement in the framework of the h-version of penalty FEM and BEM for one-body frictional contact problem is addressed in this section. The error measure, based on the energy norm of the solution, combined with normal and tangential contact terms is introduced for FEM and BEM. Then, the local residual-based error indicators are derived for both FEM and BEM and their reliability and efficiency are shown. An automatic mesh refinement procedure, based on these indicators is introduced. Finally the suggested method is illustrated on several numerical examples.

A similar error indicator was used for the h-version of FEM for frictional contact problems, but only with heuristical motivation, cf. Wriggers [72], Hu and Wriggers [36]. Another reliable residual based error indicator was obtained by Eck and Wendland in [27] for the h-version of the BEM using a different technique, while the efficiency of the error indicator has not been shown.

We estimate here the error between the solution $\boldsymbol{u}^\varepsilon$ of the weak penalty domain formulation (for FEM) or of the penalty boundary integral formulation (for BEM) and the corresponding discrete solution $\boldsymbol{U}^\varepsilon$. In order to capture the error between $\boldsymbol{u}^\varepsilon$ and the solution of the variational inequality $\boldsymbol{u}$, the penalty parameters $\varepsilon_n, \varepsilon_t$ have to be changed simultaneously with the mesh size. The relation between the penalty parameters and the mesh size is usually taken from the corresponding a priori error analysis, which guarantees the optimal order of convergence of $\boldsymbol{U}^\varepsilon$ to $\boldsymbol{u}$. For example, employing the results of the previous section, we obtain that $\varepsilon_n \sim h^{1-\epsilon}$, $0 < \epsilon \ll 1$, provides the optimal convergence rate for frictionless contact.

3.3.1 Regularization of the frictional contact problem

We return to the contact problem between an elastic body and a rigid obstacle with Tresca's law of friction, described in the introduction to Chapter 3. As shown in Section 3.1 for the case of vanishing gap function $g \equiv 0$, the classical formulation of the problem (3.1) can be written as a variational inequality, or as a minimization problem (3.11). Similar arguments provide for the general case $g \not\equiv 0$ the following minimization formulation: Find $\boldsymbol{u} \in \boldsymbol{\mathcal{K}} := \{\boldsymbol{w} \in \boldsymbol{\mathcal{V}} : v_n - g \leq 0 \text{ on } \Gamma_C\}$:

$$J(\boldsymbol{w}) \geq J(\boldsymbol{u}), \qquad \forall \boldsymbol{w} \in \boldsymbol{\mathcal{K}}, \tag{3.82}$$

where

$$J(\boldsymbol{w}) := \frac{1}{2}\langle S\boldsymbol{w}, \boldsymbol{w}\rangle_\Sigma + j(\boldsymbol{w}) - L(\boldsymbol{w}), \tag{3.83}$$

and $\boldsymbol{\mathcal{V}} := \tilde{\boldsymbol{H}}^{1/2}(\Sigma)$. The frictional functional $j(\cdot)$ and the load functional $L(\cdot)$ are given by (3.6) and (3.4) respectively. In Section 3.2 we have shown, how the inconvenient inequality constraint can be removed from the space of admissible solutions $\boldsymbol{\mathcal{K}}$ by penalizing the penetration of the body through the obstacle. This technique leads to the (frictionless) penalty formulation (3.45), which can be equivalently rewritten in terms of the minimization problem. In the case of non-vanishing friction the penalized minimization problem reads: Find $\boldsymbol{u} \in \boldsymbol{\mathcal{V}}$:

$$\bar{J}_\varepsilon(\boldsymbol{w}) \geq \bar{J}_\varepsilon(\boldsymbol{u}), \qquad \forall \boldsymbol{w} \in \boldsymbol{\mathcal{V}}, \tag{3.84}$$

where

$$\bar{J}_\varepsilon(\boldsymbol{w}) := \frac{1}{2}\langle S\boldsymbol{w}, \boldsymbol{w}\rangle_\Sigma + \left|\left|\frac{1}{(2\varepsilon_n)^{1/2}}(w_n - g)^+\right|\right|^2_{L_2(\Gamma_C)} + j(\boldsymbol{w}) - L(\boldsymbol{w}) \tag{3.85}$$

and the "positive value" function $(\cdot)^+$ is defined by (3.47). Note, that the non-differentiable frictional functional $j(\cdot)$ is still included in the penalized formulation, which is quite inconvenient for developing of numerical solution schemes. Therefore, we introduce the regularized version of $j(\cdot)$ (see [38, Section 10.4] for different examples of regularization). We use here the piecewise quadratic regularization of the absolute value function (cf. (3.18)), which can be equivalently expressed on the discrete level in terms of the *return mapping* algorithm, as described in Section 4.2.

$$\Psi_{\varepsilon_t}(x) = \begin{cases} |x| - \frac{\varepsilon_t}{2}, & |x| \geq \varepsilon_t, \\ \frac{x^2}{2\varepsilon_t}, & |x| \leq \varepsilon_t, \end{cases} \qquad \varphi_{\varepsilon_t}(x) = \begin{cases} \operatorname{sign}(x), & |x| \geq \varepsilon_t, \\ \frac{x}{\varepsilon_t}, & |x| \leq \varepsilon_t. \end{cases} \tag{3.86}$$

The regularized frictional functional is now given by

$$j_{\varepsilon_t}(\boldsymbol{w}) := \int_{\Gamma_C} \mathcal{F}\Psi_{\varepsilon_t}(w_t)\, ds$$

and the minimization problem (3.84) transforms as follows: Find $\boldsymbol{u} \in \boldsymbol{\mathcal{V}}$:

$$J_\varepsilon(\boldsymbol{w}) \geq J_\varepsilon(\boldsymbol{u}), \qquad \forall \boldsymbol{w} \in \boldsymbol{\mathcal{V}}, \tag{3.87}$$

where

$$J_\varepsilon(\boldsymbol{w}) := \frac{1}{2}\langle S\boldsymbol{w}, \boldsymbol{w}\rangle_\Sigma + \left|\left|\frac{1}{(2\varepsilon_n)^{1/2}}(w_n - g)^+\right|\right|^2_{L_2(\Gamma_C)} + j_{\varepsilon_t}(\boldsymbol{w}) - L(\boldsymbol{w}). \tag{3.88}$$

We define for brevity $f^* := \varepsilon_t \varphi_{\varepsilon_t}(f)$. Hence, according to (3.86),

$$(f(x))^* = \begin{cases} \varepsilon_t \operatorname{sign}(f(x)), & |x| \geq \varepsilon_t, \\ f(x), & |x| \leq \varepsilon_t. \end{cases} \tag{3.89}$$

The regularized functional $j_{\varepsilon_t}(\cdot)$ (and therefore $J_{\varepsilon_t}(\cdot)$) is Gâteaux-differentiable and its derivative is given by

$$\langle Dj_{\varepsilon_t}(\boldsymbol{u}), \boldsymbol{v}\rangle_{\Gamma_C} = \langle p_t^\varepsilon, v_t\rangle_{\Gamma_C}, \qquad p_t^\varepsilon := -\frac{1}{\varepsilon_t}\mathcal{F}u_t^*.$$

Thus, the problem of finding a stationary point of $J_\varepsilon(\cdot)$ can be rewritten as the following variational formulation: Find $\boldsymbol{u}^\varepsilon \in \boldsymbol{\mathcal{V}}$ such that

$$\langle S\boldsymbol{u}^\varepsilon, \boldsymbol{v}\rangle_\Sigma - \langle p_n^\varepsilon, v_n\rangle_{\Gamma_C} - \langle p_t^\varepsilon, v_t\rangle_{\Gamma_C} = L(\boldsymbol{v}), \qquad \forall \boldsymbol{v} \in \boldsymbol{\mathcal{V}}, \tag{3.90}$$

where the normal contact traction is given by the constitutive relation (cf. 3.46)

$$p_n^\varepsilon := -\frac{1}{\varepsilon_n}(u_n^\varepsilon - g)^+. \tag{3.91}$$

In order to discretize the problem (3.90), we introduce a partition $\mathcal{T}_h$ of the boundary Γ into straight line segments.

$$\overline{\Gamma} := \bigcup_{I\in\mathcal{T}_h} \overline{I}.$$

We define the space $\boldsymbol{\mathcal{V}}_h$ of admissible displacements consisting of continuous piecewise linear functions on the mesh $\mathcal{T}_h$ by

$$\boldsymbol{\mathcal{V}}_h := \left\{\boldsymbol{v} \in \tilde{\boldsymbol{H}}^{1/2}(\Sigma) : \boldsymbol{v}|_I \in \mathcal{P}_1(I), \forall I \in \mathcal{T}_h\right\}. \tag{3.92}$$

As discussed before, the Steklov-Poincaré operator S (cf. (3.40)) can not be discretized directly, since it includes the inverse V^{-1} of the single layer potential. Therefore, first, the approximation V_h of V is computed and then inverted. The construction of the discrete operator V_h requires a dual variable – the boundary traction, which must be discretized correspondingly. Therefore one can define some different mesh for discretization of the boundary traction, as it was suggested in [46]. We employ here the same mesh as for the primal variable. We define the space of discrete tractions as a space of piecewise constant functions on $\mathcal{T}_h$

$$\boldsymbol{\mathcal{W}}_h := \left\{\boldsymbol{v} \in \boldsymbol{H}^{-1/2}(\Gamma) : \boldsymbol{v}|_I \in \mathcal{P}_0(I), \forall I \in \mathcal{T}_h\right\}. \tag{3.93}$$

The same as before, we denote the discrete Steklov-Poincaré operator $\hat{S}$ and the error-operator $\hat{E}$ as follows (cf. (3.56)):

$$\begin{aligned} \hat{S} &:= W + (K' + 1/2)i_h V_h^{-1} i_h^*(K + 1/2), \\ \hat{E} &:= S - \hat{S} = (K' + 1/2)(V - i_h V_h^{-1} i_h^*)(K + 1/2). \end{aligned} \tag{3.94}$$

Then the discrete formulation reads as follows: Find $\boldsymbol{U}^\varepsilon \in \boldsymbol{\mathcal{V}}_h$.

$$\left\langle \hat{S}\boldsymbol{U}^\varepsilon, \boldsymbol{\Phi}\right\rangle_\Sigma - \langle P_n^\varepsilon, \Phi_n\rangle_{\Gamma_C} - \langle P_t^\varepsilon, \Phi_t\rangle_{\Gamma_C} = L(\boldsymbol{\Phi}), \qquad \forall \boldsymbol{\Phi} \in \boldsymbol{\mathcal{V}}_h \tag{3.95}$$

with

$$P_n^\varepsilon := -\frac{1}{\varepsilon_n}(U_n^\varepsilon - g)^+, \qquad P_t^\varepsilon := -\frac{1}{\varepsilon_t}\mathcal{F}U_t^{\varepsilon *}.$$

Remark 3.3.1. *For the finite element method one can obtain corresponding formulations. The domain variational formulation reads:*

Find $\boldsymbol{u}^\varepsilon \in \boldsymbol{\mathcal{V}}_F := \left\{\boldsymbol{v} \in \boldsymbol{H}^1(\Omega) : \boldsymbol{v} = 0 \text{ on } \Gamma_D\right\}$ *such that*

$$a(\boldsymbol{u}^\varepsilon, \boldsymbol{\phi}) - \langle p_n^\varepsilon, \phi_n\rangle_{\Gamma_C} - \langle p_t^\varepsilon, \phi_t\rangle_{\Gamma_C} = L(\boldsymbol{\phi}), \qquad \forall \boldsymbol{\phi} \in \boldsymbol{\mathcal{V}}_F. \tag{3.96}$$

The bilinear form $a(\cdot,\cdot)$ *and the linear form* $L(\cdot)$ *are given by*

$$a(\boldsymbol{u}^\varepsilon, \boldsymbol{\phi}) := \int_\Omega \sigma(\boldsymbol{u}^\varepsilon) : \varepsilon(\boldsymbol{\phi})\, dx, \qquad L(\boldsymbol{\phi}) := \int_{\Gamma_N} \hat{\boldsymbol{t}} \cdot \boldsymbol{\phi}\, ds + \int_\Omega \boldsymbol{f} \cdot \boldsymbol{\phi}\, dx,$$

where $\boldsymbol{f} \in \boldsymbol{L}_2(\Omega)$ *indicates the volume force. We introduce a piecewise linear space of admissible displacements* $\boldsymbol{\mathcal{V}}_{Fh}$ *over some (triangular or quadrilateral) mesh* $\mathcal{T}_{Fh}$ *in two-dimensional domain* Ω*. Then the discrete formulation reads: Find* $\boldsymbol{U}^\varepsilon \in \boldsymbol{\mathcal{V}}_{Fh}$ *such that*

$$a(\boldsymbol{U}^\varepsilon, \boldsymbol{\Phi}) - \langle P_n^\varepsilon, \Phi_n\rangle - \langle P_t^\varepsilon, \Phi_t\rangle = L(\boldsymbol{\Phi}), \qquad \forall \boldsymbol{\Phi} \in \boldsymbol{\mathcal{V}}_{Fh}. \tag{3.97}$$

Sometimes, we use the following vector notations for the penalized traction

$$\boldsymbol{p}^\varepsilon := p_n^\varepsilon \boldsymbol{n} + p_t^\varepsilon \boldsymbol{t}, \qquad \boldsymbol{P}^\varepsilon := P_n^\varepsilon \boldsymbol{n} + P_t^\varepsilon \boldsymbol{t}.$$

3.3.2 Residual a posteriori error estimates for finite elements

Let $\boldsymbol{u}^\varepsilon \in \boldsymbol{\mathcal{V}}_F$ be an exact solution of the domain penalty formulation (3.96) and let $\boldsymbol{U}^\varepsilon \in \boldsymbol{\mathcal{V}}_{Fh}$ be the solution of the discrete finite element problem (3.97). In order to prove an a posteriori error estimate, we have to show a monotonicity property for the tangential component of the displacement (cf. Lemma 3.2.8 for the normal component of the displacement).

Lemma 3.3.1. *For all* $\boldsymbol{u}^\varepsilon \in \boldsymbol{\mathcal{V}}_F$ *solving (3.96) and* $\boldsymbol{U}^\varepsilon \in \boldsymbol{\mathcal{V}}_{Fh}$ *solving (3.97), there holds*

$$||{\varepsilon_t}^{1/2}\mathcal{F}^{-1/2}(p_t^\varepsilon - P_t^\varepsilon)||^2_{L_2(\Gamma_C)} \leq -\langle p_t^\varepsilon - P_t^\varepsilon, u_t^\varepsilon - U_t^\varepsilon\rangle_{\Gamma_C}.$$

Proof. At first, we show that for any real numbers a, b there holds

$$(a^* - b^*)^2 \leq (a^* - b^*)(a - b)$$

We introduce a function $(\cdot)^\#$ complementary to $(\cdot)^*$, such that for any $a \in \mathbb{R}$ the decomposition $a = a^* + a^\#$ holds. Hence

$$(a^* - b^*)(a - b) = (a^* - b^*)^2 + (a^* - b^*)(a^\# - b^\#).$$

We get the desirable result, if we show that

$$(a^* - b^*)(a^\# - b^\#) \geq 0. \tag{3.98}$$

Therefore, we check the different possible cases. If $|a| \leq \varepsilon_t$ and $|b| \leq \varepsilon_t$, the inequality (3.98) trivially holds, since $a^\# = 0 = b^\#$. For $|a| \geq \varepsilon_t, |b| \leq \varepsilon_t$, according to (3.89), we obtain

$$(a^* - b^*)(a^\# - b^\#) = (\varepsilon_t \text{sign}(a) - b)a^\# = (\varepsilon_t - b\,\text{sign}(a))|a^\#| \geq 0,$$

which yields (3.98). The same holds for $|a| \leq \varepsilon_t, |b| \geq \varepsilon_t$. Finally, for $|a| \geq \varepsilon_t, |b| \geq \varepsilon_t$ there holds

$$\begin{aligned}(a^* - b^*)(a^\# - b^\#) &= \varepsilon_t(\text{sign}(a) - \text{sign}(b))(a^\# - b^\#)\\ &= \varepsilon_t(1 - \text{sign}(ab))(|a^\#| - |b^\#|\text{sign}(ab))\\ &= \left\{\begin{array}{ll} 0, & \text{if sign}(ab) = 1,\\ 2\varepsilon_t(|a^\#| + |b^\#|), & \text{if sign}(ab) = -1\end{array}\right\} \geq 0\end{aligned}$$

and (3.98) follows. Now we derive that

$$\begin{aligned}||{\varepsilon_t}^{1/2}\mathcal{F}^{-1/2}(p_t^\varepsilon - P_t^\varepsilon)||^2_{L_2(\Gamma_C)} &= \int_{\Gamma_C} \frac{\varepsilon_t}{\mathcal{F}}(p_t^\varepsilon - P_t^\varepsilon)^2\,ds = \int_{\Gamma_C} \frac{1}{\varepsilon_t}\mathcal{F}(u_t^{\varepsilon*} - U_t^{\varepsilon*})^2\,ds\\ &\leq \int_{\Gamma_C} \frac{1}{\varepsilon_t}\mathcal{F}(u_t^{\varepsilon*} - U_t^{\varepsilon*})(u_t^\varepsilon - U_t^\varepsilon)\,ds\\ &= -\left\langle p_t^\varepsilon - P_t^\varepsilon, u_t^\varepsilon - U_t^\varepsilon\right\rangle_{\Gamma_C},\end{aligned}$$

which completes the proof. □

We introduce the error measure in the finite element case as follows

$$\begin{aligned}|||\boldsymbol{u}^\varepsilon - \boldsymbol{U}^\varepsilon|||^2_F &:= a(\boldsymbol{u}^\varepsilon - \boldsymbol{U}^\varepsilon, \boldsymbol{u}^\varepsilon - \boldsymbol{U}^\varepsilon)\\ &\quad + ||{\varepsilon_n}^{1/2}(p_n^\varepsilon - P_n^\varepsilon)||^2_{L_2(\Gamma_C)} + ||{\varepsilon_t}^{1/2}\mathcal{F}^{-1/2}(p_t^\varepsilon - P_t^\varepsilon)||^2_{L_2(\Gamma_C)}.\end{aligned} \tag{3.99}$$

Reliability of the FE a posteriori error estimate

Denote for brevity by $\mathcal{E}_{Fh}$ the set of all edges in the mesh $\mathcal{T}_{Fh}$. Now we are in the position to show that the following a posteriori error estimate holds.

Theorem 3.3.1. *Let $\boldsymbol{u}^\varepsilon \in \boldsymbol{\mathcal{V}}_F$ be an exact solution of the domain penalty formulation (3.96) and let $\boldsymbol{U}^\varepsilon \in \boldsymbol{\mathcal{V}}_{Fh}$ be the solution of the discrete finite element problem (3.97). Then the error defined by (3.99) can be estimated as follows*

$$|||\boldsymbol{u}^\varepsilon - \boldsymbol{U}^\varepsilon|||^2_F \leq C \sum_{K \in \mathcal{T}_h} \eta^2_{Fh}(K),$$

where the local indicators are given by

$$\begin{aligned}
\eta_{Fh}^2(K) := h_K^2 \|\boldsymbol{f} + \operatorname{div} \sigma(\boldsymbol{U}^\varepsilon)\|^2_{\boldsymbol{L}_2(K)} \\
+ \frac{1}{2} \sum_{I \subset (\mathcal{E}_h \cup \partial K)\setminus \Gamma} h_I \|[\sigma(\boldsymbol{U}^\varepsilon)\cdot \boldsymbol{n}]\|^2_{\boldsymbol{L}_2(I)} \\
+ \sum_{I \subset \mathcal{E}_h \cap \partial K \cap \Gamma_N} h_I \|\hat{\boldsymbol{t}} - \sigma(\boldsymbol{U}^\varepsilon)\cdot \boldsymbol{n}\|^2_{\boldsymbol{L}_2(I)} \\
+ \sum_{I \subset \mathcal{E}_h \cap \partial K \cap \Gamma_C} h_I \left\| P_n^\varepsilon \boldsymbol{n} + P_t^\varepsilon \boldsymbol{t} - \sigma(\boldsymbol{U}^\varepsilon)\cdot \boldsymbol{n} \right\|^2_{\boldsymbol{L}_2(I)},
\end{aligned} \tag{3.100}$$

with some positive constant C.

Proof. Using the monotonicity properties of Lemma 3.2.8 and Lemma 3.3.1 one can write

$$\begin{aligned}
|||\boldsymbol{u}^\varepsilon - \boldsymbol{U}^\varepsilon|||_F^2 := a(\boldsymbol{u}^\varepsilon - \boldsymbol{U}^\varepsilon, \boldsymbol{u}^\varepsilon - \boldsymbol{U}^\varepsilon) \\
+ ||{\varepsilon_n}^{1/2}(p_n^\varepsilon - P_n^\varepsilon)||^2_{L_2(\Gamma_C)} + ||{\varepsilon_t}^{1/2}\mathcal{F}^{-1/2}(p_t^\varepsilon - P_t^\varepsilon)||^2_{L_2(\Gamma_C)} \\
\le a(\boldsymbol{u}^\varepsilon - \boldsymbol{U}^\varepsilon, \boldsymbol{u}^\varepsilon - \boldsymbol{U}^\varepsilon) \\
- \langle p_n^\varepsilon - P_n^\varepsilon, u_n^\varepsilon - U_n^\varepsilon\rangle_{\Gamma_C} - \langle p_t^\varepsilon - P_t^\varepsilon, u_t^\varepsilon - U_t^\varepsilon\rangle_{\Gamma_C}.
\end{aligned} \tag{3.101}$$

Subtracting (3.97) from (3.96) we obtain for arbitrary $\boldsymbol{\Phi} \in \boldsymbol{\mathcal{V}}_{Fh}$

$$0 = a(\boldsymbol{u}^\varepsilon - \boldsymbol{U}^\varepsilon, \boldsymbol{\Phi}) - \langle p_n^\varepsilon - P_n^\varepsilon, \Phi_n\rangle_{\Gamma_C} - \langle p_t^\varepsilon - P_t^\varepsilon, \Phi_t\rangle_{\Gamma_C}. \tag{3.102}$$

For some $\boldsymbol{\Psi} \in \boldsymbol{\mathcal{V}}_{Fh}$ we choose $\boldsymbol{\Phi} := \boldsymbol{U}^\varepsilon - \boldsymbol{\Psi} \in \boldsymbol{\mathcal{V}}_{Fh}$. Adding (3.102) and (3.101) we get

$$\begin{aligned}
|||\boldsymbol{u}^\varepsilon - \boldsymbol{U}^\varepsilon|||_F^2 \le a(\boldsymbol{u}^\varepsilon - \boldsymbol{U}^\varepsilon, \boldsymbol{u}^\varepsilon - \boldsymbol{U}^\varepsilon) - \langle p_n^\varepsilon - P_n^\varepsilon, u_n^\varepsilon - U_n^\varepsilon\rangle_{\Gamma_C} - \langle p_t^\varepsilon - P_t^\varepsilon, u_t^\varepsilon - U_t^\varepsilon\rangle_{\Gamma_C} \\
- a(\boldsymbol{u}^\varepsilon - \boldsymbol{U}^\varepsilon, \boldsymbol{U}^\varepsilon - \boldsymbol{\Psi}) - \langle p_n^\varepsilon - P_n^\varepsilon, U_n^\varepsilon - \Psi_n\rangle_{\Gamma_C} - \langle p_t^\varepsilon - P_t^\varepsilon, U_t^\varepsilon - \Psi_t\rangle_{\Gamma_C} \\
= a(\boldsymbol{u}^\varepsilon - \boldsymbol{U}^\varepsilon, \boldsymbol{u}^\varepsilon - \boldsymbol{\Psi}) - \langle p_n^\varepsilon - P_n^\varepsilon, u_n^\varepsilon - \Psi_n\rangle_{\Gamma_C} - \langle p_t^\varepsilon - P_t^\varepsilon, u_t^\varepsilon - \Psi_t\rangle_{\Gamma_C}.
\end{aligned}$$

With $\boldsymbol{\phi} := \boldsymbol{u}^\varepsilon - \boldsymbol{\Psi} \in \boldsymbol{\mathcal{V}}_F$, the variational formulation (3.96) reads

$$a(\boldsymbol{u}^\varepsilon, \boldsymbol{u}^\varepsilon - \boldsymbol{\Psi}) - \langle p_n^\varepsilon, u_n^\varepsilon - \Psi_n\rangle_{\Gamma_C} - \langle p_t^\varepsilon, u_t^\varepsilon - \Psi_t\rangle_{\Gamma_C} = L(\boldsymbol{u}^\varepsilon - \boldsymbol{\Psi})$$

and therefore

$$|||\boldsymbol{u}^\varepsilon - \boldsymbol{U}^\varepsilon|||_F^2 \le L(\boldsymbol{u}^\varepsilon - \boldsymbol{\Psi}) - a(\boldsymbol{U}^\varepsilon, \boldsymbol{u}^\varepsilon - \boldsymbol{\Psi}) + \langle P_n^\varepsilon, u_n^\varepsilon - \Psi_n\rangle_{\Gamma_C} + \langle P_t^\varepsilon, u_{\varepsilon t} - \Psi_t\rangle_{\Gamma_C}.$$

Applying Green's formula on each element $K \in \mathcal{T}_{Fh}$ we obtain

$$\begin{aligned}
-a(\boldsymbol{U}^\varepsilon|_K, \boldsymbol{u}^\varepsilon|_K - \boldsymbol{\Psi}|_K) = \int_K \operatorname{div} \sigma(\boldsymbol{U}^\varepsilon)\cdot(\boldsymbol{u}^\varepsilon - \boldsymbol{\Psi})\, ds \\
- \sum_{I \subset \partial K} \int_I (\sigma(\boldsymbol{U}^\varepsilon)\cdot \boldsymbol{n})\cdot(\boldsymbol{u}^\varepsilon - \boldsymbol{\Psi})\, ds.
\end{aligned}$$

This gives

$$\begin{aligned}|||\boldsymbol{u}^\varepsilon - \boldsymbol{U}^\varepsilon|||_F^2 \le \sum_{K\in\mathcal{T}_{Fh}} & \int_K (\boldsymbol{f} + \operatorname{div}\sigma(\boldsymbol{U}^\varepsilon)) \cdot (\boldsymbol{u}^\varepsilon - \boldsymbol{\Psi})\, ds \\ & + \frac{1}{2} \sum_{I\subset\mathcal{E}_h\setminus\partial\Omega} \int_I [\sigma(\boldsymbol{U}^\varepsilon)\cdot\boldsymbol{n}] \cdot (\boldsymbol{u}^\varepsilon - \boldsymbol{\Psi})\, ds \\ & + \sum_{I\subset\mathcal{E}_h\cap\Gamma_N} \int_I (\hat{\boldsymbol{t}} - \sigma(\boldsymbol{U}^\varepsilon)\cdot\boldsymbol{n}) \cdot (\boldsymbol{u}^\varepsilon - \boldsymbol{\Psi})\, ds \\ & + \sum_{I\subset\mathcal{E}_h\cap\Gamma_C} \int_I (P_n^\varepsilon \boldsymbol{n} + P_t^\varepsilon \boldsymbol{t} - \sigma(\boldsymbol{U}^\varepsilon)\cdot\boldsymbol{n}) \cdot (\boldsymbol{u}^\varepsilon - \boldsymbol{\Psi})\, ds.\end{aligned}$$

The Cauchy-Schwarz inequality provides

$$\begin{aligned}|||\boldsymbol{u}^\varepsilon - \boldsymbol{U}^\varepsilon|||_F^2 \le \sum_{K\in\mathcal{T}_{Fh}} & ||\boldsymbol{f} + \operatorname{div}\sigma(\boldsymbol{U}^\varepsilon)||_{\boldsymbol{L}_2(K)} ||\boldsymbol{u}^\varepsilon - \boldsymbol{\Psi}||_{\boldsymbol{L}_2(K)} \\ & + \sum_{I\subset\mathcal{E}_h\setminus\partial\Omega} ||[\sigma(\boldsymbol{U}^\varepsilon)\cdot\boldsymbol{n}]||_{\boldsymbol{L}_2(I)} ||\boldsymbol{u}^\varepsilon - \boldsymbol{\Psi}||_{\boldsymbol{L}_2(I)} \\ & + \sum_{I\subset\mathcal{E}_h\cap\Gamma_N} ||\hat{\boldsymbol{t}} - \sigma(\boldsymbol{U}^\varepsilon)\cdot\boldsymbol{n}||_{\boldsymbol{L}_2(I)} ||\boldsymbol{u}^\varepsilon - \boldsymbol{\Psi}||_{\boldsymbol{L}_2(I)} \\ & + \sum_{I\subset\mathcal{E}_h\cap\Gamma_C} ||P_n^\varepsilon \boldsymbol{n} + P_t^\varepsilon \boldsymbol{t} - \sigma(\boldsymbol{U}^\varepsilon)\cdot\boldsymbol{n}||_{\boldsymbol{L}_2(I)} ||\boldsymbol{u}^\varepsilon - \boldsymbol{\Psi}||_{\boldsymbol{L}_2(I)}.\end{aligned}$$

We choose now $\boldsymbol{\Psi} := \boldsymbol{U}^\varepsilon + \mathfrak{i}_h(\boldsymbol{u}^\varepsilon - \boldsymbol{U}^\varepsilon) \in \boldsymbol{\mathcal{V}}_{Fh}$, where $\mathfrak{i}_h$ is the two-dimensional Clément interpolation operator applied componentwise. Let $\boldsymbol{v} \in L_2(\Omega)$. The following estimates for the interpolation error are well-known, see e.g. [20], [49],

$$\begin{aligned}\|\boldsymbol{v} - \mathfrak{i}_h\boldsymbol{v}\|_{\boldsymbol{L}_2(K)} &\le c_1 h_K |\boldsymbol{v}|_{\boldsymbol{H}^1(\omega(K))}, \\ \|\boldsymbol{v} - \mathfrak{i}_h\boldsymbol{v}\|_{\boldsymbol{L}_2(I)} &\le c_2 h_I^{1/2} |\boldsymbol{v}|_{\boldsymbol{H}^1(\omega(I))},\end{aligned} \tag{3.103}$$

where $\omega(E)$ denotes the neighbourhood of E for $E = K, I$, i.e. the set of all (finite) elements from the mesh $\mathcal{T}_h$, which have nonempty intersection with E. Using the approximation property (3.103) we obtain the assertion of the theorem. □

Remark 3.3.2. *Note that $\boldsymbol{H}^1(\Omega)$-regularity is not enough for working with the Lagrangian interpolation operator, since $\boldsymbol{H}^1(\Omega) \not\subset \boldsymbol{C}(\Omega)$. Therefore, we need to employ an interpolation operator, as the Clément interpolation operator, which works also for nonsmooth functions.*

Efficiency of the FE a posteriori error estimate

The proof of efficiency of the suggested finite element error indicator is analogous to the proof in the boundary element case, considered below, with some standard modifications for the domain term $||\boldsymbol{f} + \operatorname{div}\sigma(\boldsymbol{U}^\varepsilon)||_{\boldsymbol{L}_2(K)}$ and for the interior jumps of the stress

$|||[\sigma(\boldsymbol{U}^\varepsilon)\cdot\boldsymbol{n}]|||_{\boldsymbol{L}_2(I)}$. The reliability and efficiency properties yield the sharpness of the a posteriori error estimate.

Theorem 3.3.2. *Let $\mathcal{T}_h$ be a quasiuniform mesh on Γ with characterictical meshsize h. Then, if the penalty parameters $\varepsilon_n, \varepsilon_t$ are chosen, such that there exists a constant $\tilde{C} > 0$, for which*

$$\varepsilon_n \geq \tilde{C}h, \qquad \varepsilon_t \geq \tilde{C}\mathcal{F}h,$$

the a posteriori error estimate is sharp, i.e. there exist constants $c, C > 0$ independent of h, such that

$$c\sum_{K\in\mathcal{T}_h}\eta_{Fh}^2(K) \leq |||\boldsymbol{u}^\varepsilon - \boldsymbol{U}^\varepsilon|||_F^2 \leq C\sum_{K\in\mathcal{T}_h}\eta_{Fh}^2(K).$$

3.3.3 Residual a posteriori error estimates for boundary elements

Let $\boldsymbol{u}^\varepsilon \in \boldsymbol{\mathcal{V}}$ be an exact solution of the boundary penalty formulation (3.90) and let $\boldsymbol{U}^\varepsilon \in \boldsymbol{\mathcal{V}}_h$ be the solution of the discrete boundary element problem (3.95). Define the traction-like functions by

$$\begin{aligned}\boldsymbol{\psi} &:= V^{-1}(K+1/2)\boldsymbol{u}^\varepsilon,\\ \boldsymbol{\Psi}^* &:= V^{-1}(K+1/2)\boldsymbol{U}^\varepsilon,\\ \boldsymbol{\Psi} &:= i_h V_h^{-1} i_h^*(K+1/2)\boldsymbol{U}^\varepsilon.\end{aligned} \tag{3.104}$$

We introduce the error measure in the boundary element case as follows

$$\begin{aligned}|||\boldsymbol{u}^\varepsilon - \boldsymbol{U}^\varepsilon|||_B^2 := {}& ||\boldsymbol{u}^\varepsilon - \boldsymbol{U}^\varepsilon||^2_{\tilde{\boldsymbol{H}}^{1/2}(\Sigma)} + ||\boldsymbol{\psi} - \boldsymbol{\Psi}||^2_{\boldsymbol{H}^{-1/2}(\Gamma)}\\ &+ ||{\varepsilon_n}^{1/2}(p_n^\varepsilon - P_n^\varepsilon)||^2_{L_2(\Gamma_C)} + ||{\varepsilon_t}^{1/2}\mathcal{F}^{-1/2}(p_t^\varepsilon - P_t^\varepsilon)||^2_{L_2(\Gamma_C)}.\end{aligned} \tag{3.105}$$

Reliability of the BE a posteriori error estimate

The following theorem provides an upper bound for $|||\boldsymbol{u}^\varepsilon - \boldsymbol{U}^\varepsilon|||_B^2$.

Theorem 3.3.3. *Let $\boldsymbol{u}^\varepsilon \in \boldsymbol{\mathcal{V}}$ be an exact solution of the boundary penalty formulation (3.90) and let $\boldsymbol{U}^\varepsilon \in \boldsymbol{\mathcal{V}}_h$ be the solution of the discrete boundary element problem (3.95). Then the following a posteriori error estimate holds for some constant $C > 0$:*

$$|||\boldsymbol{u}^\varepsilon - \boldsymbol{U}^\varepsilon|||_B^2 \leq C\sum_{I\subset\mathcal{T}_h}\eta_h^2(I) \tag{3.106}$$

where the local indicators are given by

$$\begin{aligned}\eta_h^2(I) :=\ & h_I \|\hat{\boldsymbol{t}} - \hat{S}\boldsymbol{U}^\varepsilon\|^2_{\boldsymbol{L}_2(I\cap\Gamma_N)} \\ & + h_I \|P_n^\varepsilon \boldsymbol{n} + P_t^\varepsilon \boldsymbol{t} - \hat{S}\boldsymbol{U}^\varepsilon\|^2_{\boldsymbol{L}_2(I\cap\Gamma_C)} \\ & + h_I \Big\|\frac{\partial}{\partial s}(V\boldsymbol{\Psi} - (K+1/2)\boldsymbol{U}^\varepsilon)\Big\|^2_{\boldsymbol{L}_2(I)}.\end{aligned} \tag{3.107}$$

Proof. Employing Lemma 3.2.6 we obtain

$$\begin{aligned}&||\boldsymbol{u}^\varepsilon - \boldsymbol{U}^\varepsilon||^2_W + ||\boldsymbol{\psi} - \boldsymbol{\Psi}||^2_V \\ &\quad + ||{\varepsilon_n}^{1/2}(p_n^\varepsilon - P_n^\varepsilon)||^2_{L_2(\Gamma_C)} + ||{\varepsilon_t}^{1/2}\mathcal{F}^{-1/2}(p_t^\varepsilon - P_t^\varepsilon)||^2_{L_2(\Gamma_C)} = A_1 + A_2,\end{aligned}$$

where

$$\begin{aligned}A_1 &:= \Big\langle S\boldsymbol{u}^\varepsilon - \hat{S}\boldsymbol{U}^\varepsilon, \boldsymbol{u}^\varepsilon - \boldsymbol{U}^\varepsilon \Big\rangle + ||{\varepsilon_n}^{1/2}(p_n^\varepsilon - P_n^\varepsilon)||^2_{L_2(\Gamma_C)} + ||{\varepsilon_t}^{1/2}\mathcal{F}^{-1/2}(p_t^\varepsilon - P_t^\varepsilon)||^2_{L_2(\Gamma_C)}, \\ A_2 &:= \langle V(\boldsymbol{\Psi}^* - \boldsymbol{\Psi}), \boldsymbol{\psi} - \boldsymbol{\Psi}\rangle\,.\end{aligned}$$

The Galerkin orthogonality property provides for arbitrary $\boldsymbol{\Phi} \in \boldsymbol{\mathcal{V}}_h$

$$\Big\langle S\boldsymbol{u}^\varepsilon - \hat{S}\boldsymbol{U}^\varepsilon, \boldsymbol{U}^\varepsilon - \boldsymbol{\Phi}\Big\rangle + \langle \boldsymbol{p}^\varepsilon - \boldsymbol{P}^\varepsilon, \boldsymbol{U}^\varepsilon - \boldsymbol{\Phi}\rangle_{\Gamma_C} = 0.$$

For the first term A_1, this relation in combination with Lemma 3.2.8 and Lemma 3.3.1 leads to

$$\begin{aligned}A_1 &\le \Big\langle S\boldsymbol{u}^\varepsilon - \hat{S}\boldsymbol{U}^\varepsilon, \boldsymbol{u}^\varepsilon - \boldsymbol{U}^\varepsilon\Big\rangle - \langle \boldsymbol{p}^\varepsilon - \boldsymbol{P}^\varepsilon, \boldsymbol{u}^\varepsilon - \boldsymbol{U}^\varepsilon\rangle_{\Gamma_C} \\ &= \Big\langle S\boldsymbol{u}^\varepsilon - \hat{S}\boldsymbol{U}^\varepsilon, \boldsymbol{u}^\varepsilon - \boldsymbol{U}^\varepsilon\Big\rangle - \langle \boldsymbol{p}^\varepsilon - \boldsymbol{P}^\varepsilon, \boldsymbol{u}^\varepsilon - \boldsymbol{U}^\varepsilon\rangle_{\Gamma_C} \\ &\qquad + \Big\langle S\boldsymbol{u}^\varepsilon - \hat{S}\boldsymbol{U}^\varepsilon, \boldsymbol{U}^\varepsilon - \boldsymbol{\Phi}\Big\rangle + \langle \boldsymbol{p}^\varepsilon - \boldsymbol{P}^\varepsilon, \boldsymbol{U}^\varepsilon - \boldsymbol{\Phi}\rangle_{\Gamma_C} \\ &= \Big\langle S\boldsymbol{u}^\varepsilon - \hat{S}\boldsymbol{U}^\varepsilon, \boldsymbol{u}^\varepsilon - \boldsymbol{\Phi}\Big\rangle - \langle \boldsymbol{p}^\varepsilon - \boldsymbol{P}^\varepsilon, \boldsymbol{u}^\varepsilon - \boldsymbol{\Phi}\rangle_{\Gamma_C}\,.\end{aligned}$$

Since $\boldsymbol{u}^\varepsilon - \boldsymbol{\Phi} \in \boldsymbol{\mathcal{V}}$, the variational formulation (3.90) provides

$$\langle S\boldsymbol{u}^\varepsilon, \boldsymbol{u}^\varepsilon - \boldsymbol{\Phi}\rangle - \langle \boldsymbol{p}^\varepsilon, \boldsymbol{u}^\varepsilon - \boldsymbol{\Phi}\rangle_{\Gamma_C} = \big\langle \hat{\boldsymbol{t}}, \boldsymbol{u}^\varepsilon - \boldsymbol{\Phi}\big\rangle_{\Gamma_N}$$

and therefore, together with Cauchy-Schwarz inequality, we obtain

$$\begin{aligned}A_1 &\le \Big\langle \hat{\boldsymbol{t}} - \hat{S}\boldsymbol{U}^\varepsilon, \boldsymbol{u}^\varepsilon - \boldsymbol{\Phi}\Big\rangle_{\Gamma_N} + \Big\langle \boldsymbol{P}^\varepsilon - \hat{S}\boldsymbol{U}^\varepsilon, \boldsymbol{u}^\varepsilon - \boldsymbol{\Phi}\Big\rangle_{\Gamma_C} \\ &\le \sum_{E\subset\mathcal{T}_h\cap\Gamma_N} \|\hat{\boldsymbol{t}} - \hat{S}\boldsymbol{U}^\varepsilon\|_{\boldsymbol{L}_2(E)}\|\boldsymbol{u}^\varepsilon - \boldsymbol{\Phi}\|_{\boldsymbol{L}_2(E)} + \sum_{E\subset\mathcal{T}_h\cap\Gamma_C} \|\boldsymbol{P}^\varepsilon - \hat{S}\boldsymbol{U}^\varepsilon\|_{\boldsymbol{L}_2(E)}\|\boldsymbol{u}^\varepsilon - \boldsymbol{\Phi}\|_{\boldsymbol{L}_2(E)}.\end{aligned}$$

We estimate now the summand A_2. It holds

$$A_2 := \langle V(\boldsymbol{\Psi} - \boldsymbol{\Psi}^*), \boldsymbol{\Psi} - \boldsymbol{\psi}\rangle \le \|V(\boldsymbol{\Psi} - \boldsymbol{\Psi}^*)\|_{\boldsymbol{H}^{1/2}(\Gamma)}\|\boldsymbol{\Psi} - \boldsymbol{\psi}\|_{\boldsymbol{H}^{-1/2}(\Gamma)}.$$

Further, since $\boldsymbol{U}^\varepsilon \in \boldsymbol{\mathcal{V}}_h \subset \boldsymbol{H}_0^1(\Sigma)$, $\boldsymbol{\Psi} \in \boldsymbol{\mathcal{W}}_h \subset \boldsymbol{L}_2(\Gamma)$ and $V : \boldsymbol{H}^{s-1/2} \to \boldsymbol{H}^{s+1/2}$, $W : \boldsymbol{H}^{s+1/2} \to \boldsymbol{H}^{s-1/2}$ are continuous mappings for $s \in [-1/2, 1/2]$ (cf. Lemma 1.2.1) we obtain with definition (3.104) that

$$V(\boldsymbol{\Psi} - \boldsymbol{\Psi}^*) = V\boldsymbol{\Psi} - (K + 1/2)\boldsymbol{U}^\varepsilon \in \boldsymbol{H}^1(\Gamma) \subset \boldsymbol{C}(\Gamma).$$

Lemma 3.2.7 yields that $V(\boldsymbol{\Psi} - \boldsymbol{\Psi}^*)$ is orthogonal in $L_2(\Gamma)$ to $\boldsymbol{\mathcal{W}}_h$. Furthermore, for the characteristic function $\boldsymbol{\chi}_I \in \boldsymbol{\mathcal{W}}_h$ of an element $I \in \mathcal{T}_h$ there holds

$$0 = \langle V(\boldsymbol{\Psi} - \boldsymbol{\Psi}^*), \boldsymbol{\chi}_I \rangle_\Gamma = \int_I V(\boldsymbol{\Psi} - \boldsymbol{\Psi}^*)\, ds,$$

and therefore the continuous function $V(\boldsymbol{\Psi} - \boldsymbol{\Psi}^*)$ should have a zero on each boundary segment I. Since $V(\boldsymbol{\Psi} - \boldsymbol{\Psi}^*) \in \boldsymbol{H}^1(\Gamma)$, we can apply the result of [15, Theorem 5.1], which provides existence of a positive constant C such that for quasiuniform meshes there holds

$$\|V(\boldsymbol{\Psi} - \boldsymbol{\Psi}^*)\|_{\boldsymbol{H}^{1/2}(\Gamma)} \leq C \sum_{I \subset \Gamma} h_I^{1/2} \Big\| \frac{\partial}{\partial s} V(\boldsymbol{\Psi} - \boldsymbol{\Psi}^*) \Big\|_{\boldsymbol{L}_2(I)}.$$

Since $\langle W\cdot, \cdot\rangle_\Sigma$, $\langle V\cdot, \cdot\rangle_\Gamma$ are positive definite, there exist constants $c_W, c_V > 0$ such that

$$\begin{aligned}
c_W ||\boldsymbol{u}^\varepsilon - \boldsymbol{U}^\varepsilon||^2_{\tilde{\boldsymbol{H}}^{1/2}(\Sigma)} &+ c_V ||\boldsymbol{\psi} - \boldsymbol{\Psi}||^2_{\boldsymbol{H}^{-1/2}(\Gamma)} \\
&+ ||{\varepsilon_n}^{1/2}(p_n^\varepsilon - P_n^\varepsilon)||^2_{L_2(\Gamma_C)} + ||{\varepsilon_t}^{1/2}\mathcal{F}^{-1/2}(p_t^\varepsilon - P_t^\varepsilon)||^2_{L_2(\Gamma_C)} \\
&\leq \sum_{I \subset \mathcal{T}_h \cap \Gamma_N} \|\hat{\boldsymbol{t}} - \hat{S}\boldsymbol{U}^\varepsilon\|_{\boldsymbol{L}_2(I)} ||\boldsymbol{u}^\varepsilon - \boldsymbol{\Phi}||_{\boldsymbol{L}_2(I)} \\
&\qquad + \sum_{I \subset \mathcal{T}_h \cap \Gamma_C} \|P_n^\varepsilon \boldsymbol{n} + P_t^\varepsilon \boldsymbol{t} - \hat{S}\boldsymbol{U}^\varepsilon\|_{\boldsymbol{L}_2(I)} ||\boldsymbol{u}^\varepsilon - \boldsymbol{\Phi}||_{\boldsymbol{L}_2(I)} \\
&\qquad + C \sum_{I \subset \mathcal{T}_h} h_I \Big\| \frac{\partial}{\partial s}(V\boldsymbol{\Psi} - (K + 1/2)\boldsymbol{U}^\varepsilon) \Big\|_{\boldsymbol{L}_2(I)} ||\boldsymbol{\psi} - \boldsymbol{\Psi}||_{\boldsymbol{H}^{-1/2}(\Gamma)}
\end{aligned}$$

for arbitrary $\boldsymbol{\Phi} \in \boldsymbol{\mathcal{V}}_h$. We choose $\boldsymbol{\Phi} := \boldsymbol{U}^\varepsilon + \mathrm{i}_h(\boldsymbol{u}^\varepsilon - \boldsymbol{U}^\varepsilon)$ to be the one-dimensional Clément interpolant of $\boldsymbol{u}^\varepsilon$. According to Clément [20] the following approximation property holds

$$\|\boldsymbol{u}^\varepsilon - \boldsymbol{\Phi}\|_{\boldsymbol{L}_2(I)} \leq C h_I \|\boldsymbol{u}^\varepsilon - \boldsymbol{U}^\varepsilon\|_{\boldsymbol{H}^1(\omega(I))},$$

where $\omega(I)$ is the neighbourhood of I, i.e. the set of all (boundary) elements from the mesh $\mathcal{T}_h$, which have a nonempty intersection with I. Real interpolation between $\boldsymbol{L}_2$ and $\boldsymbol{H}^1$ provides

$$\|\boldsymbol{u}^\varepsilon - \boldsymbol{\Phi}\|_{\boldsymbol{L}_2(I)} \leq C h_I^{1/2} \|\boldsymbol{u}^\varepsilon - \boldsymbol{U}^\varepsilon\|_{\boldsymbol{H}^{1/2}(\omega(I))},$$

which yields

$$
\begin{aligned}
c_W||\boldsymbol{u}^\varepsilon - \boldsymbol{U}^\varepsilon||^2_{\tilde{\boldsymbol{H}}^{1/2}(\Sigma)} &+ c_V||\boldsymbol{\psi} - \boldsymbol{\Psi}||^2_{\boldsymbol{H}^{-1/2}(\Gamma)} \\
&+ ||{\varepsilon_n}^{1/2}(p_n^\varepsilon - P_n^\varepsilon)||^2_{L_2(\Gamma_C)} + ||{\varepsilon_t}^{1/2}\mathcal{F}^{-1/2}(p_t^\varepsilon - P_t^\varepsilon)||^2_{L_2(\Gamma_C)} \\
&\leq C \sum_{I\subset \mathcal{T}_h \cap \Gamma_N} h_I \|\hat{\boldsymbol{t}} - \hat{S}\boldsymbol{U}^\varepsilon\|_{\boldsymbol{L}_2(I)} ||\boldsymbol{u}^\varepsilon - \boldsymbol{U}^\varepsilon||_{\boldsymbol{H}^{1/2}(I)} \\
&\quad + C \sum_{I\subset \mathcal{T}_h \cap \Gamma_C} h_I \|P_n^\varepsilon \boldsymbol{n} + P_t^\varepsilon \boldsymbol{t} - \hat{S}\boldsymbol{U}^\varepsilon\|_{\boldsymbol{L}_2(I)} ||\boldsymbol{u}^\varepsilon - \boldsymbol{U}^\varepsilon||_{\boldsymbol{H}^{1/2}(I)} \\
&\quad + C \sum_{I\subset \mathcal{T}_h} h_I \Big\| \frac{\partial}{\partial s}(V\boldsymbol{\Psi} - (K+1/2)\boldsymbol{U}^\varepsilon)\Big\|_{\boldsymbol{L}_2(I)} ||\boldsymbol{\psi} - \boldsymbol{\Psi}||_{\boldsymbol{H}^{-1/2}(\Gamma)}.
\end{aligned}
$$

Using Cauchy's inequality we throw the terms $||\boldsymbol{u}^\varepsilon - \boldsymbol{U}^\varepsilon||^2_{\boldsymbol{H}^{1/2}(I)}$, $||\boldsymbol{\psi} - \boldsymbol{\Psi}||^2_{\boldsymbol{H}^{-1/2}(\Gamma)}$ to the left hand side and obtain the a posteriori error estimate (3.106). $\square$

Efficiency of the BE a posteriori error estimate

In this paragraph we prove efficiency of the a posteriori error estimates. We extend the approach of Carstensen and Stephan [17], Carstensen [15] onto the frictional contact problems.

Theorem 3.3.4. *There exists a constant $c > 0$ such that for any element $I \in \mathcal{T}_h$ the local error indicator $\eta_h(I)$ defined in (3.107), can be bounded as follows*

$$
\begin{aligned}
c\eta_h^2(I) \leq & h_I||W(\boldsymbol{u}^\varepsilon - \boldsymbol{U}^\varepsilon)||^2_{\boldsymbol{L}_2(I\cap\Sigma)} + h_I||(K'+1/2)(\boldsymbol{\psi} - \boldsymbol{\Psi})||^2_{\boldsymbol{L}_2(I\cap\Sigma)} \\
&+ h_I\Big\|\frac{\partial}{\partial s}V(\boldsymbol{\psi} - \boldsymbol{\Psi})\Big\|^2_{\boldsymbol{L}_2(I)} + h_I\Big\|\frac{\partial}{\partial s}(K+1/2)(\boldsymbol{u}^\varepsilon - \boldsymbol{U}^\varepsilon)\Big\|^2_{\boldsymbol{L}_2(I)} \\
&+ h_I||\boldsymbol{p}^\varepsilon - \boldsymbol{P}^\varepsilon||^2_{\boldsymbol{L}_2(I\cap\Gamma_C)}
\end{aligned}
\tag{3.108}
$$

Proof. Consider the indicator on the Neumann boundary, i.e. the case $I \subset \Gamma_N$. Noting that $\hat{\boldsymbol{t}} \equiv S\boldsymbol{u}^\varepsilon|_{\Gamma_N}$ for the exact solution $\boldsymbol{u}^\varepsilon$, we obtain

$$
\begin{aligned}
h_I||\hat{\boldsymbol{t}} - \hat{S}\boldsymbol{U}^\varepsilon||^2_{\boldsymbol{L}_2(I)} &= h_I||S\boldsymbol{u}^\varepsilon - \hat{S}\boldsymbol{U}^\varepsilon||^2_{\boldsymbol{L}_2(I)} \\
&= h_I||W(\boldsymbol{u}^\varepsilon - \boldsymbol{U}^\varepsilon) + (K'+1/2)(\boldsymbol{\psi} - \boldsymbol{\Psi})||^2_{\boldsymbol{L}_2(I)} \\
&\leq 2h_I||W(\boldsymbol{u}^\varepsilon - \boldsymbol{U}^\varepsilon)||^2_{\boldsymbol{L}_2(I)} + 2h_I||(K'+1/2)(\boldsymbol{\psi} - \boldsymbol{\Psi})||^2_{\boldsymbol{L}_2(I)}.
\end{aligned}
$$

We used here the definition of the traction-like functions (3.104). Further, the weak formulation (3.90) yields the identity $\boldsymbol{p}^\varepsilon \equiv S\boldsymbol{u}^\varepsilon$ on the contact boundary Γ_C. Therefore, if $I \subset \Gamma_C$, then

$$
\begin{aligned}
h_I||\boldsymbol{P}^\varepsilon - \hat{S}\boldsymbol{U}^\varepsilon||^2_{\boldsymbol{L}_2(I)} &\leq 2h_I||\boldsymbol{p}^\varepsilon - \boldsymbol{P}^\varepsilon||^2_{\boldsymbol{L}_2(I)} + 2h_I||S\boldsymbol{u}^\varepsilon - \hat{S}\boldsymbol{U}^\varepsilon||^2_{\boldsymbol{L}_2(I)} \\
&\leq 2h_I||\boldsymbol{p}^\varepsilon - \boldsymbol{P}^\varepsilon||^2_{\boldsymbol{L}_2(I)} \\
&\qquad + 4h_I||W(\boldsymbol{u}^\varepsilon - \boldsymbol{U}^\varepsilon)||^2_{\boldsymbol{L}_2(I)} + 4h_I||(K'+1/2)(\boldsymbol{\psi} - \boldsymbol{\Psi})||^2_{\boldsymbol{L}_2(I)}.
\end{aligned}
$$

Finally, we have to estimate the consistency term. The identity $V\boldsymbol{\psi} \equiv (K+1/2)\boldsymbol{u}^\varepsilon$ provides for some element $I \subset \Gamma$

$$\begin{aligned} h_I \Big\| \frac{\partial}{\partial s}(V\boldsymbol{\Psi} - (K+1/2)\boldsymbol{U}^\varepsilon)\Big\|^2_{\boldsymbol{L}_2(I)} \\ \leq 2h_I \Big\| \frac{\partial}{\partial s} V(\boldsymbol{\psi} - \boldsymbol{\Psi})\Big\|^2_{\boldsymbol{L}_2(I)} + 2h_I \Big\| \frac{\partial}{\partial s}(K+1/2)(\boldsymbol{u}^\varepsilon - \boldsymbol{U}^\varepsilon)\Big\|^2_{\boldsymbol{L}_2(I)}, \end{aligned}$$

which finishes the proof. □

We need the following lemma to prove the efficiency of the a posteriori error estimate.

Lemma 3.3.2. *Let $\boldsymbol{\psi} \in \boldsymbol{L}_2(\Gamma)$ and $\Pi_h : \boldsymbol{L}_2(\Gamma) \to \boldsymbol{\mathcal{W}}_h$ be the L_2-projection operator. Then there holds*

$$||\boldsymbol{\psi} - \Pi_h \boldsymbol{\psi}||_{\boldsymbol{H}^{-1/2}(\Gamma)} \leq C h_{max}^{1/2} ||\boldsymbol{\psi}||_{\boldsymbol{L}_2(\Gamma)}.$$

In particular, there holds

$$||\boldsymbol{\psi} - \Pi_h \boldsymbol{\psi}||_{\boldsymbol{H}^{-1/2}(\Gamma)} \leq C h_{max}^{1/2} ||\boldsymbol{\psi} - \Pi_h \boldsymbol{\psi}||_{\boldsymbol{L}_2(\Gamma)}.$$

Proof. The definition of the L_2-projection operator yields

$$\big\langle \boldsymbol{\psi} - \Pi_h \boldsymbol{\psi}, \boldsymbol{\Phi} \big\rangle = 0, \qquad \forall \boldsymbol{\Phi} \in \boldsymbol{\mathcal{W}}_h.$$

By duality we obtain

$$\begin{aligned} ||\boldsymbol{\psi} - \Pi_h \boldsymbol{\psi}||_{\boldsymbol{H}^{-1}(\Gamma)} &= \sup_{\boldsymbol{w} \in \boldsymbol{H}^1(\Gamma)} \frac{\big\langle \boldsymbol{\psi} - \Pi_h \boldsymbol{\psi}, \boldsymbol{w} \big\rangle}{||\boldsymbol{w}||_{\boldsymbol{H}^1(\Gamma)}} \\ &= \sup_{\boldsymbol{w} \in \boldsymbol{H}^1(\Gamma)} \frac{\big\langle \boldsymbol{\psi} - \Pi_h \boldsymbol{\psi}, \boldsymbol{w} - \Pi_h \boldsymbol{w} \big\rangle}{||\boldsymbol{w}||_{\boldsymbol{H}^1(\Gamma)}} \\ &= \sup_{\boldsymbol{w} \in \boldsymbol{H}^1(\Gamma)} \frac{\big\langle \boldsymbol{\psi}, \boldsymbol{w} - \Pi_h \boldsymbol{w} \big\rangle}{||\boldsymbol{w}||_{\boldsymbol{H}^1(\Gamma)}} \\ &\leq ||\boldsymbol{\psi}||_{\boldsymbol{L}_2(\Gamma)} \sup_{\boldsymbol{w} \in \boldsymbol{H}^1(\Gamma)} \frac{||\boldsymbol{w} - \Pi_h \boldsymbol{w}||_{\boldsymbol{L}_2(\Gamma)}}{||\boldsymbol{w}||_{\boldsymbol{H}^1(\Gamma)}} \end{aligned} \tag{3.109}$$

since $\Pi_h \boldsymbol{w} \in \boldsymbol{\mathcal{W}}_h$. The Poincaré inequality gives

$$||\boldsymbol{w} - \Pi_h \boldsymbol{w}||_{\boldsymbol{L}_2(\Gamma)} \leq C h_{max} ||\boldsymbol{w}||_{\boldsymbol{H}^1(\Gamma)}$$

and therefore we obtain from (3.109) that

$$||\boldsymbol{\psi} - \Pi_h \boldsymbol{\psi}||_{\boldsymbol{H}^{-1}(\Gamma)} \leq C h_{max} ||\boldsymbol{\psi}||_{\boldsymbol{L}_2(\Gamma)}.$$

The L_2-projection is stable in the L_2-norm, i.e.

$$||\boldsymbol{\psi} - \Pi_h \boldsymbol{\psi}||_{\boldsymbol{L}_2(\Gamma)} \leq C ||\boldsymbol{\psi}||_{\boldsymbol{L}_2(\Gamma)}.$$

Hence, the interpolation between $\boldsymbol{H}^{-1}(\Gamma)$ and $\boldsymbol{L}_2(\Gamma)$ provides

$$||\boldsymbol{\psi} - \Pi_h \boldsymbol{\psi}||_{\boldsymbol{H}^{-1/2}(\Gamma)} \leq C h_{max}^{1/2} ||\boldsymbol{\psi}||_{\boldsymbol{L}_2(\Gamma)}.$$

In particular there holds

$$\begin{aligned} ||\boldsymbol{\psi} - \Pi_h \boldsymbol{\psi}||_{\boldsymbol{H}^{-1/2}(\Gamma)} &= ||\boldsymbol{\psi} - \Pi_h \boldsymbol{\psi} - \Pi_h(\boldsymbol{\psi} - \Pi_h \boldsymbol{\psi})||_{\boldsymbol{H}^{-1/2}(\Gamma)} \\ &\leq C h_{max}^{1/2} ||\boldsymbol{\psi} - \Pi_h \boldsymbol{\psi}||_{\boldsymbol{L}_2(\Gamma)}. \end{aligned}$$

□

Theorem 3.3.5. *Let $\mathcal{I}_h : \boldsymbol{C}(\Sigma) \to \boldsymbol{\mathcal{V}}_h$ be the Lagrangian interpolation operator and let $\Pi_h : \boldsymbol{L}_2(\Gamma) \to \boldsymbol{\mathcal{W}}_h$ be the L_2-projection operator. Assume that $\boldsymbol{u}^\varepsilon \in \boldsymbol{H}_0^1(\Sigma)$, $\boldsymbol{\psi} \in \boldsymbol{L}_2(\Gamma)$ and that the penalty parameters $\varepsilon_n, \varepsilon_t$ are chosen such that there exists a constant $\tilde{C} > 0$, for which*

$$\varepsilon_n \geq \tilde{C} h_{max}, \qquad \varepsilon_t \geq \tilde{C} \mathcal{F} h_{max}. \tag{3.110}$$

Then there exists a constant $c > 0$ such that

$$\begin{aligned} c \sum_{I \in \mathcal{T}_h} \eta_h^2(I) \leq \max\left(\frac{h_{max}}{h_{min}}, \tilde{C}^{-1}\right) |||\boldsymbol{u}^\varepsilon - \boldsymbol{U}^\varepsilon|||_B^2 \\ + \frac{h_{max}^2}{h_{min}} ||\boldsymbol{u}^\varepsilon - \mathcal{I}_h \boldsymbol{u}^\varepsilon||_{\boldsymbol{H}_0^1(\Sigma)}^2 + \frac{h_{max}^2}{h_{min}} ||\boldsymbol{\psi} - \Pi_h \boldsymbol{\psi}||_{\boldsymbol{L}_2(\Gamma)}^2. \end{aligned}$$

Proof. Summing the estimate (3.108) over all elements $I \in \mathcal{T}_h$ we obtain

$$\begin{aligned} c \sum_{I \in \mathcal{T}_h} \eta_h^2(I) \leq & h_{max} ||W(\boldsymbol{u}^\varepsilon - \boldsymbol{U}^\varepsilon)||_{\boldsymbol{L}_2(\Sigma)}^2 + h_{max} ||(K' + 1/2)(\boldsymbol{\psi} - \boldsymbol{\Psi})||_{\boldsymbol{L}_2(\Sigma)}^2 \\ & + h_{max} \Big|\Big| \frac{\partial}{\partial s} V(\boldsymbol{\psi} - \boldsymbol{\Psi}) \Big|\Big|_{\boldsymbol{L}_2(\Gamma)}^2 + h_{max} \Big|\Big| \frac{\partial}{\partial s} (K + 1/2)(\boldsymbol{u}^\varepsilon - \boldsymbol{U}^\varepsilon) \Big|\Big|_{\boldsymbol{L}_2(\Gamma)}^2 \\ & + h_{max} ||\boldsymbol{p}^\varepsilon - \boldsymbol{P}^\varepsilon||_{\boldsymbol{L}_2(\Gamma_C)}^2. \end{aligned} \tag{3.111}$$

To prove the theorem, we need to estimate the terms on the right hand side of (3.111). For the first term and for the fourth term in (3.111) we obtain

$$\begin{aligned} h_{max} ||W(\boldsymbol{u}^\varepsilon - \boldsymbol{U}^\varepsilon)||_{\boldsymbol{L}_2(\Sigma)}^2 &\leq C h_{max} ||\boldsymbol{u}^\varepsilon - \boldsymbol{U}^\varepsilon||_{\boldsymbol{H}^1(\Gamma)}^2, \\ h_{max} \Big|\Big| \frac{\partial}{\partial s} (K + 1/2)(\boldsymbol{u}^\varepsilon - \boldsymbol{U}^\varepsilon) \Big|\Big|_{\boldsymbol{L}_2(\Gamma)}^2 &\leq h_{max} \Big|\Big| (K + 1/2)(\boldsymbol{u}^\varepsilon - \boldsymbol{U}^\varepsilon) \Big|\Big|_{\boldsymbol{H}^1(\Gamma)}^2 \\ &\leq C h_{max} \Big|\Big| \boldsymbol{u}^\varepsilon - \boldsymbol{U}^\varepsilon \Big|\Big|_{\boldsymbol{H}^1(\Gamma)}^2 \end{aligned}$$

since $W : \boldsymbol{H}^{1/2+s}(\Gamma) \to \boldsymbol{H}^{-1/2+s}(\Gamma)$ and $K : \boldsymbol{H}^{1/2+s}(\Gamma) \to \boldsymbol{H}^{1/2+s}(\Gamma)$ are continuous mappings for $s \in [-1/2, 1/2]$. Here we identify functions f, supp $f \subset \Sigma$, with their zero extension onto whole Γ. Let $\mathcal{I}_h$ be the Lagrangian interpolation operator on the mesh $\mathcal{T}_h$. The triangle inequality gives

$$h_{max}\big\|\boldsymbol{u}^\varepsilon - \boldsymbol{U}^\varepsilon\big\|^2_{\boldsymbol{H}^1(\Gamma)} \leq Ch_{max}||\boldsymbol{u}^\varepsilon - \mathcal{I}_h\boldsymbol{u}^\varepsilon||^2_{\boldsymbol{H}^1(\Gamma)} + Ch_{max}||\mathcal{I}_h\boldsymbol{u}^\varepsilon - \boldsymbol{U}^\varepsilon||^2_{\boldsymbol{H}^1(\Gamma)}.$$

Since $\mathcal{I}_h\boldsymbol{u}^\varepsilon - \boldsymbol{U}^\varepsilon \in \boldsymbol{\mathcal{V}}_h$, we can apply the inverse inequality (see e.g. [14, Proposition 3])

$$\begin{aligned} h_{max}||\mathcal{I}_h\boldsymbol{u}^\varepsilon - \boldsymbol{U}^\varepsilon||^2_{\boldsymbol{H}^1(\Gamma)} &\leq C\frac{h_{max}}{h_{min}}||\mathcal{I}_h\boldsymbol{u}^\varepsilon - \boldsymbol{U}^\varepsilon||^2_{\boldsymbol{H}^{1/2}(\Gamma)} \\ &= C\frac{h_{max}}{h_{min}}||\mathcal{I}_h\boldsymbol{u}^\varepsilon - \boldsymbol{U}^\varepsilon||^2_{\tilde{\boldsymbol{H}}^{1/2}(\Sigma)} \\ &\leq C\frac{h_{max}}{h_{min}}||\boldsymbol{u}^\varepsilon - \boldsymbol{U}^\varepsilon||^2_{\tilde{\boldsymbol{H}}^{1/2}(\Sigma)} + C\frac{h_{max}}{h_{min}}||\mathcal{I}_h\boldsymbol{u}^\varepsilon - \boldsymbol{u}^\varepsilon||^2_{\tilde{\boldsymbol{H}}^{1/2}(\Sigma)}. \end{aligned}$$

Employing properties of space interpolation and approximation properties of $\mathcal{I}_h$ we get

$$\begin{aligned} ||\mathcal{I}_h\boldsymbol{u}^\varepsilon - \boldsymbol{u}^\varepsilon||^2_{\boldsymbol{H}^{1/2}(\tilde{\Sigma})} &\leq C||\mathcal{I}_h\boldsymbol{u}^\varepsilon - \boldsymbol{u}^\varepsilon||_{\boldsymbol{L}_2(\Sigma)}||\mathcal{I}_h\boldsymbol{u}^\varepsilon - \boldsymbol{u}^\varepsilon||_{\boldsymbol{H}^1_0(\Sigma)} \\ &\leq Ch_{max}||\mathcal{I}_h\boldsymbol{u}^\varepsilon - \boldsymbol{u}^\varepsilon||^2_{\boldsymbol{H}^1_0(\Sigma)} \end{aligned}$$

and therefore

$$\begin{aligned} h_{max}||W(\boldsymbol{u}^\varepsilon - \boldsymbol{U}^\varepsilon)||^2_{\boldsymbol{L}_2(\Sigma)} + h_{max}\Big\|\frac{\partial}{\partial s}(K+1/2)(\boldsymbol{u}^\varepsilon - \boldsymbol{U}^\varepsilon)\Big\|^2_{\boldsymbol{L}_2(\Gamma)} \\ \leq C\frac{h_{max}}{h_{min}}||\boldsymbol{u}^\varepsilon - \boldsymbol{U}^\varepsilon||^2_{\tilde{\boldsymbol{H}}^{1/2}(\Sigma)} + C\frac{h^2_{max}}{h_{min}}||\mathcal{I}_h\boldsymbol{u}^\varepsilon - \boldsymbol{u}^\varepsilon||^2_{\boldsymbol{H}^1_0(\Sigma)}. \end{aligned}$$

For the second term and for the third term in (3.111) there holds

$$\begin{aligned} h_{max}||(K'+1/2)(\boldsymbol{\psi} - \boldsymbol{\Psi})||^2_{\boldsymbol{L}_2(\Gamma)} &\leq h_{max}||\boldsymbol{\psi} - \boldsymbol{\Psi}||^2_{\boldsymbol{L}_2(\Gamma)}, \\ h_{max}\Big\|\frac{\partial}{\partial s}V(\boldsymbol{\psi} - \boldsymbol{\Psi})\Big\|^2_{\boldsymbol{L}_2(\Gamma)} &\leq h_{max}\big\|V(\boldsymbol{\psi} - \boldsymbol{\Psi})\big\|^2_{\boldsymbol{H}^1(\Gamma)} \leq h_{max}\big\|\boldsymbol{\psi} - \boldsymbol{\Psi}\big\|^2_{\boldsymbol{L}_2(\Gamma)}, \end{aligned}$$

since $V : \boldsymbol{H}^{-1/2+s}(\Gamma) \to \boldsymbol{H}^{1/2+s}(\Gamma)$ and $K' : \boldsymbol{H}^{-1/2+s}(\Gamma) \to \boldsymbol{H}^{-1/2+s}(\Gamma)$ are continuous mappings for $s \in [-1/2, 1/2]$. Let $\Pi_h : \boldsymbol{L}_2(\Gamma) \to \boldsymbol{\mathcal{W}}_h$ be the L_2-projection operator onto the space of piecewise constants on the mesh $\mathcal{T}_h$. Therefore, with the triangle inequality

$$h_{max}||\boldsymbol{\psi} - \boldsymbol{\Psi}||^2_{\boldsymbol{L}_2(\Gamma)} \leq h_{max}||\boldsymbol{\psi} - \Pi_h\boldsymbol{\psi}||^2_{\boldsymbol{L}_2(\Gamma)} + h_{max}||\Pi_h\boldsymbol{\psi} - \boldsymbol{\Psi}||^2_{\boldsymbol{L}_2(\Gamma)} \tag{3.112}$$

In [14, Proposition 3] the inverse inequality $||\boldsymbol{\Phi}||_{\boldsymbol{L}_2(\Gamma)} \leq Ch^{-1}_{min}||\boldsymbol{\Phi}||_{\boldsymbol{H}^{-1}(\Gamma)}$ was shown for $\forall \boldsymbol{\Phi} \in \boldsymbol{\mathcal{W}}_h$. We obtain by interpolation

$$||\boldsymbol{\Phi}||^2_{\boldsymbol{L}_2(\Gamma)} \leq Ch^{-1}_{min}||\boldsymbol{\Phi}||^2_{\boldsymbol{H}^{-1/2}(\Gamma)}, \qquad \forall \boldsymbol{\Phi} \in \boldsymbol{\mathcal{W}}_h.$$

Hence, the second term in (3.112) can be estimated as follows

$$\begin{aligned} h_{max}||\Pi_h\boldsymbol{\psi} - \boldsymbol{\Psi}||^2_{\boldsymbol{L}_2(\Gamma)} &\leq C\frac{h_{max}}{h_{min}}||\Pi_h\boldsymbol{\psi} - \boldsymbol{\Psi}||^2_{\boldsymbol{H}^{-1/2}(\Gamma)} \\ &\leq C\frac{h_{max}}{h_{min}}||\boldsymbol{\psi} - \boldsymbol{\Psi}||^2_{\boldsymbol{H}^{-1/2}(\Gamma)} + C\frac{h_{max}}{h_{min}}||\boldsymbol{\psi} - \Pi_h\boldsymbol{\psi}||^2_{\boldsymbol{H}^{-1/2}(\Gamma)} \end{aligned}$$

Employing Lemma 3.3.2 we obtain

$$\frac{h_{max}}{h_{min}}||\boldsymbol{\psi} - \Pi_h\boldsymbol{\psi}||^2_{\boldsymbol{H}^{-1/2}(\Gamma)} \leq C\frac{h^2_{max}}{h_{min}}||\boldsymbol{\psi} - \Pi_h\boldsymbol{\psi}||^2_{\boldsymbol{L}_2(\Gamma)}$$

and therefore

$$h_{max}||(K' + 1/2)(\boldsymbol{\psi} - \boldsymbol{\Psi})||^2_{\boldsymbol{L}_2(\Gamma)} + h_{max}\Big|\Big|\frac{\partial}{\partial s}V(\boldsymbol{\psi} - \boldsymbol{\Psi})\Big|\Big|^2_{\boldsymbol{L}_2(\Gamma)}$$
$$\leq C\frac{h_{max}}{h_{min}}||\boldsymbol{\psi} - \boldsymbol{\Psi}||^2_{\boldsymbol{H}^{-1/2}(\Gamma)} + C\frac{h^2_{max}}{h_{min}}||\boldsymbol{\psi} - \Pi_h\boldsymbol{\psi}||^2_{\boldsymbol{L}_2(\Gamma)}.$$

Finally, if the penalty parameters $\varepsilon_n, \varepsilon_t$ are chosen accordingly to (3.110), the contact terms can be estimated as follows

$$h_{max}||\boldsymbol{p}^\varepsilon - \boldsymbol{P}^\varepsilon||^2_{\boldsymbol{L}_2(\Gamma_C)} \leq \tilde{C}^{-1}||{\varepsilon_n}^{1/2}(p^\varepsilon_n - P^\varepsilon_n)||^2_{L_2(\Gamma_C)} + \tilde{C}^{-1}||{\varepsilon_t}^{1/2}\mathcal{F}^{-1/2}(p^\varepsilon_t - P^\varepsilon_t)||^2_{L_2(\Gamma_C)}.$$

□

Let us consider the quasiuniform meshes on Γ, i.e. meshes for which there exists a constant $C_q > 0$, independent of the meshsize, such that

$$\frac{h_{max}}{h_{min}} \leq C_q.$$

Then, with additional regularity assumptions on the solution $\boldsymbol{u}^\varepsilon \in \tilde{\boldsymbol{H}}^{1+\nu}(\Sigma)$ and $\boldsymbol{\psi} \in \boldsymbol{H}^\nu(\Gamma)$, the approximation properties of the Lagrangian interpolation operator and of the L_2-projection operator yield

$$\begin{aligned} h^{1/2}_{max}||\boldsymbol{u}^\varepsilon - \mathcal{I}_h\boldsymbol{u}^\varepsilon||_{\boldsymbol{H}^1_0(\Sigma)} &\leq Ch^{1/2+\nu}_{max}||\boldsymbol{u}^\varepsilon||_{\tilde{\boldsymbol{H}}^{1+\nu}(\Sigma)}, \\ h^{1/2}_{max}||\boldsymbol{\psi} - \Pi_h\boldsymbol{\psi}||_{\boldsymbol{L}_2(\Gamma)} &\leq Ch^{1/2+\nu}_{max}||\boldsymbol{\psi}||_{\boldsymbol{H}^\nu(\Gamma)}. \end{aligned} \tag{3.113}$$

Remark 3.3.3. *[26, Remark 7] For the contact problem with friction the best regularity which can be shown is $\boldsymbol{u}^\varepsilon \in \boldsymbol{H}^1_0(\Sigma)$, which corresponds to the case $\nu = 0$ [25], [37], [51]. For the frictionless contact problems the regularity $\boldsymbol{u}^\varepsilon \in \tilde{\boldsymbol{H}}^{3/2}(\Sigma)$ can be shown, i.e. $\nu = 1/2$ (cf. [39]). Therefore the convergence rate $\mathcal{O}(h^{1/2}_{max})$ is expected for frictional problem and the convergence rate $\mathcal{O}(h_{max})$ is expected for frictionless problem:*

Remark 3.3.4. *Based on Remark 3.3.3 we expect that if the solution does not lie in the BE space $\boldsymbol{u}^\varepsilon \notin \boldsymbol{\mathcal{V}}_h$, the convergence rate is not better then $h^{1/2+\nu}_{max}$ with $\nu = 0, 1/2$ for frictional and frictionless contact problems respectively, i.e. there exists $C > 0$ independent from the meshsize, such that*

$$Ch^{1/2+\nu}_{max} \leq |||\boldsymbol{u}^\varepsilon - \boldsymbol{U}^\varepsilon|||_B.$$

Combining Theorem 3.3.5, Remark 3.3.4 and (3.113) we obtain a sharp a posteriori error estimate.

Theorem 3.3.6. *Under above mentioned assumptions, the a posteriori error estimate is sharp, i.e. there exists $c, C > 0$ independent from the meshsize, such that*

$$c\sum_{I\in\mathcal{T}_h}\eta^2_h(I) \leq |||\boldsymbol{u}^\varepsilon - \boldsymbol{U}^\varepsilon|||^2_B \leq C\sum_{I\in\mathcal{T}_h}\eta^2_h(I).$$

3.3.4 Mesh refinement strategy for the h-version

In the numerical examples we employ the standard mesh refinement procedure for the h-version of finite elements or boundary elements, given by Algorithm 3.2 (see e.g. [67]).

The discrete problem in the case of a frictional contact problem between an elastic body and a rigid obstacle with BEM is given by (3.95), the error indicators are given by (3.107).

If FEM is used, the discrete problem is given by (3.97) and the error indicators are given by (3.100).

Algorithm 3.2. *(Mesh refinement strategy for the h-version of FEM and BEM)*

---

1. *generate an initial (coarse) mesh $\mathcal{T}_{h,0}$, discrete spaces $\boldsymbol{\mathcal{V}}_{h,0}$, $\boldsymbol{\mathcal{W}}_{h,0}$, set $k = 0$*
2. *choose a refinement criterion, refinement quota $p \in [0, 1]$, tolerance TOL*
3. *for $k = 0, 1, 2 \dots$*
   a) *solve the discrete problem (with FEM or BEM)*
   b) *compute indicators η_I for all segments $I \in \mathcal{T}_{h,k}$*
   c) *stop if $\sum_{I \in \mathcal{T}_{h,k}} \eta_I^2 \leq \frac{TOL}{C}$*
   d) *refine I, if the refinement criterion for I is satisfied*
   e) *make further refinement to preserve conformity of the mesh, obtain $\mathcal{T}_{h,k+1}$*
   f) *generate the discrete spaces $\boldsymbol{\mathcal{V}}_{h,k+1}$, $\boldsymbol{\mathcal{W}}_{h,k+1}$ based on the mesh $\mathcal{T}_{h,k+1}$*
   g) *set $k = k + 1$, go to (a)*

Some refinement criteria:

- *refine I if $\eta_I \geq p \max_{J \in \mathcal{T}_{h,k}} \eta_J$*
- *refine I if η_I belongs to $(1 - p) \cdot 100\%$ of the largest indicators*

Remark 3.3.5. *Note, that the step (e) is only necessary, when a two-dimensional mesh $\mathcal{T}_h$ is considered (BEM in 3D or FEM in 2D or 3D), or is case of one-dimensional mesh with restriction on the length the neighbours elements.*

3.3.5 Numerical results

In this section two numerical examples with automatic mesh refinement for contact problems with Coulomb's friction are presented, based on error indicators, derived in the previous sections for the penalty formulation. The problem is solved with the Newton's method. The detailed description of linearization of the contact terms and the algebraic formulation is a special case of the two-body frictional contact problem, presented in Section 4.2. We give two examples of adaptive mesh refinement for boundary elements, employing error indicators (3.107). An example for the finite elements with the error indicator (3.100) will be given in the next chapter within the two-body frictional contact framework.

Example 1

The first example is based on the same geometry as the numerical example, described in Paragraph 3.2.5. We consider a frictional contact problem of the two-dimensional elastic body, occupying $\Omega := [-1,1] \times [-1,1]$, with a rigid horizontal obstacle $\gamma := [-1,1] \times \{-1+d\}$, where d varies. The body is fixed along the upper horizontal boundary

$$\boldsymbol{u} = 0 \qquad \text{on } \Gamma_D := [-1,1] \times \{1\}.$$

The remaining part of the boundary is assumed to be the zone of possible contact with the obstacle γ

$$\Gamma_C := \partial\Omega \setminus \Gamma_D, \qquad \Gamma_N := \emptyset.$$

The elastic parameters are $E = 266926.0$, $\nu = 0.29$ and the coefficient of friction is set to be $\mu_f = 0.1$. The displacement increment $d = 0.6 \cdot 10^{-4}$ is subjected to the obstacle γ, which yields contact between the body Ω and the obstacle γ and, therefore, a deformation in Ω. The geometry of the problem is shown on Fig. 3.2.

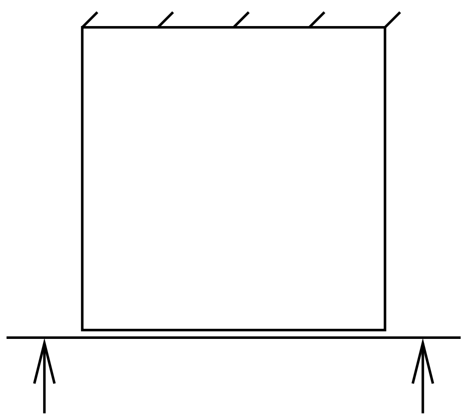

Figure 3.2: Contact geometry of Example 1

The initial uniform mesh $\mathcal{T}_h$ consists of four straight line elements per side of Ω, as it is shown on Fig. 3.3. The space $\boldsymbol{\mathcal{V}}_h$ of piecewise linear continuous functions (3.92) is used for discretization of the displacement; and the space $\boldsymbol{\mathcal{W}}_h$ of piecewise constant functions (3.93) is used for discretization of the boundary traction.

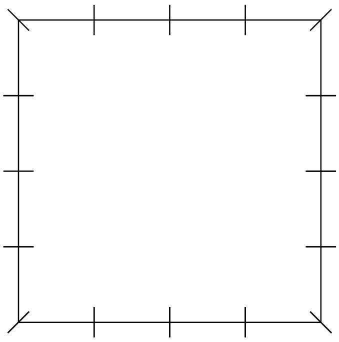

Figure 3.3: Initial mesh $\mathcal{T}_h$

The error indicator for BEM with penalty contact discretization (3.107), combined with the mesh refinement Algorithm 3.2, was used to optimize the mesh $\mathcal{T}_h$. The maximum value of the error indicator over all elements η_{max} is computed, and then compared with the local indicators η_I on elements $I \in \mathcal{T}_h$. The element I is halved, if its indicator η_I is larger than 90% of η_{max}.

The sequence of obtained the displacement meshes after each of the six refinement steps and corresponding deformed configuration is presented on Fig. 3.4. The deformed configuration is plotted for displacements, multiplied with 10^4, to make the deformation of the body visible. The red labelling in the mesh is used for the elements being refined within the current refinement step. As it can be seen from Fig. 3.4, the elements having symmetric positions are refined in each step, which is caused by the symmetry of the problem. Furthermore, most of the refinement happens in the zone of *actual* contact and near the corners of Ω. This is caused by the singularities, appearing where the boundary conditions are changing: contact / no contact near the points $(-1,-1)$, $(1,-1)$; and homogeneous Neumann / homogeneous Dirichlet near the points $(-1,1)$, $(1,1)$. Moreover, refinement of the contact boundary is also caused by the consistency error on the contact boundary, i.e. nonzero penetration.

The x- and y-components of the displacement inside the body and deformation of the auxiliary finite element mesh after the sixth refinement step, obtained by the representation formula (1.2), are shown in Fig. 3.5.

In Fig. 3.6 we compare decay of the error in the norm $|||\cdot|||_B$, defined in (3.105), for uniform and adaptive refinement. As a reference norm, we take $|||\boldsymbol{U}_{190}|||_B$, where $\boldsymbol{U}_{190}$ is the solution, obtained on the uniform mesh with 190 degrees of freedom. The curves $err(\boldsymbol{U})$, plotted in Fig. 3.6 are defined by $err(\boldsymbol{U}) := \big|\, |||\boldsymbol{U}|||_B - |||\boldsymbol{U}_{190}|||_B \big|$.

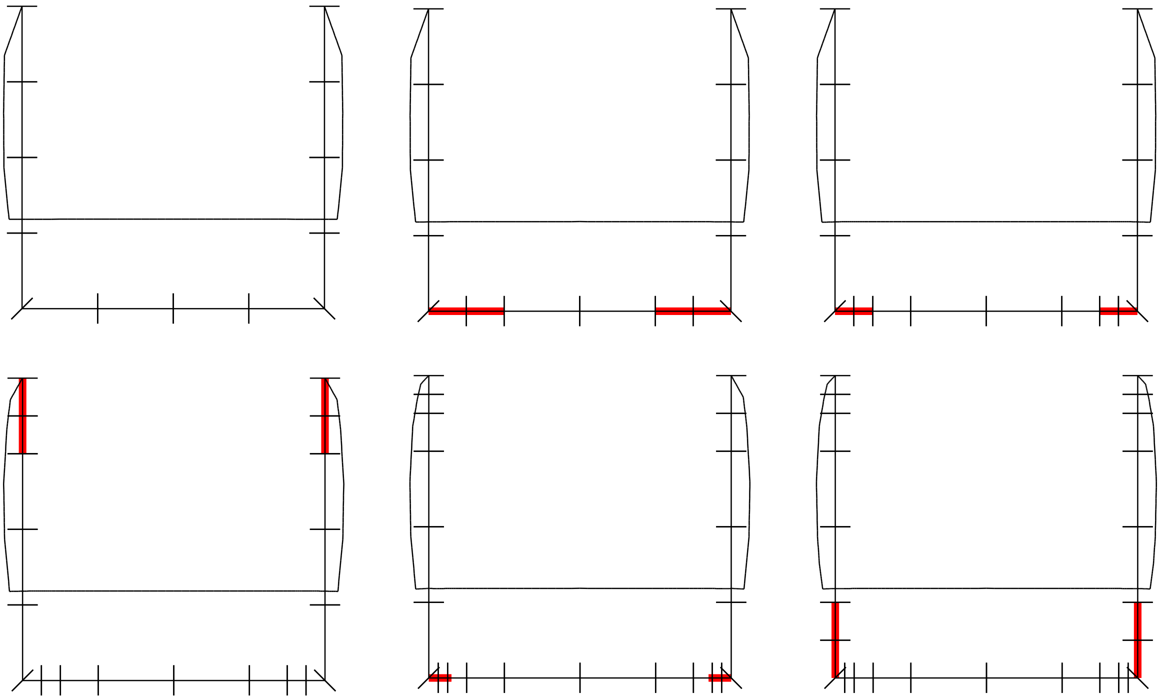

Figure 3.4: Sequence of the adaptively generated meshes and deformed geometries (value of the displacement is multiplied by 10^4)

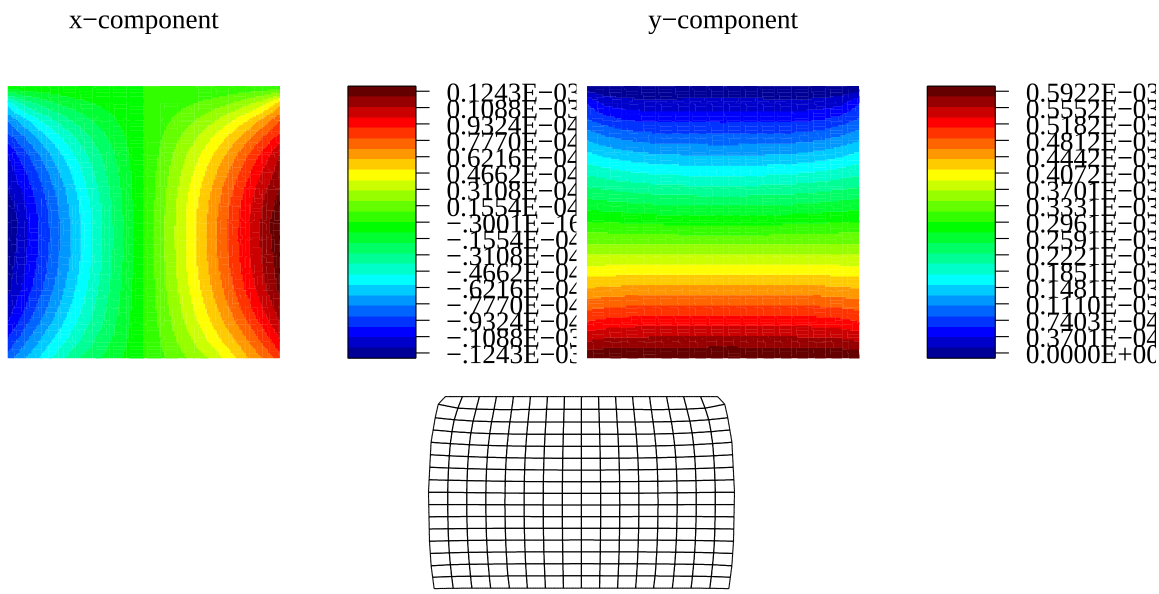

Figure 3.5: x- and y-components of the displacement inside the body and deformation of the auxiliary FE-grid after 6^{th} refinement step, obtained with the representation formula (1.2)

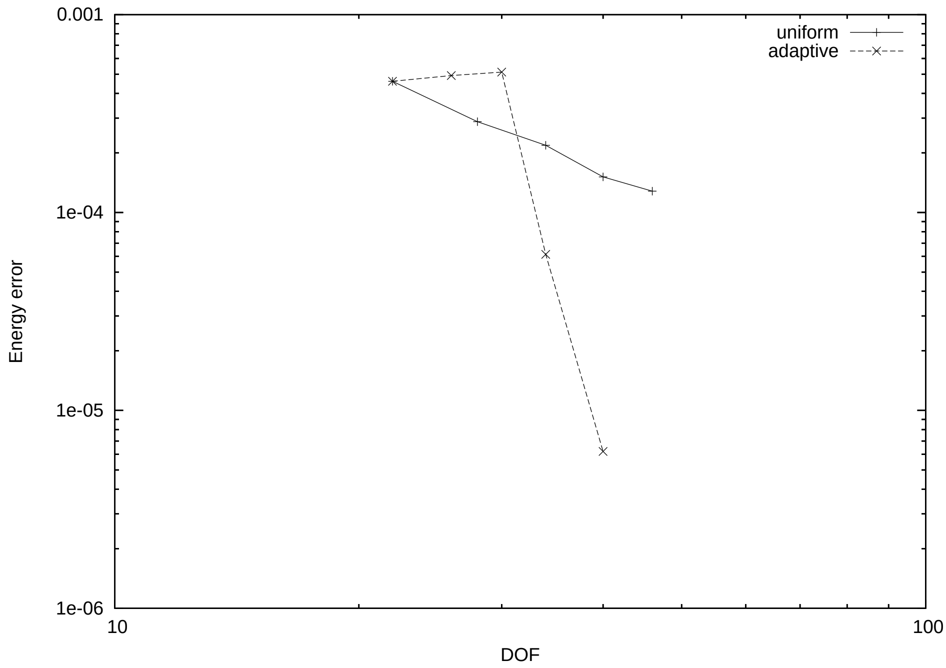

Figure 3.6: $err(\boldsymbol{U}) := \left| |||\boldsymbol{U}|||_B - |||\boldsymbol{U}_{190}|||_B \right|$ for uniform and adaptive refinement

As it can be seen from Fig. 3.6, the adaptive refinement procedure provides a better results than the uniform refinement with the same number of the degrees of freedom.

Example 2

In the second example we consider the same geometry and material parameters for the body Ω as in the Example 1, but change configuration and location of the obstacle. The obstacle now is given by $\gamma := \{-1 + d\} \times [-1/2, 1/2]$ and the displacement increment $d := 6 \cdot 10^{-4}$ brings the obstacle in contact with the body Ω.

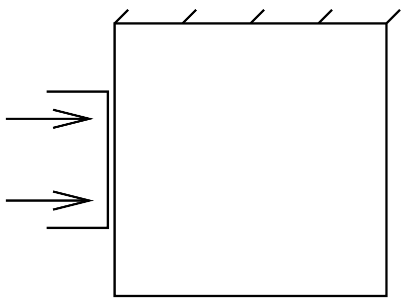

Figure 3.7: Contact geometry of Example 2

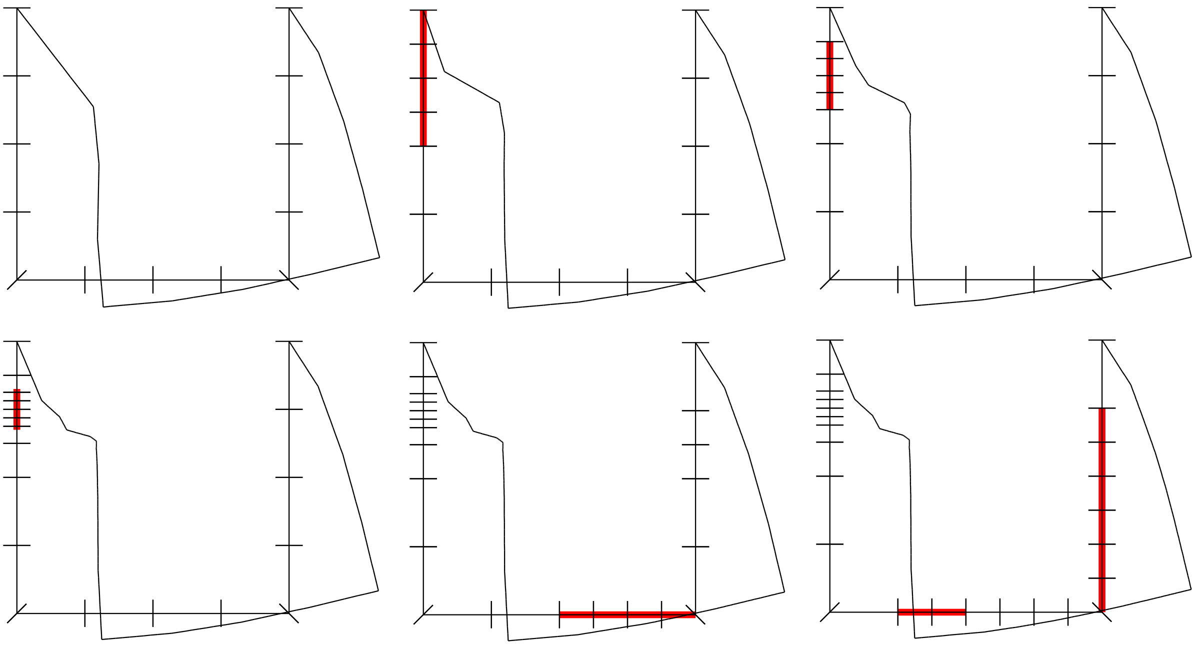

Figure 3.8: Sequence of the adaptively generated meshes and deformed geometries (value of the displacement is multiplied by 10^4)

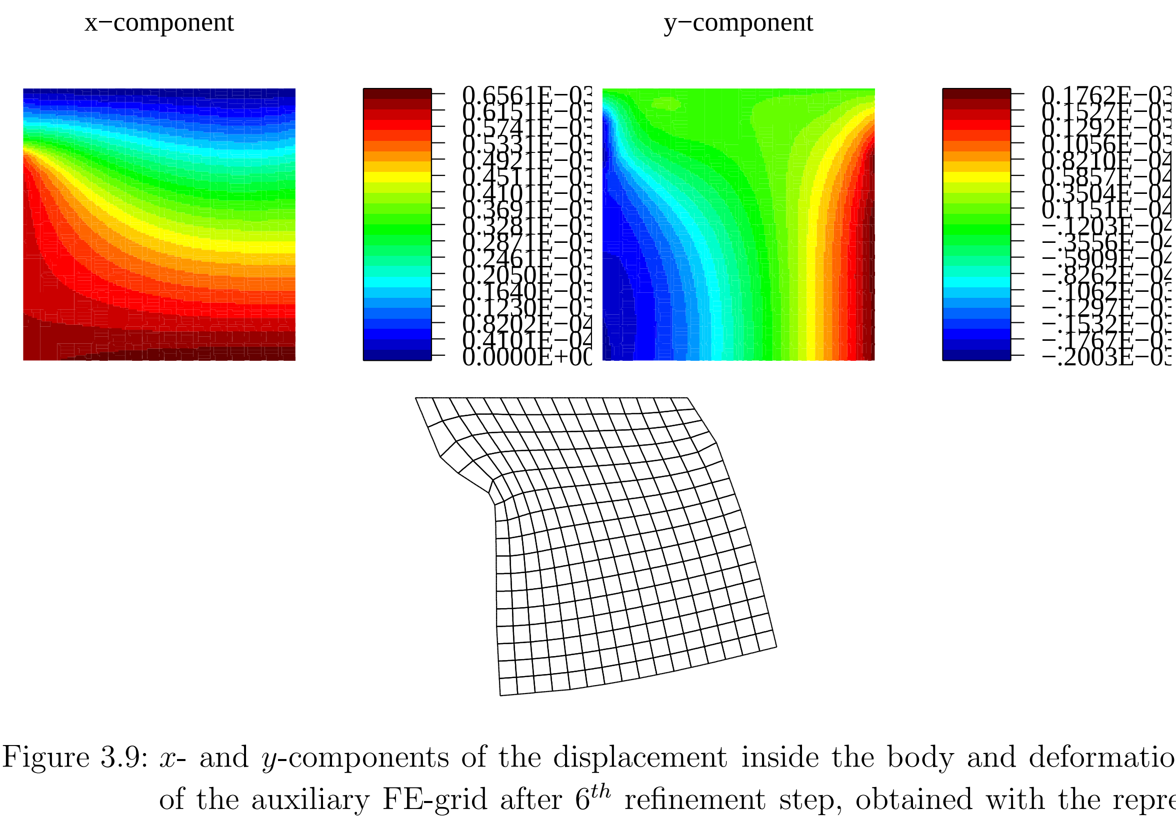

Figure 3.9: x- and y-components of the displacement inside the body and deformation of the auxiliary FE-grid after 6^{th} refinement step, obtained with the representation formula (1.2)

The initial mesh of four elements per side of Ω (Fig. 3.3) is employed again. The same refinement strategy as in Example 1 is applied, i.e. elements which indicators are larger than 90% of the maximal indicator are refined. The sequence of adaptively generated meshes is presented in Fig. 3.8. In the beginning of the refinement process we observe that most of refinement happens near the point $(-1, 1/2)$, which is caused by the large gradients of the boundary traction. On the contrary, we do not observe any refinement near the point $(-1, -1/2)$, since the boundary traction changes there not as sharp. Following the refinement process, we observe, that after four refinement steps the error near $(-1, 1/2)$ is sufficiently reduced, and the indicators near the point $(1, -1)$ provide the largest contribution.

4 Nonconforming methods for two-body contact problems with friction

This chapter is devoted to the investigation of nonconforming methods for two-body contact problems with friction. Often, it turns out that the one-body frictional contact description is not sufficient for simulation of the realistic industrial processes. For example, deformation of the tool often cannot be neglected in simulation of the stamping process. This motivates developing of a two-body frictional contact description. The independent discretization of contacting bodies is usually very convenient, e.g. it simplifies the task of global mesh generation and allows to perform an independent mesh refinement procedure. Furthermore, in many cases, e.g. for large deformation or sliding boundaries, it is the only way to avoid a time-consuming remeshing procedure. Below, we consider two different methods allowing to handle nonmatching discretizations for two-body contact problems with friction: the penalty and the mortar methods.

First, the standard classical and weak formulations for two-body contact problems with friction are briefly recalled. Then we consider the h-version of the penalty FE/BE and BE/BE coupling methods for elastoplastic two-body contact problems with Coulomb's law of friction. The suggested solution procedure as well as derivation of the linearized formulation are described in detail. The methods are demonstrated in several numerical examples.

Then, a new hp-mortar boundary element method is constructed for two-body contact problems with Tresca's law of friction in linear elasticity. We prove under mild regularity assumptions that the method converges as $\mathcal{O}((h/p)^{1/4})$, provided by suitable restrictions on the discretization parameters. We solve the discrete problem employing a Dirichlet-to-Neumann algorithm and an Uzawa algorithm. Furthermore, we perform an automatic mesh refinement procedure with the three-step hp-refinement algorithm (see e.g. Maischak and Stephan [47]), based on a heuristically motivated error indicator. Finally, the h-version of the suggested approach is generalized onto elastoplastic two-body frictional contact problems. The series of numerical examples underlines the proposed approach.

4.1 Classical and weak formulation for two-body contact problems with friction

Let Ω^1, Ω^2 be bounded two-dimensional polygonal domains with (Lipschitz) boundaries Γ^1, Γ^2. Let Γ^i, $i = 1, 2$, be decomposed into three disjoint parts Γ^i_D, Γ^i_N and Γ^i_C. Denote for brevity $\Sigma^i := \Gamma^i_N \cup \Gamma_C$, $\Omega := \Omega^1 \cup \Omega^2$, $\Gamma := \Gamma^1 \cup \Gamma^2$, $\Gamma_D := \Gamma^1_D \cup \Gamma^2_D$, $\Gamma_N := \Gamma^1_N \cup \Gamma^2_N$. We assume that the displacement $\hat{\boldsymbol{u}}$ is known along Γ_D, that the boundary traction $\hat{\boldsymbol{t}}$ is prescribed along Γ_N and $\Gamma^i_C, i = 1, 2$ are the boundary parts, where the contact can occur. We denote with $\boldsymbol{f}$ the volume forces acting inside the bodies. Then the classical formulation of the problem is given by

$$\begin{aligned} \operatorname{div} \sigma(\boldsymbol{u}) &= \boldsymbol{f} && \text{in } \Omega, \\ \boldsymbol{u} &= \hat{\boldsymbol{u}} && \text{on } \Gamma_D, \\ \sigma(\boldsymbol{u}) \cdot \boldsymbol{n} &= \hat{\boldsymbol{t}} && \text{on } \Gamma_N, \\ \left.\begin{array}{c} \sigma_n \leq 0, \quad [u_n] \leq g, \quad \sigma_n([u_n] - g) = 0, \\ |\sigma_t| \leq \mathcal{F}, \quad \sigma_t[u_t] + \mathcal{F}|[u_t]| = 0, \end{array}\right\} & && \text{on } \Gamma_C. \end{aligned} \tag{4.1}$$

Here σ stands for the stress tensor. Its dependence on the displacement field $\boldsymbol{u}$ is given by Hook's law of elasticity, i.e. under small strain assumption there holds

$$\sigma(\boldsymbol{u}) = \mathbb{C} : \varepsilon(\boldsymbol{u}) := \overline{\lambda} \mathrm{tr} \varepsilon(\boldsymbol{u}) + 2\overline{\mu}\varepsilon(\boldsymbol{u}), \qquad \varepsilon(\boldsymbol{u}) = \frac{1}{2}(\nabla \boldsymbol{u} + \nabla \boldsymbol{u}^T),$$

where $\overline{\lambda}$, $\overline{\mu}$ are the Lamé constants. Let $\boldsymbol{n}^i$, $\boldsymbol{t}^i$ denote the outer normal and tangential unit vectors to Γ^i and introduce

$$\boldsymbol{n} := \begin{cases} \boldsymbol{n}^1, & \text{on } \Gamma^1, \\ \boldsymbol{n}^2, & \text{on } \Gamma^2 \setminus \Gamma_C, \end{cases} \qquad \boldsymbol{t} := \begin{cases} \boldsymbol{t}^1, & \text{on } \Gamma^1, \\ \boldsymbol{t}^2, & \text{on } \Gamma^2 \setminus \Gamma_C. \end{cases}$$

The stress on the contact boundary is given by

$$\begin{aligned} \sigma_n &= \boldsymbol{n}^1 \cdot \sigma(\boldsymbol{u}^1) \cdot \boldsymbol{n}^1 = \boldsymbol{n}^2 \cdot \sigma(\boldsymbol{u}^2) \cdot \boldsymbol{n}^2, \\ \sigma_t \boldsymbol{t}^1 &= \sigma(\boldsymbol{u}^1) \cdot \boldsymbol{n}^1 - \sigma_n \boldsymbol{n}^1 = -(\sigma(\boldsymbol{u}^2) \cdot \boldsymbol{n}^2 - \sigma_n \boldsymbol{n}^2). \end{aligned}$$

We assume that there is a mapping between Γ^1_C and Γ^2_C, e.g. orthogonal projection of points of Γ^2_C onto Γ^1_C modified near the corners, which allows to identify Γ^1_C with Γ^2_C. We denote the "generalized" contact boundary by Γ_C. We write $[\cdot]$ for the jump of the normal displacement $u^i_n := \boldsymbol{u}^i \cdot \boldsymbol{n}$ and the tangential displacement $u^i_t := \boldsymbol{u}^i \cdot \boldsymbol{t}$ across Γ_C, namely

$$\begin{aligned} [u_n] &:= u^1_n - u^2_n \equiv \boldsymbol{u}^1 \cdot \boldsymbol{n}^1 + \boldsymbol{u}^2 \cdot \boldsymbol{n}^2, \\ [u_t] &:= u^1_t - u^2_t \equiv \boldsymbol{u}^1 \cdot \boldsymbol{t}^1 + \boldsymbol{u}^2 \cdot \boldsymbol{t}^2. \end{aligned}$$

The function $g : \Gamma_C \subset \mathbb{R}^2 \to \mathbb{R}_{\geq 0}$ is the initial distance between two bodies in normal direction, [32]. Thus $[u_n] \leq g$ has the meaning of the nonpenetration condition. The so-called given friction function $\mathcal{F} \geq 0$ defines pointwise the sticking threshold of the bodies, i.e. as it can be seen from (4.1), if the absolute value of the tangential stress does not exceed the given friction $|\sigma_t| < \mathcal{F}$, then $[u_t] = 0$ and $[u_t] \neq 0$ is only possible if $|\sigma_t| = \mathcal{F}$. In the more general case of Coulomb's friction law the given friction function is defined to be proportional to the normal stress $\mathcal{F} := \mu_f \sigma_n$, where μ_f is the friction coefficient, see e.g. Wriggers [72]. In order to derive a weak formulation for (4.1) we assume that $\hat{\boldsymbol{u}} \in \boldsymbol{H}^{1/2}(\Gamma_D)$, $\hat{\boldsymbol{t}} \in \tilde{\boldsymbol{H}}^{-1/2}(\Gamma_N)$, $\mathcal{F} \in L_2(\Gamma_C)$.

Further we will use the functional spaces and sets, defined as follows

$$\boldsymbol{\mathcal{V}}^i := \tilde{\boldsymbol{H}}^{1/2}(\Sigma^i), \qquad \boldsymbol{\mathcal{V}} := \boldsymbol{\mathcal{V}}^1 \times \boldsymbol{\mathcal{V}}^2, \tag{4.2}$$

$$\boldsymbol{\mathcal{W}}^i := \boldsymbol{H}^{-1/2}(\Gamma^i), \qquad \boldsymbol{\mathcal{W}} := \boldsymbol{\mathcal{W}}^1 \times \boldsymbol{\mathcal{W}}^2, \tag{4.3}$$

$$\boldsymbol{\mathcal{V}}_F^i := \left\{\boldsymbol{v} \in \boldsymbol{H}^1(\Omega^i) : \boldsymbol{v} = 0 \text{ on } \Gamma_D^i\right\}, \qquad \tilde{\boldsymbol{\mathcal{V}}} := \boldsymbol{\mathcal{V}}_F^1 \times \boldsymbol{\mathcal{V}}^2, \tag{4.4}$$

$$\boldsymbol{\mathcal{K}} := \left\{\boldsymbol{u} = (\boldsymbol{u}^1, \boldsymbol{u}^2) \in \boldsymbol{\mathcal{V}} : [u_n] \leq g \text{ on } \Gamma_C\right\}, \tag{4.5}$$

$$\tilde{\boldsymbol{\mathcal{K}}} := \left\{\boldsymbol{u} = (\boldsymbol{u}^1, \boldsymbol{u}^2) \in \tilde{\boldsymbol{\mathcal{V}}} : [u_n] \leq g \text{ on } \Gamma_C\right\} \tag{4.6}$$

and the spaces including the nonhomogeneous Dirichlet boundary conditions

$$\boldsymbol{\mathcal{V}}_D^i := \left\{\boldsymbol{v} \in \boldsymbol{H}^{1/2}(\Gamma^i) : \boldsymbol{v} = \hat{\boldsymbol{u}} \text{ on } \Gamma_D^i\right\}, \qquad \boldsymbol{\mathcal{V}}_D := \boldsymbol{\mathcal{V}}_D^1 \times \boldsymbol{\mathcal{V}}_D^2, \tag{4.7}$$

$$\boldsymbol{\mathcal{V}}_{F,D}^i := \left\{\boldsymbol{v} \in \boldsymbol{H}^1(\Omega^i) : \boldsymbol{v} = \hat{\boldsymbol{u}} \text{ on } \Gamma_D^i\right\}, \qquad \tilde{\boldsymbol{\mathcal{V}}}_D := \boldsymbol{\mathcal{V}}_{F,D}^1 \times \boldsymbol{\mathcal{V}}_D^2, \tag{4.8}$$

$$\boldsymbol{\mathcal{K}}_D := \left\{\boldsymbol{u} = (\boldsymbol{u}^1, \boldsymbol{u}^2) \in \boldsymbol{\mathcal{V}}_D : [u_n] \leq g \text{ on } \Gamma_C\right\}, \tag{4.9}$$

$$\tilde{\boldsymbol{\mathcal{K}}}_D := \left\{\boldsymbol{u} = (\boldsymbol{u}^1, \boldsymbol{u}^2) \in \tilde{\boldsymbol{\mathcal{V}}}_D : [u_n] \leq g \text{ on } \Gamma_C\right\}. \tag{4.10}$$

We introduce the Steklov-Poincaré operator

$$S = W + (K' + 1/2)V^{-1}(K + 1/2), \tag{4.11}$$

which is a continuous, positive definite mapping $S : \boldsymbol{\mathcal{V}} \to \boldsymbol{\mathcal{W}}$, see Lemma 1.3.1. Let the linear functionals be defined by

$$L(\boldsymbol{v}) := \langle N\boldsymbol{f}, \boldsymbol{v}\rangle_\Sigma + \left\langle \hat{\boldsymbol{t}}, \boldsymbol{v}\right\rangle_{\Gamma_N}, \qquad \forall \boldsymbol{v} \in \boldsymbol{\mathcal{V}},$$

$$\tilde{L}(\boldsymbol{v}) := (\boldsymbol{f}, \boldsymbol{v})_{\Omega^1} + \langle N\boldsymbol{f}, \boldsymbol{v}\rangle_{\Sigma^2} + \left\langle \hat{\boldsymbol{t}}, \boldsymbol{v}\right\rangle_{\Gamma_N}, \qquad \forall \boldsymbol{v} \in \tilde{\boldsymbol{\mathcal{V}}},$$

there N is the Newton potential, defined in (1.7).

Variational inequality

Similarly to the analysis of Section 3.1 for the one-body problem, it can be shown that the classical two-body problem (4.1) can be reformulated as a boundary variational inequality of the second kind. In particular, for $\hat{\boldsymbol{u}} = 0$ it reads: Find $\boldsymbol{u} \in \boldsymbol{\mathcal{K}}$:

$$\langle S\boldsymbol{u}, \boldsymbol{v} - \boldsymbol{u}\rangle_\Sigma + j([\boldsymbol{v}]) - j([\boldsymbol{u}]) \geq L(\boldsymbol{v} - \boldsymbol{u}) \qquad \forall \boldsymbol{v} \in \boldsymbol{\mathcal{K}}, \tag{4.12}$$

where the friction functional is given by

$$j([\boldsymbol{v}]) := \int_{\Gamma_C} \mathcal{F}|[v_t]|\,ds.$$

Similarly to Section 3.1 one can prove that the problem with given friction has a unique solution for sufficiently smooth given friction function $\mathcal{F}$. In the case of Coulomb's frictional law, then $\mathcal{F} := \mu_f \sigma_n$, applying ideas of Nečas, Jarušek and Haslinger [51] for the domain formulation, it can be shown that the problem has a unique solution if the coefficient of friction μ_f is small enough.

Saddle point formulation

Following the approach of Haslinger, Hlaváček and Nečas [33] based on the domain formulation, it is possible to obtain a saddle point formulation, equivalent to (4.12). We define the sets of normal and tangential Lagrange multipliers as follows

$$\begin{gathered} M_n := \left\{ q \in \tilde{H}^{-1/2}(\Gamma_C) : \langle q, v\rangle_{\Gamma_C} \geq 0, \forall v \in H^{1/2}(\Gamma_C), v \geq 0 \text{ a.e. on } \Gamma_C \right\}, \\ M_t := \{ q \in L_2(\Gamma_C) : |q| \leq \mathcal{F} \text{ a.e. on } \Gamma_C \}, \\ \boldsymbol{\mathcal{M}} := M_n \times M_t. \end{gathered} \tag{4.13}$$

The classical formulation (4.1) with $\hat{\boldsymbol{u}} = 0$ can be rewritten in a weak sense as a saddle point problem of finding $\boldsymbol{u} \in \boldsymbol{\mathcal{V}}, \boldsymbol{p} \in \boldsymbol{\mathcal{M}}$ such that

$$\begin{aligned} &\langle S\boldsymbol{u}, \boldsymbol{v}\rangle_\Sigma + b(\boldsymbol{p}, \boldsymbol{v}) = \langle \hat{\boldsymbol{t}}, \boldsymbol{v}\rangle_{\Gamma_N}, && \forall \boldsymbol{v} \in \boldsymbol{\mathcal{V}}, \\ &b(\boldsymbol{q} - \boldsymbol{p}, \boldsymbol{u}) \leq 0, && \forall \boldsymbol{q} \in \boldsymbol{\mathcal{M}}. \end{aligned} \tag{4.14}$$

with the functional $b(\boldsymbol{q}, \boldsymbol{v}) := \langle q_n, [v_n]\rangle_{\Gamma_C} + \langle q_t, [v_t]\rangle_{\Gamma_C}$ and the bilinear form generated by the Steklov-Poincaré operator S. It follows from (4.14) that $\boldsymbol{p} = -\sigma(\boldsymbol{u}^1)\cdot \boldsymbol{n}^1$ in a weak sense.

Penalty weak formulation

Both the variational inequality (4.12) and the saddle point formulation (4.14) include an inequality restriction in the set of admissible displacements or in the set of contact tractions. This makes the theoretical analysis and the implementation relatively complicated. Therefore the corresponding penalty formulation is often used. The weak penalty boundary formulation for the two-body problem with (possibly) nonhomogeneous Dirichlet boundary conditions is given by: Find $\boldsymbol{u}^\varepsilon \in \boldsymbol{\mathcal{V}}_D$ such that

$$\langle S\boldsymbol{u}^\varepsilon, \boldsymbol{v}\rangle_\Sigma - \langle \boldsymbol{p}^\varepsilon, [\boldsymbol{v}]\rangle_{\Gamma_C} = L(\boldsymbol{v}), \qquad \forall \boldsymbol{v} \in \boldsymbol{\mathcal{V}}, \tag{4.15}$$

where the contact traction is given by the constitutive relations (cf. (3.90))

$$\boldsymbol{p}^\varepsilon := p_n^\varepsilon \boldsymbol{n} + p_t^\varepsilon \boldsymbol{t}, \quad p_n^\varepsilon := -\frac{1}{\varepsilon_n}([u_n^\varepsilon] - g)^+, \quad p_t^\varepsilon := -\frac{1}{\varepsilon_t}\mathcal{F}[u_t^\varepsilon]^*, \qquad \mathcal{F} := \mu_f p_n^\varepsilon, \tag{4.16}$$

where the functions $(\cdot)^+$ and $(\cdot)^*$ are given by (3.91) and (3.89) respectively. The corresponding FE/BE coupling formulation, where finite elements are used in Ω^1 and boundary elements are used on Γ^2, reads as follows: Find $\boldsymbol{u}^\varepsilon \in \tilde{\boldsymbol{\mathcal{V}}}_D$ such that

$$(\sigma(\boldsymbol{u}^\varepsilon), \varepsilon(\boldsymbol{v}))_{\Omega^1} + \langle S\boldsymbol{u}^\varepsilon, \boldsymbol{v}\rangle_{\Sigma^2} - \langle \boldsymbol{p}^\varepsilon, [\boldsymbol{v}]\rangle_{\Gamma_C} = \tilde{L}(\boldsymbol{v}), \qquad \forall \boldsymbol{v} \in \tilde{\boldsymbol{\mathcal{V}}}, \tag{4.17}$$

Further down, if it is clear that the penalty method is considered, we will omit the upper index $^\varepsilon$ for brevity.

4.2 h-version of the penalty method

In this section we consider the h-version of penalty FE/BE coupling and pure BE methods on nonmatching meshes for elastoplastic frictional contact. The incremental loading procedure combined with the Newton's method and return mapping algorithm is applied to solve the problem. Note, that the frictional contact and the plastic subproblems are solved within one and the same Newton cycle. An implicit Euler scheme for both plasticity and frictional contact is applied in case of FE/BE coupling. In the pure BEM case, an explicit Euler scheme for plasticity and an implicit scheme for frictional contact are employed. Linearization of normal, tangential contact terms and of plasticity terms are presented in detail. The a posteriori error estimate for one-body frictional contact, derived in Chapter 3, is extended to the two-body case. The above methods are demonstrated with a number of numerical examples.

4.2.1 Constitutive relations for contact with friction

The contact conditions in the penalty approach are formulated with help of the so-called master-slave description, see e.g. Wriggers [72]. Without loss of generality we will refer to Ω^1 as to the master body and to Ω^2 as to the slave body. In this paragraph we will also use the upper indexes $(\cdot)^m$, $(\cdot)^s$ instead of $(\cdot)^1$, $(\cdot)^2$ for the values connected with Ω^1 and Ω^2 respectively.

Penetration and relative displacement

For every point from the slave side $\boldsymbol{x}^s \in \Gamma_C^s$ we can find the closest point on the master side $\hat{\boldsymbol{x}}^m(\overline{\xi}) \in \Gamma_C^m$. The bar over $\overline{\xi}$ denotes that the value of the parameter ξ is determined by $\boldsymbol{x}^s$. We define a penetration function g_n on the slave surface Γ_C^s by

$$\mathrm{g}_n := \begin{cases} \|\hat{\boldsymbol{x}}^m(\overline{\xi}) - \boldsymbol{x}^s\| = (\hat{\boldsymbol{x}}^m(\overline{\xi}) - \boldsymbol{x}^s) \cdot \overline{\boldsymbol{n}}^m, & \text{if } (\hat{\boldsymbol{x}}^m(\overline{\xi}) - \boldsymbol{x}^s) \cdot \overline{\boldsymbol{n}}^m > 0, \\ 0, & \text{if } (\hat{\boldsymbol{x}}^m(\overline{\xi}) - \boldsymbol{x}^s) \cdot \overline{\boldsymbol{n}}^m \leq 0. \end{cases}$$

Here $||\cdot||$ stands for the Euclidean norm, i.e. $||\boldsymbol{a}|| := \sqrt{\boldsymbol{a} \cdot \boldsymbol{a}}$ for some vector $\boldsymbol{a} \in \mathbb{R}^d$; and $\overline{\xi}$ is the minimizer of the distance function

$$\hat{d}(\xi) := \|\hat{\boldsymbol{x}}^m(\xi) - \boldsymbol{x}^s\| \longrightarrow \text{ MIN over all } \xi$$

for a given slave point $\boldsymbol{x}^s$. The value $\overline{\xi}$ can be obtained by the necessary condition

$$\frac{\mathrm{d}}{\mathrm{d}\xi}\hat{d}(\xi) = \frac{\hat{\boldsymbol{x}}^m(\xi) - \boldsymbol{x}^s}{\|\hat{\boldsymbol{x}}^m(\xi) - \boldsymbol{x}^s\|} \cdot \hat{\boldsymbol{x}}^m_{,\xi}(\xi) = 0. \tag{4.18}$$

The tangential vector to the master surface in point ξ can be represented as $\boldsymbol{a}^m := \boldsymbol{x}^m_{,\xi}(\xi)$. Therefore (4.18) means that $\overline{\xi}$ is defined by the condition

$$\boldsymbol{n}^m = \frac{\hat{\boldsymbol{x}}^m(\overline{\xi}) - \boldsymbol{x}^s}{\left\|\hat{\boldsymbol{x}}^m(\overline{\xi}) - \boldsymbol{x}^s\right\|},$$

or, in other words, it means that $\hat{\boldsymbol{x}}^m(\overline{\xi})$ is the orthogonal projection of $\boldsymbol{x}^s$ onto the master side Γ^m_C. Of course, on the non-smooth boundaries the normal and tangential vectors are not defined in the corner points. In this case some modification is performed, as it is described e.g. in Wriggers [72].

Let us define the relative tangential displacement $\mathbf{g}_t$ of some slave point $\boldsymbol{x}^s$ at some time step with respect to the previous one by

$$\mathbf{g}_t = [u_t]\, \boldsymbol{a}^m.$$

We will also write $\mathrm{g}_t = [u_t] \equiv |\mathbf{g}_t|$ for its absolute value.

Micromechanical constitutive relations: normal and tangential contact traction

The contact stress is determined by the penetration function g_n and the relative displacement $\mathbf{g}_t$. The normal stress p^ε_n in point $\boldsymbol{x}^s$ is given by

$$p^\varepsilon_n(\boldsymbol{x}^s) := -\frac{1}{\varepsilon_n}\mathrm{g}_n(\boldsymbol{x}^s). \tag{4.19}$$

Here ${\varepsilon_n}^{-1}$ is the normal stiffness or penalty factor (see [72], [54]). With standard arguments of elastoplastic theory of friction (see e.g. [52]), we use an additive decomposition of the relative tangential velocity into an adherence ("elastic", describing stick behaviour) and slip ("plastic", responsible for frictional slip) part

$$\mathbf{g}_t = \mathbf{g}^e_t + \mathbf{g}^p_t.$$

The tangential contact traction is set to be proportional to the "elastic" component

$$\boldsymbol{p}^\varepsilon_t = -\frac{1}{\varepsilon_t}\mathbf{g}^e_t, \tag{4.20}$$

where ${\varepsilon_t}^{-1}$ is the tangential contact stiffness. It remains to define, how to compute $\mathbf{g}^p_t$ from known $\mathbf{g}_t$, to obtain a closed formulation. Let us consider the yield domain

$$\mathbb{E} := \left\{ \boldsymbol{p}^\varepsilon_t \in \mathbb{R}^{d-1} \middle| \, \hat{f}_{fr}(\boldsymbol{p}^\varepsilon_t) \leqslant 0 \right\}$$

in the space of the contact tangential stress with the the yield function

$$\hat{f}_{fr}(\boldsymbol{p}^\varepsilon_t) = \|\boldsymbol{p}^\varepsilon_t\| - \mathcal{F}, \qquad \mathcal{F} := \mu_f |p^\varepsilon_n|,$$

representing the slip criterion function for a given contact pressure p_n^ε with friction coefficient μ_f due to Coulomb's law of friction. We define

$$\mathbf{g}_t^p = \begin{cases} 0, & \text{if } \hat{f}_{fr} \leq 0, \\ \left(1 - \dfrac{\mathcal{F}}{\|\mathbf{g}_t/\varepsilon_t\|}\right)\mathbf{g}_T, & \text{if } \hat{f}_{fr} > 0. \end{cases}$$

Therefore $\mathbf{g}_T^p = 0$ yields $\boldsymbol{p}_t^\varepsilon \in \overline{\mathbb{E}}$ and the point sticks; on the other hand, $\mathbf{g}_T^p \neq 0$ yields $\boldsymbol{p}_t^\varepsilon \in \partial\mathbb{E}$, which means that the point slips.

Remark 4.2.1. *The constitutive relation for tangential stress is simply an algorithmic description of that defined in (4.16). Basic computations show that (4.20) is identical with (4.16), if the modified penalty parameter $\varepsilon_t = \varepsilon_t\mathcal{F}$ is used in (4.16).*

4.2.2 Constitutive relations for plasticity: J_2 flow theory with isotropic / kinematic hardening

In this paragraph we make an extension of the pure elastic two-body frictional contact problem, described in (4.1), to the more general case of an elastoplastic two-body frictional contact problem. We employ an additive decomposition of the strain tensor into elastic and plastic part $\varepsilon(\boldsymbol{u}) = \varepsilon^e(\boldsymbol{u}) + \varepsilon^p(\boldsymbol{u})$. The material law is given by the Hook's tensor, connecting the stress tensor and the elastic part of the strain tensor

$$\sigma = \mathbb{C} : \varepsilon^e = \mathbb{C} : (\varepsilon - \varepsilon^p).$$

The plastic strain ε^p is computed using the classical J_2 flow theory with isotropic/kinematic hardening, described e.g. by Simo and Hughes [60, 2.3.2]. The J_2 flow theory is based on two material parameters. The equivalent plastic strain α represents isotropic hardening of the von Mises yield surface. The deviatoric tensor $\bar{\beta}$ corresponds to the center of the von Mises yield surface. We use the J_2-plasticity model with the following yield condition, flow rule and hardening law.

$$\begin{aligned}
\eta &:= \operatorname{dev}[\sigma] - \bar{\beta}, \qquad \operatorname{tr}[\bar{\beta}] := 0, \\
\hat{f}_{pl}(\sigma, \alpha, \bar{\beta}) &= ||\eta|| - \sqrt{\frac{2}{3}}K(\alpha), \\
n &:= \frac{\eta}{||\eta||} \\
\dot{\varepsilon}^p &= \gamma n, \\
\dot{\bar{\beta}} &= \gamma \frac{2}{3} H'(\alpha) n, \\
\dot{\alpha} &= \gamma \sqrt{\frac{2}{3}},
\end{aligned} \tag{4.21}$$

where $\hat{f}_{pl}$ is the yield function for plasticity, $K(\alpha)$, $H(\alpha)$ are isotropic and kinematic hardening modules, given by

$$\begin{aligned} H'(\alpha) &= (1-\theta)\bar{H}, \\ K(\alpha) &= \sigma_Y + \theta\bar{H}\alpha, \qquad \theta \in [0,1], \end{aligned} \tag{4.22}$$

where $\sigma_Y, \bar{H} \geq 0$ are material constants and σ_Y is the yield stress. The von Mises yield surface is given by the yield condition

$$\hat{f}_{pl}(\sigma, \alpha, \bar{\beta}) \leq 0.$$

The loading/unloading complimentary Kuhn-Tucker conditions are given by

$$\gamma \geq 0, \qquad \hat{f}_{pl}(\sigma, \alpha, \bar{\beta}) \leq 0, \qquad \gamma \hat{f}_{pl}(\sigma, \alpha, \bar{\beta}) = 0.$$

It is easy to check [60, 2.2.18], that the consistency parameter γ is given by

$$\gamma = \frac{(n:\varepsilon)^+}{1 + \frac{K'+H'}{2\overline{\mu}}}.$$

Here $u^+ := (u + |u|)/2$ is the positive part function. Finally, we define the elastoplastic tangent moduli $\mathbb{C}^{ep}$ with the following relation

$$\begin{aligned} \dot{\sigma} &= \mathbb{C} : (\dot{\varepsilon} - \dot{\varepsilon}^p) = \mathbb{C}^{ep} : \dot{\varepsilon}, \\ \mathbb{C} &= \kappa \mathbf{1} \otimes \mathbf{1} + 2\overline{\mu} \left(\boldsymbol{I} - \frac{1}{3} \mathbf{1} \otimes \mathbf{1} \right). \end{aligned}$$

Therefore

$$\mathbb{C}^{ep} = \kappa \mathbf{1} \otimes \mathbf{1} + 2\overline{\mu} \left(\boldsymbol{I} - \frac{1}{3} \mathbf{1} \otimes \mathbf{1} - \frac{n \otimes n}{1 + \frac{K'+H'}{3\overline{\mu}}} \right),$$

where

$$\mathbf{1} = \delta_{ij} \boldsymbol{e}_i \otimes \boldsymbol{e}_j, \qquad \boldsymbol{I} = 1/2(\delta_{ik}\delta_{jl} + \delta_{il}\delta_{jk}) \boldsymbol{e}_i \otimes \boldsymbol{e}_j \otimes \boldsymbol{e}_k \otimes \boldsymbol{e}_l$$

are second order and fourth order identity tensors respectively and $\kappa := \overline{\lambda} + 2\overline{\mu}/3$ is the bulk modulus and $\overline{\lambda}, \overline{\mu}$ are Lame constants. Note that

$$\mathbb{C} : \varepsilon = \overline{\lambda} \operatorname{tr}[\varepsilon] + 2\overline{\mu}\varepsilon = \kappa \operatorname{tr}[\varepsilon] + 2\overline{\mu} \operatorname{dev}[\varepsilon]. \tag{4.23}$$

4.2.3 FE/BE coupling for elastoplastic contact problems with friction

In this paragraph we consider a frictional contact problem between an elastic body and an elastoplastic body. We employ boundary element discretization for the elastic domain and finite elements in the elastoplastic domain. Without loss of generality we denote the elastic body as a slave body and the elastoplastic body as a master one.

Let $\mathcal{T}^m_{F,h}$ be some partition of the finite element domain Ω^m into triangles or quadrilaterals, and $\mathcal{T}^s_h$ be some partition of the boundary Γ^s into straight line segments. Define discrete spaces

$$\begin{aligned}
\boldsymbol{\mathcal{V}}^m_{F,D,h} &:= \left\{ \boldsymbol{\Phi} \in \boldsymbol{H}^1(\Omega^m) : \boldsymbol{\Phi}|_K \in \left[\mathcal{R}_1(K)\right]^2 \ \forall K \in \mathcal{T}^m_{F,h},\ \boldsymbol{\Phi}|_{\Gamma_D} = \hat{\boldsymbol{u}}^m \right\},\\
\boldsymbol{\mathcal{V}}^m_{F,h} &:= \left\{ \boldsymbol{\Phi} \in \boldsymbol{H}^1(\Omega^m) : \boldsymbol{\Phi}|_K \in \left[\mathcal{R}_1(K)\right]^2 \ \forall K \in \mathcal{T}^m_{F,h},\ \boldsymbol{\Phi}|_{\Gamma_D} = 0 \right\},\\
\boldsymbol{\mathcal{V}}^s_{D,h} &:= \left\{ \boldsymbol{\Phi} \in \boldsymbol{H}^{1/2}(\Gamma^s) : \boldsymbol{\Phi}|_I \in \left[\mathcal{P}_1(I)\right]^2 \ \forall I \in \mathcal{T}^s_h,\ \boldsymbol{\Phi}|_{\Gamma_D} = \hat{\boldsymbol{u}}^s \right\},\\
\boldsymbol{\mathcal{V}}^s_h &:= \left\{ \boldsymbol{\Phi} \in \tilde{\boldsymbol{H}}^{1/2}(\Sigma^s) : \boldsymbol{\Phi}|_I \in \left[\mathcal{P}_1(I)\right]^2 \ \forall I \in \mathcal{T}^s_h \right\},\\
\tilde{\boldsymbol{\mathcal{V}}}_{D,h} &:= \boldsymbol{\mathcal{V}}^m_{F,D,h} \times \boldsymbol{\mathcal{V}}^s_{D,h}, \qquad \tilde{\boldsymbol{\mathcal{V}}}_h := \boldsymbol{\mathcal{V}}^m_{F,h} \times \boldsymbol{\mathcal{V}}^s_h,
\end{aligned}$$

where $\mathcal{R}_1(K)$ corresponds to the space of linear functions $\mathcal{P}_1(K)$, if K is a triangle, and corresponds to the space of bilinear functions $\mathcal{Q}_1(K)$, if K is a quadrilateral. The discretized weak formulation corresponding to (4.17) consists of finding $\boldsymbol{U} = (\boldsymbol{U}^s, \boldsymbol{U}^m) \in \tilde{\boldsymbol{\mathcal{V}}}_{D,h}$:

$$\tilde{F}^{int}(\boldsymbol{U}, \boldsymbol{\Phi}) = \tilde{F}^{ext}(\boldsymbol{\Phi}) \qquad \forall \boldsymbol{\Phi} \in \tilde{\boldsymbol{\mathcal{V}}}_h, \tag{4.24}$$

where

$$\begin{aligned}
\tilde{F}^{int}(\boldsymbol{U}, \boldsymbol{\Phi}) &:= (\sigma^m, \varepsilon(\boldsymbol{\Phi}^m))_{\Omega^m} + \left\langle \hat{S}\boldsymbol{U}^s, \boldsymbol{\Phi}^s \right\rangle_{\Sigma^s} - \langle \boldsymbol{P}, [\boldsymbol{\Phi}] \rangle_{\Gamma_C},\\
\tilde{F}^{ext}(\boldsymbol{\Phi}) &:= \tilde{L}(\boldsymbol{\Phi}), \qquad \sigma^m := \sigma(\boldsymbol{U}^m),
\end{aligned}$$

and

$$\boldsymbol{P} := P_n \boldsymbol{n} + P_t \boldsymbol{t}, \qquad P_n := -\frac{1}{\varepsilon_n} \mathrm{g}_n, \qquad P_t := -\frac{1}{\varepsilon_t} \mathbf{g}^e_t \cdot \boldsymbol{t},$$

according to (4.19), (4.20). Note that the functional $\tilde{F}^{int}(\boldsymbol{U}, \boldsymbol{\Phi})$ depends on $\boldsymbol{U}$. The nonlinear behaviour is described by the contact constitutive equations, formulated in Paragraph 4.2.1, and constitutive equations for plasticity, written in Paragraph 4.2.2. We perform the loading process as a consequent application of loading increments $(\Delta \boldsymbol{f})_{j+1}$, $(\Delta \hat{\boldsymbol{t}})_{j+1}$, $(\Delta \hat{\boldsymbol{u}})_{j+1}$:

$$\begin{aligned}
\boldsymbol{f}_{j+1} &= \boldsymbol{f}^i_j + (\Delta \boldsymbol{f})_{j+1},\\
\hat{\boldsymbol{t}}_{j+1} &= \hat{\boldsymbol{t}}^i_j + (\Delta \hat{\boldsymbol{t}})_{j+1}, \qquad j = 0, 1, 2 \ldots\\
\hat{\boldsymbol{u}}_{j+1} &= \hat{\boldsymbol{u}}^i_j + (\Delta \hat{\boldsymbol{u}})_{j+1},
\end{aligned}$$

which defines the discrete external load after application of the $(j+1)$-th increment

$$\tilde{F}^{ext}_j(\boldsymbol{\Phi}) := (\boldsymbol{f}^m_j, \boldsymbol{\Phi}^m)_{\Omega^m} + \left\langle N\boldsymbol{f}^s_j, \boldsymbol{\Phi}^s \right\rangle_{\Sigma^s} + \left\langle \hat{\boldsymbol{t}}_j, \boldsymbol{\Phi} \right\rangle_{\Gamma_N}$$

and defines the pseudo-time stepping process. Define the increment-dependent functional spaces

$$\begin{aligned}
\boldsymbol{\mathcal{V}}^m_{F,D_j,h} &:= \left\{ \boldsymbol{\Phi} \in \boldsymbol{H}^1(\Omega^m) : \boldsymbol{\Phi}|_K \in \mathcal{R}_1(K),\ \boldsymbol{\Phi}|_{\Gamma^m_D} = \hat{\boldsymbol{u}}^m_j \right\},\\
\boldsymbol{\mathcal{V}}^s_{D_j,h} &:= \left\{ \boldsymbol{\Phi} \in \boldsymbol{H}^{1/2}(\Gamma^s) : \boldsymbol{\Phi}|_I \in \mathcal{P}_1(I),\ \boldsymbol{\Phi}|_{\Gamma^s_D} = \hat{\boldsymbol{u}}^s_j \right\},\\
\tilde{\boldsymbol{\mathcal{V}}}_{D_j,h} &:= \boldsymbol{\mathcal{V}}^m_{F,D_j,h} \times \boldsymbol{\mathcal{V}}^s_{D_j,h}.
\end{aligned}$$

Let $\boldsymbol{U}_0$ be the initial displacement in the bodies, $(\varepsilon^p)_0^{(0)}, \alpha_0^{(0)}, \bar{\beta}_0^{(0)}$ initial internal variables, $(\mathbf{g}_t^p)_0^{(0)}$ initial tangential macro-displacement ("plastic" slip) and let $\boldsymbol{f}_0^i, \hat{\boldsymbol{t}}_0^i, \hat{\boldsymbol{u}}_0^i$ be the initial loads. Normally, the displacement-free state $\boldsymbol{U}_0 = 0$ as well as vanishing internal variables $(\varepsilon^p)_0^{(0)} = 0, \alpha_0^{(0)} = 0, \bar{\beta}_0^{(0)} = 0, (\mathbf{g}_t^p)_0^{(0)} = 0$ are chosen as initial data. We use the *backward (implicit) Euler scheme for both contact and plasticity.* Thus the problem can be reformulated as a series of incremental problems, and every subproblem corresponding to the j-th increment can be written as follows:

Find $\Delta \boldsymbol{U}_j \in \tilde{\boldsymbol{\mathcal{V}}}_{D_j,h}$, and therefore the new displacement state $\boldsymbol{U}_j = \boldsymbol{U}_{j-1} + \Delta \boldsymbol{U}_j$, stress $\sigma_j^m = \sigma(\boldsymbol{U}_j^m)$, contact traction $\boldsymbol{P}_j = \boldsymbol{P}(\boldsymbol{U}_j)$ such that

$$\tilde{F}^{int}(\sigma_j^m, \boldsymbol{P}_j^\varepsilon, \boldsymbol{\Phi}) = \tilde{F}_j^{ext}(\boldsymbol{\Phi}) \qquad \forall \boldsymbol{\Phi} \in \tilde{\boldsymbol{\mathcal{V}}}_h, \tag{4.25}$$

where contact and plastic constitutive conditions from Paragraph 4.2.1 and Paragraph 4.2.2 are satisfied.

We use Newton's method to solve (4.25). Let $\mathfrak{U}$ be the coefficients of the expansion of $\boldsymbol{U}$ in the basis of the discrete space $\tilde{\boldsymbol{\mathcal{V}}}_{D_j,h}$. Define

$$\tilde{F}_*^{int}(\mathfrak{U}, \boldsymbol{\Phi}) := \tilde{F}^{int}(\boldsymbol{U}, \boldsymbol{\Phi}).$$

Therefore (4.25) becomes

$$\tilde{F}_*^{int}(\mathfrak{U}_j, \boldsymbol{\Phi}) = F_j^{ext}(\boldsymbol{\Phi}) \qquad \forall \boldsymbol{\Phi} \in \tilde{\boldsymbol{\mathcal{V}}}_h.$$

We perform the linearization of $\tilde{F}_*^{int}(\mathfrak{U}_j, \boldsymbol{\Phi})$. We choose the starting value

$$\mathfrak{U}_j^{(0)} := \mathfrak{U}_{j-1},$$

and introduce Newton's increment $\Delta\mathfrak{U}_j^{(k)}$ to proceed to the next iterate

$$\mathfrak{U}_j^{(k+1)} = \mathfrak{U}_j^{(k)} + \Delta\mathfrak{U}_j^{(k+1)}, \qquad k = 0, 1, 2 \ldots$$

The Taylor expansion provides

$$\tilde{F}_*^{int}(\mathfrak{U}_j^{(k+1)}, \boldsymbol{\Phi}) = \tilde{F}_*^{int}(\mathfrak{U}_j^{(k)}, \boldsymbol{\Phi}) + \frac{\partial \tilde{F}_*^{int}(\mathfrak{U}_j^{(k)}, \boldsymbol{\Phi})}{\partial \mathfrak{U}_j^{(k)}} \Delta\mathfrak{U}_j^{(k+1)}. \tag{4.26}$$

Now we are in the position to state the algebraic problem. Define for brevity the matrix $\mathfrak{A}$ and the right hand side vector $\mathfrak{b}$ by

$$\begin{aligned} \mathfrak{A} :=& \frac{\partial \tilde{F}_*^{int}(\mathfrak{U}_j^{(k)}, \boldsymbol{\Phi})}{\partial \mathfrak{U}_j^{(k)}}, \\ \mathfrak{b} :=& \tilde{F}_j^{ext}(\boldsymbol{\Phi}) - \tilde{F}_*^{int}(\mathfrak{U}_j^{(k)}, \boldsymbol{\Phi}). \end{aligned}$$

Then the algebraic problem is: Find $\mathfrak{x} = \Delta\mathfrak{U}_j^{(k+1)}$ such that

$$\mathfrak{A}\mathfrak{x} = \mathfrak{b}.$$

Now, the whole algorithm can be formulated as follows.

Algorithm 4.1. *(Incremental loading with Newton's algorithm for FE/BE coupling)*

Set initial displacement $\mathfrak{U}_0^{(0)}$, *initial internal variables* $(\varepsilon^p)_0^{(0)}, \alpha_0^{(0)}, \bar{\beta}_0^{(0)}$, *initial tangential macro-displacement* $(\mathbf{g}_t^p)_0^{(0)}$ *and initial loads* $\boldsymbol{f}_0, \hat{\boldsymbol{t}}_0, \hat{\boldsymbol{u}}_0$

1. *for* $j = 0, 1, 2, \ldots$
   a) *for* $k = 0, 1, 2, \ldots$
      i. *compute the load vector* $\mathfrak{b} := \tilde{F}_j^{ext}(\boldsymbol{\Phi}) - \tilde{F}_*^{int}(\mathfrak{U}_j^{(k)}, \boldsymbol{\Phi})$
      ii. *if* $||\mathfrak{b}||_{l_2} := \sqrt{\mathfrak{b} \cdot \mathfrak{b}} \leq TOL$ *goto 2.*
      iii. *compute the matrix* $\mathfrak{A} := \dfrac{\partial \tilde{F}_*^{int}(\mathfrak{U}_j^{(k)}, \boldsymbol{\Phi})}{\partial \mathfrak{U}_j^{(k)}}$,
      iv. *find the next displacement increment* $\mathfrak{x} = \Delta\mathfrak{U}_j^{(k+1)}$ *by solving*
      $$\mathfrak{A}\mathfrak{x} = \mathfrak{b}.$$
      v. *update the displacement field*
      $$\mathfrak{U}_j^{(k+1)} = \mathfrak{U}_j^{(k)} + \Delta\mathfrak{U}_j^{(k+1)}$$
      and the internal variables $(\varepsilon^p)_j^{(k+1)}, \alpha_j^{(k+1)}, \bar{\beta}_j^{(k+1)}$, $(\mathbf{g}_t^p)_j^{(k+1)}$. *They should satisfy the constitutive contact and plastic conditions. We use the return mapping procedure for both the frictional contact and the plastification. The details are described below.*
   b) *exit, if the prescribed tolerance is achieved; otherwise, set* $k = k + 1$, *goto (a)*
2. *initialise the next pseudo-time step*
$$\mathfrak{U}_{j+1}^{(0)} = \mathfrak{U}_j^{(k)}$$
3. *apply the next load increment*
$$\begin{aligned} \boldsymbol{f}_{j+1} &= \boldsymbol{f}_j + (\Delta\boldsymbol{f})_{j+1}, \\ \hat{\boldsymbol{t}}_{j+1} &= \hat{\boldsymbol{t}}_j + (\Delta\hat{\boldsymbol{t}})_{j+1}, \\ \hat{\boldsymbol{u}}_{j+1} &= \hat{\boldsymbol{u}}_j + (\Delta\hat{\boldsymbol{u}})_{j+1}, \end{aligned}$$

exit, if the total load is achieved; otherwise, set $j = j + 1$, *goto 1.*

Linear system

Let us consider in detail the structure of the linear system $\mathfrak{A}\mathfrak{x} = \mathfrak{b}$. After linearization of contact and plasticity terms described below we obtain

$$\begin{pmatrix} S_{\Gamma_N^s} & S^T_{\Gamma_C^s,\Gamma_N^s} & 0 & 0 \\ S_{\Gamma_C^s,\Gamma_N^s} & S_{\Gamma_C^s} + \mathcal{C}^{ss} & -\mathcal{C}^{sm} & 0 \\ 0 & -\mathcal{C}^{ms} & \mathcal{C}^{mm} + C^{pl}_{\Gamma_C^m} & (B^{pl}_{\Gamma_C^m})^T \\ 0 & 0 & B^{pl}_{\Gamma_C^m} & A^{pl}_{\Omega^m} \end{pmatrix} \begin{pmatrix} \mathfrak{x}^s_{\Gamma_N^s} \\ \mathfrak{x}^s_{\Gamma_C^s} \\ \mathfrak{x}^m_{\Gamma_C^m} \\ \mathfrak{x}^m_{\Gamma_N^m} \end{pmatrix} = \mathfrak{b}^{ext} - \mathfrak{b}^{int} + \begin{pmatrix} 0 \\ \mathfrak{b}^s_{\Gamma_C^s} \\ -\mathfrak{b}^m_{\Gamma_C^m} \\ 0 \end{pmatrix}. \tag{4.27}$$

where the stiffness matrix

$$\tilde{\mathcal{A}} := \begin{pmatrix} \mathcal{A}^s & 0 \\ 0 & \mathcal{A}^m \end{pmatrix} = \begin{pmatrix} S_{\Gamma_N^s} & S^T_{\Gamma_C^s,\Gamma_N^s} & 0 & 0 \\ S_{\Gamma_C^s,\Gamma_N^s} & S_{\Gamma_C^s} & 0 & 0 \\ 0 & 0 & C^{pl}_{\Gamma_C^m} & (B^{pl}_{\Gamma_C^m})^T \\ 0 & 0 & B^{pl}_{\Gamma_C^m} & A^{pl}_{\Omega^m} \end{pmatrix}$$

consists of the finite element and the boundary element part and does not contain the coupling terms. The submatrix $\mathcal{A}^s$ is the stiffness matrix of the boundary element part. It is dense, since nonlocal boundary integral operators are involved in the corresponding bilinear form. The submatrix $\mathcal{A}^m$ is the stiffness matrix of the finite element part. It is sparse and has a band structure. The upper index ^{pl} means that the matrix changes within the Newton cycle due to the plastic terms. The matrix block $A^{pl}_{\Omega^m}$ is generated by testing the trial functions, which correspond to the degrees of freedom in the interior of Ω^m and its Neumann boundary Γ^m_N, against themselves. The block $C^{pl}_{\Gamma_C^m}$ corresponds to the testing the trial functions, associated with the contact boundary Γ^m_C, against themselves. The block $B^{pl}_{\Gamma_C^m}$ is generated by testing the trial functions, associated with the interior of Ω^m and Γ^m_N, against the trial functions, associated with Γ^m_C. The boundary element block $S_{\Gamma_N^s}$ ($S_{\Gamma_C^s}$) is generated by testing the trial functions, which correspond to the degrees of freedom, associated with the Neumann boundary Γ^s_N (contact boundary Γ^s_C), against themselves. The block $S_{\Gamma_C^s,\Gamma_N^s}$ represents the matrix elements, obtained by testing the trial functions, associated with Γ^s_C, against the trial functions, associated with Γ^s_N.

The term $\mathfrak{b}^{ext}$ is constructed by the usual contributions of external volume forces and prescribed tractions on the Neumann boundary part. The terms $\mathcal{C}^{ss}, \mathcal{C}^{sm}, \mathcal{C}^{ms}, \mathcal{C}^{mm}, \mathfrak{b}^s_{\Gamma_C^s}, \mathfrak{b}^m_{\Gamma_C^m}$ describe coupling of the bodies along the contact boundary. They appear after the linearization of contact integrals. $\tilde{\mathcal{A}}, \mathfrak{b}^{int}$ describe internal behaviour of the bodies and reflect, for example, the plastic effects. Computation of these terms is discussed below.

4.2.4 Pure BEM for elastoplastic contact problems with friction

Boundary integral formulation for elastoplasticity

Plastic deformation is an irreversible nonlinear process. The plastic deformation is determined by the whole deformation history, and therefore it cannot be written in terms of boundary integral operators alone. The Newton's potentials must be employed. We derive the boundary integral formulation for elastoplasticity from the coupling formulation (4.17) with the plastic material law $\sigma = \mathbb{C} : (\varepsilon - \varepsilon^p)$. In particular for $\sigma^m, (\varepsilon^p)^m \in L_2(\Omega^m), \boldsymbol{u}^m \in \boldsymbol{\mathcal{V}}^m_{F,D}, \boldsymbol{\phi}^m \in \boldsymbol{\mathcal{V}}^m_F, \varepsilon(\cdot) := (\nabla(\cdot) + (\nabla(\cdot))^T)/2$ there holds

$$
\begin{aligned}
&(\sigma^m, \varepsilon(\boldsymbol{\phi}^m))_{\Omega^m} - (\boldsymbol{f}^m, \boldsymbol{\phi}^m)_{\Omega^m} \\
&\quad = (\mathbb{C} : \varepsilon(\boldsymbol{u}^m), \varepsilon(\boldsymbol{\phi}^m))_{\Omega^m} - (\mathbb{C} : (\varepsilon^p)^m, \varepsilon(\boldsymbol{\phi}^m))_{\Omega^m} - (\boldsymbol{f}^m, \boldsymbol{\phi}^m)_{\Omega^m} \\
&\quad = (\mathbb{C} : \varepsilon(\boldsymbol{u}^m), \varepsilon(\boldsymbol{\phi}^m))_{\Omega^m} + (\mathrm{div}(\mathbb{C} : (\varepsilon^p)^m), \boldsymbol{\phi}^m)_{\Omega^m} \\
&\qquad - \langle (\mathbb{C} : (\varepsilon^p)^m) \cdot \boldsymbol{n}^m, \boldsymbol{\phi}^m \rangle_{\Sigma^m} - (\boldsymbol{f}^m, \boldsymbol{\phi}^m)_{\Omega^m} \\
&\quad = (\mathbb{C} : \varepsilon(\boldsymbol{u}^m), \varepsilon(\boldsymbol{\phi}^m))_{\Omega^m} + (\mathrm{div}(\mathbb{C} : (\varepsilon^p)^m) - \boldsymbol{f}^m, \boldsymbol{\phi}^m)_{\Omega^m} \\
&\qquad - \langle (\mathbb{C} : (\varepsilon^p)^m) \cdot \boldsymbol{n}^m, \boldsymbol{\phi}^m \rangle_{\Sigma^m} \\
&\quad = \langle S\boldsymbol{u}^m, \boldsymbol{\phi}^m \rangle_{\Sigma^m} + \langle N(\mathrm{div}(\mathbb{C} : (\varepsilon^p)^m) - \boldsymbol{f}^m), \boldsymbol{\phi}^m \rangle_{\Sigma^m} \\
&\qquad - \langle (\mathbb{C} : (\varepsilon^p)^m) \cdot \boldsymbol{n}^m, \boldsymbol{\phi}^m \rangle_{\Sigma^m} .
\end{aligned}
$$

Therefore the boundary integral formulation for elastoplastic problem with frictional contact can be written as follows: Find $\boldsymbol{u} \in \boldsymbol{\mathcal{V}}_D$ such that

$$
\begin{aligned}
\langle S\boldsymbol{u}, \boldsymbol{\phi} \rangle_{\Sigma} &+ \langle N(\mathrm{div}(\mathbb{C} : (\varepsilon^p)^m)), \boldsymbol{\phi}^m \rangle_{\Sigma^m} - \langle (\mathbb{C} : (\varepsilon^p)^m) \cdot \boldsymbol{n}^m, \boldsymbol{\phi}^m \rangle_{\Sigma^m} \\
&- \langle \boldsymbol{p}(\boldsymbol{u}), [\boldsymbol{\phi}] \rangle_{\Gamma_C} = \langle N\boldsymbol{f}, \boldsymbol{\phi} \rangle_{\Sigma} + \langle \hat{\boldsymbol{t}}, \boldsymbol{\phi} \rangle_{\Gamma_N}, \qquad \forall \boldsymbol{\phi} \in \boldsymbol{\mathcal{V}},
\end{aligned}
\tag{4.28}
$$

with the continuous contact traction

$$
\boldsymbol{p} := p_n \boldsymbol{n} + p_t \boldsymbol{t}, \qquad p_n := -\frac{1}{\varepsilon_n} \mathrm{g}_n, \qquad p_t := -\frac{1}{\varepsilon_t} \mathbf{g}^e_t \cdot \boldsymbol{t}.
$$

Here the penetration and the relative tangential displacement are computed in terms of the displacement $\boldsymbol{u}$, i.e. $\mathrm{g}_n = \mathrm{g}_n(\boldsymbol{u})$, $\mathbf{g}^e_t = \mathbf{g}^e_t(\boldsymbol{u})$.

Discrete weak formulation

We discretize the weak formulation (4.28) by defining a partition $\boldsymbol{\mathcal{T}}^i_h$ of the boundary $\Gamma^i, i = s, m$ into straight line segments and introducing discrete spaces

$$
\boldsymbol{\mathcal{V}}^i_{D,h} := \left\{ \boldsymbol{\Phi} \in \boldsymbol{H}^{1/2}(\Gamma^i) : \boldsymbol{\Phi}|_I \in \left[\mathcal{P}_1(I)\right]^2 \; \forall I \in \mathcal{T}^i_h, \, \boldsymbol{\Phi}|_{\Gamma_D} = \hat{\boldsymbol{u}}^i \right\},
$$

$$\boldsymbol{\mathcal{V}}_h^i := \left\{ \boldsymbol{\Phi} \in \tilde{\boldsymbol{H}}^{1/2}(\Sigma^i) : \boldsymbol{\Phi}|_I \in \left[\mathcal{P}_1(I)\right]^2 \ \forall I \in \mathcal{T}_h^i \right\},$$
$$\boldsymbol{\mathcal{V}}_{D,h} := \boldsymbol{\mathcal{V}}_{D,h}^m \times \boldsymbol{\mathcal{V}}_{D,h}^s, \qquad \boldsymbol{\mathcal{V}}_h := \boldsymbol{\mathcal{V}}_h^m \times \boldsymbol{\mathcal{V}}_h^s.$$

The discretized version of (4.28) is given by: Find $\boldsymbol{U} = (\boldsymbol{U}^m, \boldsymbol{U}^s) \in \boldsymbol{\mathcal{V}}_D$:

$$F^{int}(\boldsymbol{U}, \boldsymbol{\Phi}) - \boldsymbol{G}((\varepsilon^p)^m, \boldsymbol{\Phi}^m) = F^{ext}(\boldsymbol{\Phi}) \qquad \forall \boldsymbol{\Phi} \in \boldsymbol{\mathcal{V}}, \tag{4.29}$$

where

$$F^{int}(\boldsymbol{U}, \boldsymbol{\Phi}) := \left\langle \hat{S}\boldsymbol{U}, \boldsymbol{\Phi} \right\rangle_\Sigma - \langle \boldsymbol{P}, [\boldsymbol{\Phi}] \rangle_{\Gamma_C}, \tag{4.30}$$
$$\boldsymbol{G}((\varepsilon^p)^m, \boldsymbol{\Phi}^m) := - \langle N(\mathrm{div}(\mathbb{C} : (\varepsilon^p)^m)), \boldsymbol{\Phi}^m \rangle_{\Sigma^m} + \langle (\mathbb{C} : (\varepsilon^p)^m) \cdot \boldsymbol{n}^m, \boldsymbol{\Phi}^m \rangle_{\Sigma^m}$$
$$F^{ext}(\boldsymbol{\Phi}) := \langle N\boldsymbol{f}, \boldsymbol{\Phi} \rangle_\Sigma + \left\langle \hat{\boldsymbol{t}}, \boldsymbol{\Phi} \right\rangle_{\Gamma_N},$$
$$\boldsymbol{P} := P_n \boldsymbol{n} + P_t \boldsymbol{t}, \qquad P_n := -\frac{1}{\varepsilon_n} \mathrm{g}_n, \qquad P_t := -\frac{1}{\varepsilon_t} \mathbf{g}_t^e \cdot \boldsymbol{t}.$$

The contact term in the functional $F^{int}(\boldsymbol{U}, \boldsymbol{\Phi})$ is nonlinear due to the constitutive contact conditions. The functional $\boldsymbol{G}((\varepsilon^p)^m, \boldsymbol{\Phi}^m)$ is nonlinear when the plastic deformations occur. Similarly to the previous section, we introduce the incremental loading process as a consequent application of loading increments $(\Delta \boldsymbol{f})_{j+1}$, $(\Delta \hat{\boldsymbol{t}})_{j+1}$, $(\Delta \hat{\boldsymbol{u}})_{j+1}$:

$$\begin{aligned} \boldsymbol{f}_{j+1} &= \boldsymbol{f}_j + (\Delta \boldsymbol{f})_{j+1}, \\ \hat{\boldsymbol{t}}_{j+1} &= \hat{\boldsymbol{t}}_j + (\Delta \hat{\boldsymbol{t}})_{j+1}, \qquad j = 0, 1, 2 \ldots \\ \hat{\boldsymbol{u}}_{j+1} &= \hat{\boldsymbol{u}}_j + (\Delta \hat{\boldsymbol{u}})_{j+1}, \end{aligned}$$

which defines the discrete external load

$$F_j^{ext}(\boldsymbol{\Phi}) := \left\langle N\boldsymbol{f}_j, \boldsymbol{\Phi} \right\rangle_\Sigma + \left\langle \hat{\boldsymbol{t}}_j, \boldsymbol{\Phi} \right\rangle_{\Gamma_N}$$

and defines the pseudo-time stepping process. We introduce the increment-dependent boundary discrete spaces

$$\boldsymbol{\mathcal{V}}_{D_j,h}^i := \left\{ \boldsymbol{\Phi} \in \boldsymbol{H}^{1/2}(\Gamma^i) : \boldsymbol{\Phi}|_I \in \mathcal{P}_1(I), \boldsymbol{\Phi}|_{\Gamma_D^i} = (\hat{\boldsymbol{u}}^i)_j \right\},$$
$$\boldsymbol{\mathcal{V}}_{D_j,h} := \boldsymbol{\mathcal{V}}_{D_j,h}^m \times \boldsymbol{\mathcal{V}}_{D_j,h}^s.$$

Let $\boldsymbol{U}_0$ be the initial displacement state of the body. Unlike as in the FE/BE description in the previous paragraph, we use *the backward Euler scheme for contact and the forward Euler scheme for plasticity.* Using the implicit scheme for the plastic terms seems to be a more sophisticated task, since in the pure BE case we need to have the displacement-degrees-of-freedom only on the boundary of the domain.

The following implicit-explicit formulation must be solved on each loading step j: Find $(\Delta \boldsymbol{U})_j \in \boldsymbol{\mathcal{V}}_{D_j,h}$, and therefore the new displacement state $\boldsymbol{U}_j = \boldsymbol{U}_{j-1} + (\Delta \boldsymbol{U})_j$, plastic strain ε_j^p, contact traction $\boldsymbol{P}_j = \boldsymbol{P}(\boldsymbol{U}_j)$ such that

$$F^{int}(\boldsymbol{U}_j, \boldsymbol{\Phi}) = \boldsymbol{G}(\varepsilon_j^p, \boldsymbol{\Phi}) + F_j^{ext}(\boldsymbol{\Phi}) \qquad \forall \boldsymbol{\Phi} \in \boldsymbol{\mathcal{V}}_h, \tag{4.31}$$

where contact and plastic constitutive conditions from Paragraph 4.2.1 and Paragraph 4.2.2 are satisfied.

In order to solve (4.31) we use Newton's method. We proceed similarly to the previous section. Let $\mathfrak{U}$ be the coefficients of the expansion of $\boldsymbol{U}$ in basis of the discrete space $\boldsymbol{\mathcal{V}}_{D,h}$. Define

$$F_*^{int}(\mathfrak{U}, \boldsymbol{\Phi}) := F^{int}(\boldsymbol{U}, \boldsymbol{\Phi}).$$

Therefore (4.31) becomes

$$F_*^{int}(\mathfrak{U}_j, \boldsymbol{\Phi}) = \boldsymbol{G}(\varepsilon_j^p, \boldsymbol{\Phi}) + F_j^{ext}(\boldsymbol{\Phi}) \qquad \forall \boldsymbol{\Phi} \in \boldsymbol{\mathcal{V}}_h.$$

We perform the linearization of $F_*^{int}(\mathfrak{U}_j, \boldsymbol{\Phi})$. We choose the starting value

$$\mathfrak{U}_j^{(0)} := \mathfrak{U}_{j-1},$$

and introduce the Newton's increment $(\Delta\mathfrak{U})_j^{(k)}$ to proceed to the next iterate

$$\mathfrak{U}_j^{(k+1)} = \mathfrak{U}_j^{(k)} + (\Delta\mathfrak{U})_j^{(k+1)}, \qquad k = 0, 1, 2 \dots$$

The Taylor expansion provides

$$F_*^{int}(\mathfrak{U}_j^{(k+1)}, \boldsymbol{\Phi}) = F_*^{int}(\mathfrak{U}_j^{(k)}, \boldsymbol{\Phi}) + \frac{\partial F_*^{int}(\mathfrak{U}_j^{(k)}, \boldsymbol{\Phi})}{\partial \mathfrak{U}_j^{(k)}} (\Delta\mathfrak{U})_j^{(k)}. \qquad (4.32)$$

Now we are on the position to formulate the algebraic problem. Define for brevity the matrix $\mathfrak{A}$ and the right hand side vector $\mathfrak{b}$ by

$$\mathfrak{A} := \frac{\partial F_*^{int}(\mathfrak{U}_j^{(k)}, \boldsymbol{\Phi})}{\partial \mathfrak{U}_j^{(k)}},$$
$$\mathfrak{b} := F_j^{ext}(\boldsymbol{\Phi}) + \boldsymbol{G}((\varepsilon^p)_j^{(k)}, \boldsymbol{\Phi}) - F_*^{int}(\mathfrak{U}_j^{(k)}, \boldsymbol{\Phi}).$$

Note, that plastic strain from the (k)-th Newton's iteration $(\varepsilon^p)_j^{(k)}$ is appears in the right hand side and makes no influence on the matrix. That corresponds to the forward Euler scheme for plasticity. Then the algebraic problem is: Find $\mathfrak{x} = (\Delta\mathfrak{U})_j^{(k+1)}$:

$$\mathfrak{A}\mathfrak{x} = \mathfrak{b}.$$

The whole algorithm can be formulated now as follows.

Algorithm 4.2. *(Incremental loading with Newton's algorithm for pure BEM)*

Set initial displacement $\mathfrak{U}_0^{(0)}$*, initial internal variables* $(\varepsilon^p)_0^{(0)}, \alpha_0^{(0)}, \bar{\beta}_0^{(0)}$*, initial tangential macro-displacement* $(\mathbf{g}_t^p)_0^{(0)}$ *and initial loads* $\boldsymbol{f}_0, \hat{\boldsymbol{t}}_0, \hat{\boldsymbol{u}}_0$

1. *for* $j = 0, 1, 2, \ldots$

   a) *for* $k = 0, 1, 2, \ldots$

      i. *compute the load vector*
      $\mathfrak{b} := F_j^{ext}(\boldsymbol{\Phi}) + \boldsymbol{G}((\varepsilon^p)_j^{(k)}, \boldsymbol{\Phi}) - F_*^{int}(\mathfrak{U}_j^{(k)}, \boldsymbol{\Phi})$

      ii. *if* $||\mathfrak{b}||_{l_2} := \sqrt{\mathfrak{b} \cdot \mathfrak{b}} \leq TOL$ *goto 2.*

      iii. *compute the matrix* $\mathfrak{A} := \dfrac{\partial F_*^{int}(\mathfrak{U}_j^{(k)}, \boldsymbol{\Phi})}{\partial \mathfrak{U}_j^{(k)}}$,

      iv. *find the next displacement increment* $\mathfrak{x} = \Delta\mathfrak{U}_j^{(k+1)}$ *by solving*

      $$\mathfrak{A}\mathfrak{x} = \mathfrak{b}.$$

      v. *update the displacement field*

      $$\mathfrak{U}_j^{(k+1)} = \mathfrak{U}_j^{(k)} + (\Delta\mathfrak{U})_j^{(k+1)}$$

      and the internal variables $(\varepsilon^p)_j^{(k+1)}, \alpha_j^{(k+1)}, \bar{\beta}_j^{(k+1)}$, $(\mathbf{g}_t^p)_j^{(k+1)}$*. They should satisfy the constitutive contact and plastic conditions. We use the return mapping procedure for both the frictional contact and the plastification. The details are described below.*

   b) *exit, if the prescribed tolerance is achieved; otherwise, set* $k = k + 1$*, goto (a)*

2. *initialize the next pseudo-time step*

   $$\mathfrak{U}_{j+1}^{(0)} = \mathfrak{U}_j^{(k)}$$

3. *apply the next load increment*

   $$\begin{aligned} \boldsymbol{f}_{j+1} &:= \boldsymbol{f}_j + (\Delta\boldsymbol{f})_{j+1}, \\ \hat{\boldsymbol{t}}_{j+1} &:= \hat{\boldsymbol{t}}_j + (\Delta\hat{\boldsymbol{t}})_{j+1}, \\ \hat{\boldsymbol{u}}_{j+1} &:= \hat{\boldsymbol{u}}_j + (\Delta\hat{\boldsymbol{u}})_{j+1}, \end{aligned}$$

   exit, if the total load is achieved; otherwise, set $j = j + 1$*, goto 1.*

Linear system

The linear system $\mathfrak{A}\mathfrak{x} = \mathfrak{b}$ has the following form

$$\begin{pmatrix} S_{\Gamma_N^s} & S^T_{\Gamma_C^s,\Gamma_N^s} & 0 & 0 \\ S_{\Gamma_C^s,\Gamma_N^s} & S_{\Gamma_C^s} + \mathcal{C}^{ss} & -\mathcal{C}^{sm} & 0 \\ 0 & -\mathcal{C}^{ms} & \mathcal{C}^{mm} + S_{\Gamma_C^m} & S^T_{\Gamma_C^m,\Gamma_N^m} \\ 0 & 0 & S_{\Gamma_C^m,\Gamma_N^m} & S_{\Gamma_M^m} \end{pmatrix} \begin{pmatrix} \mathfrak{x}^s_{\Gamma_N^s} \\ \mathfrak{x}^s_{\Gamma_C^s} \\ \mathfrak{x}^m_{\Gamma_C^m} \\ \mathfrak{x}^m_{\Gamma_N^m} \end{pmatrix} = \mathfrak{b}^{ext} - \mathfrak{b}^{int} + \mathfrak{b}_{\varepsilon^p} + \begin{pmatrix} 0 \\ \mathfrak{b}^s_{\Gamma_C^s} \\ -\mathfrak{b}^m_{\Gamma_C^m} \\ 0 \end{pmatrix}. \tag{4.33}$$

The similar notations as in the description of the linear system for the FE/BE coupling problem are used here. The only new term is $\mathfrak{b}_{\varepsilon^p}$, which reflects the contribution of the plastic terms to the right hand side. Since the pure boundary formulation is used, the submatrices, corresponding to the stiffness matrices of the bodies without contact, are dense. Therefore, the whole matrix is of dense type, but with sufficiently reduced size with respect to the FE/BE coupling described above, because the unknowns are associated only with the boundaries of the bodies.

Note that only the contact blocks $\mathcal{C}^{ss}, \mathcal{C}^{sm}, \mathcal{C}^{ms}, \mathcal{C}^{mm}$ of the matrix are updated, which corresponds to backward Euler scheme for frictional contact and to forward Euler scheme for plasticity. The details connected with linearization of the contact terms are given below.

4.2.5 Linearization of the contact terms

In this paragraph we will describe in detail the computation of the matrix elements caused by the linearization of (4.26) or (4.32). According to the definition of the functional F^{int}, the contact terms must be also linearized. Denoting the contact terms by $C(\boldsymbol{U}, \boldsymbol{\Phi}) := -\langle \boldsymbol{P}, [\boldsymbol{\Phi}] \rangle_{\Gamma_C}$ and corresponding coefficient dependent functional $C_*(\mathfrak{U}, \boldsymbol{\Phi}) := C(\boldsymbol{U}, \boldsymbol{\Phi})$, where $\mathfrak{U}$ are expansion coefficients of the discrete function $\boldsymbol{U}$ in the basis of $\boldsymbol{\mathcal{V}}_{D,h}$. Consider some (fixed) incremental loading step j. Since all the values involved correspond to this incremental step, we will omit the lower index $_j$ for brevity. The Newton's scheme is used for solution of the problem. It is an iterative process, where the next iterate is obtained from the previous one by adding corrections

$$\mathfrak{U}^{(k+1)} = \mathfrak{U}^{(k)} + \Delta\mathfrak{U}, \qquad k = 0, 1, 2 \ldots$$

which are solutions of the linear system (4.27) or (4.33). Further down we describe the computation of the matrix elements $\mathcal{C}^{ab}$, $a, b = m, s$.

Then linearization of the contact terms can be written as follows (cf. (4.32))

$$C_*(\mathfrak{U}^{(k+1)}, \boldsymbol{\Phi}) = C_*(\mathfrak{U}^{(k)}, \boldsymbol{\Phi}) + \frac{\partial C_*(\mathfrak{U}^{(k)}, \boldsymbol{\Phi})}{\partial \mathfrak{U}^{(k)}} \Delta\mathfrak{U}$$
$$= C(\boldsymbol{U}^{(k)}, \boldsymbol{\Phi}) + \frac{d}{d\alpha} C(\boldsymbol{U}^{(k)} + \alpha\Delta\boldsymbol{U}, \boldsymbol{\Phi})\Big|_{\alpha=0}. \tag{4.34}$$

We analyse the normal and tangential contact terms independently. For $\boldsymbol{U} = U_n\boldsymbol{n} + U_t\boldsymbol{t}$ we introduce the decomposition

$$C(\boldsymbol{U}, \boldsymbol{\Phi}) := C_n(U_n, \Phi_n) + C_t(U_t, \Phi_t)$$

with

$$C_n(U_n, \Phi_n) := \frac{1}{\varepsilon_n}\int_{\Gamma_C} \mathrm{g}_n(U_n)[\Phi_n]\, ds, \qquad C_t(U_t, \Phi_t) := \frac{1}{\varepsilon_n}\int_{\Gamma_C} \mathrm{g}_t^e(U_t)[\Phi_t]\, ds.$$

Linearization of the normal contact terms

For the normal contact terms we obtain with $\mathrm{g}_n(U_n) = ([U_n] - g)^+$

$$\frac{d}{d\alpha} C_n(U_n^{(k)} + \alpha(\Delta U)_n, \Phi_n)\Big|_{\alpha=0} = \frac{1}{\varepsilon_n}\int_{\Gamma_C} \frac{d}{d\alpha}\mathrm{g}_n(U_n^{(k)} + \alpha(\Delta U)_n)\Big|_{\alpha=0} [\Phi_n]\, ds + THO.$$

Further,

$$\frac{d}{d\alpha}\mathrm{g}_n(U_n^{(k)} + \alpha(\Delta U)_n)\Big|_{\alpha=0} = \frac{d}{d\alpha}([U_n^{(k)} + \alpha(\Delta U)_n] - g)^+\Big|_{\alpha=0}$$
$$= \left\{ \begin{array}{ll} [(\Delta U)_n], & \text{if } [U_n^{(k)}] - g > 0 \\ 0, & \text{if } [U_n^{(k)}] - g < 0 \end{array} \right\} = [(\Delta U)_n]\ \mathrm{sign}(\mathrm{g}_n(U_n^{(k)})).$$

Therefore

$$\frac{d}{d\alpha} C_n(U_n^{(k)} + \alpha(\Delta U)_n, \Phi_n)\Big|_{\alpha=0} = \frac{1}{\varepsilon_n}\int_{\Gamma_C} \mathrm{sign}(\mathrm{g}_n(U_n^{(k)}))\ [(\Delta U)_n]\ [\Phi_n]\, ds. \tag{4.35}$$

Remark 4.2.2. *It is worth to say that in the case $[U_n^{(k)}] = g$ the penetration function $\mathrm{g}_n(U_n^{(k)})$ is not differentiable. The lack of smoothness can lead to some problems in convergence of Newton's method. This can be avoided by an appropriate regularization of $\mathrm{g}_n(U_n^{(k)})$. But for most problems only few iterations are needed to define the active set (i.e. contact nodes, coming in contact), see [41, 4.4.2].*

Remark 4.2.3. *The expression in the right-hand side of (4.35) is linear, since the values of sign$(\mathrm{g}_n(U_n^{(k)}))$ are taken from the previous iteration. In other words, the matrix element is "switched on", if the penetration function in the corresponding point was positive in the previous iteration, i.e. the point was in contact.*

Linearization of the tangential contact terms

For brevity of notation we introduce the parameter-dependent projection operator Π_θ pointwise as follows

$$\Pi_\theta(x) := \begin{cases} x, & \text{if } |x| \le \theta, \\ \theta \operatorname{sign}(x), & \text{if } |x| \ge \theta. \end{cases}$$

It is easy to see that the constitutive conditions, described in paragraph 4.2.1 provide

$$\mathrm{g}_t^e(U_t) = \Pi_{\varepsilon_t \mathcal{F}}(\mathrm{g}_t(U_t)) = \Pi_{\varepsilon_t \mathcal{F}}([U_t]),$$

since $\mathrm{g}_t(U_t) = [U_t]$. Therefore

$$\frac{d}{d\alpha} C_t(U_t^{(k)} + \alpha(\Delta U)_t, \Phi_t)\bigg|_{\alpha=0} = \frac{1}{\varepsilon_t}\int_{\Gamma_C} \frac{d}{d\alpha}\Pi_{\varepsilon_t\mathcal{F}}(\mathrm{g}_t^e(U_t^{(k)} + \alpha(\Delta U)_t))\bigg|_{\alpha=0} [\Phi_t]\, ds + THO.$$

Remember that in case of Coulomb's frictional law there folds

$$\mathcal{F} = \mu_f |P_n^{(k)}| = \frac{\mu_f}{\varepsilon_n}\mathrm{g}_n(U_n^{(k)} + \alpha(\Delta U)_n)$$

We distinguish between stick and slip case, i.e. we need to compare $|\mathrm{g}_t(U_t^{(k)} + \alpha(\Delta U)_t)|$ and $\varepsilon_t\mathcal{F} := \mu_f \frac{\varepsilon_t}{\varepsilon_n}\mathrm{g}_n(U_n^{(k)} + \alpha(\Delta U)_n)$ under condition $\alpha = 0$. In other words we will speak about

$$\text{stick, if} \qquad |\mathrm{g}_t(U_t^{(k)})| \le \mu_f \frac{\varepsilon_t}{\varepsilon_n}\mathrm{g}_n(U_n^{(k)}),$$
$$\text{slip, if} \qquad |\mathrm{g}_t(U_t^{(k)})| > \mu_f \frac{\varepsilon_t}{\varepsilon_n}\mathrm{g}_n(U_n^{(k)}).$$

With this notation we obtain

$$\frac{d}{d\alpha}\Pi_{\varepsilon_t\mathcal{F}}(\mathrm{g}_t(U_t^{(k)} + \alpha(\Delta U)_t))\bigg|_{\alpha=0}$$
$$= \begin{cases} \dfrac{d}{d\alpha}\mathrm{g}_t(U_t^{(k)} + \alpha(\Delta U)_t)\bigg|_{\alpha=0}, & \text{for stick,} \\ \dfrac{d}{d\alpha}\left\{\mu_f\dfrac{\varepsilon_t}{\varepsilon_n}\mathrm{g}_n(U_n^{(k)} + \alpha(\Delta U)_n)\ \operatorname{sign}(\mathrm{g}_t(U_t^{(k)} + \alpha(\Delta U)_t))\right\}\bigg|_{\alpha=0}, & \text{for slip.} \end{cases}$$

In case of stick we obtain

$$\frac{d}{d\alpha}\mathrm{g}_t(U_t^{(k)} + \alpha(\Delta U)_t)\bigg|_{\alpha=0} = \frac{d}{d\alpha}[U_t^{(k)} + \alpha(\Delta U)_t]\bigg|_{\alpha=0} = [(\Delta U)_t)].$$

In case of slip there holds (cf. (4.35))

$$\frac{d}{d\alpha}\left\{\mu_f\frac{\varepsilon_t}{\varepsilon_n}\mathrm{g}_n(U_n^{(k)} + \alpha(\Delta U)_n)\ \operatorname{sign}(\mathrm{g}_t(U_t^{(k)} + \alpha(\Delta U)_t))\right\}\bigg|_{\alpha=0}$$
$$= \mu_f\frac{\varepsilon_t}{\varepsilon_n}\ \operatorname{sign}(\mathrm{g}_n(U_n^{(k)}))\ \operatorname{sign}(\mathrm{g}_t(U_t^{(k)}))[(\Delta U)_n],$$

since

$$\frac{d}{d\alpha}\ \operatorname{sign}(\mathrm{g}_t(U_t^{(k)} + \alpha(\Delta U)_t))\bigg|_{\alpha=0} = 0.$$

Remark 4.2.4. *There is no singularity in case of slip, since* $|g_t(U_t^{(k)})| > \mu_f \frac{\varepsilon_t}{\varepsilon_n} g_n(U_n^{(k)}) > 0$ *and the origin is excluded.*

Summing obtained results we obtain

$$\frac{d}{d\alpha} C_t(U_t^{(k)} + \alpha(\Delta U)_t, \Phi_t)\Big|_{\alpha=0} = \begin{cases} \displaystyle\int_{\Gamma_C} \frac{1}{\varepsilon_t}[(\Delta U)_t]\,[\Phi_t]\,ds, & \text{for stick: } |g_t(U_t^{(k)})| \le \mu_f \frac{\varepsilon_t}{\varepsilon_n} g_n(U_n^{(k)}), \\ \displaystyle\int_{\Gamma_C} \frac{\mu_f}{\varepsilon_n}\,\text{sign}(g_n(U_n^{(k)}) g_t(U_t^{(k)}))[(\Delta U)_n]\,[\Phi_t]\,ds, & \text{for slip: } |g_t(U_t^{(k)})| > \mu_f \frac{\varepsilon_t}{\varepsilon_n} g_n(U_n^{(k)}). \end{cases}$$

Contact contribution to the right hand side – Return mapping for tangential contact traction

Linearization of the nonlinear contact terms $C(\boldsymbol{U}^{(k+1)})$ produces contributions to the system matrix and to the right-hand side, according to (4.34). The following terms must be added to the right hand side

$$-C(\boldsymbol{U}^{(k)}, \boldsymbol{\Phi}) = \int_{\Gamma_C} P_n[\Phi_n]\,ds + \int_{\Gamma_C} P_t[\Phi_t]\,ds.$$

The normal and tangential contact traction are computed with the constitutive relations

$$P_n := -\frac{1}{\varepsilon_n} g_n, \qquad P_t := -\frac{1}{\varepsilon_t} g_t^e.$$

Computation of the penetration function g_n and of the micro-stick function g_t^e is described in paragraph 4.2.1. The computational algorithm for the tangential traction P_t is known in the literature as the *return mapping algorithm.* It is a two-step algorithm of the predictor-corrector type. First, the trial value of the tangential traction is computed, based on the total tangential displacement g_t

$$P_t^{trial} := -\frac{1}{\varepsilon_t} g_t, \qquad g_t := [U_t].$$

Then, it is checked, if the trial friction force P_t^{trial} satisfies the Coulomb's frictional law. For this reason the value of the frictional yield function $\hat{f}_{fr}$ is computed

$$\hat{f}_{fr}(P_t^{trial}) := |P_t^{trial}| - \mu_f |P_n|$$

and, if the Coulomb's law is violated, the correction of P_t^{trial} is performed.

$$P_t = \begin{cases} P_t^{trial}, & \text{if } \hat{f}_{fr}(P_t^{trial}) \le 0, \\ \mu_f |P_n| \dfrac{P_t^{trial}}{||P_t^{trial}||}, & \text{if } \hat{f}_{fr}(P_t^{trial}) > 0. \end{cases}$$

4.2.6 Linearization of the plasticity terms in the FE domain – Return mapping for plasticity

Since we use the backward Euler scheme for plasticity in case of FE discretization, the energy bilinear form is nonlinear. We restrict our attention to the one of bodies with FE discretization and omit upper indexes "s" and "m" marking the master or the slave body.

Let us consider the linearization of the energy bilinear form closer.

$$(\sigma(\boldsymbol{U}^{(k+1)}), \varepsilon(\boldsymbol{\Phi}))_{\Omega^m} = (\sigma(\boldsymbol{U}^{(k)}), \varepsilon(\boldsymbol{\Phi}))_{\Omega^m} + \frac{\partial}{\partial \boldsymbol{U}^{(k)}}(\sigma(\boldsymbol{U}^{(k)}), \varepsilon(\boldsymbol{\Phi}))_{\Omega^m} \Delta \boldsymbol{U}^{(k+1)}$$

The first summand makes a contribution to the right-hand side and the last one makes a contribution to the matrix of the linear system as shown in Paragraph 4.2.3. Further we define the elastoplastic tangent moduli $(\mathbb{C}^{ep})^{(k+1)}$ by

$$\begin{aligned} \frac{\partial \sigma(\boldsymbol{U}^{(k)})}{\partial \boldsymbol{U}^{(k)}} \Delta \boldsymbol{U}^{(k+1)} &= \frac{\partial}{\partial \boldsymbol{U}^{(k)}} \mathbb{C} : (\varepsilon(\boldsymbol{U}^{(k)}) - \varepsilon^p(\boldsymbol{U}^{(k)})) \Delta \boldsymbol{U}^{(k+1)} && (4.36) \\ &= (\mathbb{C}^{ep})^{(k+1)} : \varepsilon(\Delta \boldsymbol{U}^{(k+1)}). && (4.37) \end{aligned}$$

We derive the explicit expression for $(\mathbb{C}^{ep})^{(k+1)}$ below.

Discretization of the yield condition, flow rule and hardening law (4.21) with $\Delta\gamma := \gamma_{n+1}\Delta t$ provides

$$\begin{aligned} \eta^{(k+1)} &:= \mathrm{dev}[\sigma^{(k+1)}] - \bar{\beta}^{(k+1)}, \qquad \mathrm{tr}[\bar{\beta}^{(k+1)}] := 0, \\ (\hat{f}_{pl})^{(k+1)} &= ||\eta^{(k+1)}|| - \sqrt{\frac{2}{3}} K(\alpha^{(k+1)}), \\ n^{(k+1)} &:= \frac{\eta^{(k+1)}}{||\eta^{(k+1)}||} \\ (\varepsilon^p)^{(k+1)} &= (\varepsilon^p)^{(k)} + \Delta\gamma n^{(k+1)}, && (4.38) \\ \bar{\beta}^{(k+1)} &= \bar{\beta}^{(k)} + \sqrt{\frac{2}{3}} \Delta H^{(k+1)} n^{(k+1)}, \\ \alpha^{(k+1)} &= \alpha^{(k)} + \Delta\gamma \sqrt{\frac{2}{3}}, \end{aligned}$$

where

$$\Delta H^{(k+1)} := H(\alpha^{(k+1)}) - H(\alpha^{(k)}).$$

and isotropic $K(\alpha)$ and kinematic $H(\alpha)$ hardening modules are defined by (4.22). The discrete version of loading/unloading complimentary Kuhn-Tucker conditions is

$$\Delta\gamma \geq 0, \qquad (\hat{f}_{pl})^{(k+1)} \leq 0, \qquad \Delta\gamma (\hat{f}_{pl})^{(k+1)} = 0. \qquad (4.39)$$

It is easier to work with deviatoric parts of the stress and the strain tensors

$$e := \mathrm{dev}[\varepsilon], \qquad s := \mathrm{dev}[\sigma].$$

On order to obtain the stress field, which satisfies the discrete Kuhn-Tucker conditions (4.39), we use the predictor-corrector scheme [60]. The predictor step is the pure elastic step. If the discrete Kuhn-Tucker conditions are not satisfied, then the corrector step is needed, which performs a correction of the stress deviator by changing the plastic part of the strain tensor. The method can be geometrically interpreted as the closest point projection of the stress onto the yield surface $(\hat{f}_{pl})^{(k+1)} = 0$. The method is also known as the *return mapping algorithm*.

First we perform the pure elastic trial step. Relation (4.23) yields $s^{trial} = 2\overline{\mu}e$. The discretized version is

$$\begin{aligned}
&(s^{trial})^{(k+1)} := s^{(k)} + 2\overline{\mu}\Delta e^{(k+1)}, \qquad \Delta e^{(k+1)} := e^{(k+1)} - e^{(k)} \\
&(\eta^{trial})^{(k+1)} := (s^{trial})^{(k+1)} - \bar{\beta}^{(k)}.
\end{aligned}$$

If the discrete yield condition is satisfied, i.e. $\hat{f}_{pl}((s^{trial})^{(k+1)}, \alpha^{(k)}, \bar{\beta}^{(k)}) \leq 0$, then there is no plastic loading occurs in the current step and we set

$$(s^{trial})^{(k+1)} := s^{(k+1)}, \qquad \Delta\gamma := 0.$$

If $\hat{f}_{pl}((s^{trial})^{(k+1)}, \alpha^{(k)}, \bar{\beta}^{(k)}) > 0$, the corrector step should be performed. The discrete conditions (4.38) yield

$$\begin{aligned}
s^{(k+1)} &= \mathrm{dev}[\mathbb{C} : (\varepsilon^{(k+1)} - (\varepsilon^p)^{(k+1)})] \\
&= \mathrm{dev}[\mathbb{C} : (\varepsilon^{(k)} + \Delta\varepsilon^{(k+1)} - (\varepsilon^p)^{(k)} - \Delta\gamma n^{(k+1)})] \\
&= s^{(k)} + \mathrm{dev}[\mathbb{C} : (\Delta\varepsilon^{(k+1)} - \Delta\gamma n^{(k+1)})] \\
&= s^{(k)} + 2\overline{\mu}\Delta e^{(k+1)} - 2\overline{\mu}\Delta\gamma n^{(k+1)} \\
&= (s^{trial})^{(k+1)} - 2\overline{\mu}\Delta\gamma n^{(k+1)}.
\end{aligned}$$

Therefore

$$\begin{aligned}
\eta^{(k+1)} &:= s^{(k+1)} - \bar{\beta}^{(k+1)} \\
&= (s^{trial})^{(k+1)} - 2\overline{\mu}\Delta\gamma n^{(k+1)} - \bar{\beta}^{(k)} - \sqrt{\frac{2}{3}}\Delta H^{(k+1)} n^{(k+1)} \\
&= (\eta^{trial})^{(k+1)} - \left(2\overline{\mu}\Delta\gamma + \sqrt{\frac{2}{3}}\Delta H^{(k+1)}\right) n^{(k+1)} \\
&=: (\eta^{trial})^{(k+1)} - A^{(k+1)} n^{(k+1)} \\
&=: (\eta^{trial})^{(k+1)} - A^{(k+1)} \frac{\eta^{(k+1)}}{||\eta^{(k+1)}||}
\end{aligned}$$

and

$$
\begin{aligned}
(\eta^{trial})^{(k+1)} &= \frac{\eta^{(k+1)}}{||\eta^{(k+1)}||}(||\eta^{(k+1)}|| + A^{(k+1)}),\\
||(\eta^{trial})^{(k+1)}|| &= ||\eta^{(k+1)}|| + A^{(k+1)}, \qquad (4.40)\\
A^{(k+1)} &= 2\overline{\mu}\Delta\gamma + \sqrt{\frac{2}{3}}\Delta H^{(k+1)}.
\end{aligned}
$$

This provides that the normal direction $n^{(k+1)}$ is defined fully in terms of $(\eta^{trial})^{(k+1)}$:

$$
\frac{(\eta^{trial})^{(k+1)}}{||(\eta^{trial})^{(k+1)}||} = \frac{\eta^{(k+1)}}{||\eta^{(k+1)}||} =: n^{(k+1)}.
$$

As the yield condition was not satisfied after the trial step, the corrector step should return the stress on the yield surface, i.e.

$$
(\hat{f}_{pl})^{(k+1)} := ||\eta^{(k+1)}|| - \sqrt{\frac{2}{3}}K(\alpha^{(k+1)}) = 0.
$$

Finally, we obtain the closed nonlinear system for finding the consistency parameter $\Delta\gamma$

$$
\begin{aligned}
(\hat{f}_{pl})^{(k+1)} &:= ||(\eta^{trial})^{(k+1)}|| - \left(2\overline{\mu}\Delta\gamma + \sqrt{\frac{2}{3}}\Delta H^{(k+1)}\right) - \sqrt{\frac{2}{3}}K(\alpha^{(k+1)}) = 0,\\
\alpha^{(k+1)} &= \alpha^{(k)} + \sqrt{\frac{2}{3}}\Delta\gamma. \qquad (4.41)
\end{aligned}
$$

Note, that if kinematic/isotropic hardening law is given by (4.22), the system (4.41) is linear and can be rewritten as

$$
\begin{aligned}
(\hat{f}_{pl})^{(k+1)} &:= (\hat{f}_{pl}^{trial})^{(k+1)} - (2\overline{\mu} + \frac{2}{3}\bar{H})\Delta\gamma = 0,\\
(\hat{f}_{pl}^{trial})^{(k+1)} &:= ||(\eta^{trial})^{(k+1)}|| - \sqrt{\frac{2}{3}}(\sigma_Y + \theta\bar{H}\alpha^{(k)}).
\end{aligned}
$$

Now we can establish the update formula for the consistent elastoplastic tangent moduli $(\mathbb{C}^{ep})^{(k+1)}$. For the stress tensor there holds

$$
\begin{aligned}
\sigma^{(k+1)} &= \kappa\,\mathrm{tr}[\varepsilon^{(k+1)}]\mathbf{1} + s^{(k+1)}\\
&= \kappa\,\mathrm{tr}[\varepsilon^{(k+1)}]\mathbf{1} + 2\overline{\mu}e^{(k+1)} - 2\overline{\mu}\Delta\gamma n^{(k+1)}\\
&= \mathbb{C} : \varepsilon^{(k+1)} - 2\overline{\mu}\Delta\gamma n^{(k+1)}.
\end{aligned}
$$

This yields

$$
\begin{aligned}
d\sigma^{(k+1)} &= \mathbb{C} : d\varepsilon^{(k+1)} - 2\overline{\mu}(d(\Delta\gamma)n^{(k+1)} + \Delta\gamma dn^{(k+1)})\\
&= \left(\mathbb{C} - 2\overline{\mu}n^{(k+1)} \otimes \frac{\partial\Delta\gamma}{\partial\varepsilon^{(k+1)}} - 2\overline{\mu}\Delta\gamma\frac{\partial n^{(k+1)}}{\partial\varepsilon^{(k+1)}}\right) : d\varepsilon^{(k+1)} \qquad (4.42)\\
&= (\mathbb{C}^{ep})^{(k+1)} : d\varepsilon^{(k+1)}.
\end{aligned}
$$

It is easy to show [60, Lemma 3.2] that

$$\frac{\partial n^{(k+1)}}{\partial (\eta^{trial})^{(k+1)}} = \frac{1}{||(\eta^{trial})^{(k+1)}||}\left(\boldsymbol{I} - n^{(k+1)} \otimes n^{(k+1)}\right) \tag{4.43}$$

$$\frac{\partial ||(\eta^{trial})^{(k+1)}||}{\partial (\eta^{trial})^{(k+1)}} = \frac{(\eta^{trial})^{(k+1)}}{||(\eta^{trial})^{(k+1)}||} = n^{(k+1)}. \tag{4.44}$$

Furthermore, there holds

$$\frac{\partial (\eta^{trial})^{(k+1)}}{\partial \varepsilon^{(k+1)}} = 2\overline{\mu}\frac{\partial e^{(k+1)}}{\partial \varepsilon^{(k+1)}} = 2\overline{\mu}\left(\boldsymbol{I} - \frac{1}{3}\mathbf{1}\otimes\mathbf{1}\right).$$

This and (4.43) give

$$\begin{aligned}\frac{\partial n^{(k+1)}}{\partial \varepsilon^{(k+1)}} &= \frac{2\overline{\mu}}{||(\eta^{trial})^{(k+1)}||}\left(\boldsymbol{I} - n^{(k+1)} \otimes n^{(k+1)}\right) : \left(\boldsymbol{I} - \frac{1}{3}\mathbf{1}\otimes\mathbf{1}\right)\\ &= \frac{2\overline{\mu}}{||(\eta^{trial})^{(k+1)}||}\left(\boldsymbol{I} - \frac{1}{3}\mathbf{1}\otimes\mathbf{1} - n^{(k+1)} \otimes n^{(k+1)}\right).\end{aligned} \tag{4.45}$$

Differentiating the consistency condition (4.41) we obtain

$$\frac{\partial ||(\eta^{trial})^{(k+1)}||}{\partial \varepsilon^{(k+1)}} = 2\overline{\mu}\frac{\Delta\gamma}{\partial \varepsilon^{(k+1)}} + \sqrt{\frac{2}{3}}\left[K'(\alpha^{(k+1)}) + H'(\alpha^{(k+1)})\right]\frac{\alpha^{(k+1)}}{\partial \varepsilon^{(k+1)}}. \tag{4.46}$$

For the first term the chain rule and (4.44) provide

$$\begin{aligned}\frac{\partial ||(\eta^{trial})^{(k+1)}||}{\partial \varepsilon^{(k+1)}} &= \frac{\partial ||(\eta^{trial})^{(k+1)}||}{\partial (\eta^{trial})^{(k+1)}} : \frac{\partial (\eta^{trial})^{(k+1)}}{\partial \varepsilon^{(k+1)}}\\ &= 2\overline{\mu}\left(\boldsymbol{I} - \frac{1}{3}\mathbf{1}\otimes\mathbf{1}\right) : n^{(k+1)} = 2\overline{\mu}n^{(k+1)}.\end{aligned}$$

The hardening law in (4.38) yields

$$\frac{\alpha^{(k+1)}}{\partial \varepsilon^{(k+1)}} = \sqrt{\frac{2}{3}}\frac{\Delta\gamma}{\partial \varepsilon^{(k+1)}}$$

Thus, we derive from (4.46)

$$\frac{\partial \Delta\gamma}{\partial \varepsilon^{(k+1)}} = \left[1 + \frac{K'(\alpha^{(k+1)}) + H'(\alpha^{(k+1)})}{3\overline{\mu}}\right]^{-1} n^{(k+1)}. \tag{4.47}$$

Inserting relations (4.45) and (4.47) in (4.42) provides the following representation for the elastoplastic tangent moduli

$$\begin{aligned}\mathbb{C}^{ep} &= \mathbb{C} - 2\overline{\mu}n^{(k+1)} \otimes \frac{\partial \Delta\gamma}{\partial \varepsilon^{(k+1)}} - 2\overline{\mu}\Delta\gamma\frac{\partial n^{(k+1)}}{\partial \varepsilon^{(k+1)}}\\ &= \kappa\mathbf{1}\otimes\mathbf{1} + 2\overline{\mu}\left(\boldsymbol{I} - \frac{1}{3}\mathbf{1}\otimes\mathbf{1}\right)\\ &- 2\overline{\mu}\left[1 + \frac{K'(\alpha^{(k+1)}) + H'(\alpha^{(k+1)})}{3\overline{\mu}}\right]^{-1} n^{(k+1)} \otimes n^{(k+1)}\\ &- 2\overline{\mu}\Delta\gamma\frac{2\overline{\mu}}{||(\eta^{trial})^{(k+1)}||}\left(\boldsymbol{I} - \frac{1}{3}\mathbf{1}\otimes\mathbf{1} - n^{(k+1)} \otimes n^{(k+1)}\right)\end{aligned}$$

or

$$\mathbb{C}^{ep} = \kappa \mathbf{1} \otimes \mathbf{1} + 2\overline{\mu} a^{(k+1)} \left(\boldsymbol{I} - \frac{1}{3} \mathbf{1} \otimes \mathbf{1} \right) - 2\overline{\mu} b^{(k+1)} n^{(k+1)} \otimes n^{(k+1)},$$
$$a^{(k+1)} = 1 - \frac{2\overline{\mu}\Delta\gamma}{||(\eta^{trial})^{(k+1)}||}$$
$$b^{(k+1)} = \left[1 + \frac{K'(\alpha^{(k+1)}) + H'(\alpha^{(k+1)})}{3\overline{\mu}} \right]^{-1} - (1 - a^{(k+1)}).$$

This representation used in (4.36) generates the linear system matrix contribution corresponding to the plastic behaviour.

4.2.7 Numerical examples

Example 1

The model problem can be interperted as an idealised isothermic metal forming process, described as follows. An elastic stamp comes in contact with a plastic work piece and leaves some plastic deformations in it. Then the stamp changes its location, comes into contact with the work piece in the neighbours place and initiates some plastic deformations again. Without loss of generality we denote the stamp as a slave body and the work piece as a master body. The coordinates of the stamp in the moment of the first touch are $\Omega_1^s := [0.2, 1.2] \times [-1, 1]$, and in the moment of the second touch are $\Omega_2^s := [-1.8, -0.8] \times [-1, 1]$. The work piece is given by $\Omega^m := [-2, 2] \times [-3, -1]$. Both touches are performed by setting prescribed total displacement on the Dirichlet boundary of the work piece $\Gamma_D^m := [-2, 2] \times \{-3\}$ by $\boldsymbol{u}_D^m := 4, 3 \cdot 10^{-3}$. This total displacement is applied in the incremental form. The homogeneous displacement $\boldsymbol{u}_D^s = 0$ is prescribed on the Dirichlet boundary $\Gamma_{D,1}^s := [0.2, 1.2] \times \{1\}$, $\Gamma_{D,2}^s := [-1.8, -0.8] \times \{1\}$ of the stamp for the first and second touch respectively.

On Figures 4.1 - 4.4 we present the deformed mesh and the norm of the plastic strain tensor $||\varepsilon^p|| := \sqrt{\varepsilon^p : \varepsilon^p}$ in both bodies for both approaches. One can clearly observe the similar plastic deformations in the work piece for FEM and BEM modelling of the stamp. To make more feeling of deformation inside the stamp modelled with BEM, we interpolate the FE mesh, compute displacement inside the body using the representation formula and compute corresponding deformed state. The displacement is multiplied with the factor 100 to make it visible. The evolution of the stress deviator norm in dependence of the applied force in the characteristic point $X = (-0.9; -1, 1)$ in the work piece is shown on Figure 4.5. The curves for FE/FE and FE/BE simulations are very close.

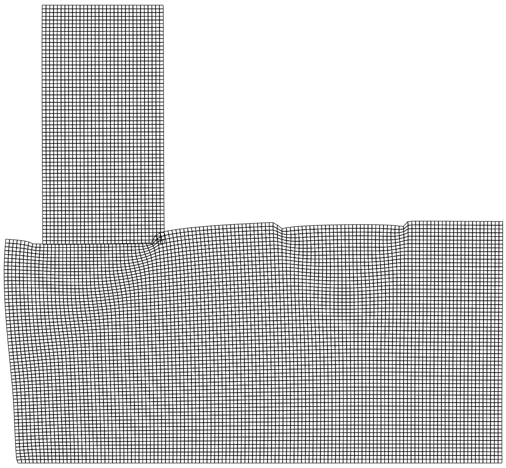

Figure 4.1: FE/FE: deformed mesh

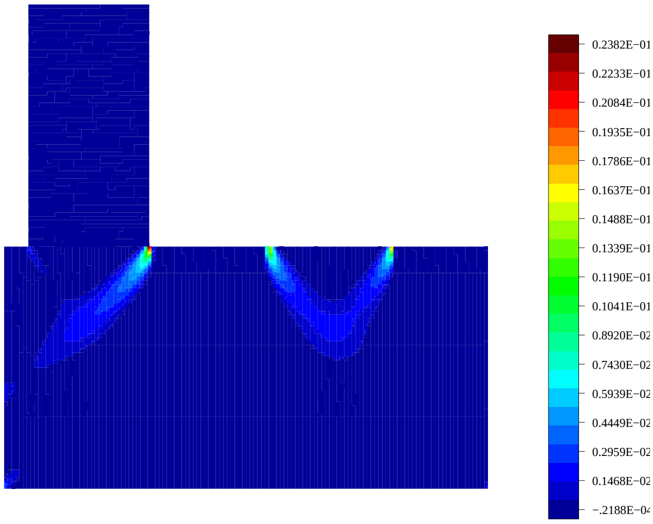

Figure 4.2: FE/FE: $||\varepsilon^p||$

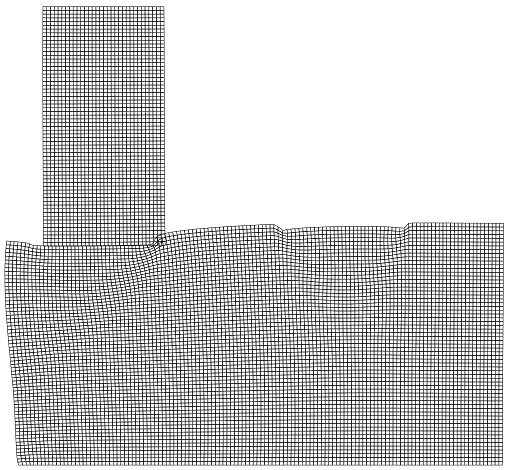

Figure 4.3: FE/BE: deformed mesh

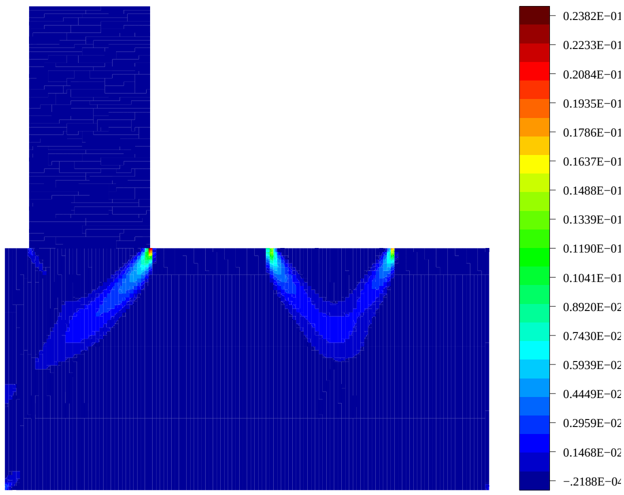

Figure 4.4: FE/BE: $||\varepsilon^p||$

Example 2

We make now a single touch in the middle of the work piece The coordinates of the stamp in the moment of the touch are $\Omega^s := [-1,1] \times [-1,0]$. The work piece is given again by $\Omega^m := [-2,2] \times [-3,-1]$. The Dirichlet boundary of the stamp $\Gamma_D^s := [-1,1] \times \{0\}$ is assumed to be fixed, i.e. $\boldsymbol{u}_D^s = 0$. The Dirichlet boundary of the work piece $\Gamma_D^m := [-2,2] \times \{-3\}$ is subjected to the total displacement $\boldsymbol{u}_D^m := 4,2 \cdot 10^{-3}$, applied incrementally.

On Figures 4.6 - 4.11 we present deformed meshes and the plastic strain norms. They reflect qualitatively the same behaviour. On Figure 4.12 we show the evolution of the norm

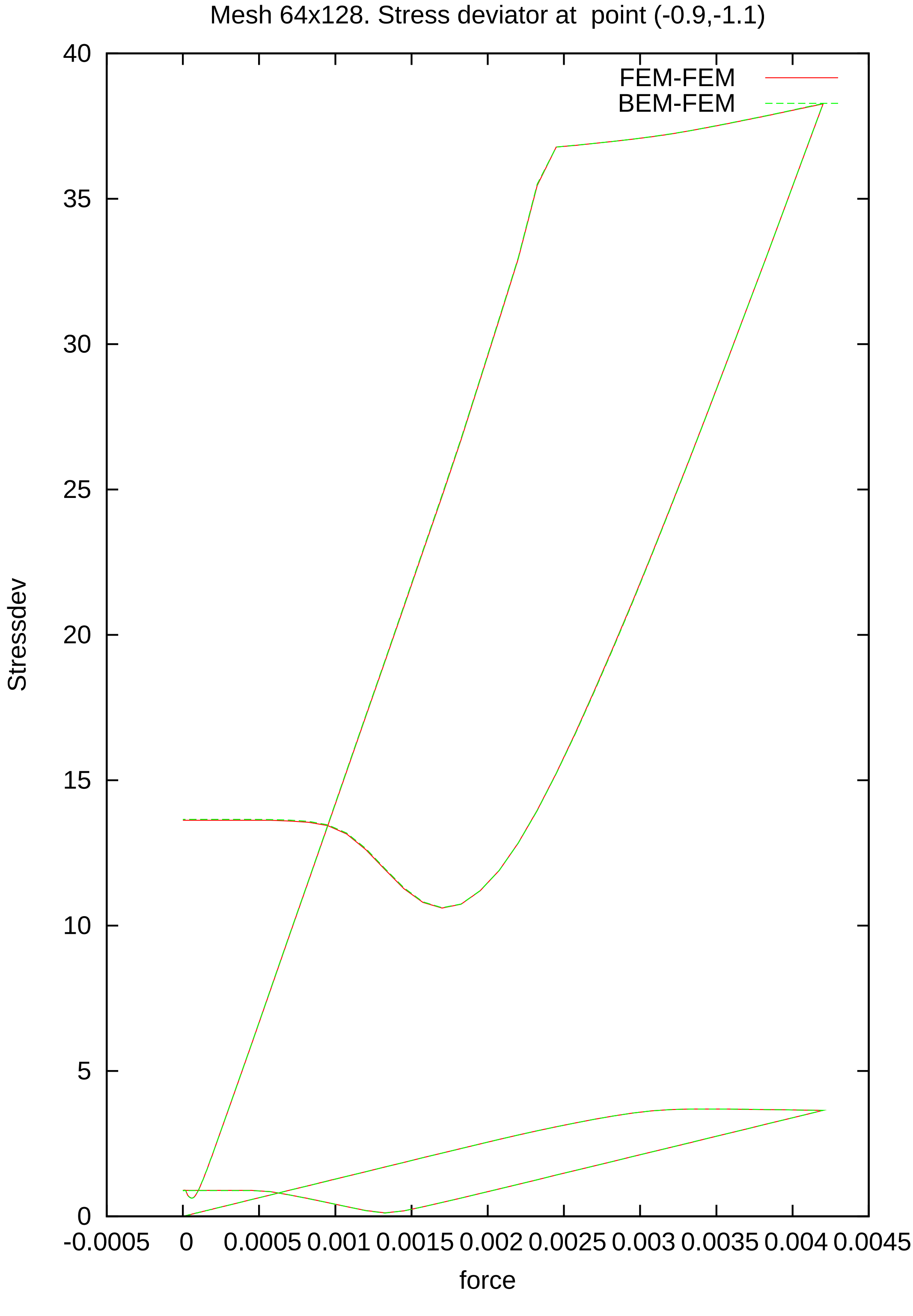

Figure 4.5: FE/FE, FE/BE: $||\,\mathrm{dev}\,\sigma||$

of the stress deviator for all three methods in the characteristic point $X = (1; -1, 1)$. One observe that both curves with the FEM modelling are pretty close to each other. The curve for BEM in the work piece shows qualitatively the similar behaviour.

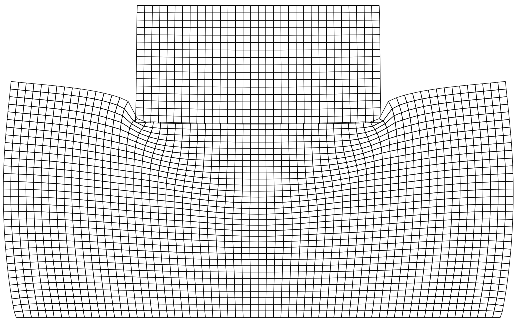

Figure 4.6: FE/FE: deformed mesh

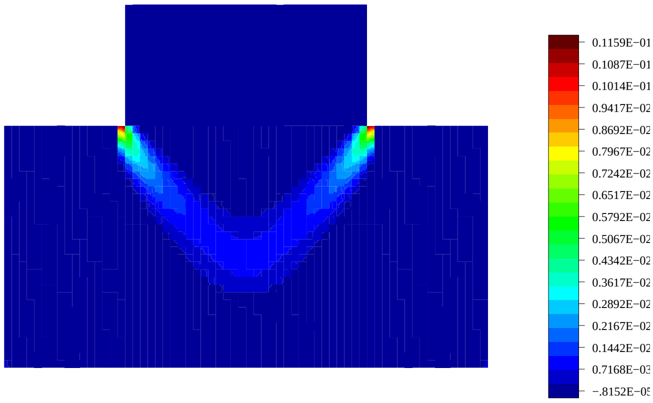

Figure 4.7: FE/FE: $||\varepsilon^p||$

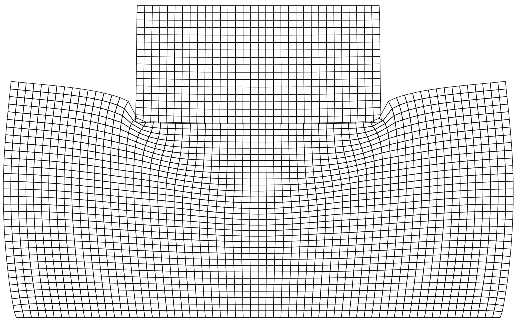

Figure 4.8: FE/BE: deformed mesh

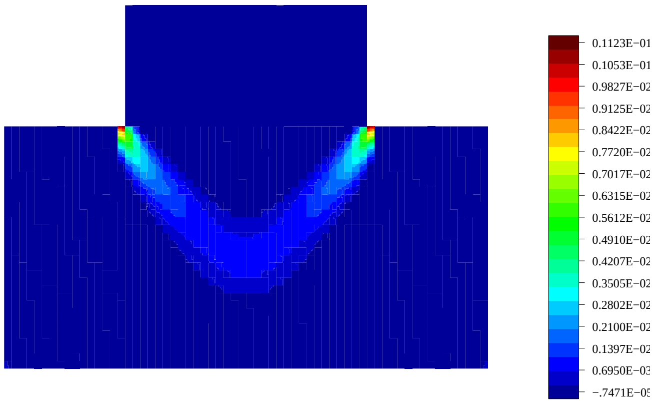

Figure 4.9: FE/BE: $||\varepsilon^p||$

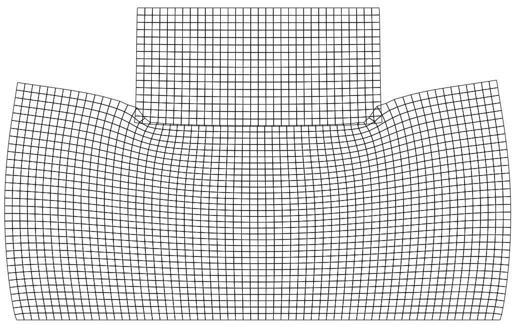

Figure 4.10: BE/BE: deformed mesh

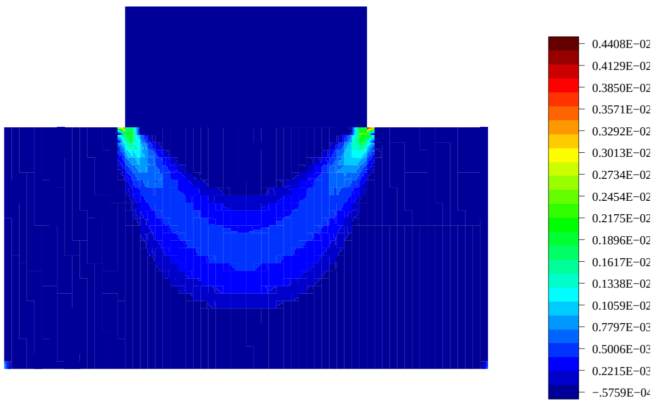

Figure 4.11: BE/BE: $||\varepsilon^p||$

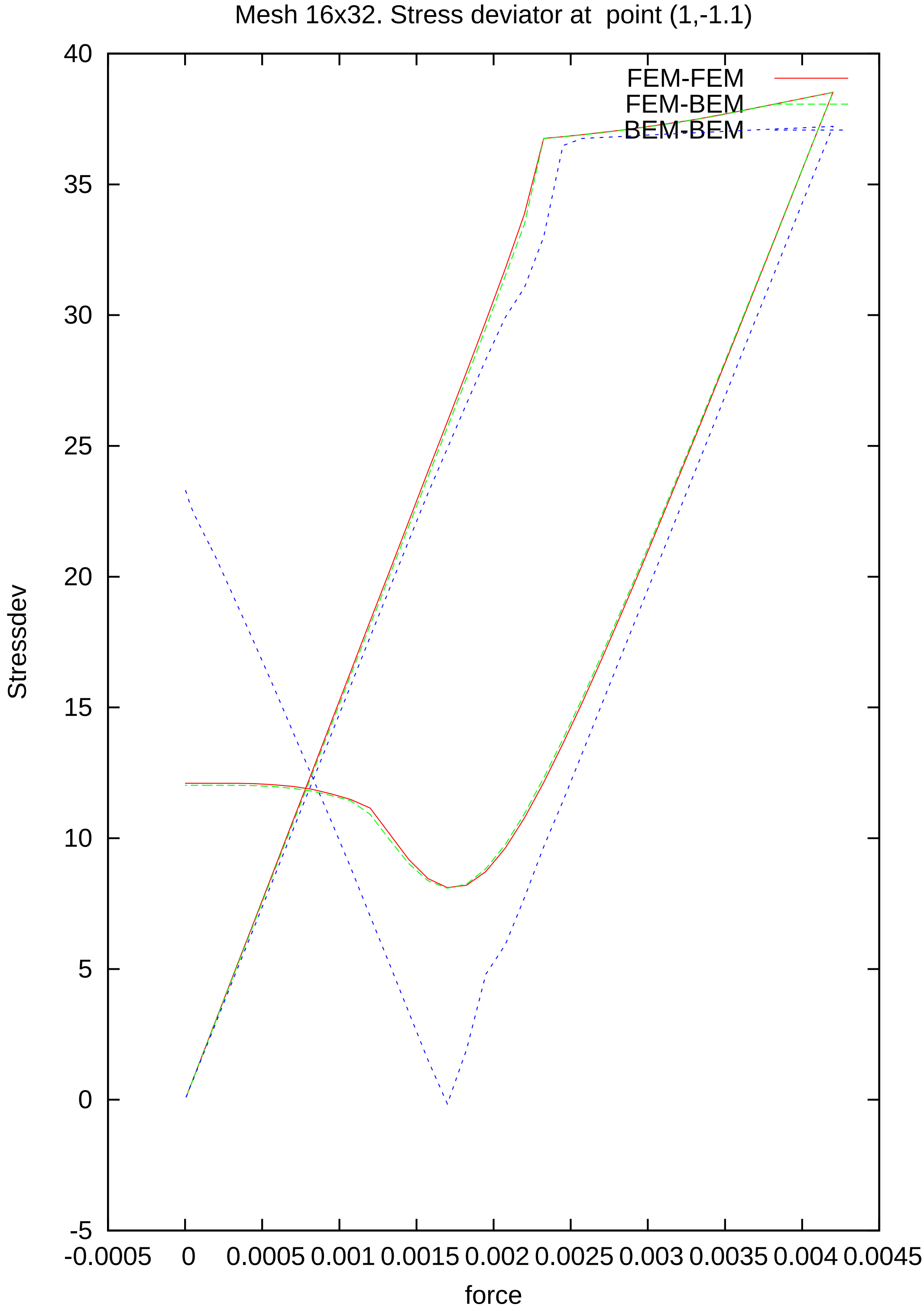

Figure 4.12: FE/FE, FE/BE, BE/BE: $||\operatorname{dev}\sigma||$

4.2.8 Numerical examples for adaptive mesh refinement

The proofs of the a posteriori error estimates from Section 3.3 for frictional contact between an elastic body and a rigid obstacle can be easily generalized to the case of two-body frictional contact problem in elasticity. Moreover, the refinement procedure can be performed in the both bodies independently. The three coupling combinations FE/FE, FE/BE and BE/BE can be performed and the FE indicator (3.100) and the BE indicator (3.107) can be applied in the FE and in the BE part respectively.

Let us consider a frictional contact problem between two elastic bodies Ω^s, Ω^m, where

$$\Omega^s := [-1/2, 1/2] \times [0, 2], \qquad \Omega^m := [-2, 2] \times [-2, 0].$$

The upper boundary of Ω^s is fixed and on the lower boundary of Ω^m the displacements are prescribed, i.e.

$$\begin{aligned} \boldsymbol{u}^s &= 0, && \text{on } \Gamma_D^s := [-1/2, 1/2] \times \{2\}, \\ \boldsymbol{u}^m &= 5 \cdot 10^{-4}, && \text{on } \Gamma_D^m := [-2, 2] \times \{-2\}. \end{aligned}$$

The remaining parts of the boundaries are treated as contact boundaries

$$\Gamma_C^s := \partial\Omega^s \setminus \Gamma_D^s, \qquad \Gamma_C^m := \partial\Omega^m \setminus \Gamma_D^m.$$

The both bodies have the same material parameters $E = 266926.0$, $\nu = 0.29$ and the coefficient of friction $\mu_f = 0.1$. The examples for boundary elements were presented for one-body frictional contact problems in Paragraph 3.3.5. We use here the FEM discretization in both bodies.

The automatic adaptive mesh refinement procedure is given by Algorithm 3.2. On each iteration step k, new meshes $\mathcal{T}_{h,k+1}^s$, $\mathcal{T}_{h,k+1}^m$ are generated, according to the values of the error indicators (3.100) and the refinement rules. Then the following discrete problem is solved: Find $\boldsymbol{U} = (\boldsymbol{U}^s, \boldsymbol{U}^m) \in \boldsymbol{\mathcal{V}}_{F,h}^s \times \boldsymbol{\mathcal{V}}_{F,D,h}^m$, such that

$$(\sigma(\boldsymbol{U}), \varepsilon(\boldsymbol{\Phi}))_{\Omega^s \cup \Omega^m} - \left\langle \boldsymbol{P}^\varepsilon, [\boldsymbol{\Phi}] \right\rangle_{\Gamma_C} = \left\langle \hat{\boldsymbol{t}}, \boldsymbol{\Phi} \right\rangle_{\Gamma_N}, \qquad \forall \boldsymbol{\Phi} \in \boldsymbol{\mathcal{V}}_{F,h}^s \times \boldsymbol{\mathcal{V}}_{F,h}^m,$$

where the discrete finite element spaces for $b = s, m$ are given by

$$\begin{aligned} \boldsymbol{\mathcal{V}}_{F,D,h}^b &:= \left\{ \boldsymbol{\Phi} \in \boldsymbol{H}^1(\Omega^b) : \boldsymbol{\Phi}|_K \in \left[\mathcal{R}^1(K)\right]^2 \ \forall K \in \mathcal{T}_{F,h}^b,\ \boldsymbol{\Phi}|_{\Gamma_D} = \hat{\boldsymbol{u}}^b \right\}, \\ \boldsymbol{\mathcal{V}}_{F,h}^b &:= \left\{ \boldsymbol{\Phi} \in \boldsymbol{H}^1(\Omega^b) : \boldsymbol{\Phi}|_K \in \left[\mathcal{R}^1(K)\right]^2 \ \forall K \in \mathcal{T}_{F,h}^b,\ \boldsymbol{\Phi}|_{\Gamma_D} = 0 \right\}, \end{aligned}$$

where $\mathcal{R}^1(K)$ represents the linear functions $\mathcal{P}^1(K)$, if K is a triangle, or the bilinear functions $\mathcal{Q}^1(K)$, if K is a quadrilateral. According to (4.19), (4.20),

$$\boldsymbol{P} := P_n \boldsymbol{n} + P_t \boldsymbol{t}, \qquad P_n := -\frac{1}{\varepsilon_n} \mathrm{g}_n, \qquad P_t := -\frac{1}{\varepsilon_t} \mathbf{g}_t^e \cdot \boldsymbol{t}.$$

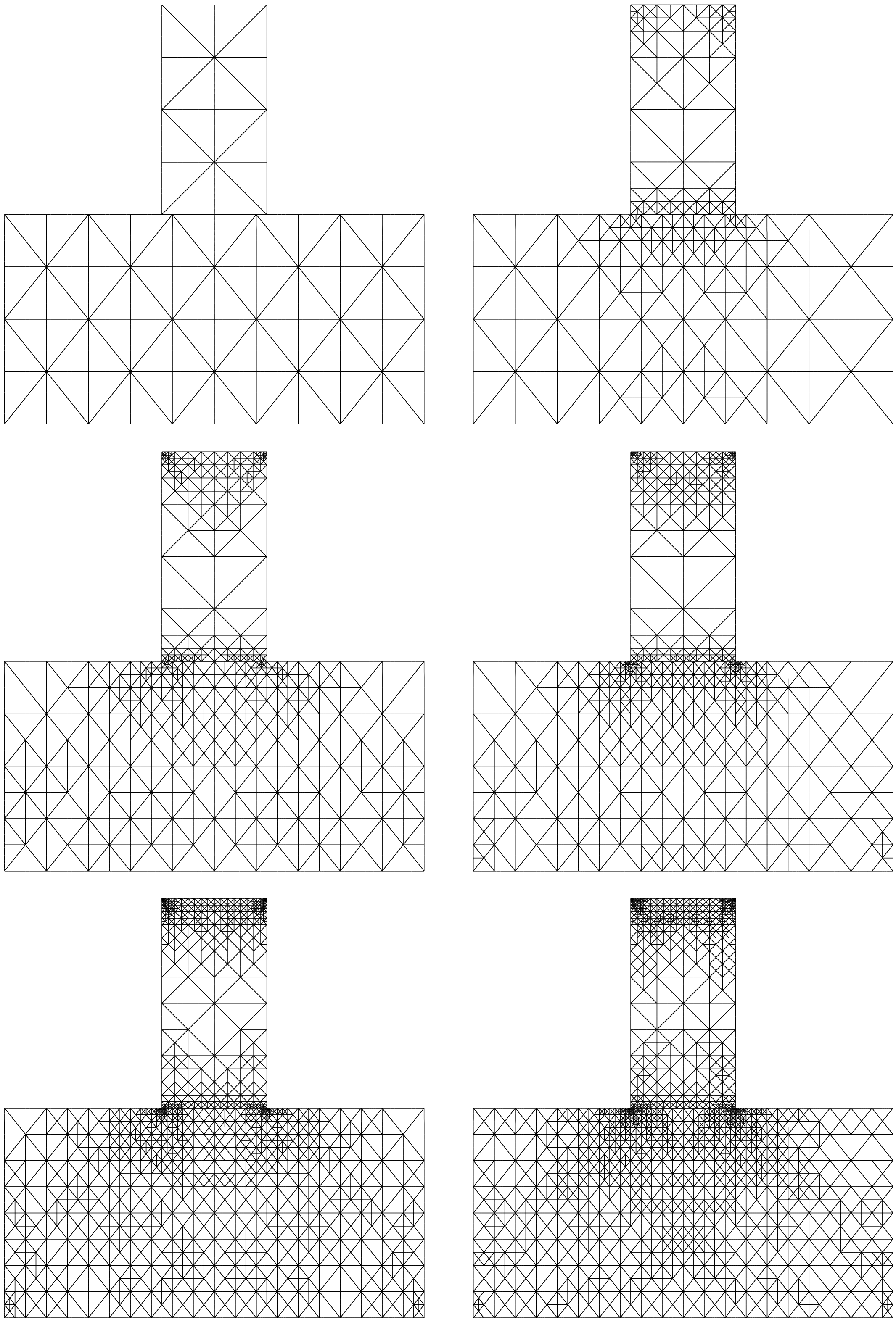

Figure 4.13: Initial mesh and adaptively generated meshes after 5^{th}, 10^{th}, 21^{st}, 36^{th} and 42^{nd} refinement steps

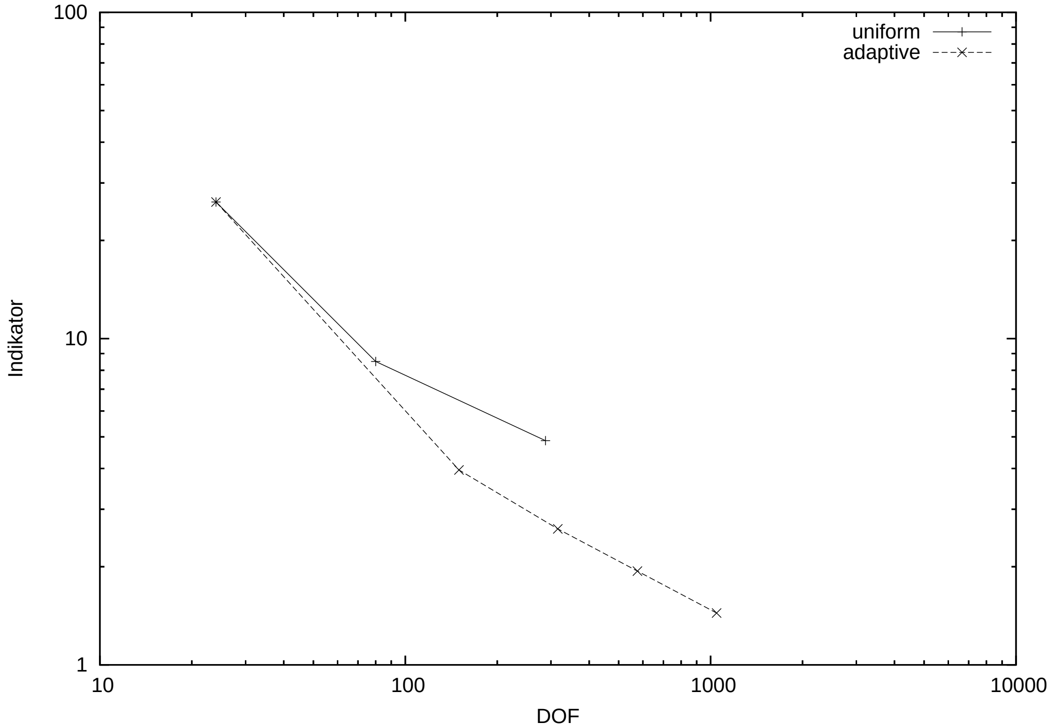

Figure 4.14: Value of error indicator (3.100) in Ω^s for uniform and adaptive mesh refinement

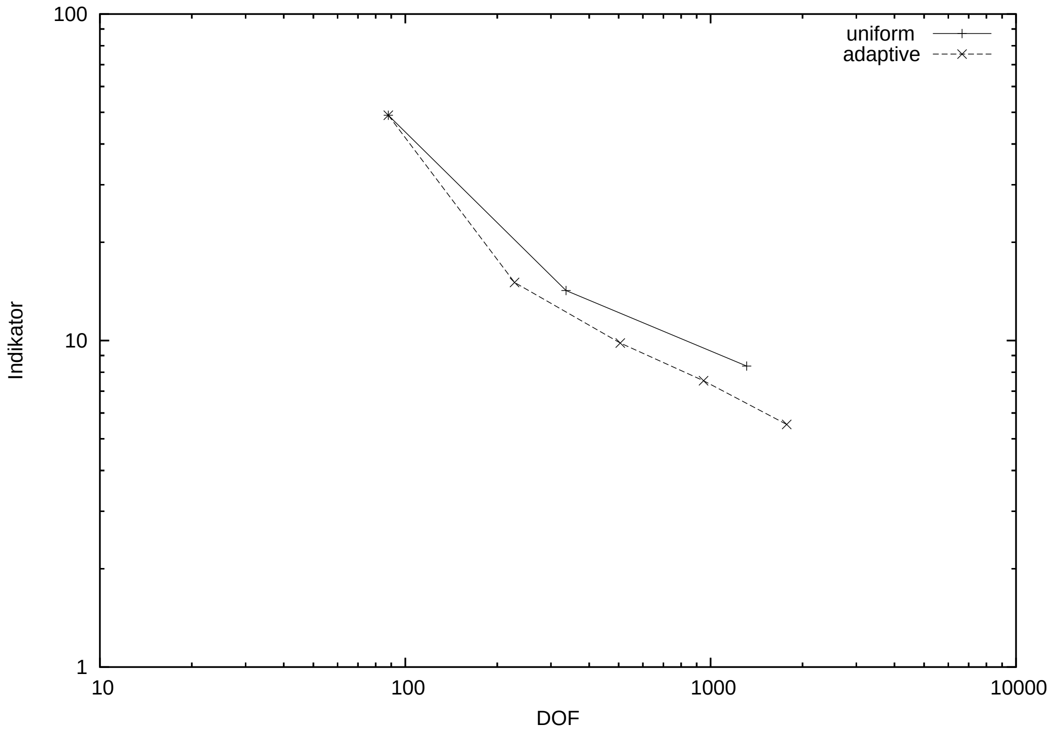

Figure 4.15: Value of error indicator (3.100) in Ω^m for uniform and adaptive mesh refinement

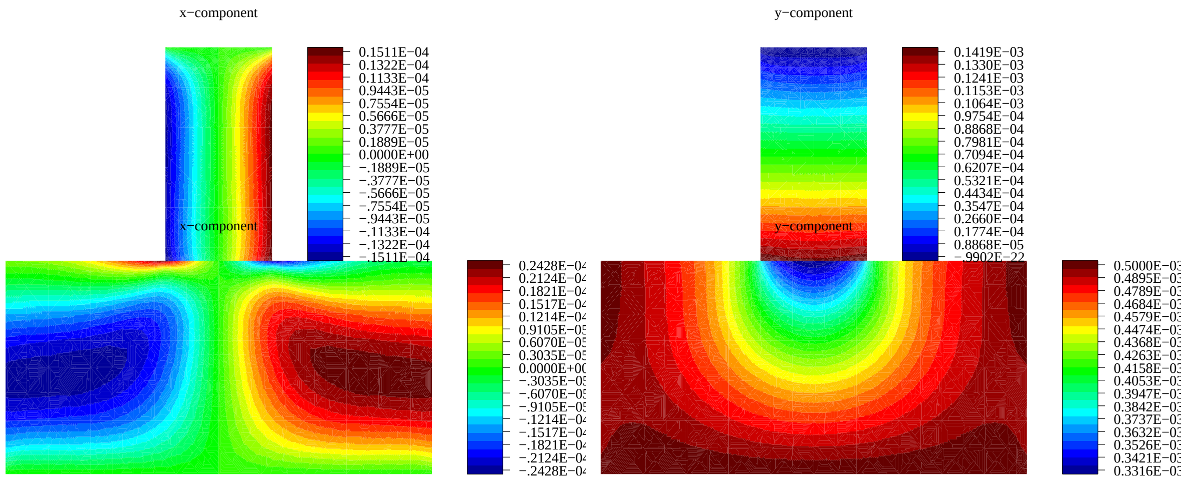

Figure 4.16: x- and y-components of the displacements after 42^{nd} refinement step

The sequence of adaptively generated meshes is shown in Figure (4.13). We observe that the most of refinement happens on the zone of *actual* contact, and near the points, where the boundary conditions change (contact / no contact or no contact / Dirichlet). We compare behaviour of the error indicators for the uniform and adaptive mesh refinement for Ω^s and Ω^m in Figure 4.14 and Figure 4.15 respectively. The x- and y-components of the displacements after 42^{nd} refinement step are given in Figure 4.16.

4.3 hp-mortar BEM for variational inequality

A novel hp-mortar BEM method for two-body frictional contact problems for non-matched discretizations is constructed in this section. The contact constraints are imposed in the weak sense on the discrete set of Gauss-Lobatto points involving the hp-mortar projection operator. The problem is reformulated as a discrete variational inequality of the second kind with the Steklov-Poincaré operator over a discrete convex set of admissible solutions. We obtain an upper bound for the discretization error in the energy norm. Due to the nonconformity of our approach, the error is decomposed into the approximation error and the consistency error. Finally, we show that for quasiuniform meshes the discrete solution converges to the exact solution as $\mathcal{O}((h/p)^{1/4})$ in the energy norm under additional assumption on the discretization parameters. We solve the discrete problem applying a Dirichlet-to-Neumann algorithm. The original two-body formulation is rewritten as a one-body contact problem and a one-body Neumann problem (see also Chernov et al. [18]). Then the global problem is solved with fixed point iterations. An alternative approach is the Uzawa algorithm, which consists of solving two independent one-body problems with a subsequent update for the contact traction. The error indicator obtained for the pure FE approach for interface problems by Wohlmuth [70] is extended here to frictional contact problems (also with boundary elements) and is applied in an automatic mesh refinement procedure together with the three-step hp-refinement algorithm (see e.g. Maischak and Stephan [47]). Then numerical examples are given, which underline the suggested approach.

4.3.1 Discretization

Consider two polygonal domains Ω^1, Ω^2 with Lipschitz boundaries $\Gamma^i := \partial\Omega^i$, $i = 1, 2$. As introduced in Section 4.1, we assume that each Γ^i consists of three disjoint parts Γ^i_D, Γ^i_N and Γ^i_C. For simplicity of presentation we assume that the bodies are initially in contact along $\Gamma_C \equiv \Gamma^1_C \equiv \Gamma^2_C$ (Γ_C can not enlarge), and that Γ_C is a straight line segment. Similarly to Section 3.2, we assume that Γ_D and Γ_C are connected curves and $\overline{\Gamma}_D \cap \overline{\Gamma}_C = \emptyset$. With each Γ^i we associate a finite family of disjoint straight line segments $\mathcal{T}^i_h$, with diameters not exceeding h_i.

$$\overline{\Gamma}^i = \bigcup_{I \in \mathcal{T}^i_h} \overline{I}.$$

We allow only conforming meshes $\mathcal{T}^i_h$, i.e. every segment from $\mathcal{T}^i_h$ is a subset of either Γ^i_D or Γ^i_N or Γ^i_C. Let $\mathcal{P}_{p_I}(I)$ define the space of polynomials on I, with degree less or equal p_I. We define the boundary element spaces on Γ^i as

$$\boldsymbol{\mathcal{V}}^i_{hp} := \left\{ \boldsymbol{U} \in \boldsymbol{\mathcal{V}}^i : \forall I \in \mathcal{T}^i_h, \boldsymbol{U} \in [\mathcal{P}_{p_I}(I)]^2 \right\}, \qquad \boldsymbol{\mathcal{V}}_{hp} := \boldsymbol{\mathcal{V}}^1_{hp} \times \boldsymbol{\mathcal{V}}^2_{hp},$$
$$\boldsymbol{\mathcal{W}}^i_{hp} := \left\{ \boldsymbol{U} \in \boldsymbol{\mathcal{W}}^i : \forall I \in \mathcal{T}^i_h, \boldsymbol{U} \in [\mathcal{P}_{p_I-1}(I)]^2 \right\}, \qquad \boldsymbol{\mathcal{W}}_{hp} := \boldsymbol{\mathcal{W}}^1_{hp} \times \boldsymbol{\mathcal{W}}^2_{hp},$$

where $\boldsymbol{\mathcal{V}}^i, \boldsymbol{\mathcal{W}}^i$ are given by (4.2) and (4.3) respectively. We assume that the meshes $\mathcal{T}_h^i$ and the polynomial degree distributions in $\boldsymbol{\mathcal{V}}_{hp}^i$ are quasiuniform, i.e.

$$\forall I, J \in \mathcal{T}_h^i \quad \exists C > 0 : \qquad \frac{|I|}{|J|} < C, \quad \frac{p_I}{p_J} < C, \qquad i = 1, 2,$$

and C is independent of I, J. Let

$$h_i := \max_{I \in \mathcal{T}_h^i} |I|, \qquad p_i := \min_{I \in \mathcal{T}_h^i} p_I$$

be the characteristic mesh size and the characteristic polynomial degree in $\boldsymbol{\mathcal{V}}_{hp}^1, \boldsymbol{\mathcal{V}}_{hp}^2$. Note that so far there is no relation imposed between h_1 and h_2 as well as between p_1 and p_2.

Since the meshes $\mathcal{T}_h^1$ and $\mathcal{T}_h^2$ induce two independent partitions of Γ_C, we can not incorporate the contact conditions directly into the set of admissible discrete solutions, as it was done for the variational formulation (4.5). In order to define discrete contact conditions we introduce an auxiliary space of normal traces on Γ_C, associated with $\mathcal{T}_h^1$ and $\mathcal{T}_h^2$

$$\mathcal{N}_{hp}^i := \left\{ W = \boldsymbol{U} \cdot \boldsymbol{n}^i|_{\Gamma_C} : \boldsymbol{U} \in \boldsymbol{\mathcal{V}}_{hp}^i \right\}, \qquad i = 1, 2 \tag{4.48}$$

and the mortar space, associated with $\mathcal{T}_h^1$

$$\mathcal{M}_{hp}^1 := \left\{ \Psi \in \mathcal{N}_{hp}^i : \Psi \in \mathcal{P}_{p_I - 1}(I), \text{ if } I \cap \partial\Gamma_C \neq \emptyset \right\}. \tag{4.49}$$

We define the hp-mortar projection operator (e.g. [59]) as the mapping $\pi_{hp}^1 : H^{1/2}(\Gamma_C) \to \mathcal{N}_{hp}^1$ with

$$\begin{aligned} \pi_{hp}^1 \varphi &= \varphi && \text{in } \partial\Gamma_C, \\ \int_{\Gamma_C} (\varphi - \pi_{hp}^1 \varphi)\, \Psi^1 \, ds &= 0 && \forall \Psi^1 \in \mathcal{M}_{hp}^1, \end{aligned} \tag{4.50}$$

The hp-mortar projection operator was studied by Bernardi, Maday, Patera in [11], [12], Ben Belgacem, Suri, Seshaiyer, Chilton in [59], [9], [7], [58] in the context of domain decomposition methods. Further, we need the following approximation and stability properties of π_{hp}^1.

Lemma 4.3.1. *[7] For any $\nu \geq 0$ there exists $C > 0$ such that $\forall \chi \in H^{1+\nu}(-1,1)$,*

$$||\chi - \pi_{hp}^1 \chi||_{\tilde{H}^{1/2}(-1,1)} \leq C \frac{h_1^{1/2+\eta}}{p_1^{1/2+\nu}} \sqrt{\log p_1} ||\chi||_{H^{1+\nu}(-1,1)}, \tag{4.51}$$

where $\eta = \min(\nu, p_1)$.

Lemma 4.3.2. *[59] If the mesh refinement is not stronger than geometric (see [59, Condition (M)]), then for $\forall \chi \in \tilde{H}^{1/2}(-1,1)$ there exists a constant $C > 0$, such that*

$$||\pi_{hp}^1 \chi||_{\tilde{H}^{1/2}(-1,1)} \leq C p_1^{3/4} ||\chi||_{\tilde{H}^{1/2}(-1,1)}. \tag{4.52}$$

Furthermore, according to [58] the stability constant can not be improved.

Let G^i_{hp} be the set of Gauss-Lobatto nodes associated with the elements of $\mathcal{T}^i_h$. Now we are in the position to define the set of admissible Galerkin solutions $\boldsymbol{\mathcal{K}}_{hp}$ of (4.55) below, by imposing non-penetration conditions only on G^1_{hp}.

$$\boldsymbol{\mathcal{K}}_{hp} := \left\{ \boldsymbol{U} \in \boldsymbol{\mathcal{V}}_{hp} : \, (U^1_n - \pi^1_{hp} U^2_n)(x) \leq 0 \;\; \forall x \in G^1_{hp} \cap \Gamma_C \right\}.$$

Note that in general $\boldsymbol{\mathcal{K}}_{hp} \not\subset \boldsymbol{\mathcal{K}}$.

The Steklov-Poincaré operator S defined in (4.11) contains the inverse of the single layer potential V^{-1}, which cannot be evaluated numerically. Therefore we introduce the discrete Steklov-Poincaré operator $\hat{S} := W + (K' + 1/2) i_{hp} V^{-1}_{hp} i^*_{hp} (K + 1/2)$ which differs from S. Here, i_{hp} stands for the canonical embedding $i_{hp} : \boldsymbol{\mathcal{W}}_{hp} \hookrightarrow \boldsymbol{H}^{-1/2}(\Gamma)$, and i^*_{hp} denotes its dual with respect to the duality product $\langle \cdot, \cdot \rangle := {}_{\boldsymbol{H}^{-1/2}(\Gamma)}\langle \cdot, \cdot \rangle_{\boldsymbol{H}^{1/2}(\Gamma)}$, cf. Section 1.4. We define the discrete single layer potential by

$$V_{hp} := i^*_{hp} V i_{hp}$$

and the consistency operator $\hat{E}$ by

$$\hat{E} := S - \hat{S} = (K' + 1/2)(V^{-1} - i_{hp} V^{-1}_{hp} i^*_{hp})(K + 1/2). \tag{4.53}$$

The following approximation properties of $\hat{E}$ are given by Lemma 1.4.2:

$$\begin{aligned} &\exists C_{\hat{E}} > 0 : && \forall \boldsymbol{u}, \boldsymbol{v} \in \boldsymbol{\mathcal{V}} \quad \langle \hat{E} \boldsymbol{u}, \boldsymbol{v} \rangle_\Sigma \leq C_{\hat{E}} ||\boldsymbol{u}||_{\tilde{\boldsymbol{H}}^{1/2}(\Sigma)} ||\boldsymbol{v}||_{\tilde{\boldsymbol{H}}^{1/2}(\Sigma)}, \\ &\exists C_0 > 0 : && \forall \boldsymbol{v} \in \boldsymbol{\mathcal{V}} \quad ||\hat{E} \boldsymbol{v}||_{\boldsymbol{H}^{-1/2}(\Gamma)} \leq C_0 \hat{e}(\boldsymbol{v}), \\ & && \text{where } \hat{e}(\boldsymbol{v}) := \inf_{\boldsymbol{\Theta} \in \boldsymbol{\mathcal{W}}_{hp}} ||V^{-1}(K + 1/2)\boldsymbol{v} - \boldsymbol{\Theta}||_{\boldsymbol{H}^{-1/2}(\Gamma)}. \end{aligned} \tag{4.54}$$

Now we are able to pose the Galerkin formulation of the problem (4.12):

Find $\boldsymbol{U} \in \boldsymbol{\mathcal{K}}_{hp}$:

$$\langle \hat{S} \boldsymbol{U}, \boldsymbol{\Phi} - \boldsymbol{U} \rangle_\Sigma + j(\boldsymbol{\Phi}^1 - \pi^1_{hp} \boldsymbol{\Phi}^2) - j(\boldsymbol{U}^1 - \pi^1_{hp} \boldsymbol{U}^2) \geq L(\boldsymbol{\Phi} - \boldsymbol{U}) \qquad \forall \boldsymbol{\Phi} \in \boldsymbol{\mathcal{K}}_{hp}. \tag{4.55}$$

The discrete set of admissible solutions $\boldsymbol{\mathcal{K}}_{hp}$ forms a convex cone. Standard arguments of convex analysis guarantee uniqueness and existence for the solution of (4.55).

Remark 4.3.1. *The formulation (4.55) is not symmetric, since the contact conditions are defined in terms of the mesh $\mathcal{T}^1_h$, associated with Γ^1. Of course, it is possible to introduce a formulation in terms of the mesh $\mathcal{T}^2_h$, associated with Γ^2.*

In the subsequent analysis we will need the Lagrange interpolation operator

$$\mathcal{I}^i_{hp} : C(\Sigma^i) \to \{ v \in C(\Sigma^i) : v|_I \in \mathcal{P}_{p_I}(I), \; \forall I \in \mathcal{T}^i_h \}$$

defined on the set of Gauss-Lobatto points G^i_{hp}. The following stability and approximation properties follow from [10, Corollary 4.6, Theorem 4.7] by scaling.

Lemma 4.3.3. *Let γ be any connected subset of Γ^i, $i = 1$ or 2. Assume that the end points of γ coincide with two mesh nodes from $\mathcal{T}_h^i$, $i = 1$ or 2 respectively. There exists a positive constant C such that for any $\forall u \in H^1(\gamma)$*

$$||\mathcal{I}_{hp}^i u||_{H^1(\gamma)} \leq C||u||_{H^1(\gamma)}. \tag{4.56}$$

Furthermore, for any real numbers μ and ν, $\nu \in [0;1]$ and $\mu > \frac{1+\nu}{2}$, there exists a positive constant C depending on μ such that the following approximation property holds for $\forall u \in H^\mu(-1;1)$:

$$||u - \mathcal{I}_{hp}^i u||_{H^\nu(\gamma)} \leq C \left(\frac{h_i}{p_i}\right)^{\mu-\nu} ||u||_{H^\mu(\gamma)}. \tag{4.57}$$

The following inverse inequality for polynomials is of importance.

Lemma 4.3.4. *(inverse inequality) For arbitrary $U \in \mathcal{N}_{hp}^i$, where $\mathcal{N}_{hp}^i$ is the space of continuous piecewise polynomials on Γ_C given by (4.48), there exists a constant $C > 0$ such that*

$$||U||_{H^1(\Gamma_C)} \leq C\frac{p_i}{h_i^{1/2}}||U||_{H^{1/2}(\Gamma_C)}. \tag{4.58}$$

Proof. The assertion of the Lemma follows from Schmidt's inequality (see e.g. [24])

$$||\varphi_p'||_{L_2(-1,1)} \leq \frac{(p+1)^2}{\sqrt{2}}||\varphi_p||_{L_2(-1,1)} \qquad \forall \varphi_p \in \mathcal{P}_p(-1,1)$$

with standard interpolation and scaling arguments. □

4.3.2 A priori error analysis

In order to derive the a priori error estimates for the error between solutions of (4.12) and (4.55) we proceed in several steps.

Lemma 4.3.5. *Suppose $\boldsymbol{u} \in \boldsymbol{\mathcal{K}}$ is the solution of the variational problem (4.12). Let $\boldsymbol{U} \in \boldsymbol{\mathcal{K}}_{hp}$ be the solution of the discrete problem (4.55). Then there exists a constant $c > 0$, such that*

$$\begin{aligned} c||\boldsymbol{u} - \boldsymbol{U}||_{\tilde{\boldsymbol{H}}^{1/2}(\Sigma)} &\leq \inf_{\boldsymbol{\Theta} \in \boldsymbol{\mathcal{W}}_{hp}} ||V^{-1}(K+1/2)\boldsymbol{u} - \boldsymbol{\Theta}||_{\boldsymbol{H}^{-1/2}(\Gamma)} \\ &+ \inf_{\boldsymbol{\Phi} \in \boldsymbol{\mathcal{K}}_{hp}} \left\{ \|\boldsymbol{u} - \boldsymbol{\Phi}\|_{\tilde{\boldsymbol{H}}^{1/2}(\Sigma)} + |\langle \sigma_n, [\Phi_n] \rangle_{\Gamma_C}|^{1/2} + \left| \int_{\Gamma_C} \sigma_t[\Phi_t] + \mathcal{F}|\Phi_t^1 - \pi_{hp}^1 \Phi_t^2| \, ds \right|^{1/2} \right\} \\ &+ \inf_{\boldsymbol{\phi} \in \boldsymbol{\mathcal{K}}} \left\{ |\langle \sigma_n, [\phi_n - U_n] \rangle_{\Gamma_C}|^{1/2} + \left| \int_{\Gamma_C} \sigma_t[\phi_t - U_t] + \mathcal{F}\left(|[\phi_t]| - |U_t^1 - \pi_{hp}^1 U_t^2|\right) ds \right|^{1/2} \right\}. \end{aligned} \tag{4.59}$$

Proof. Since the approximate Steklov-Poincaré operator $\hat{S}$ is positive definite on $\boldsymbol{\mathcal{V}}$ (cf. Lemma 1.4.1), and $\boldsymbol{u}$, $\boldsymbol{U}$ solve (4.12), (4.55), respectively, we obtain for arbitrary $\boldsymbol{\phi} \in \boldsymbol{\mathcal{K}}$ and $\boldsymbol{\Phi} \in \boldsymbol{\mathcal{K}}_{hp}$

$$\begin{aligned}
c_{\hat{S}} \|\boldsymbol{u} - \boldsymbol{U}\|_{\tilde{\boldsymbol{H}}^{1/2}(\Sigma)} &\leq \langle \hat{S}(\boldsymbol{u} - \boldsymbol{U}), \boldsymbol{u} - \boldsymbol{U} \rangle \\
&= \langle \hat{S}\boldsymbol{u}, \boldsymbol{u} \rangle + \langle \hat{S}\boldsymbol{U}, \boldsymbol{U} \rangle - \langle \hat{S}\boldsymbol{u}, \boldsymbol{U} \rangle - \langle \hat{S}\boldsymbol{U}, \boldsymbol{u} \rangle \\
&\leq \langle S\boldsymbol{u}, \boldsymbol{\phi} \rangle + j([\boldsymbol{\phi}]) - j([\boldsymbol{u}]) + L(\boldsymbol{u} - \boldsymbol{\phi}) \\
&\quad + \langle \hat{S}\boldsymbol{U}, \boldsymbol{\Phi} \rangle + j(\boldsymbol{\Phi}^1 - \pi_{hp}^1 \boldsymbol{\Phi}^2) - j(\boldsymbol{U}^1 - \pi_{hp}^1 \boldsymbol{U}^2) + L(\boldsymbol{U} - \boldsymbol{\Phi}) \\
&\quad - \langle S\boldsymbol{u}, \boldsymbol{U} \rangle - \langle S\boldsymbol{U}, \boldsymbol{u} \rangle \\
&\quad - \langle \hat{E}\boldsymbol{u}, \boldsymbol{u} \rangle + \langle \hat{E}\boldsymbol{u}, \boldsymbol{U} \rangle + \langle \hat{E}\boldsymbol{U}, \boldsymbol{u} \rangle \\
&= \langle S\boldsymbol{u}, \boldsymbol{\phi} - \boldsymbol{U} \rangle - L(\boldsymbol{\phi} - \boldsymbol{U}) \\
&\quad + \langle S\boldsymbol{u}, \boldsymbol{\Phi} - \boldsymbol{u} \rangle - L(\boldsymbol{\Phi} - \boldsymbol{u}) \\
&\quad - \langle S\boldsymbol{u}, \boldsymbol{\Phi} - \boldsymbol{u} \rangle + \langle \hat{S}\boldsymbol{U}, \boldsymbol{\Phi} \rangle - \langle S\boldsymbol{U}, \boldsymbol{u} \rangle \\
&\quad - \langle \hat{E}\boldsymbol{u}, \boldsymbol{u} \rangle + \langle \hat{E}\boldsymbol{u}, \boldsymbol{U} \rangle + \langle \hat{E}\boldsymbol{U}, \boldsymbol{u} \rangle \\
&\quad + j([\boldsymbol{\phi}]) - j([\boldsymbol{u}]) + j(\boldsymbol{\Phi}^1 - \pi_{hp}^1 \boldsymbol{\Phi}^2) - j(\boldsymbol{U}^1 - \pi_{hp}^1 \boldsymbol{U}^2).
\end{aligned}$$

The partial integration provides

$$\begin{aligned}
\langle S\boldsymbol{u}, \boldsymbol{\phi} - \boldsymbol{U} \rangle - L(\boldsymbol{\phi} - \boldsymbol{U}) &= \langle \sigma_n \boldsymbol{n} + \sigma_t \boldsymbol{t}, [\boldsymbol{\phi} - \boldsymbol{U}] \rangle_{\Gamma_C}, \\
\langle S\boldsymbol{u}, \boldsymbol{\Phi} - \boldsymbol{u} \rangle - L(\boldsymbol{\Phi} - \boldsymbol{u}) &= \langle \sigma_n \boldsymbol{n} + \sigma_t \boldsymbol{t}, [\boldsymbol{\Phi} - \boldsymbol{u}] \rangle_{\Gamma_C}.
\end{aligned}$$

Furthermore, since $S = \hat{S} + \hat{E}$, it is easy to see that

$$\begin{aligned}
&-\langle S\boldsymbol{u}, \boldsymbol{\Phi} - \boldsymbol{u} \rangle + \langle \hat{S}\boldsymbol{U}, \boldsymbol{\Phi} \rangle - \langle S\boldsymbol{U}, \boldsymbol{u} \rangle - \langle \hat{E}\boldsymbol{u}, \boldsymbol{u} \rangle + \langle \hat{E}\boldsymbol{u}, \boldsymbol{U} \rangle + \langle \hat{E}\boldsymbol{U}, \boldsymbol{u} \rangle \\
&= \langle \hat{S}\boldsymbol{u}, \boldsymbol{u} - \boldsymbol{\Phi} \rangle + \langle \hat{E}\boldsymbol{u}, \boldsymbol{u} - \boldsymbol{\Phi} \rangle + \langle \hat{S}\boldsymbol{U}, \boldsymbol{\Phi} \rangle - \langle \hat{S}\boldsymbol{U}, \boldsymbol{u} \rangle - \langle \hat{E}\boldsymbol{u}, \boldsymbol{u} \rangle + \langle \hat{E}\boldsymbol{u}, \boldsymbol{U} \rangle \\
&= \langle \hat{S}\boldsymbol{u}, \boldsymbol{u} - \boldsymbol{\Phi} \rangle + \langle \hat{E}\boldsymbol{u}, \boldsymbol{u} - \boldsymbol{\Phi} \rangle - \langle \hat{S}\boldsymbol{U}, \boldsymbol{u} - \boldsymbol{\Phi} \rangle - \langle \hat{E}\boldsymbol{u}, \boldsymbol{u} \rangle + \langle \hat{E}\boldsymbol{u}, \boldsymbol{U} \rangle \\
&= \langle \hat{S}(\boldsymbol{u} - \boldsymbol{U}), \boldsymbol{u} - \boldsymbol{\Phi} \rangle + \langle \hat{E}\boldsymbol{u}, \boldsymbol{u} - \boldsymbol{\Phi} \rangle + \langle \hat{E}\boldsymbol{u}, \boldsymbol{U} - \boldsymbol{u} \rangle.
\end{aligned}$$

Using (4.54) we obtain for some $\alpha_1 > 0$

$$\begin{aligned}
&\langle \hat{E}\boldsymbol{u}, \boldsymbol{u} - \boldsymbol{\Phi} \rangle + \langle \hat{E}\boldsymbol{u}, \boldsymbol{U} - \boldsymbol{u} \rangle \\
&\qquad \leq \|\hat{E}\boldsymbol{u}\|_{\boldsymbol{H}^{-1/2}(\Gamma)} \left(\|\boldsymbol{u} - \boldsymbol{U}\|_{\tilde{\boldsymbol{H}}^{1/2}(\Sigma)} + \|\boldsymbol{u} - \boldsymbol{\Phi}\|_{\tilde{\boldsymbol{H}}^{1/2}(\Sigma)} \right) \\
&\qquad \leq C_0 \left(\frac{\alpha_1}{2} \|\boldsymbol{u} - \boldsymbol{U}\|^2_{\tilde{\boldsymbol{H}}^{1/2}(\Sigma)} + \frac{\alpha_1 + 1}{2\alpha_1} \hat{e}(\boldsymbol{u})^2 + \frac{1}{2} \|\boldsymbol{u} - \boldsymbol{\Phi}\|^2_{\tilde{\boldsymbol{H}}^{1/2}(\Sigma)} \right).
\end{aligned}$$

Continuity of the discrete Steklov-Poincaré operator $\hat{S}$ (Lemma 1.4.1) provides for $\alpha_2 > 0$

$$\begin{aligned}
\langle \hat{S}(\boldsymbol{u} - \boldsymbol{U}), \boldsymbol{u} - \boldsymbol{\Phi} \rangle &\leq C_{\hat{S}} \|\boldsymbol{u} - \boldsymbol{U}\|_{\tilde{\boldsymbol{H}}^{1/2}(\Sigma)} \|\boldsymbol{u} - \boldsymbol{\Phi}\|_{\tilde{\boldsymbol{H}}^{1/2}(\Sigma)} \\
&\leq C_{\hat{S}} \left(\frac{\alpha_2}{2} \|\boldsymbol{u} - \boldsymbol{U}\|^2_{\tilde{\boldsymbol{H}}^{1/2}(\Sigma)} + \frac{1}{2\alpha_2} \|\boldsymbol{u} - \boldsymbol{\Phi}\|^2_{\tilde{\boldsymbol{H}}^{1/2}(\Sigma)} \right).
\end{aligned}$$

Therefore, combining these results we obtain for the global error

$$\begin{aligned}\left(c_{\hat{S}} - C_0\frac{\alpha_1}{2} - C_{\hat{S}}\frac{\alpha_2}{2}\right) \|\boldsymbol{u} - \boldsymbol{U}\|^2_{\tilde{H}^{1/2}(\Sigma)} \\ \leq C_0\frac{\alpha_1+1}{2\alpha_1}\hat{e}(\boldsymbol{u})^2 + \left(\frac{C_0}{2} + \frac{C_{\hat{S}}}{2\alpha_2}\right) \|\boldsymbol{u} - \boldsymbol{\Phi}\|^2_{\tilde{H}^{1/2}(\Sigma)} \\ + |\langle \sigma_n, [\Phi_n - u_n]\rangle| + \left| \int_{\Gamma_C} \left(\sigma_t[\Phi_t - u_t] + \mathcal{F}|\Phi_t^1 - \pi_{hp}^1\Phi_t^2| - \mathcal{F}|[u_t]|\right) ds \right| \\ + |\langle \sigma_n, [\phi_n - U_n]\rangle| + \left| \int_{\Gamma_C} \left(\sigma_t[\phi_t - U_t] + \mathcal{F}|[\phi_t]| - \mathcal{F}|U_t^1 - \pi_{hp}^1 U_t^2|\right) ds \right|.\end{aligned}$$

Since we are free in choosing $\boldsymbol{\phi} \in \boldsymbol{\mathcal{K}}$, $\boldsymbol{\Phi} \in \boldsymbol{\mathcal{K}}_{hp}$, we are able to take the infimum in the above inequality. The assertion of the lemma follows by noting that due to contact conditions in (4.1) there holds

$$\sigma_n\,[u_n] = 0, \qquad \sigma_t[u_t] + \mathcal{F}|[u_t]| = 0.$$

□

Remark 4.3.2. *It was shown in Lemma 4.3.5, that the global error consists of three parts. The first infimum in (4.59) is the approximation error of the space $\boldsymbol{\mathcal{W}}_{hp}$ initiated by the approximation of the Steklov-Poincaré operator by $\hat{S}$. The approximation property of $\mathcal{W}_{hp}$ provides that there exists $C > 0$:*

$$\inf_{\boldsymbol{\Theta} \in \boldsymbol{\mathcal{W}}_{hp}} ||V^{-1}(K + 1/2)\boldsymbol{u} - \boldsymbol{\Theta}||_{\boldsymbol{H}^{-1/2}(\Gamma)} \leq C\left(\frac{h_1}{p_1} + \frac{h_2}{p_2}\right) ||T\boldsymbol{u}||_{\boldsymbol{H}^{1/2}(\Gamma)}. \tag{4.60}$$

Here $T := V^{-1}(K + 1/2)$ is the non-symmetric representation of the Dirichlet-to-Neumann operator, introduced in Section 1.3. The second infimum in (4.59) is standard even for conforming problems and corresponds to the approximation property of the space $\boldsymbol{\mathcal{K}}_{hp}$. The last infimum in (4.59) is the consistency error and is caused by nonconformity of our approach, i.e. $\boldsymbol{\mathcal{K}}_{hp} \not\subset \boldsymbol{\mathcal{K}}$. It disappears in case of matching meshes on the contact boundary with piecewise linear basis functions.

Remark 4.3.3. *Note, that there holds*

$$\sigma_n = T\boldsymbol{u}^1 \cdot \boldsymbol{n}^1|_{\Gamma_C}, \qquad \sigma_t = T\boldsymbol{u}^1 \cdot \boldsymbol{t}^1|_{\Gamma_C}.$$

We proceed further with the approximation error.

Lemma 4.3.6. *Let $\boldsymbol{u} \in \boldsymbol{\mathcal{K}} \cap \tilde{\boldsymbol{H}}^{3/2}(\Sigma)$ be the solution of (4.12) and $\sigma_n \in H^{1/2}(\Gamma_C)$ and $\sigma_t \in H^{1/2}(\Gamma_C)$ are the normal and tangential contact traction respectively. Then there exists $\boldsymbol{\Phi} \in \boldsymbol{\mathcal{K}}_{hp}$ and $C > 0$ such that*

$$\|\boldsymbol{u} - \boldsymbol{\Phi}\|_{\tilde{\boldsymbol{H}}^{1/2}(\Sigma)} \leq C\left(\frac{h_1}{p_1}\log p_1 + \frac{h_2}{p_2}\right) \|\boldsymbol{u}\|_{\tilde{\boldsymbol{H}}^{3/2}(\Sigma)}, \tag{4.61}$$

$$|\langle \sigma_n, [\Phi_n]\rangle_{\Gamma_C}|^{1/2} \leq C\left(\frac{h_1}{p_1}\right)^{3/4} \sqrt[4]{\log p_1}\|\sigma_n\|^{1/2}_{H^{1/2}(\Gamma_C)}\|\boldsymbol{u}\|^{1/2}_{\tilde{\boldsymbol{H}}^{3/2}(\Sigma)}, \tag{4.62}$$

$$\left| \int_{\Gamma_C} \sigma_t[\Phi_t] + \mathcal{F} | \Phi_t^1 - \pi_{hp}^1 \Phi_t^2 | \, ds \right|^{1/2}$$
$$\leq C \left(\left(\frac{h_1}{p_1} \log p_1 \right)^{1/2} + \left(\frac{h_2}{p_2} \right)^{1/2} \right) \|\mathcal{F}\|_{L_2(\Gamma_C)}^{1/2} \|\boldsymbol{u}\|_{\tilde{\boldsymbol{H}}^{3/2}(\Sigma)}^{1/2}. \qquad (4.63)$$

Proof. We denote the jump of the normal displacement $r_n := [u_n] \leq 0$ on Γ_C and $\boldsymbol{r} := r_n^* \boldsymbol{n}^1$ where r_n^* is an extension of r_n onto Σ^1 satisfying

$$||r_n^*||_{\tilde{H}^{3/2}(\Sigma^1)} \leq C ||r_n||_{H^{3/2}(\Gamma_C)},$$

Existence of such an extension can be shown similarly to Lemma 3.2.2. Further we introduce $\boldsymbol{w} := (\boldsymbol{u}^1 - \boldsymbol{r}, \boldsymbol{u}^2)$. Note that there holds $[w_n] = 0$ in all points of Γ_C and

$$||\boldsymbol{w}||_{\tilde{\boldsymbol{H}}^{3/2}(\Sigma)} \leq ||\boldsymbol{u}||_{\tilde{\boldsymbol{H}}^{3/2}(\Sigma)} + C ||r_n||_{H^{3/2}(\Gamma_C)} \leq C ||\boldsymbol{u}||_{\tilde{\boldsymbol{H}}^{3/2}(\Sigma)}.$$

Let R_{hp}^1 be the zero extension operator from Γ_C onto Σ^1. Due to the definition of the $\tilde{H}^{1/2}$-norm there holds

$$||R_{hp}^1 \Psi||_{\tilde{H}^{1/2}(\Sigma^i)} = ||\Psi||_{\tilde{H}^{1/2}(\Gamma_C)}$$

for arbitrary $\Psi \in \tilde{H}^{1/2}(\Gamma_C)$. Similarly to the approach of Hild [34] for the h-version of FEM, we define a piecewise polynomial function $\boldsymbol{W} := (\boldsymbol{W}^1, \boldsymbol{W}^2)$.

$$\begin{aligned} \boldsymbol{W}^1 &:= \mathcal{I}_{hp}^1 \boldsymbol{w}^1 + R_{hp}^1 (\pi_{hp}^1 (\mathcal{I}_{hp}^2 w_n^2 - \mathcal{I}_{hp}^1 w_n^1)) \boldsymbol{n}, \\ \boldsymbol{W}^2 &:= \mathcal{I}_{hp}^2 \boldsymbol{w}^2. \end{aligned}$$

The operator R_{hp}^1 is an identity operator on Γ_C and $\pi_{hp}^1 \mathcal{I}_{hp}^1 w_n^1 = \mathcal{I}_{hp}^1 w_n^1$ on Γ_C; thus in all points of Γ_C there holds

$$W_n^1 - \pi_{hp}^1 W_n^2 = \mathcal{I}_{hp}^1 w_n^1 + R_{hp}^1 (\pi_{hp}^1 (\mathcal{I}_{hp}^2 w_n^2 - \mathcal{I}_{hp}^1 w_n^1)) - \pi_{hp}^1 \mathcal{I}_{hp}^2 w_n^2 = 0. \qquad (4.64)$$

Using the approximation property of the Lagrange interpolation operator (4.57) we obtain

$$\|\boldsymbol{w} - \mathcal{I}_{hp} \boldsymbol{w}\|_{\tilde{\boldsymbol{H}}^{1/2}(\Sigma)} \leq C \left(\frac{h_1}{p_1} + \frac{h_2}{p_2} \right) \|\boldsymbol{w}\|_{\tilde{\boldsymbol{H}}^{3/2}(\Sigma)} \leq C \left(\frac{h_1}{p_1} + \frac{h_2}{p_2} \right) \|\boldsymbol{u}\|_{\tilde{\boldsymbol{H}}^{3/2}(\Sigma)}.$$

Moreover, stability of R_{hp}^1 provides

$$\begin{aligned} \|\mathcal{I}_{hp} \boldsymbol{w} - \boldsymbol{W}\|_{\tilde{\boldsymbol{H}}^{1/2}(\Sigma)} &= \left\| \mathcal{I}_{hp}^1 \boldsymbol{w}^1 - \boldsymbol{W}^1 \right\|_{\tilde{\boldsymbol{H}}^{1/2}(\Sigma^1)} \\ &= \left\| R_{hp}^1 \left(\pi_{hp}^1 (\mathcal{I}_{hp}^1 w_n^1 - \mathcal{I}_{hp}^2 w_n^2) \right) \right\|_{\tilde{H}^{1/2}(\Sigma^1)} \\ &\leq C \left\| \pi_{hp}^1 \left(\mathcal{I}_{hp}^1 w_n^1 - \mathcal{I}_{hp}^2 w_n^2 \right) \right\|_{\tilde{H}^{1/2}(\Gamma_C)}. \end{aligned} \qquad (4.65)$$

The stability constant in (4.52) of the mortar projection π^1_{hp} includes the factor $p_1^{3/4}$, therefore direct application of (4.52) leads to the reduced rate of convergence. To overcome this we perform a splitting, and employing (4.51) we estimate

$$\begin{aligned}\left\|\pi^1_{hp}\left(\mathcal{I}^1_{hp}w^1_n - \mathcal{I}^2_{hp}w^2_n\right)\right\|_{\tilde{H}^{1/2}(\Gamma_C)} &\leq \left\|(\mathcal{I}^1_{hp}w^1_n - \mathcal{I}^2_{hp}w^2_n) - \pi^1_{hp}\left(\mathcal{I}^1_{hp}w^1_n - \mathcal{I}^2_{hp}w^2_n\right)\right\|_{\tilde{H}^{1/2}(\Gamma_C)} \\ &\quad + \left\|\mathcal{I}^1_{hp}w^1_n - \mathcal{I}^2_{hp}w^2_n\right\|_{\tilde{H}^{1/2}(\Gamma_C)} \\ &\leq C\left(\frac{h_1}{p_1}\right)^{1/2}\sqrt{\log p_1}\left\|\mathcal{I}^1_{hp}w^1_n - \mathcal{I}^2_{hp}w^2_n\right\|_{H^1(\Gamma_C)} \\ &\quad + \left\|\mathcal{I}^1_{hp}w^1_n - \mathcal{I}^2_{hp}w^2_n\right\|_{\tilde{H}^{1/2}(\Gamma_C)}.\end{aligned} \tag{4.66}$$

Further, we use the approximation property of the Lagrange interpolation operator (4.57) to obtain

$$\begin{aligned}\left\|\mathcal{I}^1_{hp}w^1_n - \mathcal{I}^2_{hp}w^2_n\right\|_{\tilde{H}^{1/2}(\Gamma_C)} &\leq \left\|\mathcal{I}^1_{hp}w^1_n - w^1_n\right\|_{\tilde{H}^{1/2}(\Gamma_C)} + \left\|w^2_n - \mathcal{I}^2_{hp}w^2_n\right\|_{\tilde{H}^{1/2}(\Gamma_C)} \\ &\leq C\left(\frac{h_1}{p_1} + \frac{h_2}{p_2}\right)\|\boldsymbol{w}\|_{\tilde{H}^{3/2}(\Sigma)}, \\ \left\|\mathcal{I}^1_{hp}w^1_n - \mathcal{I}^2_{hp}w^2_n\right\|_{H^1(\Gamma_C)} &\leq \left\|\mathcal{I}^1_{hp}w^1_n - w^1_n\right\|_{H^1(\Gamma_C)} + \left\|w^2_n - \mathcal{I}^2_{hp}w^2_n\right\|_{H^1(\Gamma_C)} \\ &\leq C\left(\left(\frac{h_1}{p_1}\right)^{1/2} + \left(\frac{h_2}{p_2}\right)^{1/2}\right)\|\boldsymbol{w}\|_{\tilde{H}^{3/2}(\Sigma)},\end{aligned}$$

since $[w_n] = 0$ by construction. This together with (4.65) and (4.66) gives

$$\begin{aligned}\|\mathcal{I}_{hp}\boldsymbol{w} - \boldsymbol{W}\|_{\tilde{\boldsymbol{H}}^{1/2}(\Sigma)} &\leq C\left(\left(\frac{h_1}{p_1}\right)\sqrt{\log p_1} + \left(\frac{h_1}{p_1}\frac{h_2}{p_2}\right)^{1/2}\sqrt{\log p_1} + \frac{h_2}{p_2}\right)\|\boldsymbol{u}\|_{\tilde{H}^{3/2}(\Sigma)} \\ &\leq C\left(\frac{h_1}{p_1}\log p_1 + \frac{h_2}{p_2}\right)\|\boldsymbol{u}\|_{\tilde{H}^{3/2}(\Sigma)}.\end{aligned}$$

Therefore, there holds

$$\begin{aligned}\|\boldsymbol{w} - \boldsymbol{W}\|_{\tilde{\boldsymbol{H}}^{1/2}(\Sigma)} &\leq \|\boldsymbol{w} - \mathcal{I}_{hp}\boldsymbol{w}\|_{\tilde{\boldsymbol{H}}^{1/2}(\Sigma)} + \|\mathcal{I}_{hp}\boldsymbol{w} - \boldsymbol{W}\|_{\tilde{\boldsymbol{H}}^{1/2}(\Sigma)} \\ &\leq C\left(\frac{h_1}{p_1}\log p_1 + \frac{h_2}{p_2}\right)\|\boldsymbol{u}\|_{\tilde{\boldsymbol{H}}^{3/2}(\Sigma)}.\end{aligned}$$

Now, we introduce $\boldsymbol{\Phi} := \left(\boldsymbol{W}^1 + \mathcal{I}^1_{hp}\boldsymbol{r}, \boldsymbol{W}^2\right)$. It follows with (4.64) that $\boldsymbol{\Phi} \in \boldsymbol{\mathcal{K}}_{hp}$, since

$$\Phi^1_n - \pi^1_{hp}\Phi^2_n = W^1_n + \mathcal{I}^1_{hp}r_n - \pi^1_{hp}W^2_n = \mathcal{I}^1_{hp}r_n = \mathcal{I}^1_{hp}[u_n]\big|_{(x)} \leq 0 \qquad \forall x \in G^1_{hp} \cap \Gamma_C.$$

Note that

$$\boldsymbol{u} - \boldsymbol{\Phi} = (\boldsymbol{w}^1 + \boldsymbol{r}, \boldsymbol{w}^2) - (\boldsymbol{W}^1 + \mathcal{I}^1_{hp}\boldsymbol{r}, \boldsymbol{W}^2) = \boldsymbol{w} - \boldsymbol{W} + (\boldsymbol{r} - \mathcal{I}^1_{hp}\boldsymbol{r}, 0).$$

Alltogether

$$\begin{aligned}\|\boldsymbol{u}-\boldsymbol{\Phi}\|_{\tilde{\boldsymbol{H}}^{1/2}(\Sigma)} &\leq \|\boldsymbol{w}-\boldsymbol{W}\|_{\tilde{\boldsymbol{H}}^{1/2}(\Sigma)} + \left\|\boldsymbol{r}-\mathcal{I}_{hp}^{1}\boldsymbol{r}\right\|_{\tilde{\boldsymbol{H}}^{1/2}(\Sigma^1)} \\ &\leq C\left(\frac{h_1}{p_1}\log p_1 + \frac{h_2}{p_2}\right)\|\boldsymbol{u}\|_{\tilde{\boldsymbol{H}}^{3/2}(\Sigma)} + C\frac{h_1}{p_1}\|[u_n]\|_{H^{3/2}(\Gamma_C)} \\ &\leq C\left(\frac{h_1}{p_1}\log p_1 + \frac{h_2}{p_2}\right)\|\boldsymbol{u}\|_{\tilde{\boldsymbol{H}}^{3/2}(\Sigma)}\end{aligned}$$

and (4.61) follows. In order to show (4.62) we decompose

$$\int_{\Gamma_C}\sigma_n[\Phi_n-u_n]\,ds = \int_{\Gamma_C}\sigma_n[W_n]\,ds + \int_{\Gamma_c}\sigma_n\left(\mathcal{I}_{hp}^{1}r_n - r_n\right)\,ds. \tag{4.67}$$

For the second term there holds

$$\begin{aligned}\int_{\Gamma_c}\sigma_n\left(\mathcal{I}_{hp}^{1}r_n-r_n\right)\,ds &\leq \|\sigma_n\|_{L_2(\Gamma_C)}\left\|r_n-\mathcal{I}_{hp}^{1}r_n\right\|_{L_2(\Gamma_C)} \\ &\leq C\|\sigma\|_{L_2(\Gamma_C)}\left(\frac{h_1}{p_1}\right)^{3/2}\|[u_n]\|_{H^{3/2}(\Gamma_C)} \\ &\leq C\left(\frac{h_1}{p_1}\right)^{3/2}\|\sigma\|_{L_2(\Gamma_C)}\|\boldsymbol{u}\|_{\tilde{\boldsymbol{H}}^{3/2}(\Sigma)}.\end{aligned} \tag{4.68}$$

Note, that we cannot achieve a better result, since the error of the interpolant cannot be optimally bounded in Sobolev spaces with negative index. Furthermore, it is crucial to use the interpolation operator in the definition of $\boldsymbol{\Phi}$ to show that $\boldsymbol{\Phi}\in\boldsymbol{\mathcal{K}}_{hp}$. Using again that R_{hp}^{1} is identity on Γ_C, definition of the mortar projection (4.50) and stability property (4.56) we get with the approximation property of $\mathcal{M}_{hp}^{1}$ (cf. [63])

$$\begin{aligned}\int_{\Gamma_C}\sigma_n[W_n]\,ds &= \int_{\Gamma_C}\sigma_n\left(\pi_{hp}^{1}\mathcal{I}_{hp}^{2}w_n^2-\mathcal{I}_{hp}^{2}w_n^2\right)\,ds \\ &= \inf_{\Theta\in\mathcal{M}_{hp}^{1}}\int_{\Gamma_C}(\sigma_n-\Theta)\left(\pi_{hp}^{1}\mathcal{I}_{hp}^{2}w_n^2-\mathcal{I}_{hp}^{2}w_n^2\right)\,ds \\ &\leq \inf_{\Theta\in\mathcal{M}_{hp}^{1}}\|\sigma_n-\Theta\|_{H^{-\frac{1}{2}}(\Gamma_c)}\left\|\mathcal{I}_{hp}^{2}w_n^2-\pi_{hp}^{1}\mathcal{I}_{hp}^{2}w_n^2\right\|_{\tilde{H}^{1/2}(\Gamma_C)} \\ &\leq C\inf_{\Theta\in\mathcal{M}_{hp}^{1}}\|\sigma_n-\Theta\|_{H^{-\frac{1}{2}}(\Gamma_c)}\left(\frac{h_1}{p_1}\right)^{1/2}\sqrt{\log p_1}\left\|\mathcal{I}_{hp}^{2}w_n^2\right\|_{H^{1}(\Gamma_c)} \\ &\leq C\left(\frac{h_1}{p_1}\right)^{3/2}\sqrt{\log p_1}\|\sigma_n\|_{H^{1/2}(\Gamma_C)}\|\boldsymbol{u}\|_{\tilde{\boldsymbol{H}}^{3/2}(\Sigma)}.\end{aligned} \tag{4.69}$$

Combining (4.68), (4.69) we obtain (4.62). For the frictional term (4.63) we use again that for the exact solution of (4.12) there holds $\sigma_t[u_t] + \mathcal{F}|[u_t]| = 0$. Thus

$$\begin{aligned}\int_{\Gamma_C} \sigma_t[\Phi_t] + \mathcal{F}|\Phi_t^1 - \pi_{hp}^1 \Phi_t^2|\, ds &= \int_{\Gamma_C} \sigma_t[\Phi_t] - \sigma_t[u_t] + \mathcal{F}(|\Phi_t^1 - \pi_{hp}^1 \Phi_t^2| - |[u_t]|)\, ds \\ &\le \int_{\Gamma_C} \sigma_t\left[\Phi_t - u_t\right] + \mathcal{F}\left|\Phi_t^1 - \pi_{hp}^1 \Phi_t^2 - [u_t]\right|\, ds \\ &\le \int_{\Gamma_C} \mathcal{F}|\left[\Phi_t - u_t\right]| + \mathcal{F}\left|\Phi_t^1 - \pi_{hp}^1 \Phi_t^2 - [u_t]\right|\, ds.\end{aligned}$$

We decompose $\Phi_t^1 - \pi_{hp}^1 \Phi_t^2 - [u_t] = \Phi_t^1 - u_t^1 + \pi_{hp}^1(u_t^2 - \Phi_t^2) + (u_t^2 - \pi_{hp}^1 u_t^2)$. Thus

$$\begin{aligned}&\int_{\Gamma_C} \sigma_t[\Phi_t] + \mathcal{F}|\Phi_t^1 - \pi_{hp}^1 \Phi_t^2|\, ds \\ &\qquad \le \int_{\Gamma_C} \mathcal{F}(|[\Phi_t - u_t]| + \left|\Phi_t^1 - u_t^1\right| + \left|\pi_{hp}^1(u_t^2 - \Phi_t^2)\right| + \left|(u_t^2 - \pi_{hp}^1 u_t^2)\right|)\, ds \\ &\qquad \le \|\mathcal{F}\|_{L_2(\Gamma_C)}(2\|\Phi_t - u_t\|_{L_2(\Gamma_C)} + ||\pi_{hp}^1(u_t^2 - \Phi_t^2)||_{L_2(\Gamma_C)} + ||(u_t^2 - \pi_{hp}^1 u_t^2)||_{L_2(\Gamma_C)}).\end{aligned}$$

By definition $\Phi_t = \left(\mathcal{I}_{hp}^1 u_t^1, \mathcal{I}_{hp}^2 u_t^2\right)$, therefore

$$\|\Phi_t - u_t\|_{L_2(\Gamma_C)} \le \left(\left(\frac{h_1}{p_1}\right)^{3/2} + \left(\frac{h_2}{p_2}\right)^{3/2}\right) \|\boldsymbol{u}\|_{\tilde{\boldsymbol{H}}^{3/2}(\Sigma)},$$

$$\begin{aligned}||\pi_{hp}^1(u_t^2 - \Phi_t^2)||_{L_2(\Gamma_C)} &\le ||\pi_{hp}^1(u_t^2 - \mathcal{I}_{hp}^2 u_t^2)||_{H^{1/2}(\Gamma_C)} \\ &\le ||(u_t^2 - \mathcal{I}_{hp}^2 u_t^2) - \pi_{hp}^1(u_t^2 - \mathcal{I}_{hp}^2 u_t^2)||_{H^{1/2}(\Gamma_C)} + ||u_t^2 - \mathcal{I}_{hp}^2 u_t^2||_{H^{1/2}(\Gamma_C)} \\ &\le \left(\frac{h_1}{p_1}\right)^{1/2} \sqrt{\log p_1}||u_t^2 - \mathcal{I}_{hp}^2 u_t^2||_{H^1(\Gamma_C)} + ||u_t^2 - \mathcal{I}_{hp}^2 u_t^2||_{H^{1/2}(\Gamma_C)} \\ &\le C\left(\frac{h_1}{p_1}\log p_1 + \frac{h_2}{p_2}\right)\|\boldsymbol{u}\|_{\tilde{\boldsymbol{H}}^{3/2}(\Sigma)},\end{aligned}$$

and

$$\begin{aligned}||u_t^2 - \pi_{hp}^1 u_t^2||_{L_2(\Gamma_C)} &\le C\frac{h_1}{p_1}\sqrt{\log p_1}||u_t^2||_{H^{3/2}(\Gamma_C)} \\ &\le C\frac{h_1}{p_1}\sqrt{\log p_1}\|\boldsymbol{u}\|_{\tilde{\boldsymbol{H}}^{3/2}(\Sigma)},\end{aligned}$$

which provides (4.63). □

Lemma 4.3.7. *Let $\boldsymbol{u} \in \boldsymbol{\mathcal{K}} \cap \tilde{\boldsymbol{H}}^{3/2}(\Sigma)$ be the solution of (4.12), let $\sigma_n \in H^{1/2}(\Gamma_C)$ and $\sigma_t \in H^{1/2}(\Gamma_C)$ be the corresponding normal and tangential contact tractions, and let $\boldsymbol{U} \in \boldsymbol{\mathcal{K}}_{hp}$ be the solution of (4.55). Then there exists $\boldsymbol{\phi} \in \boldsymbol{\mathcal{K}}$, constants $\alpha_3, \alpha_4 \in (0;1)$*

and a constant $C > 0$ such that there holds

$$\left| \int_{\Gamma_C} \sigma_n [\phi_n - U_n] \, ds \right|^{1/2} \leq \alpha_3 ||\boldsymbol{u} - \boldsymbol{U}||_{\tilde{\boldsymbol{H}}^{1/2}(\Sigma)} + \frac{C}{\alpha_3} \gamma_{n,hp} \|\sigma_n\|_{H^{1/2}(\Gamma_C)} + C \left(\frac{h_1}{p_1} \right)^{1/4} \|\boldsymbol{u}\|_{\tilde{\boldsymbol{H}}^{3/2}(\Sigma)}, \tag{4.70}$$

$$\left| \int_{\Gamma_C} \sigma_t [\phi_t - U_t] + \mathcal{F}(|[\phi_t]| - |U_t^1 - \pi_{hp}^1 U_t^2|) \, ds \right|^{1/2} \leq \alpha_4 ||\boldsymbol{u} - \boldsymbol{U}||_{\tilde{\boldsymbol{H}}^{1/2}(\Sigma)} + \frac{C}{\alpha_4} \gamma_{t,hp} \|\sigma\|_{H^{1/2}(\Gamma_C)} + C \gamma_{t,hp}^u \|\boldsymbol{u}\|_{\tilde{\boldsymbol{H}}^{3/2}(\Sigma)}. \tag{4.71}$$

where

$$\gamma_{n,hp} := \left(\frac{h_1}{p_1} \right)^{1/4} + \sqrt{\log p_1} \frac{p_2}{p_1} \frac{h_1}{h_2^{1/2}},$$
$$\gamma_{t,hp} := \sqrt{\log p_1} \frac{p_2}{p_1^{3/2}} \frac{h_1^{3/2}}{h_2^{1/2}} + \sqrt[4]{\log p_1} \left(\frac{h_1}{p_1} \right)^{3/4} h_2^{1/4} + \sqrt[4]{\log p_1} \frac{h_1}{p_1},$$
$$\gamma_{t,hp}^u := \sqrt[4]{\log p_1} \left(\frac{h_1}{p_1} \right)^{3/4} h_2^{1/4} + \sqrt[4]{\log p_1} \frac{h_1}{p_1}.$$

Proof. Since the solution $\boldsymbol{U}$ of the discrete formulation (4.55) lies in $\boldsymbol{\mathcal{K}}_{hp}$, there holds

$$\pi_{hp}^1 [U_n]|_{(x)} = U_n^1 - \pi_{hp}^1 U_n^2|_{(x)} \leq 0 \qquad \forall x \in G_{hp}^1 \cap \Gamma_C.$$

Following [46] we define continuous functions $\inf(f_1, f_2)$, $\sup(f_1, f_2)$ for continuous f_1, f_2 as follows

$$\inf(f_1, f_2)(x) := \inf(f_1(x), f_2(x)), \qquad \sup(f_1, f_2)(x) := \sup(f_1(x), f_2(x)).$$

Now, choose

$$\begin{aligned} \phi_n^1 &:= U_n^1, \\ \phi_n^2 &:= U_n^1 - \inf\left(\pi_{hp}^1 [U_n], 0\right) \\ \phi_t^1 &:= U_t^1, \\ \phi_t^2 &:= \pi_{hp}^1 U_t^2, \\ \boldsymbol{\phi}^1 &:= \phi_n^1 \boldsymbol{n}^1 + \phi_t^1 \boldsymbol{t}^1, \\ \boldsymbol{\phi}^2 &:= \phi_n^2 \boldsymbol{n}^2 + \phi_t^2 \boldsymbol{t}^1. \end{aligned} \tag{4.72}$$

Thus in all points of Γ_C there holds

$$[\phi_n] = \phi_n^1 - \phi_n^2 = \inf(\pi_{hp}^1 [U_n], 0) \leq 0,$$

which yields $\boldsymbol{\phi} := (\boldsymbol{\phi}^1, \boldsymbol{\phi}^2) \in \boldsymbol{\mathcal{K}}$. In order to prove the first inequality in the assertion of the theorem, we split

$$\begin{aligned}\int_{\Gamma_C} \sigma_n[\phi_n - U_n]\,ds &= \int_{\Gamma_C} \sigma_n \left(\inf(\pi^1_{hp}[U_n], 0) - [U_n]\right)\,ds \\ &= \int_{\Gamma_C} \sigma_n \left(\pi^1_{hp}[U_n] - [U_n]\right)\,ds - \int_{\Gamma_C} \sigma_n \sup\left(\pi^1_{hp}[U_n], 0\right)\,ds \qquad (4.73) \\ &= \int_{\Gamma_C} \sigma_n \left(U^2_n - \pi^1_{hp}U^2_n\right)\,ds - \int_{\Gamma_C} \sigma_n \sup\left(\pi^1_{hp}[U_n], 0\right)\,ds.\end{aligned}$$

For the first term we use definition of the mortar projection (4.50) and get

$$\begin{aligned}\int_{\Gamma_C} \sigma_n \left(U^2_n - \pi^1_{hp}U^2_n\right)\,ds &= \inf_{\Theta\in\mathcal{M}^1_{hp}} \int_{\Gamma_C} (\sigma_n - \Theta)\left(U^2_n - \pi^1_{hp}U^2_n\right)\,ds \qquad (4.74) \\ &\le \inf_{\Theta\in\mathcal{M}^1_{hp}} \|\sigma_n - \Theta\|_{H^{-1/2}(\Gamma_C)}\|U^2_n - \pi^1_{hp}U^2_n\|_{\tilde{H}^{1/2}(\Gamma_C)} \\ &\le C\frac{h_1}{p_1}\|\sigma\|_{H^{1/2}(\Gamma_C)}\|U^2_n - \pi^1_{hp}U^2_n\|_{\tilde{H}^{1/2}(\Gamma_C)}. \qquad (4.75)\end{aligned}$$

In order to estimate the second term in (4.73) we observe that $\mathcal{I}^1_{hp}\sup\left(\pi^1_{hp}[U_n], 0\right) \equiv 0$, since $\sup\left(\pi^1_{hp}[U_n], 0\right) = 0$ in all $x \in G^1_{hp} \cap \Gamma_C$. Here $\mathcal{I}^1_{hp}$ is the Lagrange interpolation operator in Gauss-Lobatto nodes $G^1_{hp} \cap \Gamma_C$. Therefore

$$\|\sup(\pi^1_{hp}[U_n], 0) - 0\|_{L_2(\Gamma_C)} \le C\frac{h_1}{p_1}\|\sup(\pi^1_{hp}[U_n], 0)\|_{H^1(\Gamma_C)} \le C\frac{h_1}{p_1}\|\pi^1_{hp}[U_n]\|_{H^1(\Gamma_C)}$$

Thus, interpolation between $L_2(\Gamma_C)$ and $H^1(\Gamma_C)$ gives

$$\|\sup(\pi^1_{hp}[U_n], 0) - 0\|_{L_2(\Gamma_C)} \le C\left(\frac{h_1}{p_1}\right)^{1/2}\|\pi^1_{hp}[U_n]\|_{H^{1/2}(\Gamma_C)}. \qquad (4.76)$$

The Cauchy-Schwarz inequality combined with the approximation property (4.76) allows to estimate the second term in (4.73) as follows

$$\begin{aligned}-\int_{\Gamma_C} \sigma_n \sup\left(\pi^1_{hp}[U_n], 0\right)\,ds &\le \|\sigma_n\|_{L_2(\Gamma_C)}\|\sup(\pi^1_{hp}[U_n], 0)\|_{L_2(\Gamma_C)} \\ &\le C\left(\frac{h_1}{p_1}\right)^{1/2}\|\pi^1_{hp}[U_n]\|_{H^{1/2}(\Gamma_C)}\|\sigma_n\|_{L_2(\Gamma_C)} \qquad (4.77) \\ &\le C\left(\frac{h_1}{p_1}\right)^{1/2}\left(\|U^2_n - \pi^1_{hp}U^2_n\|_{H^{1/2}(\Gamma_C)} + \|[U_n]\|_{H^{1/2}(\Gamma_C)}\right)\|\sigma_n\|_{L_2(\Gamma_C)}.\end{aligned}$$

Therefore putting (4.74) and (4.77) together we obtain

$$\int_{\Gamma_C} \sigma_n[\phi_n - U_n]\,ds \le C\left(\frac{h_1}{p_1}\right)^{1/2}\left(\|U^2_n - \pi^1_{hp}U^2_n\|_{\tilde{H}^{1/2}(\Gamma_C)} + \|[U_n]\|_{H^{1/2}(\Gamma_C)}\right)\|\sigma\|_{H^{1/2}(\Gamma_C)}. \qquad (4.78)$$

The term $\|U_n^2 - \pi_{hp}^1 U_n^2\|_{H^{1/2}(\Gamma_C)}$ must be estimated in terms of the norms $\|\boldsymbol{u}\|_{\tilde{\boldsymbol{H}}^{3/2}(\Sigma)}$ and $\|\boldsymbol{u} - \boldsymbol{U}\|_{H^{1/2}(\Gamma_C)}$. Unfortunately, for the mortar projection operator π_{hp}^1 only the stability estimate (4.52) with the factor $p_1^{3/4}$ holds, and as it was shown in [57], [58] this estimate is sharp. Direct application of (4.52) provides poor estimates, therefore it is necessary to involve inverse inequality (4.58), which holds for piecewise polynomial functions. Further, we decompose

$$\begin{aligned} U_n^2 - \pi_{hp}^1 U_n^2 = (U_n^2 - \mathcal{I}_{hp}^2 u_n^2) - \pi_{hp}^1 (U_n^2 - \mathcal{I}_{hp}^2 u_n^2) \\ + (\mathcal{I}_{hp}^2 u_n^2 - u_n^2) - \pi_{hp}^1 (\mathcal{I}_{hp}^2 u_n^2 - u_n^2) \\ + (u_n^2 - \pi_{hp}^1 u_n^2), \end{aligned} \tag{4.79}$$

which relates to the *bootstrap* procedure used e.g. in [8, Lemma 4.4]. Now the term $\|U_n^2 - \pi_{hp}^1 U_n^2\|_{H^{1/2}(\Gamma_C)}$ can be bounded as a sum of three terms, corresponding to the lines of (4.79). Each of them must be estimated separately. For the first term approximation properties (4.51), (4.57) and inverse inequality (4.58) provide

$$\begin{aligned} \|(U_n^2 - \mathcal{I}_{hp}^2 u_n^2) - \pi_{hp}^1 (U_n^2 - \mathcal{I}_{hp}^2 u_n^2)\|_{\tilde{H}^{1/2}(\Gamma_C)} &\le C\sqrt{\log p_1} \left(\frac{h_1}{p_1}\right)^{1/2} \|U_n^2 - \mathcal{I}_{hp}^2 u_n^2\|_{H^1(\Gamma_C)} \\ &\le C\sqrt{\log p_1} \left(\frac{h_1}{p_1}\right)^{1/2} \frac{p_2}{h_2^{1/2}} \|U_n^2 - \mathcal{I}_{hp}^2 u_n^2\|_{H^{1/2}(\Gamma_C)} \\ &\le C\sqrt{\log p_1} \left(\frac{h_1}{p_1}\right)^{1/2} \frac{p_2}{h_2^{1/2}} \left(\|U_n^2 - u_n^2\|_{H^{1/2}(\Gamma_C)} + \|u_n^2 - \mathcal{I}_{hp}^2 u_n^2\|_{H^{1/2}(\Gamma_C)}\right) \\ &\le C\sqrt{\log p_1} \left(\frac{h_1}{p_1}\right)^{1/2} \frac{p_2}{h_2^{1/2}} \|U_n^2 - u_n^2\|_{H^{1/2}(\Gamma_C)} \\ &\quad + C\sqrt{\log p_1} \left(\frac{h_1 h_2}{p_1}\right)^{1/2} \|u_n^2\|_{H^{3/2}(\Gamma_C)}. \end{aligned} \tag{4.80}$$

The remaining terms can be estimated as follows:

$$\begin{aligned} \|(\mathcal{I}_{hp}^2 u_n^2 - u_n^2) - \pi_{hp}^1 (\mathcal{I}_{hp}^2 u_n^2 - u_n^2)\|_{\tilde{H}^{1/2}(\Gamma_C)} &\le C\sqrt{\log p_1} \left(\frac{h_1}{p_1}\right)^{1/2} \|\mathcal{I}_{hp}^2 u_n^2 - u_n^2\|_{H^1(\Gamma_C)} \\ &\le C\sqrt{\log p_1} \left(\frac{h_1}{p_1}\frac{h_2}{p_2}\right)^{1/2} \|u_n^2\|_{H^{3/2}(\Gamma_C)} \end{aligned} \tag{4.81}$$

and

$$\|u_n^2 - \pi_{hp}^1 u_n^2\|_{H^{1/2}(\Gamma_C)} \le C\frac{h_1}{p_1}\sqrt{\log p_1} \|u_n^2\|_{H^{3/2}(\Gamma_C)}. \tag{4.82}$$

Combining (4.80) – (4.82) gives

$$\|U_n^2 - \pi_{hp}^1 U_n^2\|_{H^{1/2}(\Gamma_C)} \le C\delta_1 \|U_n^2 - u_n^2\|_{H^{1/2}(\Gamma_C)} + C\delta_2 \|u_n^2\|_{H^{3/2}(\Gamma_C)}, \tag{4.83}$$

with

$$\delta_1 = \delta_1(h_1, h_2, p_1, p_2) := \sqrt{\log p_1} \left(\frac{h_1}{p_1}\right)^{1/2} \frac{p_2}{h_2^{1/2}} \tag{4.84}$$

$$\delta_2 = \delta_2(h_1, h_2, p_1, p_2) := \sqrt{\log p_1} \left(\frac{h_1}{p_1}\right)^{1/2} \left(h_2^{1/2} + \left(\frac{h_1}{p_1}\right)^{1/2}\right) \tag{4.85}$$

Recalling (4.78) and noting that

$$\|[U_n]\|_{H^{1/2}(\Gamma_C)} \leq \|u_n - U_n\|_{H^{1/2}(\Gamma_C)} + \|u_n\|_{H^{1/2}(\Gamma_C)}$$

we derive

$$\begin{aligned}
\int_{\Gamma_C} \sigma_n[\phi_n - U_n]\, ds &\leq C \left(\frac{h_1}{p_1}\right)^{1/2} ((1 + C\delta_1)\|u_n - U_n\|_{H^{1/2}(\Gamma_C)} \\
&\qquad + (1 + C\delta_2)\|u_n\|_{H^{3/2}(\Gamma_C)})\|\sigma\|_{H^{1/2}(\Gamma_C)} \\
&\leq \alpha_3 \|u_n - U_n\|^2_{H^{1/2}(\Gamma_C)} + \frac{C}{\alpha_3}\frac{h_1}{p_1}(1 + \delta_1^2)\|\sigma\|^2_{H^{1/2}(\Gamma_C)} \\
&\qquad + C\left(\frac{h_1}{p_1}\right)^{1/2} (\|\sigma\|^2_{H^{1/2}(\Gamma_C)} + \|\boldsymbol{u}\|^2_{\tilde{\boldsymbol{H}}^{3/2}(\Sigma)}),
\end{aligned}$$

since $\delta_2 < 1$ for sufficiently fine meshes. Here $\alpha_3 \in (0;1)$ is a constant to be specified later. Noting that $h_1/p_1 < 1$ for sufficiently fine meshes we obtain

$$\begin{aligned}
\int_{\Gamma_C} \sigma_n[\phi_n - U_n]\, ds &\leq \alpha_3 \|u_n - U_n\|^2_{H^{1/2}(\Gamma_C)} \\
&\quad + \frac{C}{\alpha_3}\left(\left(\frac{h_1}{p_1}\right)^{1/2} + \frac{h_1}{p_1}\delta_1^2\right)\|\sigma\|^2_{H^{1/2}(\Gamma_C)} + \left(\frac{h_1}{p_1}\right)^{1/2} \|\boldsymbol{u}\|^2_{\tilde{\boldsymbol{H}}^{3/2}(\Sigma)} \\
&\leq \alpha_3 \|u_n - U_n\|^2_{H^{1/2}(\Gamma_C)} + \frac{C}{\alpha_3}\gamma^2_{n,hp}\|\sigma\|^2_{H^{1/2}(\Gamma_C)} + \left(\frac{h_1}{p_1}\right)^{1/2} \|\boldsymbol{u}\|^2_{\tilde{\boldsymbol{H}}^{3/2}(\Sigma)},
\end{aligned}$$

where

$$\gamma_{n,hp} = \gamma_{n,hp}(h_1, h_2, p_1, p_2) := \left(\frac{h_1}{p_1}\right)^{1/4} + \sqrt{\log p_1}\frac{p_2}{p_1}\frac{h_1}{h_2^{1/2}}$$

In order to show (4.71), we choose $\phi_t^1 := U_t^1$, $\phi_t^2 := \pi^1_{hp} U_t^2$ (see (4.72)) and derive

$$\begin{aligned}
\int_{\Gamma_C} \sigma_t[\phi_t - U_t] + \mathcal{F}(|[\phi_t]| - |U_t^1 - \pi^1_{hp}U_t^2|)\, ds &\leq \int_{\Gamma_C} \sigma_t(U_t^2 - \pi^1_{hp}U_t^2)\, ds \\
&\leq \inf_{\Theta \in \mathcal{M}^1_{hp}} \int_{\Gamma_C} (\sigma_t - \Theta)(U_t^2 - \pi^1_{hp}U_t^2)\, ds \\
&\leq \inf_{\Theta \in \mathcal{M}^1_{hp}} ||\sigma_t - \Theta||_{H^{-1/2}(\Gamma_C)} ||U_t^2 - \pi^1_{hp}U_t^2||_{\tilde{H}^{1/2}(\Gamma_C)} \\
&\leq C\frac{h_1}{p_1}||\sigma_t||_{H^{1/2}(\Gamma_C)} ||U_t^2 - \pi^1_{hp}U_t^2||_{\tilde{H}^{1/2}(\Gamma_C)},
\end{aligned} \tag{4.86}$$

Performing the same decomposition as in (4.79) with U_t^2, u_t^2 instead of U_n^2, u_n^2 and proceeding further in a similar way we obtain (cf. (4.83))

$$\|U_t^2 - \pi_{hp}^1 U_t^2\|_{H^{1/2}(\Gamma_C)} \le C\delta_1 \|U_t^2 - u_t^2\|_{H^{1/2}(\Gamma_C)} + C\delta_2 \|u_t^2\|_{H^{3/2}(\Gamma_C)},$$

where δ_1, δ_2 are defined in (4.84), (4.85) respectively. Therefore from (4.86) we obtain for some constant $\alpha_4 \in (0;1)$

$$\begin{aligned}\int_{\Gamma_C} \sigma_t[\phi_t - U_t] + \mathcal{F}(|[\phi_t]| - |U_t^1 - \pi_{hp}^1 U_t^2|)\, ds \\ &\le C\frac{h_1}{p_1}(\delta_1 \|U_t^2 - u_t^2\|_{H^{1/2}(\Gamma_C)} + C\delta_2 \|u_t^2\|_{H^{3/2}(\Gamma_C)})||\sigma_t||_{H^{1/2}(\Gamma_C)} \\ &\le \alpha_4 \|U_t^2 - u_t^2\|^2_{H^{1/2}(\Gamma_C)} + \frac{C}{\alpha_4}\gamma_{t,hp}^2 ||\sigma_t||^2_{H^{1/2}(\Gamma_C)} + C\frac{h_1}{p_1}\delta_2 ||\boldsymbol{u}||^2_{\tilde{\boldsymbol{H}}^{3/2}(\Sigma)},\end{aligned}$$

where $\gamma_{t,hp}$ is defined by

$$\begin{aligned}\left(\left(\frac{h_1}{p_1}\delta_1\right)^2 + \frac{h_1}{p_1}\delta_2\right)^{1/2} &\le \frac{h_1}{p_1}\delta_1 + \left(\frac{h_1}{p_1}\delta_2\right)^{1/2} \\ &\le \sqrt{\log p_1}\frac{h_1^{3/2}}{h_2^{1/2}}\frac{p_2}{p_1^{3/2}} + \sqrt[4]{\log p_1}\left(\frac{h_1}{p_1}\right)^{3/4} h_2^{1/4} + \sqrt[4]{\log p_1}\frac{h_1}{p_1} =: \gamma_{t,hp}\end{aligned}$$

which provides (4.71). □

Now we are can formulate the main result.

Theorem 4.3.1. *Let $\boldsymbol{u} \in \boldsymbol{\mathcal{K}} \cap \tilde{\boldsymbol{H}}^{3/2}(\Sigma)$ be the solution of (4.12), and let $\boldsymbol{U} \in \boldsymbol{\mathcal{K}}_{hp}$ be the solution of (4.55). Suppose that $\|\sigma_n\|_{H^{1/2}(\Gamma_C)} + \|\sigma_t\|_{H^{1/2}(\Gamma_C)} + \|\mathcal{F}\|_{L_2(\Gamma_C)} \le C\|\boldsymbol{u}\|_{\tilde{\boldsymbol{H}}^{3/2}(\Sigma)}$, where σ_n, σ_t are the normal and tangential contact tractions, corresponding to the solution $\boldsymbol{u}$, and $\mathcal{F}$ is a "given friction" function. Then for some constant $C > 0$ there holds*

$$\|\boldsymbol{u} - \boldsymbol{U}\|_{\tilde{\boldsymbol{H}}^{1/2}(\Sigma)} \le C\gamma_{hp}\|\boldsymbol{u}\|_{\tilde{\boldsymbol{H}}^{3/2}(\Sigma)},$$

where

$$\gamma_{hp} := \left(\frac{h_1}{p_1}\right)^{1/4} + \left(\frac{h_2}{p_2}\right)^{1/2} + \sqrt{\log p_1}\frac{p_2}{p_1}\frac{h_1}{h_2^{1/2}}$$

Proof. The assertion of the theorem follows after combining Lemma 4.3.5 with Lemma 4.3.6 and Lemma 4.3.7. The convergence rates in estimates (4.61) - (4.63) from Lemma 4.3.6 as well as the convergence rates $\gamma_{n,hp}, \gamma_{t,hp}$ in estimates (4.70) and (4.71) from Lemma 4.3.7 are obviously dominated by γ_{hp} for sufficiently refined meshes. □

Corollary 4.3.1. *Connecting the mesh parameters by*

$$h_2 := h_1^\alpha, \qquad p_2 := p_1^\beta$$

we observe that the convergence rate γ_{hp} *is given by*

$$\gamma_{hp} = \left(\frac{h_1}{p_1}\right)^{1/4} + \frac{h_1^{\alpha/2}}{p_1^{\beta/2}} + \sqrt{\log p_1}\frac{h_1^{1-\alpha/2}}{p_1^{1-\beta}}.$$

Thus $\gamma_{hp} = \left(\frac{h_1}{p_1}\right)^{1/4}$ *is optimal and is achieved for*

$$\frac{1}{2} \leq \alpha \leq \frac{3}{2}, \qquad \frac{1}{2} \leq \beta < \frac{3}{4}.$$

Furthermore, the minimal number of the degrees of freedom in the algebraic system is asymptotically achieved for largest h_2 *and smallest* p_2*, i.e. when* $\alpha = \beta = 1/2$.

Remark 4.3.4. *The condition* $\|\sigma_n\|_{H^{1/2}(\Gamma_C)} + \|\sigma_t\|_{H^{1/2}(\Gamma_C)} \leq C\|\boldsymbol{u}\|_{\tilde{\boldsymbol{H}}^{3/2}(\Sigma)}$ *in Theorem 4.3.1 can be treated as the continuity condition of the Dirichlet-to-Neumann operator* $T := V^{-1}(K + 1/2)$*, since* $T\boldsymbol{u}|_{\Gamma_C} = \sigma_n \boldsymbol{n}^1 + \sigma_t \boldsymbol{t}^1$.

Furthermore, the condition $\|\mathcal{F}\|_{L_2(\Gamma_C)} \leq C\|\boldsymbol{u}\|_{\tilde{\boldsymbol{H}}^{3/2}(\Sigma)}$ *in Theorem 4.3.1 is not restrictive. In practice, where the Coulomb's friction law is used,* $\mathcal{F}$ *is replaced with* $\mu_f\sigma_n$ *and the condition is satisfied, if the Dirichlet-to-Neumann operator* T *is continuous.*

4.3.3 Dirichlet-to-Neumann algorithm

We employ a Dirichlet-to-Neumann (DtN) algorithm (see e.g. [40] , [18]) to solve the discrete problem (4.55), which allows to decompose the two-body problem into two separate subproblems in each body - a mixed boundary value problem and a frictional contact problem between an elastic body and a rigid obstacle. The data transfer is realized in terms of a mortar projection and its adjoint. The convergence of the DtN algorithm is analysed for the h-version of FEM in [4], [28].

The mortar projection $\Phi^1 := \pi_{hp}^1(\Phi^2)$ on $\mathcal{T}_h^1 \cap \Gamma_C$ of some function Φ^2 on $\mathcal{T}_h^2 \cap \Gamma_C$ is according to (4.50) given by

$$\int_{\Gamma_C} \Phi^1 \Psi^1 ds = \int_{\Gamma_C} \Phi^2 \Psi^1 ds, \qquad \forall \Psi^1 \in \mathcal{M}_{hp}^1. \tag{4.87}$$

Thus, its algebraic form is $\Phi^1 = D^{-1}B\Phi^2$, with the sparse mass matrix D, produced by the left hand side of (4.87), and the matrix B, produced by the right hand side respectively. Note, that B is also sparse, since the basis functions on the meshes $\mathcal{T}_h^1$, $\mathcal{T}_h^2$ have local supports. The boundary tractions are transferred by the adjoint operator

π_{hp}^{1*}. Thus, the algebraic form of the adjoint mortar projection is given by the transposed matrices $\pi_{hp}^{1*}(\Phi^2) = B^T D^{-T} \Phi^1$. We denote

$$\boldsymbol{X}_{hp}^i := \left\{ \boldsymbol{\Phi}|_{\Gamma_C} : \boldsymbol{\Phi} \in \boldsymbol{\mathcal{V}}_{hp}^i \right\}.$$

The case of an initial gap $g \neq 0$ can be incorporated in our problem. We measure the initial gap in the normal direction to Γ_C^1 (see [32] for more details).

Algorithm 4.3. *(Dirichlet-to-Neumann algorithm)*

---

1. *Choose* $\omega_D, \omega_N \in (0,1)$, *set* $\boldsymbol{X}_{hp}^1 \ni \boldsymbol{Q}_0 := 0, \boldsymbol{X}_{hp}^2 \ni \boldsymbol{P}_1 := 0$
2. *Solve elastic inhomogeneous Neumann problem with BEM:*
   Find $\boldsymbol{U}_k^2 \in \boldsymbol{\mathcal{V}}_{hp}^2$:
   $$\left\langle \hat{S}\boldsymbol{U}_k^2, \boldsymbol{W}^2 \right\rangle = L(\boldsymbol{W}^2) - \langle \boldsymbol{P}_k, \boldsymbol{W}^2 \rangle_{\Gamma_C}, \qquad \forall \boldsymbol{W}^2 \in \boldsymbol{\mathcal{V}}_{hp}^2 \tag{4.88}$$
3. *Transfer obstacle, damping* $\boldsymbol{Q}_k := (1-\omega_D)\boldsymbol{Q}_{k-1} + \omega_D D^{-1} B \boldsymbol{U}_k^2$
4. *Solve elastic frictional contact problem with BEM:*
   Find $\boldsymbol{U}_k^1 \in \boldsymbol{\mathcal{K}}_{\boldsymbol{Q}_k} := \{\boldsymbol{U}_k^1 : U_{kn}^1 - Q_{kn} \leq g \text{ in } G_{hp}^1 \cap \Gamma_C^1\}$ *such that* $\forall \boldsymbol{W}^1 \in \boldsymbol{\mathcal{K}}_{\boldsymbol{Q}_k}$
   $$\langle \hat{S}\boldsymbol{U}_k^1, \boldsymbol{W}^1 - \boldsymbol{U}_k^1 \rangle + j(W_t^1 - Q_{kt}) - j(U_{kt}^1 - Q_{kt}) \geq L(\boldsymbol{W}^1 - \boldsymbol{U}_k^1) \tag{4.89}$$
5. *Compute contact traction* $\boldsymbol{R}_k^1 \in \boldsymbol{X}_{hp}^1 : \langle \boldsymbol{R}_k^1, \boldsymbol{W}^1 \rangle := \langle \hat{S}\boldsymbol{U}_k^1, \boldsymbol{W}^1 \rangle - L(\boldsymbol{W}^1)$
6. *Transfer contact traction, damping*
   $$\boldsymbol{P}_{k+1} := (1-\omega_N)\boldsymbol{P}_k + \omega_N B^T D^{-T} \boldsymbol{R}_k^1$$
7. *Set* $k = k+1$, *repeat with 2, stop if* $||\boldsymbol{P}_k - \boldsymbol{P}_{k-1}|| \leq \mathrm{TOL}_{DtN} \cdot ||\boldsymbol{P}_{k-1}||$

Remark 4.3.5. *The FEM techniques can be easily used in one or in both bodies, as well as for nonlinear material behaviour. In case of contact of an elastic body with an elastoplastic body, the problem can be decomposed into the Neumann problem with plasticity and the contact problem with elasticity. Therefore separation of nonlinearities is achieved. Numerical example for this elastoplastic contact problem are given in Section 4.4.*

In order to solve the elastic problem with frictional contact, we rewrite formulation (4.89) in an equivalent form with a Lagrange multiplier, cf. (3.16):
Find $\boldsymbol{U}^1 \in \boldsymbol{\mathcal{K}}_{\boldsymbol{Q}_k}, \lambda_u \in \Lambda$:

$$\begin{aligned} &\langle \hat{S}\boldsymbol{U}^1, \boldsymbol{W}^1 - \boldsymbol{U}^1 \rangle + \int_{\Gamma_C} \mathcal{F}\lambda_u (W_t^1 - U_t^1)\, ds \geq L(\boldsymbol{W}^1 - \boldsymbol{U}^1), \\ &\lambda_u (U_t^1 - Q_{kt}) = |U_t^1 - Q_{kt}| \text{ a.e. on } \Gamma_C, \qquad \forall \boldsymbol{W}^1 \in \boldsymbol{\mathcal{K}}_{\boldsymbol{Q}_k}, \end{aligned} \tag{4.90}$$

where $\Lambda = \{\lambda \in L^2(\Gamma_C) : |\lambda| \leq 1 \text{ a.e. on } \Gamma_C\}$. The product $\mathcal{F}\lambda_u$ plays the role of the tangential contact traction. The Lagrange multiplier λ_u itself has the meaning of the sliding direction, if sliding occurs. Problem (4.90) is solved by the Uzawa algorithm.

Algorithm 4.4. *(Uzawa algorithm)*

---

1. *Choose* $\lambda^0 \in \Lambda$, $\rho > 0$
2. *Solve frictionless contact with Polyak [53] (modified CG) algorithm*
   Find $\boldsymbol{U}_m^1 \in \boldsymbol{\mathcal{K}}_{\boldsymbol{Q}_k}, \lambda_m \in \Lambda$:

   $$\langle \hat{S}\boldsymbol{U}_m^1, \boldsymbol{W}^1 - \boldsymbol{U}_m^1 \rangle \geq L(\boldsymbol{W}^1 - \boldsymbol{U}_m^1) - \int_{\Gamma_C} \mathcal{F}\lambda_k (W_t^1 - U_{mt}^1)\, ds, \qquad \forall \boldsymbol{W}^1 \in \boldsymbol{\mathcal{K}}_{\boldsymbol{Q}_k}$$

3. *Set* $\lambda_{m+1} := P_\Lambda(\lambda_m + \rho \mathcal{F}(U_{mt}^1 - Q_{kt}))$
4. *Set* $m = m + 1$, *repeat with 2, stop if* $||\lambda_m - \lambda_{m-1}|| \leq \mathrm{TOL}_U \cdot ||\lambda_{m-1}||$

Here P_Λ is given pointwise by

$$P_\Lambda(x) := \begin{cases} 1, & \text{if } x > 1, \\ -1, & \text{if } x < -1, \\ x, & \text{otherwise.} \end{cases}$$

Theorem 3.1.8 provides that the Uzawa algorithm converges for sufficiently small ρ.

4.3.4 Numerical examples

We solve the discrete contact problem with given friction (4.55) with the Dirichlet-to-Neumann algorithm, described above. In our model problem we consider two bodies Ω^1, Ω^2, which are given by their boundaries $\Gamma^i := \partial\Omega^i = \Gamma_D^i \bigcup \Gamma_N^i \bigcup \Gamma_C^i$ as follows

$$\begin{aligned} &\Gamma_D^1 = [-1,1] \times \{2\}, && \Gamma_D^2 = [-1,1] \times \{-2\} \textstyle\bigcup \{-1,1\} \times [-1,0], \\ &\Gamma_N^1 = \{-1,1\} \times [0,2], && \Gamma_N^2 = \emptyset, \\ &\Gamma_C^1 = \gamma, && \Gamma_C^2 = -[1,1] \times \{0\}, \end{aligned}$$

where γ is the arc of a circle including the points $(-1, 0.1)$, $(0, 0)$, $(1, 0.1)$. We denote the characteristic length by $L := 2$. The bodies are coming into contact due to prescribed displacements on the Dirichlet boundary $\boldsymbol{U}^1 := (0, -0.09)$ on Γ_D^1 and $\boldsymbol{U}^2 := (0, 0)$ on Γ_D^2. The Young's modulus and Poisson's ratio are $E = 266926.0$, $\nu = 0.29$ respectively. We choose $\mathcal{F} = 0.1$, $\rho = 1.0$. The tolerances $TOL_{DtN} = TOL_U = 10^{-6}$ are used for the stopping criteria.

We solve a frictional contact problem on Γ^1 and a nonhomogeneous Neumann problem on Γ^2. We associate the mortar space $\mathcal{M}_{hp}^1$ with the mesh, induced from Γ^1, i.e. the mesh $\mathcal{T}_h^1 \cap \Gamma^1$. We present numerical examples on quasiuniform meshes.

$\omega_D \backslash \omega_N$	0.3	0.5	0.7	0.9
0.3	42	30	21	16
0.5	30	23	17	18
0.7	21	17	20	-
0.9	23	18	-	-

Table 4.1: Number of Dirichlet-to-Neumann iterations

First we study convergence of the DtN algorithm for different damping parameters. We choose the piecewise quadratic polynomial approximation with 16 elements in $\mathcal{T}_h^1 \cap \Gamma^1$ and 12 elements in $\mathcal{T}_h^2 \cap \Gamma^2$, i.e. $h_1 := L/16$, $h_2 := L/12$. The corresponding initial and deformed meshes on Γ^1 and Γ^2 are given on Fig. 4.17. The number of Dirichlet-to-Neumann iterations related to the damping parameters is given in Table 4.1. We observe, that the smallest number of iterations is achieved in case $\omega_D + \omega_N \in [1.2; 1.4]$.

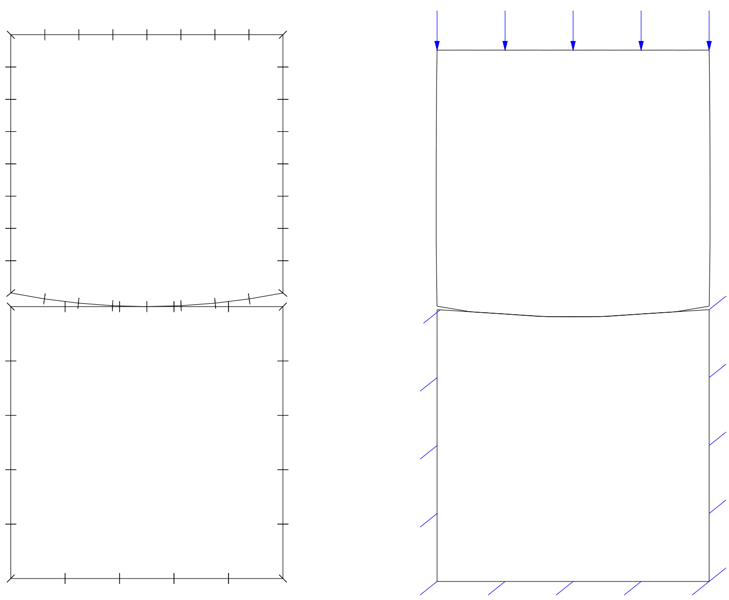

Figure 4.17: Initial mesh and deformed configuration

In case of high damping parameters $\omega_D + \omega_N \geq 1.6$ no convergence is observed.

In order to study convergence of our *hp*-mortar method we perform a series of experiments for $h_1 : h_2 = 4 : 3$, $h_1 = L/4$, $L/8$, $L/16$, $L/32$, $L/64$ and $(p_1, p_2) = (1,1)$, $(2,1)$, $(2,2)$. The norm in the space $\tilde{\boldsymbol{H}}^{1/2}(\Sigma)$ can be expressed in terms of the hypersingular integral operator W as

$$||\boldsymbol{U}||_{\tilde{H}^{1/2}(\Sigma)} \approx \left(\langle W\boldsymbol{U}^1, \boldsymbol{U}^1\rangle_{\Sigma^1} + \langle W\boldsymbol{U}^2, \boldsymbol{U}^2\rangle_{\Sigma^2}\right)^{1/2} =: ||\boldsymbol{U}||_W.$$

We compute $||\boldsymbol{U}||_{W,\delta}$ for each combination $\delta := ((h_1, h_2); (p_1, p_2))$. The limit norm $||\boldsymbol{U}||_{W,\infty} \approx 6.110073$ is obtained by extrapolation. The behaviour of $\big|\, ||\boldsymbol{U}||_{W,\delta} - ||\boldsymbol{U}||_{W,\infty} \big|$ is shown on Fig. 4.18. We observe the convergence rate ≈ 0.63 for the piecewise linear polynomial discretization, whereas in the piecewise quadratic case the convergence rate ≈ 1.89 is obtained.

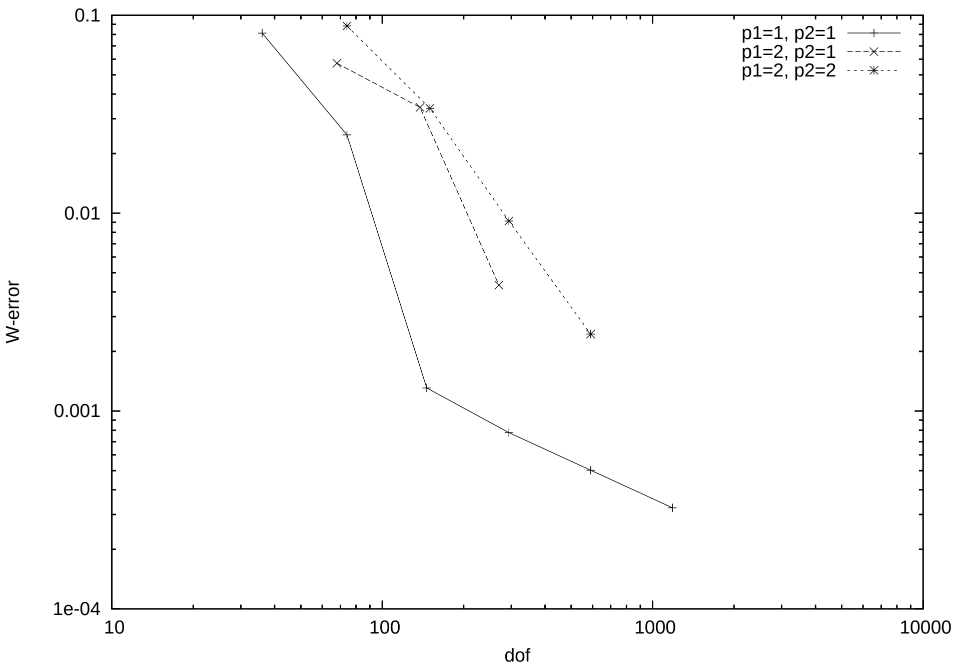

Figure 4.18: Convergence of $\big|\, ||\boldsymbol{U}||_{W,\delta} - ||\boldsymbol{U}||_{W,\infty} \big|$

4.3.5 Uzawa algorithm and hp-adaptive error control

In this section we describe an alternative solution procedure - the Uzawa algorithm. We make a heuristic motivation for the a posteriori error indicator and give a numerical example of a two-body contact problem with hp-mesh refinement.

The solution procedure is based on the mixed formulation (4.14), equivalent to the variational inequality (4.12). In order to construct a discretized version of (4.14), we use the following continuous piecewise polynomial discrete spaces

$$\boldsymbol{\mathcal{V}}_{hp}^i := \left\{ \boldsymbol{U} \in \tilde{\boldsymbol{H}}^{1/2}(\Sigma^i) : \forall I \in \mathcal{T}_{hp}^i, \boldsymbol{U} \in [\mathcal{P}_{p_I}(I)]^2 \right\}, \qquad \boldsymbol{\mathcal{V}}_{hp} := \boldsymbol{\mathcal{V}}_{hp}^1 \times \boldsymbol{\mathcal{V}}_{hp}^2,$$

$$Y_{hp}^1 := \left\{ P \in H^{1/2}(\Gamma_C) : \forall I \in \mathcal{T}_{hp}^1 \cap \Gamma_C, P \in \mathcal{P}_{p_I}(I) \right\}.$$

The main difficulty in the discretization of (4.14) lies in the correct interpretation of the non-penetration condition, hidden in the space of tractions $\boldsymbol{\mathcal{M}}$, defined in (4.13). For instance, the use of pointwise contact response, as in the penalty method, seems to be problematic. We employ here the mortar technique, which performs the data transfer across the boundary with nonmatched meshes in terms of the mortar projection and its adjoint operator. We define

$$\begin{aligned} M_{n,hp} &:= \left\{ P_n \in Y_{hp}^1 : P_n(x) \geq 0, \forall x \in G_{hp}^1 \cap \Gamma_C \right\}, \\ M_{t,hp} &:= \left\{ P_t \in Y_{hp}^1 : |P_t(x)| \leq \mathcal{F}(x), \forall x \in G_{hp}^1 \cap \Gamma_C \right\}. \end{aligned}$$

Here the positivity condition is enforced only on the discrete set of the Gauss-Lobatto points G_{hp}^1 on Γ^1. We introduce the discrete version of (4.14) as follows:
Find $\boldsymbol{U} \in \boldsymbol{\mathcal{V}}_{hp}, \boldsymbol{P} \in \boldsymbol{\mathcal{M}}_{hp} := M_{n,hp} \times M_{t,hp}$ such that

$$\begin{aligned} &\left\langle \hat{S}\boldsymbol{U}, \boldsymbol{\Phi} \right\rangle_{\Sigma} + b(\boldsymbol{P}, \boldsymbol{\Phi}) = \left\langle \hat{\boldsymbol{t}}, \boldsymbol{\Phi} \right\rangle_{\Gamma_N}, \qquad && \forall \boldsymbol{\Phi} \in \boldsymbol{\mathcal{V}}_{hp}, \\ &b(\boldsymbol{Q} - \boldsymbol{P}, \boldsymbol{U}) \leq 0, && \forall \boldsymbol{Q} \in \boldsymbol{\mathcal{M}}_{hp}. \end{aligned} \tag{4.91}$$

In this section we apply the Uzawa algorithm for solution of global problem, an alternative approach to the Dirichlet-to-Neumann method, used in the previous section. Here the two-body problem is decomposed into two one-body Neumann problems. In this case we can avoid nested cycles and compute the solution of the general contact problem with *Coulomb's friction* in a single loop. Moreover, in contrast to DtN, the Uzawa algorithm can be easily parallelized, since both one-body Neumann problems can be solved independently. The discrete mortar projection for displacement is given by the matrix $B^{-1}D$ (cf. (4.87)). The Uzawa algorithm for contact with Coulomb's friction is listed below.

Algorithm 4.5. *(Uzawa algorithm for the global problem)*

1. *Choose* $\rho > 0$*, set* $\boldsymbol{\mathcal{V}}_{hp} \ni \boldsymbol{U}_0 := 0, \boldsymbol{\mathcal{M}}_{hp} \ni \boldsymbol{P}_0 := 0, k := 0$
2. *Solve Neumann problems on* Γ^1 *and* Γ^2*: Find* $\boldsymbol{U}_k^i \in \boldsymbol{\mathcal{V}}_{hp}^i$ *such that*
$$\left\langle \hat{S}\boldsymbol{U}_k^i, \boldsymbol{\Phi}^i \right\rangle = \left\langle \hat{\boldsymbol{t}}, \boldsymbol{\Phi}^i \right\rangle + (-1)^i \langle \boldsymbol{P}_k, \boldsymbol{\Phi}^i \rangle_{\Gamma_C}, \quad \forall \boldsymbol{\Phi}^i \in \boldsymbol{\mathcal{V}}_{hp}^i,\ i = 1, 2$$
3. *Compute contact tractions* $\boldsymbol{P}_{k+1} := \Pi_{\boldsymbol{\mathcal{M}}_{hp}}(\boldsymbol{P}_k - \rho(\boldsymbol{U}_k^1 - B^{-1}D\boldsymbol{U}_k^2))$
4. *Set* $k = k + 1$*, repeat with 2, stop if* $k \geq 3$ *and* $||\boldsymbol{P}_k - \boldsymbol{P}_{k-1}|| \leq \mathrm{TOL} \cdot ||\boldsymbol{P}_2 - \boldsymbol{P}_1||$

Here
$$\Pi_{\boldsymbol{\mathcal{M}}_{hp}} = \begin{cases} \Pi_{\mathcal{M}_{n,hp}} & : \quad Y_{hp}^1 \times Y_{hp}^1 \to \mathcal{M}_{n,hp}, \\ \Pi_{\mathcal{M}_{t,hp}} & : \quad Y_{hp}^1 \times Y_{hp}^1 \to \mathcal{M}_{t,hp} \end{cases}$$
is a projection onto $\boldsymbol{\mathcal{M}}_{hp}$, defined pointwise as follows. If $x \in G_{hp}^1 \cap \Gamma_C$, i.e. x is a Gauss-Lobatto point, then the value $\boldsymbol{P}(x) = (P_n(x), P_t(x))$ of a function $\boldsymbol{P} \in \boldsymbol{\mathcal{V}}_{hp}^1$ is projected by
$$\Pi_{\mathcal{M}_{n,hp}}(P_n(x)) := P_n(x)\mathrm{sign}(P_n(x)),$$
$$\Pi_{\mathcal{M}_{t,hp}}(P_t(x)) := \max(-\mu_f P_n(x), \min(\mu_f P_n(x), P_t(x)))$$

Our model problem and a test computation for quadratic polynomials and nonmatched uniform meshes with $h_1 : h_2 = 41 : 25$ are shown on Fig.4.19.

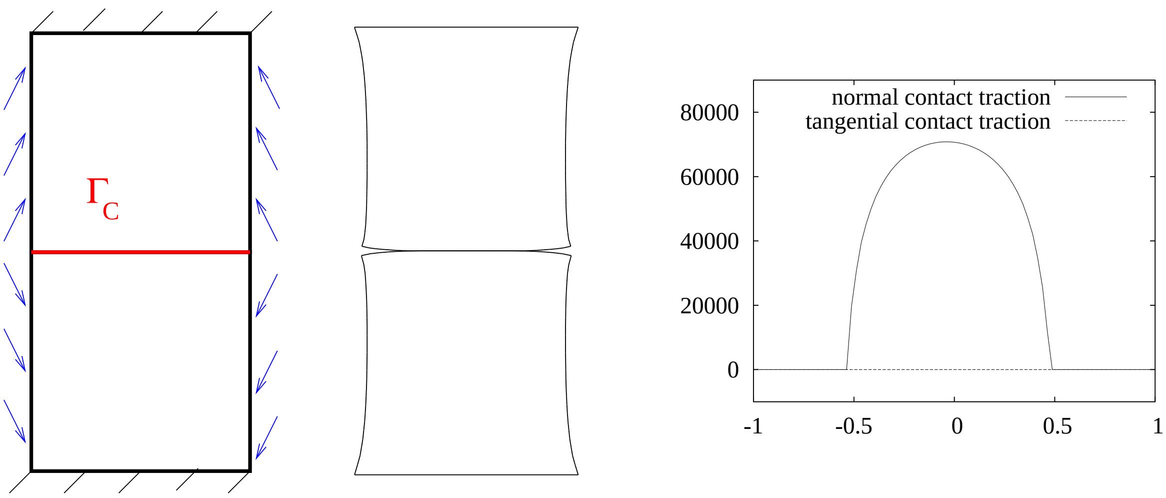

Figure 4.19: Model problem, deformed configuration, contact stress

In our numerical experiments we use the error indicator η, consisting of three parts

$$\eta := \left(\eta_C^2 + \eta_N^2 + \eta_{\hat{S}}^2\right)^{1/2},$$

where

$$\eta_C^2 := \sum_{I\in\mathcal{T}_h^1\subset\Gamma_C} \frac{h_I}{p_I}||[\boldsymbol{P}]||^2_{\boldsymbol{L}_2(I)} + \left(\frac{h_I}{p_I}\right)^{-1} ||[U_n]^+||^2_{L_2(I)} + \frac{h_I}{p_I}||(-\boldsymbol{P}) - \hat{S}\boldsymbol{U}||^2_{\boldsymbol{L}_2(I)},$$
$$\eta_N^2 := \sum_{I\in\mathcal{T}_h\subset\Gamma_N} \frac{h_I}{p_I}||\hat{\boldsymbol{t}} - \hat{S}\boldsymbol{U}||^2_{\boldsymbol{L}_2(I)},$$
$$\eta_{\hat{S}}^2 := \sum_{I\in\mathcal{T}_h} \frac{h_I}{p_I}||V\boldsymbol{\Psi} - (K+1/2)\boldsymbol{U}||^2_{\boldsymbol{L}_2(I)}.$$

Here $\boldsymbol{U}\in\boldsymbol{\mathcal{V}}_{hp}, \boldsymbol{P}\in\boldsymbol{\mathcal{M}}_{hp}$ is the solution of (4.91), and $\boldsymbol{\Psi} := i_{hp}V_{hp}^{-1}i_{hp}^*(K+1/2)\boldsymbol{U}$ is the discrete traction, cf. (3.59). We also need two other traction-like functions, given by

$$\boldsymbol{\psi} := V^{-1}(K+1/2)\boldsymbol{u},$$
$$\boldsymbol{\Psi}^* := V^{-1}(K+1/2)\boldsymbol{U}.$$

The motivation for using η is based on the identity, shown in Lemma 3.2.6. Thus,

$$||\boldsymbol{u}-\boldsymbol{U}||^2_{\tilde{\boldsymbol{H}}^{1/2}(\Sigma)} + ||\boldsymbol{\psi} - \boldsymbol{\Psi}||^2_{\boldsymbol{H}^{-1/2}(\Gamma)} \le C\left(\left\langle S\boldsymbol{u} - \hat{S}\boldsymbol{U}, \boldsymbol{u}-\boldsymbol{U}\right\rangle + \left\langle V(\boldsymbol{\Psi}^* - \boldsymbol{\Psi}), \boldsymbol{\psi} - \boldsymbol{\Psi}\right\rangle\right) \tag{4.92}$$

For the second summand in the right-hand side of (4.92) there holds

$$\left\langle V(\boldsymbol{\Psi}^* - \boldsymbol{\Psi}), \boldsymbol{\psi} - \boldsymbol{\Psi}\right\rangle \le \alpha||\boldsymbol{\psi} - \boldsymbol{\Psi}||^2_{\boldsymbol{H}^{-1/2}(\Gamma)} + \frac{1}{4\alpha}||V\boldsymbol{\Psi} - (K+1/2)\boldsymbol{U}||^2_{\boldsymbol{H}^{1/2}(\Gamma)},$$

and the indicator $\eta_{\hat{S}}^2$ is the discrete analogue of the term $||V\boldsymbol{\Psi} - (K+1/2)\boldsymbol{U}||^2_{\boldsymbol{H}^{1/2}(\Gamma)}$. Further, formulations (4.14) and (4.91) yield the identity

$$\left\langle S\boldsymbol{u} - \hat{S}\boldsymbol{U}, \boldsymbol{u}-\boldsymbol{U}\right\rangle = \left\langle \hat{\boldsymbol{t}} - \hat{S}\boldsymbol{U}, \boldsymbol{u} - \boldsymbol{\Phi}\right\rangle_{\Gamma_N} + \left\langle (-\boldsymbol{P}) - \hat{S}\boldsymbol{U}, \boldsymbol{u} - \boldsymbol{\Phi}\right\rangle_{\Gamma_C} - b(\boldsymbol{p}-\boldsymbol{P}, \boldsymbol{u}-\boldsymbol{U}), \tag{4.93}$$

for arbitrary $\boldsymbol{\Phi}\in\boldsymbol{\mathcal{V}}_{hp}$, which motivates with the standard arguments the indicator η_N^2 and the last summand in η_C^2. In order to motivate the remaining indicators, let us consider an interface problem, where the transmission conditions $[\boldsymbol{u}] = 0$ and $[\boldsymbol{p}] = 0$ are enforced on Γ_C. Then, for the interface problem, the last term in (4.93) yields

$$-b(\boldsymbol{p}-\boldsymbol{P}, \boldsymbol{u}-\boldsymbol{U}) \le \alpha||\boldsymbol{p}-\boldsymbol{P}||^2_{\tilde{H}^{-1/2}(\Gamma_C)} + \frac{1}{4\alpha}||[\boldsymbol{U}]||^2_{H^{1/2}(\Gamma_C)}. \tag{4.94}$$

The term $||\boldsymbol{p}-\boldsymbol{P}||^2_{\tilde{H}^{-1/2}(\Gamma_C)}$ corresponds to the term $||\boldsymbol{\psi} - \boldsymbol{\Psi}||^2_{\boldsymbol{H}^{-1/2}(\Gamma)}$ in (4.92), and it can be moved to the left-hand side of (4.92); while the term $||[\boldsymbol{U}]||^2_{H^{1/2}(\Gamma_C)}$ makes a contribution to the indicator. It represents the error due to violation of the interface condition $[\boldsymbol{u}] = 0$. Unfortunately, the estimate (4.94) is in general wrong for the contact problems. We replace it by adding the two first indicators in η_C^2, which should control the error due to violation of the contact conditions $[\boldsymbol{p}] = 0$ and $[u_n] \leq 0$ (or equivalently $[u_n]^+ = 0$).

The error indicator η is very similar to the indicator obtained for interface problems by Wohlmuth [70], and applied by Krause and Wohlmuth [40] to the contact problems. We use the three-step *hp*-adaptive algorithm (Algorithm 4.6) used e.g. by Maischak and Stephan [46].

The h-refinement is performed for all elements, which indicator is larger then 90% of the largest indicator value; and the p-refinement is used, if the indicator value is between 85% and 90% of the largest indicator value. The sequence of meshes and polynomial degrees obtained with our approach is shown in Figure 4.20.

Algorithm 4.6. *(Mesh refinement strategy for the h-version)*

---

1. *generate an initial (coarse) mesh* $\mathcal{T}_{hp,0}$, *discrete spaces* $\boldsymbol{\mathcal{V}}_{hp,0}$, $\boldsymbol{\mathcal{W}}_{hp,0}$, *set* $k = 0$
2. *choose a refinement criterion, refinement quota* $0 < q_1 < q_2 < 1$, *tolerance* TOL
3. *for* $k = 0, 1, 2 \ldots$
   a) *solve the discrete problem*
   b) *compute indicators* η_I *for all segments* $I \in \mathcal{T}_{hp,k}$
   c) *stop if* $\sum_{I \in \mathcal{T}_{hp,k}} \eta_{\mathcal{I}}^2 \leq TOL$
   d) *split the element* I *increase the polynomial degree on* I *according to the following rules*
      i. *if* $\eta_I \geq q_2 \eta_{max}$, *split the element* I *into two elements of equal length and inherit the polynomial degree*
      ii. *if* $q_1 \eta_{max} \leq \eta_I \leq q_2 \eta_{max}$, *increase the polynomial degree on* I
      iii. $\eta_I \leq q_1 \eta_{max}$ *do nothing*
   e) *compute the resulting mesh* $\mathcal{T}_{hp,k+1}$
   f) *generate the discrete spaces* $\boldsymbol{\mathcal{V}}_{hp,k+1}$, $\boldsymbol{\mathcal{W}}_{hp,k+1}$ *based on the mesh* $\mathcal{T}_{h,k+1}$
   g) *set* $k = k + 1$, *go to (a)*

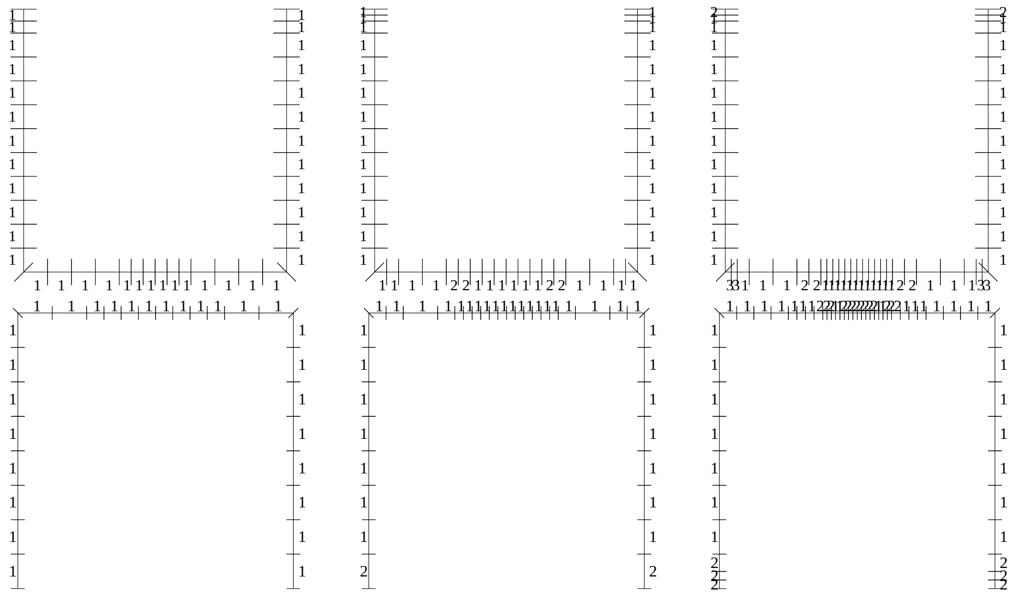

Figure 4.20: Adaptively generated meshes and polynomial degrees after 3, 6 and 9 refinement steps

4.4 Mortar and penalty methods for elastoplastic contact problems

In this section we compare the mortar method and the penalty method for frictional contact problem between an elastic body and an elastoplastic body. We use the pure FEM discretization with continuous piecewise bilinear basis functions on quadrilaterals for the mortar method. For the penalty method we use the FE/BE coupling method with continuous piecewise bilinear basis functions on quadrilaterals in the FE domain and continuous piecewise linear basis functions in the BE domain.

We employ the Dirichlet-to-Neumann (DtN) algorithm (Algorithm 4.3) as a solution procedure for the mortar method with the following modifications. In the step 2 the inhomogeneous Neumann elastoplastic problem is solved with finite elements by the Newton method, and in the step 4 corresponding frictional contact problem is solved also with finite elements.

We assume that an elastic body occupies the domain

$$\Omega^s := [-1/2, 1/2] \times [0, 2]$$

and an elastoplastic body occupies the domain

$$\Omega^m := [-2, 2] \times [-2, 0].$$

We fix the upper boundary of Ω^s and prescribe a nonzero displacement on the lower boundary of Ω^m

$$\hat{\boldsymbol{u}}^s = 0, \qquad \text{on } \Gamma^s_D := [-1/2, 1/2] \times \{2\},$$
$$\hat{\boldsymbol{u}}^m = 10^{-4}, \qquad \text{on } \Gamma^m_D := [-2, 2] \times \{-2\}.$$

The remaining parts of the boundaries are treated as contact boundaries

$$\Gamma^s_C := \partial\Omega^s \setminus \Gamma^s_D, \qquad \Gamma^m_C := \partial\Omega^m \setminus \Gamma^m_D.$$

The both bodies have the same material parameters $E = 266926.0$, $\nu = 0.29$ and the given friction function $\mathcal{F} = 0.22$. The yield stress and the hardening parameter in Ω^m are $\sigma^m_Y = 4.0, h^m_Y = 450.0$. The damping parameters of the DtN algorithm are $\omega_D = 0.5, \omega_N = 0.7$. The damping parameter for the Uzawa algorithm is $\rho = 8.264 \cdot 10^5$. The DtN and Uzawa tolerances are $\mathrm{TOL}_{DtN} = \mathrm{TOL}_U = 10^{-6}$, the tolerance of the Newton method, used for solving the elastoplastic subproblem, is $\mathrm{TOL}_N = 10^{-4}$.

The results of the numerical tests for the mortar method are presented in the Figure 4.21. The norm of the stress deviator is plotted only for the elastoplastic body Ω^m, since Ω^s is assumed to be linear elastic. The brown region in the plot of the norm of the stress deviator corresponds to its maximum value, i.e. represents the plastic region. Table 4.2 shows the number of DtN iterations depending on the damping parameters. The number of the Uzawa iterations in the first DtN iteration is given in parenthesis.

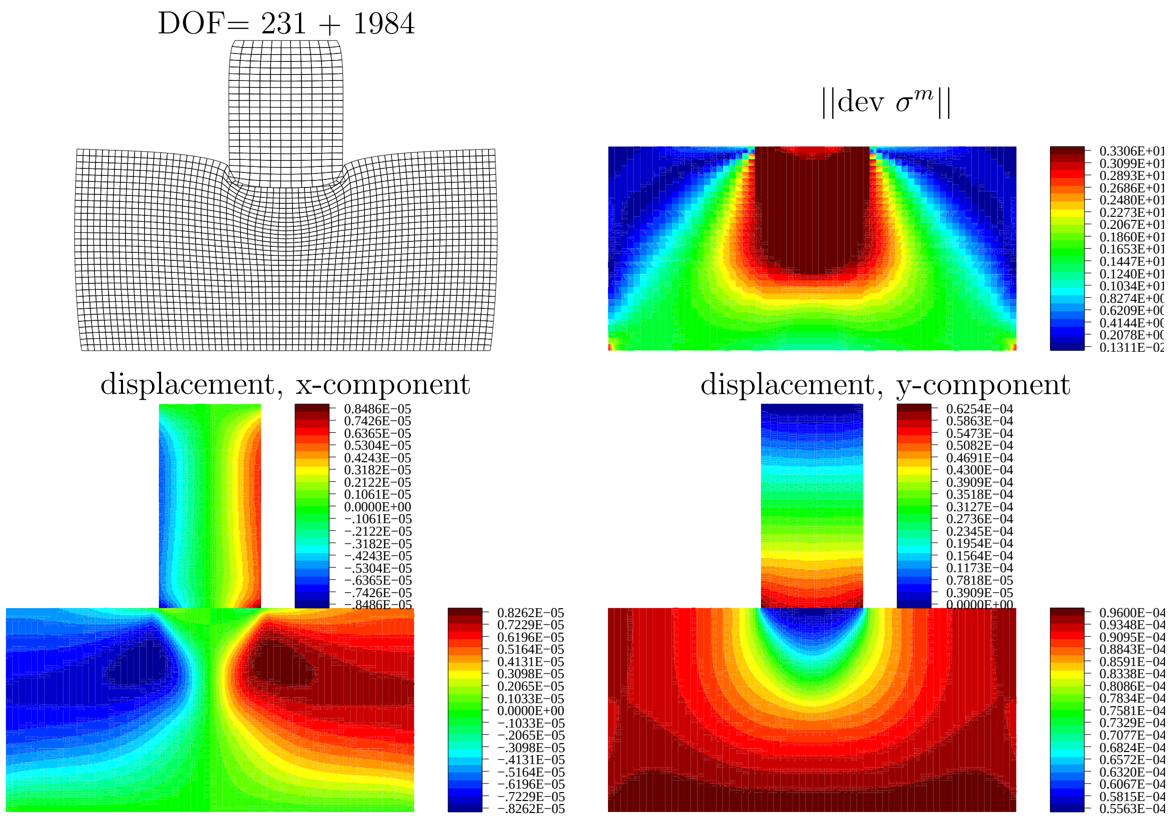

Figure 4.21: Numerical experiments for mortar method with DtN algorithm

$\omega_D \setminus \omega_N$	0.3	0.5	0.7	0.9	1.0
0.3	27(34)	19(34)	13(34)	9(34)	9(34)
0.5	19(17)	13(17)	11(17)	-	-
0.7	12(13)	11(12)	-	-	-
0.9	13(9)	-	-	-	-

Table 4.2: Number of DtN (Uzawa) iterations for mortar method

Since the sliding direction is correctly recognized after the first DtN iteration, the Uzawa algorithm needs only 2 iterations starting from the second DtN iteration. The damping parameter $\rho = 8.264 \cdot 10^5$ for the Uzawa algorithm is chosen experimentally. Table 4.2 shows that the optimal values of the damping parameters ω_D, ω_N are between 0.5 and 0.7. For large damping parameters there is no convergence observed. The numerical example with the penalty method is performed for the same geometry and the same boundary conditions, as in the mortar simulation. But in the experiment with the penalty method, Coulomb's law of friction is used, instead of Tresca's frictional law, used for the mortar method. The value $\mu_f = 0.2$ of the friction coefficient is chosen, since it provides nearly the same maximal tangential displacements in Ω^s. Newton's method, described in Algorithm 4.1, is applied to solve the problem. The tolerance is $\mathrm{TOL}_N = 10^{-4}$ is chosen in the stopping criterion. The results of the numerical experiments are presented in Figure 4.22 and in Table 4.3.

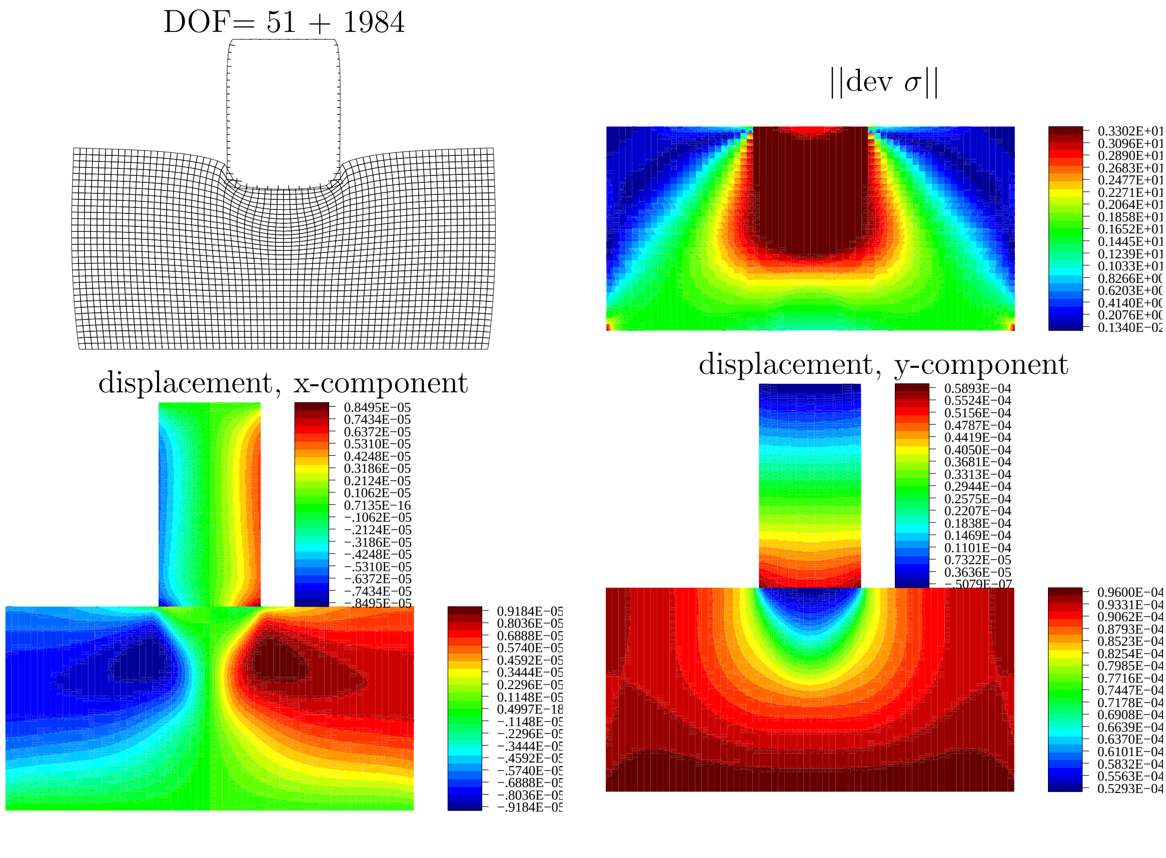

Figure 4.22: Numerical experiments for penalty method with Newton's method

The pure FEM mortar and the FE/BE penalty approaches are in a good agreement: 5-8% difference in displacement and 2-3% difference in stress. The numbers of Newton iterations needed are given in Table 4.3. Note, smaller penalty parameters reduce the L_2-norm of the penetration function $([u_n]-g)^+$. But, on the other hand, it increases the condition number of the Galerkin matrix as well as the number of Newton iterations.

$1/\varepsilon_n$	$1/\varepsilon_t$	# Newton iterations	$\|\|([u_n]-g)^+\|\|_{L_2(\Gamma_C)}$
$20 \cdot E^m$	$10 \cdot E^m$	520	$0.8 \cdot 10^{-6}$
$10 \cdot E^m$	$5 \cdot E^m$	356	$0.15 \cdot 10^{-5}$
$5 \cdot E^m$	$2.5 \cdot E^m$	248	$0.29 \cdot 10^{-5}$
$2.5 \cdot E^m$	$1.25 \cdot E^m$	175	$0.55 \cdot 10^{-5}$

Table 4.3: Number of iterations and the L_2-norm of penetration for penalty method

The mortar method and the penalty method, provide the similar results. Nethertheless, the mortar method and the penalty method have their advantages and disadvantages. The mortar approach contains no additional parameters (as penalty parameters). The discrete solution of the mortar formulation converges to the solution of the variational inequality, if the mesh size tends to zero. Unfortunately, the solution procedures for the mortar method are more complicated. The suggested DtN iteration procedure contains nested loops, where the inner loops solve the one-body problems. The convergence of the DtN algorithm depends strongly on the damping parameters, which are not allowed to be sufficiently large. The penalty approach consists only of a single loop. Here the disadvantage lies in the dependence on the penalty parameters. The smaller values of the penalty parameters give physically more relevant results, i.e. lead to the smaller penetration, but it increases the condition number of the Galerkin matrix, and therefore the time, required for solving the problem.

Bibliography

[1] R. A. Adams, *Sobolev spaces*, Academic Press [A subsidiary of Harcourt Brace Jovanovich, Publishers], New York-London, 1975. Pure and Applied Mathematics, Vol. 65.

[2] I. Babuška, B. Q. Guo, and E. P. Stephan, *On the exponential convergence of the h-p version for boundary element Galerkin methods on polygons*, Math. Methods Appl. Sci., 12 (1990), pp. 413–427.

[3] W. Bangerth and R. Rannacher, *Adaptive finite element methods for differential equations*, Lectures in Mathematics ETH Zürich, Birkhäuser Verlag, Basel, 2003.

[4] G. Bayada, J. Sabil, and T. Sassi, *Algorithme de Neumann-Dirichlet pour des problèmes de contact unilatéral: résultat de convergence*, C. R. Math. Acad. Sci. Paris, 335 (2002), pp. 381–386.

[5] R. Becker, P. Hansbo, and R. Stenberg, *A finite element method for domain decomposition with non-matching grids*, M2AN Math. Model. Numer. Anal., 37 (2003), pp. 209–225.

[6] F. Ben Belgacem, *The mortar finite element method with Lagrange multipliers*, Numer. Math., 84 (1999), pp. 173–197.

[7] F. Ben Belgacem, L. K. Chilton, and P. Seshaiyer, *The hp-mortar finite-element method for the mixed elasticity and Stokes problems*, Comput. Math. Appl., 46 (2003), pp. 35–55. p-FEM2000: p and hp finite element methods—mathematics and engineering practice (St. Louis, MO).

[8] F. Ben Belgacem, P. Hild, and P. Laborde, *Extension of the mortar finite element method to a variational inequality modeling unilateral contact*, Math. Models Methods Appl. Sci., 9 (1999), pp. 287–303.

[9] F. Ben Belgacem, P. Seshaiyer, and M. Suri, *Optimal convergence rates of hp mortar finite element methods for second-order elliptic problems*, M2AN Math. Model. Numer. Anal., 34 (2000), pp. 591–608.

[10] C. Bernardi and Y. Maday, *Polynomial interpolation results in Sobolev spaces*, J. Comput. Appl. Math., 43 (1992), pp. 53–80. Orthogonal polynomials and numerical methods.

[11] C. Bernardi, Y. Maday, and A. T. Patera, *Domain decomposition by the mortar element method*, in Asymptotic and numerical methods for partial differential equations with critical parameters (Beaune, 1992), vol. 384 of NATO Adv. Sci. Inst. Ser. C Math. Phys. Sci., Kluwer Acad. Publ., Dordrecht, 1993, pp. 269–286.

[12] ——, *A new nonconforming approach to domain decomposition: the mortar element method*, in Nonlinear partial differential equations and their applications. Collège de France Seminar, Vol. XI (Paris, 1989–1991), vol. 299 of Pitman Res. Notes Math. Ser., Longman Sci. Tech., Harlow, 1994, pp. 13–51.

[13] D. Braess, *Finite elements*, Cambridge University Press, Cambridge, second ed., 2001. Theory, fast solvers, and applications in solid mechanics, Translated from the 1992 German edition by Larry L. Schumaker.

[14] C. Carstensen, *Efficiency of a posteriori BEM-error estimates for first-kind integral equations on quasi-uniform meshes*, Math. Comp., 65 (1996), pp. 69–84.

[15] C. Carstensen, *A posteriori error estimate for the symmetric coupling of finite elements and boundary elements*, Computing, 57 (1996), pp. 301–322.

[16] C. Carstensen, O. Scherf, and P. Wriggers, *Adaptive finite elements for elastic bodies in contact*, SIAM J. Sci. Comput., 20 (1999), pp. 1605–1626 (electronic).

[17] C. Carstensen and E. P. Stephan, *Adaptive coupling of boundary elements and finite elements*, RAIRO Modél. Math. Anal. Numér., 29 (1995), pp. 779–817.

[18] A. Chernov, S. Geyn, M. Maischak, and E. P. Stephan, *Finite element/boundary element coupling for two-body elastoplastic contact problems with friction*, in Analysis and Simulation of Contact Problems, P. Wriggers and U. Nackenhorst, eds., vol. 27 of Lecture Notes in Applied and Computational Mechanics, Springer-Verlag, 2006, pp. 171–178.

[19] A. Chernov, M. Maischak, and E. P. Stephan, *A priori error estimates for hp penalty bem for contact problems in elasticity*, Comput. Methods Appl. Mech. Engrg., (2006). Submitted.

[20] P. Clément, *Approximation by finite element functions using local regularization*, Rev. Française Automat. Informat. Recherche Opérationnelle Sér. RAIRO Analyse Numérique, 9 (1975), pp. 77–84.

[21] M. Costabel, *Boundary integral operators on Lipschitz domains: elementary results*, SIAM J. Math. Anal., 19 (1988), pp. 613–626.

[22] M. Costabel and E. Stephan, *Boundary integral equations for mixed boundary value problems in polygonal domains and Galerkin approximation*, in Mathematical models and methods in mechanics, vol. 15 of Banach Center Publ., PWN, Warsaw, 1985, pp. 175–251.

[23] M. Costabel and E. P. Stephan, *Duality estimates for the numerical solution of integral equations*, Numer. Math., 54 (1988), pp. 339–353.

[24] M. R. Dorr, *The approximation theory for the p-version of the finite element method*, SIAM J. Numer. Anal., 21 (1984), pp. 1180–1207.

[25] C. Eck and J. Jarušek, *Existence results for the static contact problem with Coulomb friction*, Math. Models Methods Appl. Sci., 8 (1998), pp. 445–468.

[26] C. Eck, O. Steinbach, and W. L. Wendland, *A symmetric boundary element method for contact problems with friction*, Math. Comput. Simulation, 50 (1999), pp. 43–61. Modelling '98 (Prague).

[27] C. Eck and W. L. Wendland, *A residual-based error estimator for BEM-discretizations of contact problems*, Numer. Math., 95 (2003), pp. 253–282.

[28] C. Eck and B. Wohlmuth, *Convergence of a contact-Neumann iteration for the solution of two-body contact problems*, Math. Models Methods Appl. Sci., 13 (2003), pp. 1103–1118.

[29] R. Glowinski, J.-L. Lions, and R. Trémolières, *Numerical analysis of variational inequalities*, vol. 8 of Studies in Mathematics and its Applications, North-Holland Publishing Co., Amsterdam, 1981. Translated from the French.

[30] J. Gwinner and E. P. Stephan, *A boundary element procedure for contact problems in plane linear elastostatics*, RAIRO Modél. Math. Anal. Numér., 27 (1993), pp. 457–480.

[31] A. Hansbo, P. Hansbo, and M. G. Larson, *A finite element method on composite grids based on Nitsche's method*, M2AN Math. Model. Numer. Anal., 37 (2003), pp. 495–514.

[32] J. Haslinger and I. Hlaváček, *Contact between elastic bodies. I. Continuous problems*, Apl. Mat., 25 (1980), pp. 324–347.

[33] J. Haslinger, I. Hlaváček, and J. Nečas, *Numerical methods for unilateral problems in solid mechanics*, in Handbook of numerical analysis, Vol. IV, Handb. Numer. Anal., IV, North-Holland, Amsterdam, 1996, pp. 313–485.

[34] P. Hild, *Problèmes de contact unilatéral et maillages éléments finis incompatibles*, PhD thesis, l'Université Paul Sabatier, Toulouse 3, 1998.

[35] P. Hild and P. Laborde, *Quadratic finite element methods for unilateral contact problems*, Appl. Numer. Math., 41 (2002), pp. 401–421.

[36] G. Hu and P. Wriggers, *On the adaptive finite element method of steady-state rolling contact for hyperelasticity in finite deformations*, Comput. Methods Appl. Mech. Engrg., 191 (2002), pp. 1333–1348.

[37] J. Jarušek, *Contact problems with bounded friction coercive case*, Czechoslovak Math. J., 33(108) (1983), pp. 237–261.

[38] N. Kikuchi and J. T. Oden, *Contact problems in elasticity: a study of variational inequalities and finite element methods*, vol. 8 of SIAM Studies in Applied Mathematics, Society for Industrial and Applied Mathematics (SIAM), Philadelphia, PA, 1988.

[39] D. Kinderlehrer, *Remarks about Signorini's problem in linear elasticity*, Ann. Scuola Norm. Sup. Pisa Cl. Sci. (4), 8 (1981), pp. 605–645.

[40] R. Krause and B. Wohlmuth, *A Dirichlet-Neumann type algorithm for contact problems with friction*, Comput. Visual. Sci., 5 (2002), pp. 139–148.

[41] T. A. Laursen, *Computational contact and impact mechanics*, Springer-Verlag, Berlin, 2002. Fundamentals of modeling interfacial phenomena in nonlinear finite element analysis.

[42] T. A. Laursen and J. C. Simo, *Algorithmic symmetrization of Coulomb frictional problems using augmented Lagrangians*, Comput. Methods Appl. Mech. Engrg., 108 (1993), pp. 133–146.

[43] R. D. Lazarov, S. Z. Tomov, and P. S. Vassilevski, *Interior penalty discontinuous approximations of elliptic problems*, Comput. Methods Appl. Math., 1 (2001), pp. 367–382.

[44] P. Le Tallec and T. Sassi, *Domain decomposition with nonmatching grids: augmented Lagrangian approach*, Math. Comp., 64 (1995), pp. 1367–1396.

[45] M. Maischak and E. P. Stephan, *Adaptive hp-versions of BEM for elastic contact problems*, Comput. Mech. to appear.

[46] ——, *Adaptive hp-versions of BEM for Signorini problems*, Appl. Numer. Math., 54 (2005), pp. 425–449.

[47] ——, *A FEM-BEM coupling method for a nonlinear transmission problem modelling Coulomb friction contact*, Comput. Methods Appl. Mech. Engrg., 194 (2005), pp. 453–466.

[48] M. Maischak, E. P. Stephan, and T. Tran, *Multiplicative Schwarz algorithms for the Galerkin boundary element method*, SIAM J. Numer. Anal., 38 (2000), pp. 1243–1268 (electronic).

[49] J. M. Melenk, *hp-interpolation of nonsmooth functions and an application to hp-a posteriori error estimation*, SIAM J. Numer. Anal., 43 (2005), pp. 127–155 (electronic).

[50] U. Nackenhorst and O. von Estorff, *Numerical analysis of tire rolling noise radiation - a state of the art review*, in Internoise, Hague, 2001.

[51] J. Nečas, J. Jarušek, and J. Haslinger, *On the solution of the variational inequality to the Signorini problem with small friction*, Boll. Un. Mat. Ital. B (5), 17 (1980), pp. 796–811.

[52] J. T. Oden and J. A. C. Martins, *Models and computational methods for dynamic friction phenomena*, Comput. Methods Appl. Mech. Engrg., 52 (1985), pp. 527–634. FENOMECH '84, Part III, IV (Stuttgart, 1984).

[53] D. P. O'Leary, *A generalized conjugate gradient algorithm for solving a class of quadratic programming problems*, Linear Algebra Appl., 34 (1980), pp. 371–399.

[54] D. Perić and D. R. J. Owen, *Finite-element applications to the nonlinear mechanics of solids*, Rep. Progr. Phys., 61 (1998), pp. 1495–1574.

[55] S. Sauter and C. Schwab, *Randelementmethoden*, B. G. Teubner, 2004.

[56] C. Schwab, *p- and hp-finite element methods*, Numerical Mathematics and Scientific Computation, The Clarendon Press Oxford University Press, New York, 1998. Theory and applications in solid and fluid mechanics.

[57] P. Seshaiyer, *Non-conforming hp finite element methods*, PhD thesis, Department of Mathematics and Statistics, University of Maryland, Baltymore County, 1998.

[58] ——, *Stability and convergence of nonconforming hp finite-element methods*, Comput. Math. Appl., 46 (2003), pp. 165–182. p-FEM2000: p and hp finite element methods—mathematics and engineering practice (St. Louis, MO).

[59] P. Seshaiyer and M. Suri, *Uniform hp convergence results for the mortar finite element method*, Math. Comp., 69 (2000), pp. 521–546.

[60] J. C. Simo and T. J. R. Hughes, *Computational inelasticity*, vol. 7 of Interdisciplinary Applied Mathematics, Springer-Verlag, New York, 1998.

[61] O. Steinbach, *Numerische Näherungsverfahren für elliptische Randwertprobleme. Finite Elemente und Randelemente.*, Advances in Numerical Mathematics, B. G. Teubner, 2003.

[62] E. P. Stephan, *Coupling of boundary element methods and finite element methods*, in Encyclopedia of computational mechanics, vol. I. Fundamentals, E. Stein, R. de Borst, and T. J. R. Hughes, eds., John Wiley & Sons Ltd, Amsterdam, 2004, pp. 375–412.

[63] E. P. Stephan and M. Suri, *On the convergence of the p-version of the boundary element Galerkin method*, Math. Comp., 52 (1989), pp. 31–48.

[64] ——, *The h-p version of the boundary element method on polygonal domains with quasiuniform meshes*, RAIRO Modél. Math. Anal. Numér., 25 (1991), pp. 783–807.

[65] B. Szabó and I. Babuška, *Finite element analysis*, A Wiley-Interscience Publication, John Wiley & Sons Inc., New York, 1991.

[66] T. Tran and E. P. Stephan, *Two-level additive Schwarz preconditioners for the h-p version of the Galerkin boundary element method for 2-d problems*, Computing, 67 (2001), pp. 57–82.

[67] R. Verfürth, *A review of a posteriori error estimation and adaptive mesh-refinement techniques*, John Wiley & Sons Ltd. and B. G. Teubner, Chichester, Stuttgart, 1996.

[68] T. Warburton and J. S. Hesthaven, *On the constants in hp-finite element trace inverse inequalities*, Comput. Methods Appl. Mech. Engrg., 192 (2003), pp. 2765–2773.

[69] W. L. Wendland and E. P. Stephan, *A hypersingular boundary integral method for two-dimensional screen and crack problems*, Arch. Rational Mech. Anal., 112 (1990), pp. 363–390.

[70] B. I. Wohlmuth, *A residual based error estimator for mortar finite element discretizations*, Numer. Math., 84 (1999), pp. 143–171.

[71] ——, *Discretization methods and iterative solvers based on domain decomposition*, vol. 17 of Lecture Notes in Computational Science and Engineering, Springer-Verlag, Berlin, 2001.

[72] P. Wriggers, *Computational contact mechanics*, John Wiley & Sons Ltd, 2002.

[73] P. Wriggers and C. Miehe, *Contact constraints within coupled thermomechanical analysis—a finite element model*, Comput. Methods Appl. Mech. Engrg., 113 (1994), pp. 301–319.

Curriculum Vitae

Personal Details:

Name:	Alexey Chernov
Email:	chernov@ifam.uni-hannover.de
Born:	13th August 1981, Moscow, Russia
Family Status:	married

Education:

since 10/2003	Ph.D. Student and Junior Researcher at Institute of Applied Mathematics, University of Hanover, Germany
09/1998 - 06/2003	Student of Mathematics and Mechanics at Department of Computational Mechanics, Faculty of Mechanics and Mathematics, Moscow State Lomonosov University, Russia
09/1988 - 06/1998	Secondary School N 491, Moscow, Russia

Examinations:

25/06/2003	Honours Diploma in Mechanics and Applied Mathematics
26/06/1998	State Examination awarded with a Silver Medal (Honours School-Leaving Certificate)

Professional history:

since 10/2003	Junior Researcher; Scholarship Holder in the DFG Graduiertenkolleg 615 "Interaction of Modeling, Computation Methods and Software Concepts for Scientific-Technological Problems", University of Hanover, Germany
06/2003-10/2003	Junior Researcher at Moscow State Geological Prospecting University, Russia
09/2002-05/2003	Software Test Designer at the Group of Companies "Cellular Business Operation Support System", Moscow, Russia
09/1998-06/2003	Student of Mathematics and Mechanics at Department of Computational Mechanics, Faculty of Mechanics and Mathematics, Moscow State Lomonosov University, Russia

Research Interests: Frictional Contact, Interface Problems, Nonconforming Methods, Finite Elements, Boundary Elements and their Coupling, *hp*-Methods, Adaptive Error Control, Software Development

Language Skills: native language Russian, fluent English, fluent German